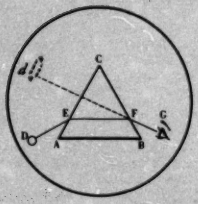

optics and spectroscopy

volume viii
number 3
march 1960

OPTICAL SOCIETY OF AMERICA

RUSSIAN EDITORIAL STAFF FOR OPTIKA I SPEKTROSKOPIYA

sponsored by

USSR ACADEMY OF SCIENCES

Editor: S. E. FRISH

Assistant Editor: P. P. FEOFILOV

Corresponding Secretary: L. S. SAZONOV

Associate Editors:

M. M. GUREVICH M. A. EL'IASHEVICH A. A. LEBEDEV V. P. LINNIK
S. L. MANDEL'SHTAM I. V. OBREIMOV V. K. PROKOF'EV
N. N. SOBOLEV A. N. TERENIN A. I. TUDOROVSKII

Translated on the Initiative of

THE OPTICAL SOCIETY OF AMERICA, INC.

With a Grant-in-Aid from

THE NATIONAL SCIENCE FOUNDATION

TRANSLATION EDITORIAL STAFF

Scientific Editors

FRED W. BEHNKE, *Perkin-Elmer Corp.*

CYRUS FELDMAN, *Oak Ridge National Laboratory*

GEORGE HERRMAN, *Columbia University*

Administrative Editor: PATRICIA R. WAKELING, *OSA*

Published monthly by the Optical Society of America, Inc. Executive office: 1155 Sixteenth Street, N.W., Washington, D.C. Subscriptions for one year to members of the Society: Associates $13.00; Regular members and Fellows $17.00. Subscriptions for non-members of the Society: One year U. S. and Possessions, $25.00; Foreign $28.00. Back numbers: $3.00 per copy. Subscriptions, changes of address and undeliverable copies should be referred to the Executive offices in Washington, D.C. The office of publication is 2500 South State Street, Ann Arbor, Michigan. Second class postage paid at Ann Arbor, Michigan.

Printed in the U.S.A. by Edwards Brothers, Inc., Ann Arbor, Michigan.

THE HYPERFINE STRUCTURE OF MULTIELECTRON ATOMS

G. M. Bukat, A. Z. Dolginov, and R. A. Zhitnikov

Received 18 June 1959

We have calculated the electronic matrix elements which enter into the hyperfine structure constants for atoms with several equivalent electrons in an unfilled shell. Cases with LS- and jj-coupling were considered. The fractional parentage coefficients for terms of maximum multiplicity of configurations f^n were given a form convenient for calculation. It was shown how, in certain cases, application of the sum rule makes it possible to solve the problem without calculating the fractional parentage coefficients.

INTRODUCTION

Hyperfine interaction, i.e., the interaction of the magnetic and electric moments of an atomic nucleus with the electron shells, has been adequately studied theoretically only for atoms with one electron (or "hole") in an unfilled shell.[1,2] A number of papers[3,4] have been devoted to the theory of hyperfine structure of atoms with several valence electrons. Trees'[4] work, together with Racah's[5,6] results, permit one to calculate the magnetic dipole and electric quadrupole interaction of a nucleus with electron shells containing s, p, and d electrons, using the approximation of the central field and LS-coupling.

In certain important cases, however, this is insufficient. For example, the rare earth atoms, in which the unfilled shells contain several equivalent electrons with orbital quantum number $l = 3$, constitute such a case. Here there is also significant octupole interaction to be taken into account. Furthermore, this is an interesting opportunity to apply the sum rule, which Goudsmit[7] used in studying magnetic dipole interaction, to the calculation of the interaction of any multipolarity in multielectronic atoms.

1. The Hamiltonian of the hyperfine interaction can be written in the form[2]

$$H = \sum_{k>0} \mathbf{T}_k \cdot \mathbf{P}_k, \tag{1}$$

where $\mathbf{T}_k \cdot \mathbf{P}_k$ is the operator of the electric (if k is even) or magnetic (if k is odd) 2^k-pole interaction of the nucleus with the atomic electron shells. It is the scalar product of irreducible tensor operators of rank k in the space of the momenta J (the operator $\mathbf{T}_k$) and I (the operator $\mathbf{P}_k$). J and I are the total angular momenta of the electron shell and the nucleus, respectively. The expression for $\mathbf{T}_k$ has the form[2]

$$\mathbf{T}_k = \begin{cases} \mathbf{T}_k^{el} = -e\sum_i r_i^{k-1} \mathbf{C}_k(i), & (k \text{ even}) \quad (2a) \\ \mathbf{T}_k^{mg} = \sum_i \mu_e \left(\Delta r_i^{k-1} \mathbf{C}_k(i)\right) \cdot \left(\frac{2}{k}\mathbf{l}(i) - 2\mathbf{s}(i)\right), & (k \text{ odd}) \quad (2b) \end{cases}$$

where e is the charge of an electron; μ_e is the Bohr magneton; ∇ is the gradient operator; $\mathbf{l}(i)$, $\mathbf{s}(i)$ are the orbital and spin momentum operators, respectively, acting on the i-th electron with coordinates r_i, ϑ_i, φ_i; $\mathbf{C}_k(i)$ is an irreducible tensor operator, the components of which are $\sqrt{4\pi/(2k+1)}\, Y_{kq}(\vartheta_i, \varphi_i)$, where $Y_{kq}(\vartheta_i, \varphi_i)$ are spherical functions.

Since the explicit form of the operator $\mathbf{P}_k$ is not used here, we will not introduce it. The diagonal matrix element of the component P_{k0} of the operator $\mathbf{P}_k$ in a state with $M_I = I$

$$(II\,|\mathbf{P}_k|\,II) = \frac{1}{\sqrt{2I+1}} C^{II}_{II\,k0} (I\,\|\mathbf{P}_k\|\,I) = \begin{cases} M_k & (k \text{ odd}) \\ Q_k & (k \text{ even}) \end{cases} \tag{3}$$

is called the nuclear electric (with k even) or magnetic (with k odd) 2^k-pole moment. Here C^{II}_{IIk0} is the Clebsch-Gordon coefficient; $(I\,\|\,\mathbf{P}_k\,\|\,I)$ is the reduced matrix element[3] of the operator $\mathbf{P}_k$. The multipole momenta M_1, Q_2, and M_3 are connected with the usual nuclear momenta μ (magnetic dipole[7]), Q (electric quadrupole[7]), and Ω (magnetic octupole[8]) in the following way:

$$\mu = M_1; \quad Q = 2Q_2; \quad \Omega = -M_3.$$

2. In the absence of an external field, the energy of the hyperfine interaction, in the first approximation of perturbation theory, has the form

$$E_J^{(1)}(F) = (\gamma I \alpha J F m\,|H|\,\gamma I \alpha J F m), \tag{4}$$

where $|\gamma I \alpha J F m)$ is the wave function of an atom with total angular momentum $\mathbf{F} = \mathbf{I} + \mathbf{J}$ and its z projection m. Here and henceforth in this paper, γ and α denote all the quantum numbers of the nucleus and electron shells respectively, besides being used as indices of the wave function in explicit form.

When the fine structure intervals are not too large in comparison with the hyperfine interaction energy, a second approximation is needed:

$$E_J^{(2)}(F) = \sum_{J'} \frac{|(\gamma I \alpha J F m\,|H|\,\gamma I \alpha J' F m)|^2}{E_J - E_{J'}}, \tag{5}$$

where E_J is the fine structure energy level. In a number of cases the effect of neighboring electron configurations can be taken into account with the help of Schwartz' method.[2]

3. A general expression for matrix elements of the type in Eq. (5) was given by Racah.[6] In accordance with his results

$$(\gamma I \alpha J F m\,|\,\mathbf{T}_k \cdot \mathbf{P}_k|\,\gamma I \alpha' J' F m)$$
$$= (-1)^{I+J'-F} W(IIJJ'; kF)\,(\alpha J\,\|\mathbf{T}_k\|\,\alpha J')\,(\gamma I\|\,\mathbf{P}_k\|\,\gamma I). \tag{6}$$

Here $W(IIJJ'; kF)$ are Racah coefficients.[9] They are tabulated in references 8 and 9. According to reference 2, $E_J^{(2)}(F)$ can be written thus

$$E_J^{(2)}(F) = \sum_{k>0} A_k M(IJ; F; k), \tag{7}$$

where

$$A_k = (\alpha J J\,|\mathbf{T}_{kk}|\,\alpha J J)\,(\gamma I I\,|\,\mathbf{P}_{kk}|\,\gamma I I),$$
$$M(IJ; F; k) = (-1)^{I+J-F} \frac{1}{a_k} W(IIJJ; kF),$$
$$a_k = \frac{1}{\sqrt{(2J+1)(2I+1)}} C^{JJ}_{JJ\,k0} C^{II}_{II\,k0}. \tag{8}$$

The functions M for the first four k's are presented in the above-mentioned paper by Schwartz. The quantities A_k are called the hyperfine structure constants. They are connected with the ordinary constants of magnetic dipole (a), electric quadrupole (b), and magnetic octupole (c) interaction[10] in the following way:

$$A_1 = lJa; \quad A_2 = \frac{1}{4}b; \quad A_3 = c.$$

Due to the orthogonality of the M functions, the constants A_k are expressed through $E_J^{(k)}(F)$ in the form

$$A_k = (2k+1)\,a_k^{-1}\sum_F (2F+1)\,M(IJ;\ F;\ k)\,E_J^{(k)}(F). \qquad (9)$$

The value of the hyperfine structure constant $A_k^{(k)}$ can be determined to a first approximation from (9), or, if it is assumed that formula (7) gives $E_J(F)$ completely, from the system of equations (7) for various F's, together with the experimental values of the hyperfine structure intervals. The second approximation is taken into account by the correction

$$A_k^{(2)} = -(2k+1)\,a_k^{-1}\sum_F (2F+1)\,M(IJ;\ F;\ k)\,E_J^{(2)}(F). \qquad (10)$$

The nuclear moments can be found by using (8) to calculate the values of A_k, if the corresponding matrix elements of the electron operators are known.

THE COUPLING OF MATRIX ELEMENTS IN LSJM$_J$ AND LSM$_L$M$_S$ REPRESENTATIONS

In this section the values of $(\alpha LSJ \| T_k \| \alpha LSJ')$ for the case of LS-coupling are expressed by diagonal matrix elements of the ordinary operators in LSM$_L$M$_S$ representation using Racah's algebra.[8] The matrix elements of the operator T_k must be diagonal with respect to J for (8), but are required to be nondiagonal with respect to J for calculating the second approximation by formulas (10) and (5).

Let us consider the matrix elements of the operator T_k^{k1}. Since T_k^{k1} acts only on the spatial coordinates of the electrons, we have

$$(\alpha LSJ\,\|T_k^{k1}\|\,\alpha LSJ') = (-1)^{S-L-J+k+1}\,e\sqrt{(2J+1)(2J'+1)}$$
$$\times W(LLJJ';\ kS)\,(\alpha LS\,\|\sum_i r_i^{k-1}C_k(i)\|\,\alpha LS). \qquad (11)$$

Now let us calculate the matrix element of the operator T_k^{k2}. After removing the parentheses in (2b), the q-component of the operator T_k^{k2} can be written in the form

$$T_{kq}^{k2} = \sum_i a_i\sqrt{i^{k-2}}\sqrt{(k+1)(2k+3)}\left(\frac{2}{k}\,\tau_{kq}^{1}(i) - 2\tau_{kq}^{2}(i)\right). \qquad (12)$$

where

$$\tau_{kq}^{1}(i) = \sum_p C_{k+1\,q+p\,1-p}^{kq}\,C_{k+1\,q+p}(i)\,l_{-p}(i)$$

is the q-component of the tensor product of rank k of the operators $C_{k+1}(i)$ and $1(i)$, and $\tau_{kq}^{2}(i)$ is the component of the similar tensor product of the operators $C_{k+1}(i)$ and $s(i)$. Since τ_k^1 acts only on the spatial coordinates of the electrons, we obtain for the "orbital" operator T_k^{k1}

$$(\alpha LSJ\,\|T_k^{k1}\|\,\alpha LSJ') = (-1)^{S-L-J+k}\sqrt{(2J+1)(2J'+1)(k+1)(2k+3)}$$
$$\times P_1\frac{2}{k}\,W(LLJJ';\ kS)\,(\alpha LS\,\|\sum_i r_i^{k-2}\tau_k^1(i)\|\,\alpha LS). \qquad (13)$$

The matrix element of the "spin" operator T_k^{k2} has the form

$$(\alpha LSJ\,\|T_k^{k2}\|\,\alpha LSJ') = 2a_1\sqrt{(k+1)(2k+1)(2k+3)(2J+1)(2J'+1)}$$
$$\times X(SLJ';\ SLJ';\ 1k+1k)\,(\alpha LS\,\|\sum_i r_i^{k-2}C_{k+1}(i)\,s(i)\|\,\alpha LS), \qquad (14)$$

where X(SLJ; SLJ'; 1k + 1k) is Fano's[11] function, and $C_{k+1}(i)s(i)$ is a dual tensor, acting as an irreducible tensor operator of rank k + 1 in coordinate space and rank 1 in spin space.

In this way we obtain expressions for the first three interaction constants

$$A_1 = 2a_1\sqrt{\frac{J(2J+1)}{J+1}}\,[(-1)^{S-L-J+1}\,W(LLJJ';\ 1S)$$
$$\times(\alpha LS\,\|\sum_i r_i^{-2}\tau_1^1(i)\|\,\alpha LS) - \sqrt{3}\,X(SLJ';\ SLJ';\ 121)$$
$$\times(\alpha LS\,\|\sum_i r_i^{-2}C_2(i)\,s(i)\|\,\alpha LS)]\,M_1, \qquad (15a)$$

$$A_2 = (-1)^{S-L-J+1}\,e\sqrt{\frac{J(2J-1)(2J+1)}{(J+1)(2J+3)}}$$
$$\times W(LLJJ';\ 2S)\,(\alpha LS\,\|\sum_i r_i^{-3}C_2(i)\|\,\alpha LS)\,Q_2, \qquad (15b)$$

$$A_3 = 4a_1a_2\sqrt{\frac{J(J-1)(2J-1)(2J+1)}{(J+1)(J+2)(2J+3)}}$$
$$\times[(-1)^{S-L-J+1}\,W(LLJJ';\ 3S)\,(\alpha LS\,\|\sum_i r_i^{-3}\tau_2^1(i)\,\|\,\alpha LS)$$
$$-3\sqrt{7}\,X(SLJ';\ SLJ';\ 143)\,(\alpha LS\,\|\sum_i r_i^{-3}C_3(i)\,s(i)\|\,\alpha LS)]\,M_3. \qquad (15c)$$

Expressions (15a) and (15b) were derived somewhat differently in reference 4.

CALCULATION OF MATRIX ELEMENTS USING COEFFICIENTS OF FRACTIONAL PARENTAGE

The calculation of matrix elements in LSM$_L$M$_S$ representation does not present any difficulty for atoms in which unfilled shells contain no equivalent electrons, since the wave function of such an atom can be constructed by the usual laws of vector addition from the one-electron wave function $R_{1l}(r_i)Y_{1,m_l}(\vartheta_i\varphi_i)\chi_{\sigma_i}$; where $Y_{1,m_l}(\vartheta_i\varphi_i)$ is a spherical function, $\chi_{\sigma i}$ is the Pauli spinor, and $R_{1l}(r_i)$ is the radial part of the function.

The construction of wave functions of several (n) equivalent electrons is complicated by the necessity of antisymmetrization of the functions. For configurations consisting of equivalent electrons with orbital quantum number l, the resulting antisymmetric wave function can be written with the help of the fractional parentage coefficients[8] $(l^{n-1}(a_1L_1S_1)lLS\,\|\,l^n\alpha LS)$ in the form

$$|\,l^n\alpha LSM_LM_S) = \sum_{a_1;\,L_1;\,S_1}(l^{n-1}(a_1L_1S_1)\,lLS\,\|\,l^n\alpha LS)\,|$$
$$\times l^{n-1}(a_1L_1S_1)\,lLSM_LM_S), \qquad (16)$$

where

$$\left|\,l^{n-1}(a_1L_1S_1)\,lLSM_LM_S) = \sum_{M_{L_1};\,m_l;\,\sigma}C_{L_1M_{L_1}lm}^{LM_L}\,C_{S_1M_{S_1}\sigma_i}^{SM_S}\,\right|$$
$$\times l^{n-1}a_1L_1S_1M_{L_1}M_{S_1})\,|l\,l_{zm}\sigma).$$

Racah[8] has derived fractional parentage coefficients for equivalent p^n and d^n electrons. Reference 12 is devoted to calculating them for equivalent f^n electrons by group theory methods. The fractional parentage coefficients for terms of maximum multipolarity of the basic ($n \le 7$) configurations are presented in Table 1 in a form convenient for practical use. For terms of additional ($n > 7$) configurations, they can be found from Table 1 by means of the formulas in reference 6.

The reduced matrix elements of the operator

$$T_k = \sum_i t_k(i),$$

where $t_k(i)$ acts on the spatial coordinates of the i-th

Table 1A. Coefficients of Fractional Parentage $(f^2(^2L')f\,{}^4L \,\|\, f^3\,{}^4L)$ for f^3 Configuration

^2L / ^4L	^4S	^4D	^4F	^4G	^4I
^3P	0	$\sqrt{\frac{3}{7}}$	$\frac{1}{\sqrt{2\cdot 7}}$	$\sqrt{\frac{11}{2\cdot 3\cdot 7}}$	0
^3F	1	$\frac{\sqrt{2}}{3}$	$-\sqrt{\frac{2}{3}}$	$\frac{\sqrt{2}}{3}$	$\frac{\sqrt{2}}{3}$
^3H	0	$\frac{1}{3}\sqrt{\frac{2\cdot 11}{7}}$	$\sqrt{\frac{11}{2\cdot 3\cdot 7}}$	$\frac{1}{3}\sqrt{\frac{5\cdot 13}{2\cdot 7}}$	$-\frac{\sqrt{7}}{3}$

Table 1B. Coefficients of Fractional Parentage $(f^2(^2L')f\,{}^2L \,\|\, f^3\,{}^2L)$ for f^3 Configuration

^2L / ^4L	^2S	^2D	^2F	^2G	^2I
^4S	0	0	$\frac{1}{\sqrt{7}}$	0	0
^4D	0	$\sqrt{\frac{2}{7}}$	$-\frac{1}{2}\sqrt{\frac{5}{2\cdot 7}}$	$\frac{1}{2}\sqrt{\frac{5\cdot 11}{2\cdot 3\cdot 7}}$	0
^4F	1	$-\frac{1}{2\sqrt{2}}$	$\frac{1}{2}\sqrt{\frac{3}{2}}$	$\frac{1}{2\sqrt{2}}$	$\frac{1}{2\sqrt{2}}$
^4G	0	$-\frac{1}{2}\sqrt{\frac{3\cdot 11}{2\cdot 7}}$	$-\frac{3}{2\sqrt{2\cdot 7}}$	$-\frac{5}{2}\sqrt{\frac{5}{2\cdot 7\cdot 11}}$	$\frac{1}{2}\sqrt{\frac{3\cdot 7}{2\cdot 11}}$
^4I	0	0	$-\frac{1}{2}\sqrt{\frac{13}{2\cdot 7}}$	$\frac{1}{2}\sqrt{\frac{7\cdot 13}{2\cdot 3\cdot 11}}$	$\sqrt{\frac{7}{11}}$

Table 1C. Coefficients of Fractional Parentage $(f^2(^3L')f\,{}^3L \,\|\, f^3\,{}^3L)$ for f^3 Configuration

^2L / ^4L	^3P	^3F	^3H
^3S	0	$\sqrt{\frac{3}{5\cdot 7}}$	0
^3D	$\sqrt{\frac{3}{7}}$	$\sqrt{\frac{2}{3\cdot 7}}$	$\sqrt{\frac{2}{5\cdot 7}}$
^3F	$\frac{1}{\sqrt{2\cdot 5}}$	$-\sqrt{\frac{2}{5}}$	$\frac{1}{\sqrt{2\cdot 5}}$
^3G	$\sqrt{\frac{3\cdot 11}{2\cdot 5\cdot 7}}$	$-\sqrt{\frac{2\cdot 3}{5\cdot 7}}$	$-\sqrt{\frac{3\cdot 13}{2\cdot 7\cdot 11}}$
^3I	0	$-\sqrt{\frac{2\cdot 11}{3\cdot 5\cdot 7}}$	$\sqrt{\frac{7\cdot 13}{3\cdot 5\cdot 11}}$

Table 1D. Coefficients of Fractional Parentage $(f^3(^2L')f\,{}^2L \,\|\, f^4\,{}^2L)$ for f^4 Configuration

^3L / ^5L	^3P
^4P	$\frac{1}{\sqrt{7}}$
^4F	$\frac{1}{\sqrt{3}}$
^4H	$\sqrt{\frac{11}{3\cdot 7}}$

Table 1E. Coefficients of Fractional Parentage $(f^3(^3L')f\,{}^3L \,\|\, f^4\,{}^3L)$ for f^4 Configuration

^3L / ^5L	^3S
^3F	1

electron, can be expressed in terms of one-electron parameters by utilizing Racah's algebra:

$$(f^n\alpha LS\,\|\,T_k\,\|\,f^n\alpha'L'S') = \delta_{SS'}\sqrt{(2L+1)(2L'+1)}\,(l\,\|\,t_k\,\|\,l) \times n\sum_{\alpha_1L_1S_1}(-1)^{L'+l-k-L_1+S'+1/2-S}\,W(LL'll;\,kL_1)\,W(SS'1/2\,1/2;\,kS_1) \times (f^{n-1}\alpha_1L_1S_1,\,lL'S')\,f^n\alpha'L'S')\,(f^n\alpha LS\,[f^{n-1}(\alpha_1L_1S_1)\,lL]S), \quad (17)$$

where $(l \,\|\, t_k \,\|\, l)$ is the one-electron reduced matrix element. Similarly for $T_{kq} = \sum_i t_{kq}(i)$, where $t_{kq}(i)$ is the dual tensor operator, we have the relationship

$$(f^n\alpha LS\,\|\,T_k\,\|\,f^n\alpha'L'S') = \sqrt{(2L+1)(2L'+1)(2S+1)(2S'+1)}\,(l^{1/2}\,\|\,t_k\,\|\,l^{1/2}) \times n\sum_{\alpha_1L_1S_1}(-1)^{L'+l-k-L_1+S'+1/2-S}\,W(LL'll;\,kL_1)\,W(SS'1/2\,1/2;\,kS_1) \times (f^{n-1}\alpha_1L_1S_1,\,lL'S')\,f^n\alpha'L'S')\,(f^n\alpha LS\,[f^{n-1}(\alpha_1L_1S_1)\,lL]S). \quad (18)$$

In particular, from a comparison of

$$(f^nLS\,\|\,L\,\|\,f^nLS) = \sqrt{L(L+1)(2L+1)}$$

with (17) we find

$$\sum_{\alpha_1L_1S_1}(-1)^{L+l+1-L_1}\,(f^{n-1}(\alpha_1L_1S_1)\,lLS]\,f^nLS)\,(f^nLS\,[f^{n-1}(\alpha_1L_1S_1)\,lLS) \times W(LLll;\,1L_1) = \frac{1}{n}\sqrt{\frac{L(L+1)}{l(l+1)(2l+1)(2L+1)}} \quad (19)$$

If we introduce the notation $U_k = \sum_i u_k(i)$; $V_{1k} = \sum_i u_k(i)s(i)$, where u_k is an irreducible tensor operator of rank k, acting on the spacial coordinates and satisfying the spacialship $(1 \,\|\, u_k \,\|\, 1) = 1$, then we will have for the equivalent electrons

$$\left.\begin{aligned}
&(f^n\alpha LS\,\|\,\sum_i r_i^{k-1}\,C_k(i)\,\|\,f^n\alpha LS) \\
&= \langle r^{k-1}\rangle_l\,(l\,\|\,C_k\,\|\,l)\,(f^n\alpha LS\,\|\,U_k\,\|\,f^n\alpha LS); \\
&(f^n\alpha LS\,\|\,\sum_i r_i^{k-3}\tau_k^1\,(i)\,\|\,f^n\alpha LS) \\
&= \langle r^{k-2}\rangle_l\,(l\,\|\,\tau_k^1\,\|\,l)\,(f^n\alpha LS\,\|\,U_k\,\|\,f^n\alpha LS); \\
&(f^n\alpha LS\|\sum_i r_i^{k-3}\,C_{k+1}(i)\,s\,(i)\,\|\,f^n\alpha LS) \\
&= \langle r^{k-2}\rangle_l\,(l\,\|\,C_{k+1}\|\,l)\,(f^n\alpha LS\,\|\,V_{1k}\|\,f^n\alpha LS),
\end{aligned}\right\} \quad (20)$$

where, according to reference 5,

$$(l\,\|\,C_k\|\,l) = \frac{1+(-1)^k}{2}\,(-1)^{\frac{k}{2}}\,\frac{(k-1)!!}{k!!} \times (2l+1)\sqrt{\frac{(2l-k-1)!!\,(2l+k)!!}{(2l+k+1)!!\,(2l-k)!!}}, \quad (21)$$

and for $(1 \,\|\, \tau_k^1 \,\|\, 1)$ we obtain by direct calculation

$$(l\,\|\,\tau_k^1\|\,l) = -\frac{1}{2}\,(l\,\|\,C_{k+1}\|\,l)\sqrt{\frac{(k+1)(2l-k)(2l+k+2)}{(2k+3)}} \quad (22)$$

The radial integrals must be evaluated by conventional approximation methods[13] or found with the help of fine structure data.[4, 14]

The matrix elements of the operators U_k and V_{1k} are given by formulas (17) and (18) in which it is essential to take into account that $(1 \,\|\, u_k \,\|\, 1) = 1$; $(1^1/_2 \,\|\, u_k \,\|\, 1^1/_2) = \sqrt{4}/_3$.

Racah[3, 9] tabulated these matrix elements for configurations of p- and d-electrons with k = 2. The matrix elements of the operators U_k and V_{1k} for configurations of f-electrons with parallel spins and the maximum possible values of L_i (the rare earths) were calculated using the coefficients of fractional parentage from Table 1. These are presented in Table 2. When k = 1 we have from Eq. (19)

$$(f^nLS\,\|\,U_1\|\,f^nLS) = \sqrt{\frac{L(L+1)(2L+1)}{l(l+1)(2l+1)}}. \quad (23)$$

In this section, atoms with one group of equivalent electrons in the unfilled shell were considered. By means

Table 2

n	Term	$(l^n LS \| U_1 \| l^n LS)$	$(l^n LS \| V_{11} \| l^n LS)$
1	^2F	1	$\sqrt{\frac{2}{2}}$
2	^3H	$\frac{1}{3}\sqrt{\frac{11\cdot 13}{2\cdot 7}}$	$\frac{1}{2}\sqrt{\frac{11\cdot 13}{3\cdot 7}}$
3	^4I	$\sqrt{\frac{13}{2\cdot 3\cdot 11}}$	$\frac{1}{3}\sqrt{\frac{5\cdot 13}{2\cdot 11}}$
4	^5I	$-\sqrt{\frac{13}{2\cdot 3\cdot 11}}$	$-\frac{1}{4}\sqrt{\frac{5\cdot 13}{11}}$
5	^6H	$-\frac{1}{3}\sqrt{\frac{11\cdot 13}{2\cdot 7}}$	$-\frac{1}{2}\sqrt{\frac{11\cdot 13}{3\cdot 5}}$
6	^7F	-1	$-\sqrt{\frac{7}{3}}$
7	^8S	0	0

Note: for $n > 7$

$$(l^n LS \| U_k \| l^n LS) = (-1)^{k+1} (l^{14-n} LS \| U_k \| l^{14-n} LS),$$
$$(l^n LS \| V_{1k} \| l^n LS) = (-1)^k (l^{14-n} LS \| V_{1k} \| l^{14-n} LS).$$

of references 5 and 16 these results were generalized to cover cases in which there are several such groups.

CALCULATION OF MATRIX ELEMENTS USING THE SUM RULE

In a number of cases it is considerably simpler to calculate matrix elements by making use of the sum rule. It is embodied in the statement that the trace of a matrix of any operator O is invariant to any unitary transformation; i.e., it does not depend on which of the representations associated with the unitary transformation are used to calculate the matrix of this operator.

Let us consider the diagonal elements of the matrix of the operator $O = \sum_i o(i)$ in the $LSM_L M_S$ representation and in the A representation, where A is the antisymmetrized and normalized product of one-electron functions of the form $R_l(r_i) Y_{lm_l}(\vartheta_i \varphi_i) \chi_{\sigma_i}$. When $\sum m_i = M_L$ and $\sum \sigma_i = M_S$, these two representations are linked by the Clebsch-Gordon unitary matrix coefficients. According to reference 15

$$(A \mid O \mid A) = \sum (l^3 \, {}_{\gamma} m_1 \sigma_1 \mid o(i) \mid l^3 \, {}_{\gamma} m_1 \sigma_1).$$

Equating the traces of the matrices gives a system of equations

$$\sum_{\alpha;\ L \supset |M_L|;\ S \supset |M_S|} (l^n \alpha L S M_L M_S \mid O \mid l^n \alpha L S M_L M_S) = \sum_{m_1;\ \sigma_1;\ i} (l^3 \, {}_{\gamma} m_1 \sigma_1 \mid o(i) \mid l^3 \, {}_{\gamma} m_1 \sigma_1) \tag{24}$$

with $M_L = \sum m_i$ and $M_S = \sum \sigma_i$. The summation on the right-hand side includes only those values of the magnetic quantum numbers which are permitted by the Pauli principle.

The system (24) contains a sufficient number of equations to determine the matrix elements of those terms which occur once in the given configurations. If a term is encountered in the configuration β times, then one can only determine the sum

$$\sum_{\alpha}^{\beta} (l^n \alpha L S M_L M_S \mid O \mid l^n \alpha L S M_L M_S).$$

For $O = U_k$ and $O = V_{1k}$ the system has the form

$$\sum_{\alpha;\ L \supset |M_L|;\ S \supset |M_S|} C^{LM_L}_{LM_L k 0} \frac{1}{\sqrt{2L+1}} (l^n \alpha L S \| U_k \| l^n \alpha L S) = \frac{1}{\sqrt{2l+1}} \sum_{m_1;\ \sigma_1;\ i} C^{lm_l}_{lm_l k 0}, \tag{25}$$

$$\sum_{\alpha;\ L \supset |M_L|;\ S \supset |M_S|} C^{LM_L}_{LM_L k 0} \frac{M_S}{\sqrt{S(S+1)(2S+1)(2L+1)}} (l^n \alpha L S \| V_{1k} \| l^n \alpha L S) = \frac{1}{\sqrt{2l+1}} \sum_{m_1;\ \sigma_1;\ i} \sigma_i C^{lm_l}_{lm_l k 0}. \tag{26}$$

In both systems $M_L = \sum m_i$ and $M_S = \sum \sigma_i$, but the summation of the right-hand parts is carried out only over those values of m_i and σ_i that are simultaneously allowed by the Pauli principle. Application of the sum rule is especially effective for terms with maximum multiplicity and the maximum value of L allowed for given S's (such a situation occurs in the rare earths, for example). In such cases the sums on the left-hand sides of expressions (25) and (26) each degenerate to a single term, and solution of one simple expression is required for calculation of the matrix elements of the operators U_k and V_{1k}. In particular, the expression

$$\sqrt{\frac{L(2L-1)}{(L+1)(2L+1)(2L+3)}} (l^n \alpha L S \| U_k \| l^n \alpha L S) = \frac{1}{\sqrt{(2l-1) l (l+1) (2l+1) (2l+3)}} \sum_{m_1;\ \sigma_1;\ i} [3m_i^2 - l(l+1)] \tag{27}$$

at once gives the matrix elements needed for calculation of the quadrupole electric interaction of the nucleus with the electron shells for such cases.

CALCULATION OF MATRIX ELEMENTS IN THE jj REPRESENTATION

In a number of cases (for example, in excited states of heavy atoms) the interaction under consideration is well described in an approximation of jj-coupling.

Let us consider for simplicity the case of a single group of equivalent electrons forming an unfilled shell. Its wave function can be written in a form analogous to (16) using the fractional parentage coefficients for jj-coupling:

$$|l^n J M_J) = \sum_{\alpha_1; J_1} (l^{n-1} (\alpha_1 J_1) j J \mid l^n \alpha J) \mid l^{n-1} (\alpha_1 J_1) j \, J M_J); \tag{28}$$

and for the matrix elements of an operator of type (2) we obtain

$$(l^n \alpha J \| T_k \| l^n \alpha J') = \sqrt{(2J+1)(2J'+1)} (j \| t_k \| j) \times \sum_{\alpha_1; J_1} (-1)^{J'+j-k-J_1} W(jjJJ'; kJ_1) \times (l^n \alpha J \mid l^{n-1} (\alpha_1 J_1) j J) (l^{n-1} (\alpha_1 J_1) j J' \mid l^n \alpha J'). \tag{29}$$

For the electric interaction

$$(j \| T^{el}_k \| j) = -e \langle r^{k-k_1} \rangle_l (j \| C_k \| j),$$

where $(j \| C_k \| j)$ are given in references 5 and 2.

For the magnetic interaction direct computation gives

$$(j \| T^{mg}_k \| j) = -\mu_0 \langle r^{k-k_1} \rangle_l \frac{(2j+1)(k+1)}{(2j+1)k} (l \| C_{k+1} \| l) \times \sqrt{[2j+1+(-1)^{j+l+1/2}(k+2)][2j+1+(-1)^{j+l+1/2}(k+1)]}. \tag{30}$$

The diagonal matrix elements can be calculated both by using (29) if the fractional parentage coefficients are known, and by using a sum rule that is written in a form similar to equation (25), i.e.,

$$\sum_{\alpha;\ J \supset |M_J|} C^{JM_J}_{JM_J k 0} \frac{1}{\sqrt{2J+1}} (l^n \alpha J \| T_k \| l^n \alpha J) = (j \| t_k \| j) \frac{1}{\sqrt{2j+1}} \sum_{\mu_l;\ i} C^{jm_j}_{jm_j k 0} \quad \text{for } M_J = \sum_i \mu_i, \tag{31}$$

where the summation on the right-hand side is carried out only over those values of μ_i that are simultaneously allowed by the Pauli principle.

REFERENCES

1. E. Fermi and E. Segre. Z. Physik **82**, 729 (1933).
2. C. Schwartz. Phys. Rev. **97**, 380 (1955).
3. S. Goudsmit. Phys. Rev. **37**, 662 (1931).
4. R. E. Trees. Phys. Rev. **92**, 308 (1953).
5. G. Racah. Phys. Rev. **62**, 438 (1942).
6. G. Racah. Phys. Rev. **63**, 667 (1943).
7. J. Blatt and V. Weiskopf. "Teoreticheskaya Yadernaya fizika." (Theoretical Nuclear Physics), Izd. Inostrannoi Lit., Moscow, 1954.
8. L. C. Biedenharn. ORNL Rept. 1098.
9. Ann. Tokyo Astron. Observ. **3**, 89 (1952); Ibid. **4**, 3, 77 (1954).
10. V. Jaccarino, J. G. King, R. A. Satten, and H. H. Stroke. Phys. Rev. **94**, 1798 (1954).
11. H. Matsunobo and H. Takebe. Progr. Theoret. Phys. (Kyoto) **14**, 58 (1955).
12. G. Racah. Phys. Rev. **76**, 1352 (1949).
13. R. Sternheimer. Phys. Rev. **80**, 102 (1950).
14. M. A. El'yashevich. "Spektry redkikh zemel'." (Spectra of the Rare Earths), Moscow, 1953.
15. E. Condon and G. Shortley. "Teoriya atomnykh spektrov." (The Theory of Atomic Spectra), Izd. Inostrannoi Lit., Moscow, 1949.
16. V. V. Balashov, K. A. Tomanov, and Iu. M. Shirokov. Sbornik "Yadernye reaktsii pri malykh i srednikh energiyakh," p. 548. (Collection, Nuclear Reactions at Low and Intermediate Energies), Moscow, 1958.

AN APPROXIMATE METHOD FOR CALCULATING FRANCK-CONDON FACTORS

L. M. Biberman and I. T. Yakubov

Received 9 June 1959

An approximate method is given for calculating Franck-Condon factors for diatomic molecules. The method is applicable in the region of large values of the vibrational quantum number.

The intensity distribution in a system of electronic vibrational bands of a diatomic molecule is determined by Franck-Condon factors, that is, by squares of the integrals of the overlap of the vibrational wave functions of the upper and lower electronic states:

$$q(v', v'') = |(v', v'')|^2 = \left[\int_0^\infty \Psi^{v'}(r) \cdot \Psi^{v''}(r)\, dr\right]^2. \qquad (1)$$

A large number of papers has been devoted to the calculation of Franck-Condon factors. Nevertheless, the subject cannot be considered closed, since the methods given in the literature are applicable only for small quantum numbers v.

We give an approximate method which permits the calculation of Franck-Condon factors for large v.

1. EXISTING METHODS OF CALCULATING FRANCK-CONDON FACTORS

As a rule, the potential curve of a diatomic molecule is well approximated by a Morse function

$$U = D\left(1 - e^{-\alpha(r-r_e)}\right)^2, \qquad (2)$$

where D and α are constants.

(v', v''), the overlap integral of the eigenfunctions of the Schrödinger equation with the Morse potential, is a troublesome integral of the product of two Laguerre functions. The difficulty of directly calculating (v', v'') increases sharply with increasing v, since the number of significant figures which are lost during the calculation begins to exceed the number of places available on the computer.[1] This situation results from the alternation of signs in the generalized Laguerre polynomials. For the same reason, the tabulation of these polynomials, which would be useful in a calculation of (v', v'') by means of graphical integration,[2] is a very laborious task.

In some of the approximate methods of calculating Franck-Condon factors, the harmonic oscillator wave functions, that is, the Hermite polynomials tabulated in the literature,[3] are used. However, their direct application involves very large errors even for small quantum numbers, since the magnitude of the overlap integral is very sensitive to small changes in the wave functions.

In the method of "distorted wave functions,"[4] the Hermite polynomials are distorted in such a way as to increase their outward resemblance to the Laguerre polynomials, after which (v', v'') is found by the method of graphical integration. The error in this method increases rapidly with increasing v. It is scarcely recommended for $v > 3$ in the case of a molecule with normal anharmonicity.

The method given by Wu[5] for the approximate calculation of the integral in the expression for (v', v'') is very laborious, and the vanishing of significant figures as a result of the alternation of signs in the generalized Laguerre polynomials makes it inapplicable for $(v' + v'') > 5$.

If the constants α_1 and α_2 of the Morse potentials are equal, the integration of (v', v'') is very easy. This fact is made use of in the method of "average α,"[6,7] in which α_1 and α_2 are replaced by a suitably chosen α_{av} which is used for both of the potential curves. Such a replacement means a distortion of the potential curves which increases with increasing v. Thus, by introducing α_{av} we actually make the wave functions inexact and obtain an error in the values of the Franck-Condon factors which increases with increasing v. Calculations made by us as a check have shown that the error may exceed 100% even for relatively small values of one of the quantum numbers ($v \sim 10$), even when α_1 and α_2 differ only by 10-20%. The refinements of the method of "average α" which are proposed in reference 7 seem ineffective.

On the whole, one may say that existing methods for calculating Franck-Condon factors are valid only for small values of $(v' + v'')$.

2. APPROXIMATE METHOD FOR CALCULATING FRANCK-CONDON FACTORS

It was remarked above that great difficulty arises in the calculation of Franck-Condon factors because of the special properties of the generalized Laguerre polynomials. At the same time, and, in particular, for large v, the Laguerre functions may be replaced by

asymptotic expressions which we obtain by application of the wentzel-Kramers-Brillouin method (W. K. B. method) to the solution of the Schrödinger equation with a Morse potential.* In the neighborhood of the points of

*In reference 5 Wu discusses the possibility of using the W. K. B. method, but only for cases in which the Morse function is not a satisfactory approximation to the experimental potential curve.

reversal, where the W. K. B. method is not applicable, we approximate the Laguerre polynomials with the aid of monotonic parts of Hermite polynomials chosen in a certain way. The functions obtained are comparatively easy to plot, and (v', v'') can be obtained by graphical integration. The accuracy of the results increases with increasing v' and v'' as long as the Morse function is a sufficiently good representation of the experimental potential curve.

Certain problems do not require a highly accurate knowledge of q(v', v''). For use in such cases, a method of approximate calculation of Franck-Condon factors is explained below. The method uses asymptotic expressions of the Laguerre functions, but does not require their graphing. This greatly reduces the labor involved in the calculation.

A. USE OF THE W. K. B. METHOD

The quasi-classical functions representing approximate solutions in the oscillatory and monotonic regions and going to infinity at the points of reversal are as follows:

$$\Psi(r) \cong \frac{C}{2}\frac{1}{\sqrt{|p|}}\exp\left[-\frac{1}{\hbar}\int_r^{r_1}|p|\,dr\right], \quad r<r_1 \tag{3a}$$

$$\Psi(r) \cong C\frac{1}{\sqrt{p}}\cos\left[\frac{1}{\hbar}\int_{r_1}^{r} p\,dr-\frac{\pi}{4}\right], \quad r_2>r>r_1 \tag{3b}$$

$$\Psi(r) \cong \frac{C}{2}\frac{1}{\sqrt{|p|}}\exp\left[-\frac{1}{\hbar}\int_{r_2}^{r}|p|\,dr\right], \quad r>r_2, \tag{3c}$$

where p(r) is the momentum and r_1 and r_2 are the coordinates of the points of reversal:

$$r_{1,2} = -\frac{1}{a}\ln(1\pm\sqrt{\beta}), \quad \beta = \frac{E}{D}. \tag{4}$$

When expression (2) is substituted into (3), it is essential that all of the integrals be expressed in terms of elementary functions.* For example, the integral in Eq.

*As a result of this, we obtain an asymptotic expression for associated Laguerre polynomials L_v^a of high degree v and having large fractional indices a. This in itself may be of some interest.

(3b) is equal to

$$J(r) = \frac{1}{\hbar}\int_{r_1}^{r} p(r)\,dr - \frac{\pi}{4} =$$

$$-\frac{\sqrt{2\mu D}}{a\hbar}\left[\sqrt{\beta-(1-e^{-a(r-r_e)})^2}-\arcsin\frac{1-e^{-a(r-r_e)}}{\sqrt{\beta}}\right.$$

$$\left.-\sqrt{1-\beta}\cdot\arcsin\frac{\beta+e^{-a(r-r_e)}-1}{e^{-a(r-r_e)}\sqrt{\beta}}+\frac{\pi}{2}(\sqrt{1-\beta}-1)\right]-\frac{\pi}{4}, \tag{5}$$

where μ is the reduced mass of the molecule.

We calculate the normalization constant in accordance with reference 9: $C = \sqrt{\frac{2a\sqrt{2\mu D}}{\pi}}\cdot\sqrt[4]{1-\beta}$.

The question of the practical utilization of the functions (3) depends on the relative magnitude of the region of applicability of the W. K. B. method. The quasi-classical condition for a system may be written as:[10]

$$\left|\frac{3}{4}\left(\frac{p'}{p^2}\right)^2-\frac{p''}{2p^3}\right|\hbar^2 \ll 1, \tag{6}$$

where p' and p'' are the first and second derivatives of the momentum.

We cannot immediately determine how sensitive the deviation of the quasi-classical functions from the Laguerre functions is to the magnitude of the left-hand side of inequality (6), since no tabulation of the Laguerre polynomials exists. Condition (6) may prove too severe. Hence it is necessary to investigate the applicability of the W. K. B. method to the dimensionless harmonic oscillator; also, since from the point of view of the applicability of the W. K. B. method there is no essential difference between harmonic and anharmonic oscillators, we must compare the ranges of applicability of the W. K. B. method for each of the two sides of the potential curves of the two oscillators. However, by making the estimate for a dimensionless oscillator, we eliminate the possibility of explaining the result in terms of the particular properties of a given electronic state.

As a result of the comparison of the Hermite polynomials and the asymptotic functions obtained by the W. K. B. method, we can make a decision as to the possibility of using the quasi-classical expressions for relatively small v. Figure 1 shows the Hermitian polynomial for v = 5 and its quasi-classical approximation, plotted as a function of the dimensionless variable:

$$\xi = \sqrt{a_r}\cdot(r-r_e) = \sqrt[4]{\frac{k_2}{\hbar^2}}(r-r_e), \tag{7}$$

where k is the force constant.

We introduce the small quantity $\Delta = \xi_0 - \xi$, where $\xi_0 = \sqrt{2v+1}$ is the point of reversal of the classical harmonic oscillator. It appears that the amplitudes of the quasi-classical functions differ by less than 5% from the values of the Hermitian polynomials for $\xi < \xi_0 - \Delta_0$, where Δ_0 is the solution of the equation obtained by setting the left-

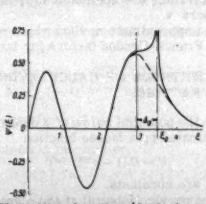

Fig. 1. Hermitian function (dashed curve) and quasi-classical function approximating it (continuous curve) (v = 5).

hand side of (6) equal to one third, that is,

$$\Delta_0 \cong \sqrt[3]{\frac{0.47}{\xi_0}}.$$

We define corresponding magnitudes for the Morse oscillator thus:

$$\Delta_1 = \frac{\Delta_0}{\xi_0}(r_e - r_1), \tag{9a}$$

$$\Delta_2 = \frac{\Delta_0}{\xi_0}(r_2 - r_e). \tag{9b}$$

B. USE OF THE HERMITIAN POLYNOMIALS

We approximate the Laguerre polynomials in the neighborhood of the points of reversal, as well as in the regions of monotonic damping, by corresponding portions of the Hermite polynomials. For this we make the points of reversal of the anharmonic and harmonic levels coincide, and do the same for the minima of the potential wells. The coefficient of the Hermite polynomial $\sqrt{\alpha_\Gamma}$ must then be chosen as:

$$\sqrt{\alpha_\Gamma}(1,2) = \frac{\sqrt{2\nu+1}}{r_{1,2}}. \qquad (10)$$

This suggestion is based not on the formal resemblance of the functions, but on a trial calculation. The harmonic oscillator functions were used in reference 1 to calculate $q(\nu', \nu'')$ for the β-system of NO. The authors of this work chose $\sqrt{\alpha_\Gamma}$ in such a way as to obtain the best agreement between the (ν', ν'') which they found and the overlap integrals of the Laguerre polynomials calculated for small $\nu' + \nu''$ with the aid of a computer. It may be shown that the value of $\sqrt{\alpha_\Gamma}$ which they found agrees well with that calculated by means of Eq. (10). It is essential to note, however, that they compared their calculated values of $q(\nu', \nu'')$ with the exact values of the Franck-Condon factors only in cases where they resulted from the overlapping of monotonic portions of the wave functions. It is not surprising that good agreement was found for such (ν', ν'').

However, the authors of reference 1 extrapolate this result without proof to cases where this condition is not fulfilled.

It should be noted that the choice of normalization constant of the Hermitian polynomial made in reference 1 is not satisfactory, since the probability amplitude is unity at both the left and the right points of reversal. It is more correct to make the quasi-classical and harmonic functions come together at the points $r = r_2 - \Delta_2$ and $r = r_1 + \Delta_1$. For example, Fig. 2 shows the approximation for the last maximum of the Laguerre polynomial $\psi^{\nu=9}(r)$, $B^3\Pi_g$, N_2.

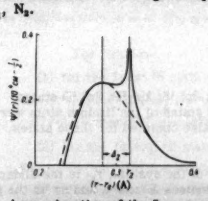

Fig. 2. Approximation of the Laguerre function in the neighborhood of a point of reversal and in the region of monotonic damping (ν = 9, $B^3\Pi_g$, N_2). Continuous curve: quasi-classical function of the Morse oscillator; dashed curve: Hermite polynomial.

Thus, in order to construct a function which will approximate a Laguerre polynomial for $\nu \geq 4$, we use Eq. (7) for the oscillating region and the tabulated Hermitian polynomials. The parameters of the Hermitian functions are determined with the aid of (10).

C. APPROXIMATE METHOD OF INTEGRATING (ν', ν'')

The function $\psi^{\nu'}\psi^{\nu''}(r)$, which is under the integral sign in (ν', ν''), has multiple roots. Let us assume that the form of the "semiwave" function $\psi^{\nu'}\psi^{\nu''}(r)$ is approximately sinusoidal. This is suggested by qualitative considerations, as well as by direct consideration of graphs of the overlap function. For example, the overlap function for

$$\Psi^{\nu=9}(r),\ A^3\Sigma,\ N_2 \text{ and } \Psi^{\nu=10}(r),\ B^3\Pi_g,\ N_2$$

is plotted in Fig. 3.

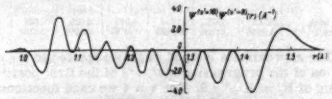

Fig. 3. Graph of the overlap function of the oscillatory wave functions $\psi^{\nu'=9}(r)$, $A^3\Sigma$ and $\psi^{\nu'=10}(r)$, $B^3\Pi_g$ of the N_2 molecule.

On the basis of this assumption, we obtain

$$(\nu', \nu'') \cong \frac{2}{\pi} \sum_i \Psi^{\nu'}(r_{m_i}) \cdot \Psi^{\nu''}(r_{m_i}) \cdot \Delta r_i, \qquad (11)$$

where Δr_i is the distance between two adjacent roots of the overlap function and r_{m_i} is the coordinate of the midpoint of the i-th section.

With respect to this calculation, it must be noted that the sections forming the monotonic portions of the overlap functions themselves are known to be nonsinusoidal. The accuracy of Eq. (11) may be improved by carrying out a graphical integration over these sections.

We suggest the following actual calculational procedure:

1. The roots of the function $\psi^{\nu'}\psi^{\nu''}(r)$ are the roots of $\cos I_1(r)$ and $\cos I_2(r)$, where the functions $I_1(r)$ and $I_2(r)$ may be plotted with the aid of Eq. (5). Since their values at the points r_1 and r_2 are known, an expansion of I(r) in powers of $\alpha(r - r_e)$ significantly reduces the labor. The expansion is as follows:

$$I(r) = I(r_e) + \frac{\sqrt{2\mu D}}{\hbar}\sqrt{3}(r - r_e)\left[1 - \frac{a^2}{6}(r - r_e)^2\right] + \ldots \qquad (12)$$

2. Knowing $I_1(r)$ and $I_2(r)$, we find the roots of the function $\psi^{\nu'}\psi^{\nu''}(r)$ and then find the Δr_i, r_{m_i}, $I_1(r_{m_i})$ and $I_2(r_{m_i})$.

3. The momentum of the particle at the points r_{m_i}, which is needed for the calculation of $\psi(r_{m_i})$ (See Eq. 3b), may be determined directly from a graph of the potential function U(r). However, if we are calculating a large square table of $q(\nu', \nu'')$, then it is more convenient to draw the family of curves $(1/\sqrt{p})(r)$, starting from the graph of U(r) just mentioned.

4. The form of the monotonic sections of the Hermitian polynomials is simple. In order not to have to draw up tables of these functions, such as those introduced in reference 3, for each case, we may select some simple approximation for them.

5. With the aid of Eq. (11) we calculate (ν', ν''), and then $q(\nu', \nu'')$.

3. VERIFICATION OF THE APPROXIMATE METHOD

The overlap integrals of the harmonic oscillator wave functions, calculated with the aid of a computer, are given in reference 1. In order to make an explicit check of the method proposed in Section 2C, while retaining the assumptions of reference 1 and using the tabulated Hermite functions, we carried out an analogous calculation with the aid of this method.

We calculated values of the progression $q(\nu', \nu'')$ for $\nu'' = 12 = \text{const}$. The results are given in Table 1, where

they are compared with corresponding results from reference 1.

Table 1. Values of q(v', v")

	v'						
	0	1	2	3	4	5	6
Present work . . .	0.053	0.120	0.014	0.073	0.025	0.048	0.002
Reference 1	0.0557	0.1100	0.0033	0.0599	0.0158	0.0382	0.0198

The approximate method was also applied to the calculation of the progression q(v', v") of the first positive system of N_2 with v" = 8. For v ≥ 4 we used functions obtained by means of the W. K. B. method. For v = 2 and 3, "distorted" functions were constructed by Pillow's method,[4] except that the coordinate of the central zero (maximum) of the distorted function was determined using the linear part of the expansion (12)

$$\Delta r_s(\nu) = \frac{a - I(r_0)}{\frac{\sqrt{2\mu D}}{h}\sqrt{3}}, \qquad (13)$$

where a is greater than $I(r_e)$ and is the nearest multiple of π/2 or π, depending on the evenness of oddness of v. For v = 0 or v = 1 the harmonic functions were used.

In Table 2 the results of the present work are compared with those of reference 2. This reference gives the only large table of Franck-Condon factors to be found in the literature in which the values may be considered of sufficient accuracy. Nicholls and Jarmain carried out a graphical integration of the Laguerre function, performing a great deal of laborious calculation, as they themselves remark.

Consideration of Tables 1 and 2 shows that the proposed method gives completely satisfactory results. The

Table 2. Values of q(v', v")

	v'											
	0	1	2	3	4	5	6	7	8	9	10	11	12
Reference 2	0.000	0.009	0.043	0.089	0.063	0.000	0.074	0.040	0.035	0.077	0.055	0.080	0.267
Present work	0.000	0.011	0.048	0.100	0.082	0.000	0.087	0.038	0.027	0.102	0.073	0.074	0.290

average error in the values of the Franck-Condon factors does not exceed 20%. Because of the constancy of the absolute error, the calculated results for large Franck-Condon factors, which are of basic interest, are necessarily more accurate than the results for small ones.

REFERENCES

1. B. Kivel, H. Mayer, and H. Bethe. Annals of Physics 2, 57 (1957).
2. W. Jarmain and R. Nicholls. Canad. J. Phys. 32, 201 (1954).
3. M. Pillow. Proc. Phys. Soc. A62, 237 (1949); Ibid. A63, 940 (1950).
S. Weniger. J. phys. Radium 15, 428 (1954).
4. M. Pillow. Proc. Phys. Soc. A64, 773 (1951).
5. Ta You-Wu. Proc. Phys. Soc. A65, 965 (1952).
6. P. Fraser and W. Jarmain. Proc. Phys. Soc. A66, 1145 (1953).
7. P. Fraser and W. Jarmain. Proc. Phys. Soc. A66, 1153 (1953).
8. I. T. Yakubov. Izvest Vyssh. Shkoly, Ser.-Mat. (in press).
9. W. Furry. Phys. Rev. 71, 360 (1957).
10. E. Kemble. "Fundamental Principles of Quantum Mechanics." McGraw-Hill, New York, 1937.

CALCULATION OF THE PROBABILITY OF AUTOIONIZATION IN HELIUM AND LITHIUM ATOMS

R. Kh. Propin

Received 17 April 1959

The probabilities of the autoionization of the $2s^2\ ^1S$; $2s2p^1\ ^3P$; $2p^2\ ^1S$; $2p^2\ ^3P$; $2p^2\ ^1D$ states of the helium atom and the $1s2s^2\ ^2S$; $1s2s2p\ ^2P$; $1s2p^2\ ^2S$; $1s2p^2\ ^2D$ states of the lithium atom were calculated. Approximate wave functions and energy values were also obtained for these states.

It is well known that the probability of autoionization in light atoms (where possible) is far greater than the probability of optical transition.[1] Consequently, this phenomenon is of interest for its own sake. In helium and lithium it can take place only from doubly excited states; for example, states which may be produced under electron impact. Autoionization manifests itself experimentally in the absence of lines corresponding to optical transitions for which such states are the initial or final state. Lines corresponding to transitions from a doubly excited state which is not subject to autoionization by virtue of selection rules are an exception. In fact, Wu[2] showed that He 320.4A can be explained by a $1s2P\ ^3P - 2p^2\ ^3P$ transition.

The probability of autoionization is calculated by the formula

$$w = \frac{2\pi}{h}\left|\int \psi_i^* \left(\sum_{k>j}\frac{1}{r_{kj}}\right)\psi_f d\tau\right|^2, \qquad (1)$$

where ψ_i and ψ_f are the wave functions for the initial and final states of the system, r_{kj} is the distance between electrons with indices k and j, and dτ is the product of the elementary volumes of all electrons (the summation and integration are carried out over all electrons).

This paper is devoted to the calculation of autoionization probabilities in helium and lithium atoms. The variational method was used to determine the initial state functions. Trial functions were assumed to be linear combinations of the form

$$\psi_i = \sum_k c_k \varphi_k. \qquad (2)$$

The functions φ_k are chosen such that the total spin S, the total orbital angular momentum L and its projection M on the z axis have fixed values. In the case of helium the functions φ_k are made up of one-electron Coulomb functions for a field with a charge of 2μ. For lithium, the 1s electrons are considered as being in a field with a charge of 3μ; the remaining electrons, in a field of charge 2μ. Then coefficients c_k and the scale parameter μ are determined from the condition of mini-

mum energy of the system. Moreover, the quantum numbers of one of the functions ψ_k must correspond to the state that we are considering. The remaining functions ψ_k are considered as superfluous in this instance.

It should be noted that there is an infinitely large number of states with energies lower than those under consideration. Consequently it is impossible to satisfy all the orthogonality conditions required by the variational principle, and hence it cannot be proved that the energy values obtained are not lower than the true ones.

If the functions ψ_k are labeled by the symbols of the corresponding states, then the wave functions of the initial states can be written in the following form.

For helium

(1) for the $2s^2\ ^1S$ state:

$$\Psi = N^{-1}[\psi(2s^2\,^1S) + c_1\psi(2s3s\,^1S) + c_2\psi(2p^2\,^1S) + c_3\psi(2p3p\,^1S)],$$

$$N^2 = 1.379,\ \mu = 0.947,\ c_1 = -0.118,\ c_2 = 0.575,\ c_3 = -0.184;$$

(2) for the $2s2p\ ^1P$ state:

$$\Psi = N^{-1}[\psi(2s2p\,^1P) + c_1\psi(2s3p\,^1P) + c_2\psi(2p3s\,^1P) + c_3\psi(2p3d\,^1P)],$$

$$N^2 = 1.415,\ \mu = 1.023,\ c_1 = -0.287,\ c_2 = -0.431,\ c_3 = -0.382;$$

(3) for the $2s2p\ ^3P$ state:

$$\Psi = N^{-1}[\psi(2s2p\,^3P) + c_1\psi(2s3p\,^3P) + c_2\psi(2p3s\,^3P) + c_3\psi(2p3d\,^3P)],$$

$$N^2 = 1.048,\ \mu = 0.941,\ c_1 = -0.151,\ c_2 = 0.115,\ c_3 = -0.109;$$

(4) for the $2p^2\ ^1S$ state:

$$\Psi = N^{-1}[\psi(2p^2\,^1S) + c_1\psi(2s^2\,^1S) + c_2\psi(2s3s\,^1S) + c_3\psi(2p3p\,^1S)],$$

$$N^2 = 2.352,\ \mu = 1.070,\ c_1 = -0.554,\ c_2 = 0.697,\ c_3 = -0.747;$$

(5) for the $2p^2\ ^3P$ state:

$$\Psi = N^{-1}[\psi(2p^2\,^3P) + c_1\psi(2p3p\,^3P) + c_2\psi(3p^2\,^3P) + c_3\psi(3d^2\,^3P)],$$

$$N^2 = 1.114,\ \mu = 0.952,\ c_1 = -0.326,\ c_2 = -0.058,\ c_3 = -0.070;$$

(6) for the $2p^2\ ^1D$ state:

$$\Psi = N^{-1}[\psi(2p^2\,^1D) + c_1\psi(2p3p\,^1D) + c_2\psi(2s3d\,^1D)],$$

$$N^2 = 1.453,\ \mu = 1.040,\ c_1 = -0.574,\ c_2 = 0.351.$$

For lithium

(1) for the $1s2s^2\ ^2S$ state:

$$\Psi = N^{-1}[\psi(1s2s^2\,^2S) + c\psi(1s2p^2\,^2S)],$$

$$N^2 = 1.142,\ \mu = 1.007,\ c = 0.410;$$

(2) for the $1s2s2p\ ^2P$ state:

$$\Psi = N^{-1}[\psi(1s2s2p\,^2P) + c\psi(1s2s3p\,^2P)],$$

$$N^2 = 1.102,\ \mu = 1.000,\ c = -0.342;$$

(3) for the $1s2p^2\ ^2S$ state:

$$\Psi = N^{-1}[\psi(1s2p^2\,^2S) + c\cdot\psi(1s2s^2\,^2S)],$$

$$N^2 = 1.187,\ \mu = 0.962,\ c = -0.438;$$

(4) for the $1s2p^2\ ^2D$ state:

$$\Psi = N^{-1}[\psi(1s2p^2\,^2D) + c\cdot\psi(1s2p3p\,^2D)],$$

$$N^2 = 1.208,\ \mu = 1.000,\ c = -0.456.$$

When an ejected electron is at infinity, the wave function of the final state must be simply the product of the wave function of the remaining atom and the wave function of the ejected electron. In conformity with this, the wave function of the final state for helium takes the form

$$\Psi = \frac{1}{\sqrt{2}}[\psi_{100}(1)\,\psi_{\mathrm{Elm}}(2) \pm \psi_{\mathrm{Elm}}(1)\,\psi_{100}(2)], \qquad (3)$$

where

$$\psi_{100} = \sqrt{\frac{\delta}{\pi}}\cdot e^{-\delta r}\ \text{(in atomic units)}.$$

The analogous function for lithium takes the form

$$\Psi = \frac{1}{\sqrt{6}}\begin{vmatrix} \psi_{100}(1)\,\eta_+(1); & \psi_{100}(2)\,\eta_+(2); & \psi_{100}(3)\,\eta_+(3) \\ \psi_{100}(1)\,\eta_-(1); & \psi_{100}(2)\,\eta_-(2); & \psi_{100}(3)\,\eta_-(3) \\ \psi_{\mathrm{Elm}}(1)\,\eta_+(1); & \psi_{\mathrm{Elm}}(2)\,\eta_+(2); & \psi_{\mathrm{Elm}}(3)\,\eta_+(3) \end{vmatrix}, \qquad (4)$$

where η_+ and η_- are spin functions,

$$\psi_{100} = \sqrt{\frac{27\mu^3}{\pi}}\cdot e^{-3\mu r},$$

$\mu = 0.89583$, and in both cases ψ_{Elm} takes the form of a coulomb function of a continuous spectrum for an electron in the field of the residual atom normalized to δ—a function of energy. The quantum numbers of the final state are determined from the conditions of energy conservation E, total spin S, orbital momentum L, its projection M, and parities.

Table 1. Probability of Autoionization in a Helium Atom

State	Our data		Data of reference 2	
	Energy (ry)	w (sec^{-1})	Energy (ry)	w (sec^{-1})
$2s^2\ ^1S$	−1.5443	$2.51\cdot10^{14}$	−1.4440	$4\cdot10^{14}$
$2s2p\ ^1P$	−1.3890	$3.84\cdot10^{13}$	—	—
$2s2p\ ^3P$	−1.5112	$5.01\cdot10^{12}$	−1.5043	$5\cdot10^{12}$
$2p^2\ ^1S$	−1.1939	$5.86\cdot10^{13}$	—	—
$2p^2\ ^3P$	−1.4088	0	−1.4109	0
$2p^2\ ^1D$	−1.3826	$1.33\cdot10^{14}$	−1.3280	$1\cdot10^{14}$

The calculated values of the probabilities w are presented in the table. The probability of autoionization of lithium atoms[2] from the $1s2s2p\ ^4P$, $1s2p^2\ ^2P$, and $1s2p^2\ ^4P$ states is zero by virtue of selection rules.

Table 2. Probability of Autoionization in a Lithium Atom

State	Energy (ry)	w (sec^{-1})
$1s2s^{22}S$	−10.6922	$8.03\cdot10^{14}$
$1s2s2p^4P$	−10.5801	$5.88\cdot10^{14}$
$1s2p^{22}S$	−11.1100	$2.8\cdot10^{13}$
$1s2p^{22}D$	−10.3765	$2.18\cdot10^{13}$

The results of calculations for helium performed by Wu[2] are shown for comparison. In reference 2 the wave functions of the ejected electron are determined by numerical solution of an integral-differential equation; however, the functions for the initial state were less precise than in this work. The agreement of the results allows us to consider the order of magnitude of the autoionization probability as being correct. This is a most important point, since there are no direct experimental data on these values.

We note in conclusion that as far as we know, calculations of this type have not been previously performed for lithium.

In closing, I would like to thank B. T. Geilikman for the suggested topic and constant consultation.

REFERENCES

1. G. Wentzel. Z. Physik 43, 524 (1927).
2. Ta-You Wu. Phys. Rev. 66, 291 (1944).

TRANSITION PROBABILITIES IN THE γ- AND β- BAND SYSTEMS OF NO

S. P. Erkovich and Yu. V. Pisarevsky

Received 24 March 1959

This paper presents a calculation of the electronic transition moment $R_e(r)$ for the γ- and β-band systems in the absorption spectrum of the NO molecule.

The absolute intensities of electronic transitions to the ground state in NO molecules have recently attained great significance in conjunction with the calculation of the emissivity of hot air (see, for instance, reference 1).

The purpose of this paper is to present a calculation of the electronic transition moment $R_e(r)$ for the γ- and β-band systems of NO (transitions $A^2\Sigma - X^2\Pi$ and $B^2\Pi - X^2\Pi$) on the basis of Marmo's[2] and Mayence's[3] experimental data on absorption spectra. The computations presented here were carried out by employing the method proposed in reference 1, although this method has been somewhat modified because of the strong dependence of the electronic moment on the internuclear distances.

If ν_i is the wave number corresponding to the center of the transmission band, and a the width of the transmission band of the spectrograph (0.85 A in Marmo's experiments), the transmission coefficient of a gas layer of thickness l and of the spectrograph described by the transmission function $f(|\nu - \nu_i|, a)$ can be determined from the expression

$$T = \frac{I}{I_0} = 1 - \frac{1}{a} \sum_j f(|\nu_j - \nu_i|, a) \cdot 2\sqrt{S_j l}. \qquad (1)$$

Here ν_j stands for the wave number of the center of the line, characterized by the rotational quantum number of the lower level $j = j''$. The summation in Eq. (1) is extended over all lines within the transmission band of the spectrograph.

The total absorption in the region of the individual line

$$S_j = \int_0^\infty k_{j,\nu} d\nu$$

is obtained from the equation

$$S_j = \frac{8\pi^3 e^2 \nu_j}{3hc} \frac{n_{v''j''}}{2j''+1} i_{j''} q(v', v'') R_e^2(\bar{r}). \qquad (2)$$

In this equation $n_{v''j''}$ signifies the molecular concentration in the lower electronic vibrational-rotational level, and $q(v', v'')$ represents the Franck-Condon factor; i_j is the square of the matrix element of the rotational transition (Hönl-London intensity factor); and $\bar{r}$ represents the average value of internuclear separation in the transition $v' - v''$ (r – centroid) defined by the equation

$$\bar{r} = \frac{\int \psi_{v'} r \psi_{v''}(r)\, dr}{\int \psi_{v'} \psi_{v''} dr}. \qquad (3)$$

where $\psi_{v'}$ and $\psi_{v''}$ are the vibrational wave functions corresponding to the upper and lower electron states. The damping constant γ entering Eq. (1) can be obtained from

$$\gamma = \frac{1}{4\pi c} A_{v'v''} = \frac{16\pi^3 e^2 \nu_i^3}{3hc} R_e^2. \qquad (4)$$

After substituting Eqs. (4) and (2) into (1), the following expression for the absorption function A = 1 – T is obtained:

$$A = \frac{16\pi^3 e^2 \nu_i^3}{3hcs} R_e^2(\bar{r}) \sum_j f(|\nu_j - \nu_i|, a) \sqrt{2l \frac{n_{v'j''}}{2j''+1} i_{j''} q(v', v'')}. \qquad (5)$$

Comparing this relationship with the experimental value of the absorption function for definite values of ν_i, i.e., with the quantity

$$A_{exp.} = 1 - T_{exp.} = 1 - e^{-\frac{kpl}{760}}, \qquad (6)$$

we ultimately obtain the expression

$$R_e^2(\bar{r}) = \frac{1 - e^{-\frac{kpl}{760}}}{\frac{16\pi^3 e^2 \nu_i^3}{3hcs} \sum_j f(|\nu_j - \nu_i|, a) \sqrt{2l \frac{n_{v'j''}}{2j''+1} i_{j''} q(v', v'')}}. \qquad (7)$$

In Eq. (6) the quantity p represents the pressure of NO in mm Hg, and k represents the experimentally determined absorption coefficient defined by the equation

$$I = I_0 e^{-kl}$$

and converted to standard pressure.

Since the absolute values of ν_i are not accurately known from experimental data on absorption, we calculated values of the denominator in Eq. (1) for a number of values of ν_i within the given band. This made it possible to determine the maximum values of the denominator corresponding to the two band maxima, after which the electronic transition moment was obtained from the quantities k_{max}.

The molecular concentration $n_{v''j''}$ was computed from the formulas quoted in reference 4.

For the evaluation of the functions $f(|\nu - \nu_i|, a)$ we used data from the rotational structure analysis of these bands obtained by Schmidt[5] and Lagerquist and Miescher.[6] Following reference 7, we assumed the function $f(|\nu - \nu_i|, a)$ to be of the form

$$f(|\nu - \nu_i|, a) = \begin{cases} 0 & \nu \leqslant \nu_i - a \\ (\nu - \nu_i + a)\frac{1}{a} & \nu_i - a \leqslant \nu \leqslant \nu_i \\ (\nu_i - \nu + a)\frac{1}{a} & \nu_i \leqslant \nu \leqslant \nu_i + a \\ 0 & \nu \geqslant \nu_i + a. \end{cases} \qquad (8)$$

The values of the Franck-Condon factor have been taken from the work by Kivel, Mayer, and Bethe.[1] The Hönl-London intensity factors have been taken in the form published by Herzberg.[8]

Results of calculations for the β-band system of NO, obtained by using Marmo's[2] experimental data for the β-band region, (5,0) are presented in Table 1. We utilized the values of the electronic transition moments for the

normalization of the relative dependence $R_e(\bar{r})$ established by Robinson and Nicholls.[9] Unfortunately, reference 9 does not contain relative data for values of the internuclear separation close to our case. This fact compelled us to resort to extrapolation. The normalized function $R_e(\bar{r})$ shown in the figure can be expressed by the following empirical formula, where r is in Angstrom units.

$$R_e(r) = 0.122\,(-1 + 1.807r) \text{ (atomic units)}. \qquad (9)$$

Table 1. Electronic Transition Moment for the β-band System of NO, Computed from data relating to the $\beta(5,0)$ band ($\bar{r}$ = 1.204 A)

p (mm Hg)	k (cm^{-1}) according to ref. 2	R_e (atomic units)	Remarks
4.00	2.24	0.115	Short wavelength band maximum
14.8	1.16	0.112	
50.0	0.582	0.109	
101	0.43	0.106	
4.00	2.50	0.117	Long wavelength band maximum
14.8	1.36	0.120	
50.0	0.86	0.109	
101	0.55	0.114	

Mulliken[10] has demonstrated that for parallel electronic resonance transitions (including the β-band system of NO) the electronic moment can readily be estimated by using a linear combination of atomic orbitals. This leads to the expression

$$R_e \simeq \frac{\sigma r_e}{2\sqrt{1 - \left|\int \varphi_A \varphi_B d\tau\right|^2}}, \qquad (10)$$

where φ_A and φ_B are atomic orbital functions. Remembering that the second term under the square root sign is small small compared to unity, and substituting numerical values into Eq. (10), one finally obtains $R_e \simeq 1.2$ atomic units, which agrees well with our results.

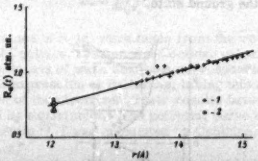

Electronic transition moment for β-band systems of NO as function of the internuclear separation. 1—values obtained from relative data[9] by chosing a suitable scaling factor; 2—absolute values obtained from reference 2.

Nicholls' work[11] is devoted to the experimental investigation of the dependence of the electronic transition $R_e(r)$ in diatomic molecules upon the internuclear separation. Nicholls' work briefly mentions that for γ-bands of NO the quantity $R_e(r)$ is practically independent of r. Thus, in reference 4 we considered it possible to characterize the probability of the given transition by means of the oscillator strength. However, the oscillator strength cannot in itself characterize the probability of the entire optical transition of band systems in those cases where R_e is strongly dependent upon r. In subsequent work by Robinson and Nicholls[9] it was disclosed that for the γ-bands of NO, such a strong dependence actually exists. For that reason we have also computed the electronic transition moments for the γ-band system of NO by means of Eq. (7). The results of these computations, based on Marmo's[2] experimental data and those of Mayence[3] for the region of both maxima of the $\gamma(1,0)$ and $\gamma(2,0)$ bands and the short wavelength maximum of the $\gamma(0,0)$ band, are listed in Table 2.

Table 2. Electronic Transition Moments for γ-band Systems of NO

Band	p (mm Hg)	l (cm)	k (cm^{-1})	R_e (atomic units)	Remarks
γ (2,0) ($\bar{r}$ = 1.162 A) Long wavelength maximum	4.0	4.7	7.9	0.138	Based on data from reference 2
	7.9	4.7	4.8	0.129	
	14.8	4.7	4.4	0.138	
	50.0	4.7	4.1	0.145	
	14.8	4.7	4.7	0.144	
γ (1,0) ($\bar{r}$ = 1.135 A) Long wavelength maximum	10	0.1	20.9	0.129	
	10	1.0	8.3	0.136	
	10	5.0	3.7	0.129	
	10	0.5	1.5	0.129	
γ (1,0) ($\bar{r}$ = 1.135 A) Short wavelength maximum	10	0.1	34.8	0.136	Based on data from reference 3
	10	1.0	15.0	0.153	
	10	5.0	6.2	0.143	
	14.8	4.7	8.9	0.166	
γ (0,0) ($\bar{r}$ = 1.108 A) No-Short wavelength maximum	14.8	4.7	4.8	0.154	Based on data from reference 2

REFERENCES

1. B. Kivel, H. Mayer, and H. Bethe. Ann. Phys. (N.Y.) **2**, 57 (1957).
2. F. F. Marmo. J. Opt. Soc. Am. **43**, 1186 (1953).
3. J. Mayence. Ann. phys. **7**, 453 (1952).
4. S. P. Erkovich. Opt. i Spektr. **6**, 297 (1959).
5. R. Schmid. Z. Physik **64**, 84 (1930); Z. Physik **49**, 428 (1928)
6. A. Lagerquist and E. Miescher. Helv. Phys. Acta **31**, 221 (1958).
7. J. R. Nielsen, V. Tornton, and E. B. Dale. Revs. Modern Phys. **16**, 307 (1944).
8. G. Herzberg. "Spectra of Diatomic Molecules." New York, 1950.
9. D. Robinson and R. W. Nicholls. Proc. Phys. Soc. **A71**, 957 (1958).
10. R. S. Mulliken. J. Chem. Phys. **7**, 14, 20 (1939).
11. R. W. Nicholls. Proc. Phys. Soc. **A69**, 741 (1956).

COEFFICIENT OF CONTINUOUS ABSORPTION OF RADIATION BY QUASI MOLECULES OF HYDROGEN

S. P. Erkovich

Received 28 March 1959

We obtain the dependence of the absorption coefficient of quasi molecules of hydrogen on temperature and the concentration of H atoms. It is shown that over a wide range of temperatures and pressures, quasi-molecular absorption plays an important role. A table is given from which k_λ may be evaluated under specific conditions.

It is well known that the hydrogen molecule, in passing from the excited $1s\sigma 2s\sigma\,^3\Sigma_u^+$ state to the unstable $1s\sigma 2p\sigma\,^3\Sigma_g^+$ state, emits a continuous spectrum extending from 1800 to 4000 A. In the process the H_2 molecule dissociates into two unexcited atoms of H. By a process inverse to the dissociation of an H_2 molecule with emission of a continuous spectrum, recombination can occur by collision of two H atoms which are following the potential curve of the unstable state. This reaction involves the absorption of light and the formation of a molecule of H_2 in the $^3\Sigma_g^+$ state. The yield coefficient for such continuous absorption is proportional to the number of atoms in the collision state.

In case of a dipole transition in the molecule the absorption coefficient may be defined according to the well-known relation[1]

$$k_\nu d\nu = \frac{8\pi^3 n\nu h\nu}{3hc}\,\frac{dD^2}{d\nu}\,d\nu, \tag{1}$$

where n is the concentration of absorbing molecules, ν is the frequency, and D the matrix element of the transition. For a transition in the hydrogen molecule from a vibrational level ν of the electronic state $^3\Sigma_g^+$ to the unstable state $^3\Sigma_u^+$ we may write:[2]

$$\frac{dD^2}{d\nu}\,d\nu = \left|\int \psi_\nu(r)\,\psi_E(r)\,dr \int M_e \psi_1(r, r')\,\psi_2(r, r')\,dr'\right|^2 \frac{dN}{d\nu}\,d\nu, \tag{2}$$

where M_e is the dipole moment of the electronic transition, $\psi_\nu(r)$ and $\psi_E(r)$ are the oscillatory wave functions of states $^3\Sigma_g^+$ and $^3\Sigma_u^+$, respectively, in which the higher state is characterized by the vibrational quantum number v and the lower by energy E from a continuum of values; $\psi_1(r, r')$ and $\psi_2(r, r')$ are the electron wave functions of states $^3\Sigma_g^+$ and $^3\Sigma_u^+$, depending on both the electron coordinates r′ and the internuclear distance r;

$$\frac{dN}{d\nu}\,d\nu = l\left(\frac{2\mu}{E}\right)^{\frac{1}{2}} d\nu$$

is the number of states in the frequency interval $d\nu$ of the continuous spectrum; E is the kinetic energy of the relative motion of the H atoms; and μ is the reduced mass. The quantity l denotes the average distance between hydrogen atoms in the absorbing gas. We are not interested in the numerical value of l, because it is eliminated by normalization of the transition probability in accordance with the sum rule.[3]

Substituting (2) into (1), we obtain

$$k_{\nu\nu}\,d\nu = \frac{8\pi^3 n\nu^2}{3hc}\left|\int \psi_\nu(r)\,\psi_E(r)\,dr \int M_e \psi_1(r, r')\,\psi_2(r, r')\,dr'\right|^2 l\left(\frac{2\mu}{E}\right)^{\frac{1}{2}} d\nu, \tag{3}$$

where $k_{\nu\nu}$ is the absorption coefficient associated with the formation of an H_2 molecule in electronic state $^3\Sigma_g^+$ and vibrational state v.

The number of quasi molecules n may be defined as the number of pairs of H atoms with parallel spins per unit volume which are found in a state of collision with an energy of relative motion between E and E + dE along the line of centers; i.e., assuming a Boltzman distribution of energy

$$n\,dE = \frac{3}{8}\,d_0^2\left(\frac{8\pi}{\mu kT}\right)^{\frac{1}{2}} n_H^2\, e^{-\frac{E}{kT}}\,h d\nu, \tag{4}$$

where d_0 is the gas kinetic collision diameter of the atoms, and n_H is the concentration of H atoms in the ground state.

Let us express E in terms of the frequency ν (see Fig. 1):

$$E = T_e + \omega_e'\left(v+\tfrac{1}{2}\right) - \omega_e' x_e'\left(v+\tfrac{1}{2}\right)^2 - h\nu - D, \tag{5}$$

where $\omega_e' = 2664.83\ \text{cm}^{-1}$, $T_e = 95938\ \text{cm}^{-1}$, and $\omega_e' x_e' = 71.65\ \text{cm}^{-1}$ are the vibrational constant, the electronic term, and the anharmonicity constant of the $^3\Sigma_g^+$ state; D = 4.4776 ev is the dissociation energy of the H_2 molecule from the ground state.

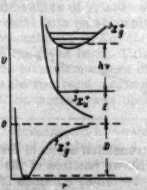

Fig. 1. Diagram showing the origin of the continuous absorption.

From Eqs. (3)-(5) we have

$$k_{\nu\nu} = \frac{4\pi^3 n\nu^2}{c}\,d_0^2\left(\frac{\pi}{kT}\right)^{\frac{1}{2}} n_H^2\, e^{\frac{h\nu}{kT}}\,F(\nu, v) \times \exp\left(-\frac{h\nu}{kT}\left[T_e - D + \omega_e'\left(v+\tfrac{1}{2}\right) - \omega_e' x_e'\left(v+\tfrac{1}{2}\right)^2\right]\right), \tag{6}$$

where for the sake of abbreviation we introduce the notation

$$F(\nu, v) = \frac{\nu l}{E^{\frac{1}{2}}}\left|\int \psi_\nu(r)\,\psi_E(r)\,dr \int M_e \psi_1(r, r')\,\psi_2(r, r')\,dr'\right|^2. \tag{7}$$

The total absorption coefficient at frequency ν will be equal to the sum of $k_{\nu\nu}$ over all vibrational states v with ν = const., i.e.,

$$k_\nu = \sum_v k_{\nu v} = \frac{4\pi^2\nu^2}{c} d_0^2 \left(\frac{\pi}{kT}\right)^{\frac{1}{2}} n_H^2 \frac{h\nu}{kT} \exp\left[-\frac{hc}{kT}(T_e - D)\right]$$

$$\times \sum_v F(\nu, v) \exp\left(-\frac{hc}{kT}\left[\omega_e'\left(v+\frac{1}{2}\right) - \omega_e' x_e'\left(v+\frac{1}{2}\right)^2\right]\right). \quad (8)$$

To calculate the double integral in (7) we make use of the repulsion method of Winans and Stueckelberg,[4] who replace the oscillatory wave function of a repulsion state by δ functions, which are different from zero only at the classical turning points. As shown by James and Coolidge,[5] the repulsion method gives very good results for the present transition. In this case

$$F(\nu, v) = \frac{\nu l}{E^{\frac{1}{2}}} R_e^2(r)\,\psi_v^2(r), \quad (9)$$

where the values r correspond to turning points for the given energy E, and

$$R_e(r) = \int M \psi_{1'}(r, r')\,\psi_n(r, r')\,dr'$$

is the matrix element of the dipole moment of the electron transition.

The vibrational wave functions $\psi_v(r)$ in the stable $^3\Sigma_g^+$ state of the molecule are calculated with the aid of the Morse potential functions

$$u(r) = D_e\{1 - \exp[-a(r - r_e)]\}^2, \quad (10)$$

where r_e = 0.9887 A is the equilibrium internuclear distance of the $^3\Sigma_g^+$ state, and the quantities a and D_e are connected with the constants of the molecule by the relations

$$a = \sqrt{\frac{8\pi^2\mu c\omega_e' x_e'}{h}}, \quad (11)$$

$$D_e = \frac{\omega_e'}{4\omega_e' x_e'}. \quad (12)$$

The values of $R_e(r)$ were taken from the work of James and Coolidge.[5] James and Coolidge calculated $R_e(r)$ with the aid of wave functions corresponding to the variational expression of Hylleraas, taking into account correlation of the electrons. Their results have been confirmed by experiment.[6] The potential curve of the repulsion state $^3\Sigma_u^+$ was calculated by Coolidge, James, and Present.[7]

The gas kinetic collision diameter d_0 of hydrogen atoms was defined in a quasi-classical approximation for which the potential curves of repulsion, as presented in reference 7, were approximated for large r by the expression (see Fig. 2)

$$u(r) = \frac{A}{r^8}, \quad (13)$$

where $A = 6.4 \times 10^{-36}$ erg cm^8.

The indicated approximation should hold for $r \gtrsim \sqrt{\pi A/h\nu}$ (see, for example, reference 8), which for velocities corresponding to the mean kinetic energy at temperatures of the order of $T = 10^3$–10^4°K gives $r \gtrsim$ 10–6 atomic units. As seen from Fig. 2, Eq. (13) is valid for internuclear distances between 2.5 and 4 atomic units. When $r > 4$ atomic units, (for which calculations were not performed in reference 7) and we have to deal with the interactions of identical atoms in different states (1s and 2p), with different parities and with orbital moments differing from unity, the interaction energy at large distances (in view of the presence of exchange degeneracy) will be determined by the nonzero off-diagonal matrix elements of the dipole moment for transitions between these states. In the first approximation of perturbation theory this gives (see, for example, reference 8)

$$u(r) \sim \frac{1}{r^6}. \quad (14)$$

i.e., Eq. (13) may also be used for $r > 4$ atomic units. The condition for the quasi-classical treatment $8\pi^3M^2vA/h^3 \gg 1$, where $M = 1.6734 \times 10^{-24}$ gm is the mass of the hydrogen atom, is fulfilled down to a very low velocity v of the order of 10^2 cm/sec.

Under these conditions, the effective collision diameter turns out to be

$$d_0^2 = \frac{16\pi^2 A}{h\nu}, \quad (15)$$

or, substituting the value of the mean relative velocity,

$$d_0^2 = \frac{A \cdot 4\pi^{3/2} M^{1/2}}{h\,(kT)^{1/2}}. \quad (16)$$

We note that the validity of (13) for U(r) and the fact that the coefficients of proportionality in (13) and (14) must be equal are also confirmed by the fact that the values of d_0 obtained from (15) coincide accurately (within 7%) with the optical diameter obtained from the collision broadening of the H_α line (1s – 2p transition), as defined by[9] the equation

$$d^2 = \frac{\pi e^2}{mv\nu} f, \quad (17)$$

where $f = 0.416$ is the oscillator strength of the H_α line.

To evaluate the role of quasi-molecular absorption it is useful to compare it with absorption by negative ions of hydrogen (see reference 10). Figure 3 shows curves of the ratio of our coefficient of quasi-molecular absorption $k(H_2)$ to the absorption coefficient of negative hydrogen $k(H^-)$ ions in hydrogen gas at thermodynamic equilibrium. As seen from these curves, quasi-molecular absorption plays an important role over a wide range of pressures and temperatures. Bearing in mind the practical significance of the absorption coefficient (calculation of the degree of blackness of gases in problems of radiative heat exchange, studies of the structure of the solar and stellar atmospheres, various gaseous discharge problems, etc.), we present a table of the function $F(\nu, v)$, making it possible to obtain $k(H_2)$ under specific conditions according to (8). It should be noted that to calculate $k(H_2)$ at high temperatures ($T > 6000$°K) it is necessary to extend the table of $F(\nu, v)$ to larger values of v.

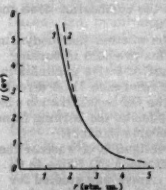

Fig. 2

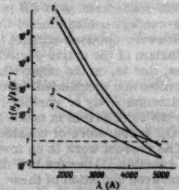

Fig. 3

Fig. 2. Repulsion potential. Curve 1—Coolidge, James, and Present;[7] curve 2—Eq. (13).

Fig. 3. Ratio of the quasi-molecular absorption coefficient to the coefficient of absorption by H^- ions. Curve 1—T = 2000°K, total pressure p = 0.1 atm; curve 2—T = 2000°K, p = 10 atm; curve 3—T = 6000°K, p = 0.1 atm; curve 4—T = 6000°K, p = 10 atm.

Table of the function $F(\nu, v) \cdot 10^8$ cm$^2 \cdot$ g$^{-1/2}$

ν(cm^{-1})	v = 0	1	2	3	ν(cm^{-1})	v = 0	1	2	3
$1.5 \cdot 10^3$	1.2	0.85	3.7	8.7	$3.8 \cdot 10^3$	25.8	2.2	11.8	8.9
$1.6 \cdot 10^3$	1.6	1.5	4.3	9.1	$3.9 \cdot 10^3$	22.8	5.0	12.9	7.0
$1.7 \cdot 10^3$	2.1	2.5	5.1	9.6	$4.0 \cdot 10^3$	19.1	9.7	13.1	4.6
$1.8 \cdot 10^3$	2.5	3.9	6.0	10.0	$4.1 \cdot 10^3$	14.9	13.9	12.3	2.1
$1.9 \cdot 10^3$	3.0	5.5	7.2	10.4	$4.2 \cdot 10^3$	10.8	17.0	9.2	0.3
$2.0 \cdot 10^3$	3.8	7.0	9.0	10.7	$4.3 \cdot 10^3$	7.2	19.4	4.0	0.0
$2.1 \cdot 10^3$	4.7	8.8	10.5	9.8	$4.4 \cdot 10^3$	4.8	20.8	0.8	3.8
$2.2 \cdot 10^3$	5.9	10.8	12.0	10.8	$4.5 \cdot 10^3$	3.2	21.1	0.0	7.4
$2.3 \cdot 10^3$	7.2	12.2	12.8	10.5	$4.6 \cdot 10^3$	2.0	20.5	0.8	9.8
$2.4 \cdot 10^3$	8.8	13.8	13.0	10.0	$4.7 \cdot 10^3$	1.1	18.4	4.9	10.7
$2.5 \cdot 10^3$	10.6	15.4	12.8	9.2	$4.8 \cdot 10^3$	0.5	14.0	9.0	10.0
$2.6 \cdot 10^3$	12.6	16.4	12.3	7.8	$4.9 \cdot 10^3$	0.2	9.8	12.2	8.3
$2.7 \cdot 10^3$	14.6	17.0	11.0	5.9	$5.0 \cdot 10^3$	0.08	6.4	15.3	5.2
$2.8 \cdot 10^3$	16.7	16.8	9.1	3.5	$5.1 \cdot 10^3$	0.0	3.9	13.2	0.4
$2.9 \cdot 10^3$	18.8	15.8	6.7	1.4	$5.2 \cdot 10^3$	0.0	2.2	19.1	0.0
$3.0 \cdot 10^3$	20.9	14.2	4.2	0.15	$5.3 \cdot 10^3$	0.0	1.1	17.9	0.5
$3.1 \cdot 10^3$	23.0	12.3	1.9	0.05	$5.4 \cdot 10^3$	—	0.4	14.6	3.0
$3.2 \cdot 10^3$	24.9	9.4	0.4	0.8	$5.5 \cdot 10^3$	—	0.05	10.6	6.4
$3.3 \cdot 10^3$	26.7	6.8	0.0	3.4	$5.6 \cdot 10^3$	—	0.0	6.7	9.7
$3.4 \cdot 10^3$	28.1	3.8	1.1	6.2	$5.7 \cdot 10^3$	—	0.0	3.9	11.1
$3.5 \cdot 10^3$	29.1	1.2	3.3	8.1	$5.8 \cdot 10^3$	—	—	1.7	9.9
$3.6 \cdot 10^3$	29.1	0.3	5.9	9.1	$5.9 \cdot 10^3$	—	—	0.4	6.8
$3.7 \cdot 10^3$	28.1	0.4	8.7	9.5	$6.0 \cdot 10^3$	—	—	0.0	2.0

REFERENCES

1. R. S. Mulliken. J. Chem. Phys. 7, 14 (1939).
2. E. Condon. Phys. Rev. 28, 1182 (1926); Phys. Rev. 32, 858 (1928).
3. G. Herzberg. "Spectra of Diatomic Molecules." New York, 1950.
4. J. G. Winans and E. C. Stueckelberg. Proc. Natl. Acad. Sci. 14, 867 (1928).
5. H. M. James and A. S. Coolidge. Phys. Rev. 55, 184 (1939).
6. A. S. Coolidge. Phys. Rev. 65, 236 (1944).
7. A. S. Coolidge, H. M. James, and R. D. Present. J. Chem. Phys. 4, 193 (1936).
8. L. D. Landau and E. M. Lifshitz. "Kvantovaya mekhanika." Moscow-Leningrad, 1948.
9. A. Unsöld. "Physik der Sternatmosphären." 2nd ed., 1955.
10. S. Chandrasekhar and F. Breen. Astrophys. J. 104, 430 (1936).

THE IMPORTANCE OF H_2O IN THE COMBUSTION OF CARBON MONOXIDE IN OXYGEN

R. B. Tagirov

Received 21 May 1959

The infrared radiation from a CO diffusion flame in O_2 was studied. It is shown that dissociated water molecules have an active part in the flame.

Research by Kondrat'ev and his pupils,[1,2] and by others,[3] was established that H_2O molecules have an active part in the combustion of CO in O_2 at low pressures. They are also important in the slow oxidation $CO + O_2$ outside the ignition region;[4] here, as in combustion inside the ignition region in low-pressure flames, the chain reaction occurs:

$$OH \xrightarrow{(+CO)} H \xrightarrow{(+O_2)} OH \xrightarrow{(+CO)} H \xrightarrow{(+O_2)}, \qquad (1)$$

in consequence of which thermodynamic equilibrium in the concentration of active particles should prevail. Reaction rate measurements support the conclusion that the hydoxyl radical and atomic H are active in the mechanism of slow oxidation only for CO; for low-pressure flames the conclusion is based on measurements of the absolute concentration of OH in the combustion zone and the percentage combustion of CO.

However opinions conflict on whether thermodynamic equilibrium of the active particles prevails in burning flames, that is, on the importance of active particles in the combustion mechanism (see reference 2). A direct experimental study of whether the OH concentration rises above the equilibrium in cases such as the burning flame, $CO + O_2$, is therefore of considerable interest.

The present work is an investigation of whether the chain reaction (1) occurs in a diffusion CO flame in O_2. The infrared radiation of these flames was studied for this purpose.

EXPERIMENTAL METHOD

An IKS-11 infrared spectrometer was used for the experiment. A spherical aluminized mirror was placed a distance equal to its radius of curvature behind the flame, which almost doubled its radiance. A flat burner was used to increase the radiating volume of the flame. Technical hydrogen, and CO obtained by the reaction of heated formic and sulfuric acids, were used as the fuel. The carbon monoxide was stored in a galvanized sheet gas-holder over water at a pressure of ~20 mm Hg. The flame temperature* was measured by reversal of the sodium doublet 5890/96 A.

*The temperature of a diffusion flame varies greatly with the height of the flame. We measured it at the top of the dark cone inside the mantel (T = 2800°K). The flame temperature at this height varies with the burner size and material and the fuel feed velocity.[5]

The temperatures of the CO and H_2 flames in O_2 were equalized by adjusting the fuel and oxygen feed rates. The gas feed was monitored with a flow meter.

EXPERIMENTAL DATA AND DISCUSSION

Ordinarily, the absolute values of the atom and radical concentrations in flames in equilibrium are measured to determine the ratio of their concentrations; to verify that the temperature and radiation have equilibrium values their adherence to the Boltzmann equation is examined. These questions, especially the first, cause great difficulties and introduce errors.

A simple and reliable method of determining the degree of dissociation of H_2O in a CO flame in O_2 is the comparison method; we used this for determining the CO_2 molecule excitation mechanism in flames,[7] with the infrared radiation from an H_2 flame in O_2 as the standard. The data in the literature indicate that the excitation of the vibrational-rotational levels of the ground state of H_2O [7,8] and OH [9,10] is thermal in nature in diffusion flames at atmospheric pressure. It follows from this that in H_2 and CO flames at equal temperatures in O_2 the relative concentrations of H_2O and OH can be expressed

through their relative infrared radiances. On the other hand there are indications[11] that in burning flames and also in low-pressure hydrogen flames,[1, 2] the OH radical concentration exceeds the equilibrium value. On this basis we can use the infrared emission spectrum of an H_2 diffusion flame in O_2 to establish the manner of formation of OH in the combustion zone. Since we were not interested in the absolute concentration of active particles but only the relative concentrations of OH and H_2O in different flames, we used as a criterion the ratio of the intensity of the OH line* $\nu = 2945\ cm^{-1}$ to that of the R-branch* of the H_2O band $\nu = 3755.8\ cm^{-1}$ (Fig. 1a, marked with crosses).

*Weaker OH lines from transitions between higher levels are superimposed on this line.

*In CO and hydrocarbon flame spectra the R-branch of the water band is free from superimposed bands of other particles. CO_2 bands are superimposed on other branches of the H_2O band, and this spectral region is strongly distorted by absorption in the LiF prism.

If we assume a chemical mechanism for OH formation in the combustion zone of an oxygen-hydrogen diffusion flame in agreement with reference 11, from the measurement (Fig. 1a) we obtain the following required criterion:

$$\frac{I_{OH}}{I_{H_2O}} \geq \frac{1}{230}. \qquad (2)$$

Figure 1b shows the same spectral region for a wet CO flame in O_2 in which there are an H_2O band and OH lines. From the data corresponding to this Figure we find:

$$\frac{I_{OH}}{I_{H_2O}} \simeq \frac{1}{10}. \qquad (3)$$

This value is two orders of magnitude greater than for the hydrogen flame. This indicates that the dissociation of H_2O in a CO flame cannot be caused by purely thermal factors.

The values that we obtained for ratios (2) and (3) are somewhat in error due to radiation from the outer layers of the flame in which the reaction is almost absent. To evaluate this error we determined the values of these ratios for flames of pre-mixed gases $H_2 + O_2$ and $CO + O_2$, in which the combustion is almost completed in the inner cones. We found:

$$\frac{I_{OH}}{I_{H_2O}} \simeq \frac{1}{120} \quad \text{for the } H_2 + O_2 \text{ flame;}$$

$$\frac{I_{OH}}{I_{H_2O}} \simeq \frac{1}{3} \quad \text{for the } CO + O_2 \text{ flame.}$$

Therefore I_{OH}/I_{H_2O} in the $CO + O_2$ flame is 40 times greater than in the $H_2 + O_2$ flame in this case. This indicates in the $CO + O_2$ flame the chemical mechanism of OH formation is considerably more important.

Figure 2 justifies using the criterion that we have chosen; it shows the intensity I (in arbitrary units) of CO_2, H_2O, and CO bands and OH lines at different heights, h, of the flame.

Within the limits of experimental error, the OH line intensity follows strictly the CO band intensity change and the positions of their maxima almost coincide. However,

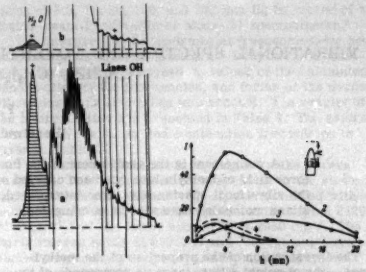

Fig. 1 Fig. 2

Fig. 1. H_2O band and OH lines in the spectra of (a) H_2 and (b) CO flames in O_2.
Fig. 2. Intensity of bands of CO (curve 1), CO_2 (curve 2), H_2O (curve 3) and OH lines (curve 4) in the spectrum of a CO flame in O_2, plotted against the height h (the OH line intensity is an approximate estimate.

the water band intensity reaches a considerably higher maximum than that of the other molecules.

The experimental data presented show that in wet $CO + O_2$ flames the H_2O molecules dissociate considerably and therefore must have an important part in the CO in O_2 combustion process.

Finally, the author thanks V. N. Kondrat'ev and V. V. Voevodskii for discussion of the work and valuable advice on preparing it for publication.

REFERENCES

1. V. N. Kondvat'ev. "Spektroskopicheskoe izuchenie khimicheskikh gazovykh reaktsii." (The Spectroscopic Study of Chemical Gas Reactions), Izd. Akad. Nauk SSSR, Moscow-Leningrad, 1944.
2. V. N. Kondrat'ev. "Kinetika khimicheskikh gazovykh reaktsii." (The Kinetics of Chemical Gas Reactions), Izd. Akad. Nauk SSSR, Moscow, 1958.
3. B. Lewis and G. Von Elbe. "Gorenie, plamya i vzryvy v gazakh." (Combustion, Flames, and Explosions of Gases), Izd. Inostrannoi Lit., Moscow, 1948.
4. V. I. Tsvetkova, V. V. Voevodskii, and N. M. Chirkov. Zhur. Fiz. Khim. 29, 380 (1955).
5. (Missing from Russian original.)
6. S. Sapega. Thesis, Kazan State University, 1958.
7. R. B. Tagirov. Opt. i Spektr. 6, 137 (1959).
8. A. Gaydon. "Spektroskopiya i Theoriya Goreniya." (Spectroscopy and Combustion Theory) Izd. Inostrannoi Lit., Moscow, 1950.
9. D. A. Dows, E. Whittle, and G. C. Pimentel. J. Chem. Phys. 23, 499 (1955).
10. J. A. A. Ketelaar, C. Haas, F. N. Hooge, and R. Brockhuijsen. Physica 21, 695 (1955).
11. W. S. Benedict, E. K. Plyler, and C. J. Hemphreys. J. Chem. Phys. 21, 398 (1953).

VIBRATIONAL SPECTRA AND POTENTIAL FUNCTIONS OF THE METHYLSILANES CH_3SiH_3, $(CH_3)_2SiH_2$, AND $(CH_3)_3SiH$

I. F. Kovalev

Received 11 July 1959

A refinement in the assignment of the fundamental frequencies and in the calculation of the force field of methylsilane has been carried out. The force coefficients have been evaluated, the vibrational spectra have been interpreted, and the frequencies of the dimethyl- and trimethylsilane molecules have also been computed.

The investigation of the properties of the methylsilanes— the simplest silicon-organic compounds of the series $(CH_3)_nSiH_{4-n}$ (n = 1-4)—offers considerable theoretical and practical interest. We were confronted with the problem of studying the force fields and the vibrational spectra of the molecules of these compounds. Earlier in the process of solving this problem, a calculation of the corresponding parameters for the molecules SiH_4 [1] and $(CH_3)_4Si$ [2] was carried out, and a first attempt at such a calculation for the CH_3SiH_3 [3] molecule was also made.* The experimental information accumulated up to the present time made it possible to introduce a number of refinements into the calculations for the CH_3SiH_3 molecule and to carry out corresponding studies of the compounds $(CH_3)_2SiH_2$ and $(CH_3)_3SiH$.

*References to works of other authors devoted to this question are given in references 1-3.

In the calculation of the force field, frequencies, and forms of the normal vibrations, the procedures of Vol'kenshtein, El'yashevich, and Stepanov[4] and of Mayants[5] were used. The computations were carried out simultaneously for the whole series of methylsilanes $(CH_3)_nSiH_{4-n}$, taking into account the results obtained earlier for ethane and disilane (see references in reference 3). The problem was solved with the "spectroscopic mass" of hydrogen.

To characterize the force fields of the four methylsilanes, 100 constants were chosen. The remaining coefficients, corresponding to the bonds and angles most distant from one another, were set equal to zero. The force constants $k_{\gamma\alpha}$, h_α, h_δ, h_γ, a, $l_{\alpha\alpha}$, $l_{\alpha\delta}$, a_δ, b_δ, $a_{\gamma\gamma}$, b_γ, $m_{\delta\gamma}$, $n_{\delta\gamma}$, $m_{\delta\varepsilon}$, $n_{\delta\varepsilon}$, $l^*_{\gamma\gamma}$, $l_{\gamma\varepsilon}$, k_ε, and b_ε* were taken to be respectively equal in magnitude for the entire series of molecules under study. Of these, the first 11 were derived from the results of the calculation for the C_2H_6 and Si_2H_6 molecules. In addition, we took $B_\delta = B_\gamma = B_\varepsilon$, $b_\gamma = b_\varepsilon$, $l_{\delta\delta} = l^*_{\gamma\gamma}$, and we also assumed that $l_{\delta\gamma}$ differs only slightly from the corresponding coefficient in disilane, that $l_{\beta\beta}$ differs only slightly from $l_{\alpha\beta}$, and $l_{\gamma\varepsilon}$ from $l_{\delta\gamma}$.

*We shall use the same designations as in references 2 and 3; the constant $l^*_{\gamma\gamma}$ refers to the interaction of angles γ having a side Si—C in common.

As a result, there were 63 experimental frequencies for finding 40 unknowns. The problem was solved according to the variation method, using values calculated according to Mayants' procedure[6] for the sensitivities of the frequencies to change in the force coefficients. The calculated values of the potential constants are presented in Table 1.

1. CALCULATION FOR METHYLSILANE

We have previously accomplished a first attempt at the calculation of the force field and the vibrational frequencies of the CH_3SiH_3 molecule.[3] In the present work,

Table 1. Dynamic Coefficients of the Methylsilanes (in 10^5 cm^{-2})

Coefficients \ Molecule	CH_3SiH_3	$(CH_3)_2SiH_2$	$(CH_3)_3SiH$	$(CH_3)_4Si$
K_Q	4.850	4.850	4.830	4.820
$k_{\gamma(1)}$(Si—H)	4.494	4.415	4.350	—
$k_{\gamma(2)}$(C—H)	5.050	5.050	5.050	5.050
k_α	—	0.856	0.856	0.856
k_β	0.690	0.690	0.680	0.675
k_γ	0.710	0.689	0.670	0.660
k_δ	0.752	0.770	—	—
k_ε	0.870	0.7905	0.8253	—
H_1	—	0.050	0.100	0.150
H_2	—0.008	—0.008	—0.008	—
h_α	0.070	0.070	0.070	0.070
h_δ	0.030	0.030	—	—
$A_1 - B_1$	—	—	0.300	0.300
$A_1 - B_2$	—	—	0.348	—
$A_2 - B_2$	—	0.300	—	—
$A_2 - B_3$	—	0.300	—	—
$A_1 - B_1$	—	0.346	0.348	—
$A_1 - B_3$	0.348	—	—	—
$A_2 - B_2$	0.370	0.320	0.270	0.225

Coefficients \ Molecule	CH_3SiH_3	$(CH_3)_2SiH_2$	$(CH_3)_3SiH$	$(CH_3)_4Si$
a	0.350	0.350	0.350	0.350
a_δ	0.220	0.220	—	—
b_δ	—0.030	—	—	—
a_γ	0.300	0.300	0.300	—
b_γ	—0.040	—0.040	—	—
b_ε	—	—0.040	—0.040	—
$l_{\alpha\alpha} = l_{\gamma\gamma}$	—0.035	—0.035	—0.035	—0.035
$l_{\alpha\beta}$	—0.045	—0.040	—0.040	—0.040
$l_{\beta\beta}$	—	—	0.040	0.081
$l_{\gamma\gamma}$	0.115	0.115	—	—
$l_{\beta\gamma}$	0.080	0.093	—	—
$l_{\gamma\delta}$	0.115	—	—	—
$l_{\gamma\varepsilon}$	—	0.093	0.093	—
$l^*_{\gamma\gamma}$	—	—0.0245	—0.0672	—
$m_{\beta\gamma}$	—	0.080	0.080	0.080
$n_{\beta\gamma}$	—	—0.010	—0.010	—0.010
$m_{\gamma\gamma}$	—0.023	—0.023	—0.023	—
$n_{\gamma\gamma}$	—0.010	—0.010	—0.010	—

*Corresponds to the interaction of angles γ having a side Si-H in common.

the coefficients of the potential function of methylsilane were refined in connection with the solution of the problem for the other molecules of the $(CH_3)_nSiH_{4-n}$ series, taking into account the new experimental data.[7] The equilibrium configuration of the molecule, the coordinate system adopted, the interaction coefficients in the general form, and other details of the calculation are presented in reference 3. The calculated frequencies of the vibrational spectrum, as well as corrections in the identification of the fundamental frequencies, are presented in Table 2.

Table 2. Fundamental Frequencies of the Vibrational Spectrum of the CH_3SiH_3 Molecule (in cm^{-1})

Symbols	Coordinates	Vibration type	Experimental frequency values: According to ref. 8	Experimental frequency values: According to ref. 7	Calculated frequency values
ν_1	$q_1^{(1)}$	A_1	—	2167	2147
ν_2	$\delta = -\gamma$		940—952 (v. s.)	940	946
ν_3	Q		686 701 (s.) 716	700	704
ν_4	$q_1^{(2)}$		2900	2927	2899
ν_5	$\alpha = -\beta$		1250 1268 (s.) 1282	1267	1267
ν_6	$q_1^{(1)}$	E	2130 (v. s.)	2167	2160
ν_7	α		1386—1464(w.)	1430	1434
ν_8	γ			540	547
ν_9	$q_1^{(2)}$		2966 (m.)	2983	2966
ν_{10}	δ		930 (s.)	980	934
ν_{11}	β		860—886 (s.)	870	872
ν_{12}	τ	A_2	—	—	183

Note. Symbols for the line intensities in infrared absorption spectra: v.w. – very weak, w. – weak, m. – medium, s. – strong, v.s. – very strong.

2. CALCULATION FOR DIMETHYLSILANE

1. The dimethylsilane molecule has the symmetry C_{2v}. The 27-term representation of this point group can be separated into irreducible representations according to the law

$$\Gamma = 9A_1 + 5A_2 + 7B_1 + 6B_2.$$

By the selection rules, vibrations of all four types are allowed in the Raman spectrum, and those of types A_1, B_1, and B_2 in the infrared spectrum.

We had at our disposal experimental data on only the infrared spectrum of $(CH_3)_2SiH_2$ gas, obtained at pressures of 13 and 740 mm Hg in a 5 cm gas cell with the help of a double beam Baird spectrophotometer,[8] and also at pressures of 2.5, 17, 50, 100, and 200 mm Hg by means of a double-beam Perkin-Elmer Model 21 spectrometer.[9]

Table 3. Interpretation of the Combination Frequencies and Overtones in the Infrared Absorption Spectra of Dimethylsilane (Frequencies in cm^{-1})

Frequency according to ref. 8*	Interpretation	Frequency according to ref. 8*	Interpretation
4575 (w.) 4400 (w.)	$\nu_4 + \nu_9 + \nu_{10}\,(B_1)$ $\nu_9 + \nu_{12}\,(B_2)$	1733 (v. w.) 1647 (v. w.)	$2\nu_{10}\,(A_1)$ $\nu_{10} + \nu_{12}\,(A_1)$
3870 (w.)	$\nu_{11} + \nu_{12}\,(B_1)$	1566	
3580 (v. w.)	$\nu_3 + \nu_{12}\,(B_1)$	1545 (v. w.)	$\nu_3 + \nu_5\,(A_1)$
3450 (v. w.)	$\nu_{10} + \nu_{11}\,(A_1)$	1522	
3180 (v. w.)	$\nu_3 + \nu_8\,(A_2)$	1400 (m.)	$\nu_3 + \nu_{10}\,(B_1)$
3060 (w.)**	$\nu_1 + \nu_{11}\,(B_1)$	1385	
2960 (w.)**	$\nu_7 + \nu_{12}\,(B_1)$	1190	
2670 (v. w.)	$\nu_{11} + \nu_{12}\,(A_1)$	1180 (v. w.)	$\nu_5 + \nu_8\,(A_2)$
2590 (v. w.)	$\nu_{10} + \nu_{11}\,(A_1)$	1171	
2295 (w.)	$\nu_1 + \nu_{11}\,(B_2)$	1148 1138 (w.) 1129	$\nu_3 + \nu_{12}\,(B_1)$
1966 (w.) 1912 (w.)**	$\nu_8 + \nu_{10}\,(B_2)$ $2\nu_8\,(A_1)$	1069— —1085 (w.)	$\nu_3 + \nu_{12}\,(B_1)$
1820 ** 1804 (w.) 1780	$\nu_3 + \nu_8\,(A_2)$		

*For the symbols of line intensities (in parentheses), see Table 2.
**Frequencies also recorded in reference 9.

In interpreting the fundamental frequencies, we used information on the band contours.[9] Data on the intensities, degrees of depolarization, values of the calculated sensitivities of the frequencies, and forms of the normal vibrations were also taken into account. The results of the interpretation are presented in Table 4. The assignment of the overtones and combination frequencies is given in Table 3.

In connection with the foregoing we make several remarks. The frequencies corresponding to the stretching vibrations ν(Si—H) and ν(C—H) are identified without particular difficulty. The former lie in the region 2120–2150 cm^{-1},[9,10] the latter around 2900–2980 cm^{-1}. The fairly intense bands at 650–680 and 706–748 cm^{-1} are assigned respectively to the A_1 and B_1 vibration types which are primarily associated with changes in the length of the Si—C band. Study of the alkyl- and alkylhalosilanes[3,9] shows that the stretching vibration of the Si—C type actually lies in the region under consideration. The frequency of this vibration goes down systematically on replacement of the methyl groups by ethyl groups.

The bands at 1380–1440, 1240–1270, and 820–880 cm^{-1} are characteristic of the methylsilanes. The assignment of the frequencies associated with the vibrations of the $=SiH_2$ group presents the greatest difficulty. We have identified the fairly characteristic frequency 946–972 cm^{-1} with the internal deformation vibration, the frequency 919 cm^{-1} with the rocking vibration within the C—Si—C plane, and the frequency 467 cm^{-1} perpendicular to it. The second has a contour of type A, and the third a contour of type C. Absorption is not observed for the $(CH_3)_4Si$ molecule in the regions under consideration. The twisting vibration of the $=SiH_2$ group is inactive in the infrared spectrum.

2. In the calculation for dimethylsilane, we have taken as natural vibrational coordinates (see Fig. 1): Q_1 (i = a, b), $q_i^{(1)}$ (i = 1, 2), $q_i^{(2)}$ (i = 3–8), δ, γ_{1a}, γ_{1b}, γ_{2a}, γ_{2b}, ε, α_{ij} (i, j = 3–8; $i \neq j$), β_i (i = 3–8). Torsional vibrations of the CH_3 groups (ν_{11} and ν_{12} in Table 4) were not considered. Among the angular coordinates there were 3 additional conditions:

$$\gamma_{1a} + \gamma_{1b} + \gamma_{2a} + \gamma_{2b} + \delta + \varepsilon = 0,$$
$$\alpha_{34} + \alpha_{45} + \alpha_{53} + \beta_3 + \beta_4 + \beta_5 = 0,$$
$$\alpha_{67} + \alpha_{78} + \alpha_{86} + \beta_6 + \beta_7 + \beta_8 = 0.$$

The following geometrical parameters were taken for the calculation:

r (Si—C) = 1.86 A,
r (C—H) = 1.09 A,
r (Si—H) = 1.48 A [11],

and the angles were assumed to be tetrahedral.

The calculated values of the frequencies and the forms of the normal vibrations are presented in Table 4.

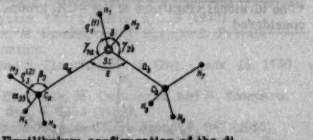

Fig. 1. Equilibrium configuration of the dimethylsilane molecule.

3. CALCULATION FOR TRIMETHYLSILANE

1. The trimethylsilane molecule has three Si—C bonds and belongs to the point group C_{3v}. The 36 term

Table 4. Vibrational Spectrum of Dimethylsilane (Frequencies in cm^{-1})

Symbols	Coordinates	Vibration type	Experimental frequency values: according to ref. 8*	according to ref. 9*	Calculated frequency values	Forms of the vibrations: $q^{(1)}$	Q	$q_1^{(2)}$	$q_2^{(2)}$	δ	τ	α_1	α_2	β_1
ν_1	$q^{(1)}$		2120 (s.)	2145 (s.)	2132	1	−0.026	−0.005	0.002	0.001	−0.013	0.010	−0.009	−0.013
ν_2	Q		660—680 (s.)	650 (s.)	658	0.008	1	−0.001	0.001	0.383	−0.024	−0.078	0.057	−0.345
ν_3	$q_1^{(2)}$		2966 (s.)	2920—	2987	0.006	−0.001	1	−0.705	−0.002	0.044	0.072	−0.051	0.057
ν_4	$q_2^{(2)}$		2900 (s.)	—2980 (m.)	2899	0.002	−0.059	0.706	1	0.001	−0.001	−0.028	−0.039	0.039
ν_5	$\delta = -\tau$	A_1	946—972 (v. s.)	961 (v. s.)	949	−0.006	0.035	0.007	−0.010	1	−0.467	0.113	0.015	0.073
ν_6	$\tau = -\delta$		—	—	227	−0.106	−0.025	−0.037	0.038	0.048	1	−0.197	0.050	−0.287
ν_7	$\alpha_1 = -\beta_1$		1434 (s.)	1380—1440 (m.)	1432	−0.006	−0.004	0.029	−0.021	−0.011	0.024	1	−0.701	−0.174
ν_8	$\alpha_2 = -\beta_2$		1261 (s.)	1260 (s.)	1266	0.004	0.142	−0.026	−0.036	−0.088	0.044	0.897	1	−0.991
ν_9	$\beta_1 = -\beta_1$		860—881	855 (s.)	882	0.009	0.101	0.068	−0.041	−0.333	0.290	0.300	−0.326	1
ν_{10}	Q		706—748 (s.)	730 (s.)	724	—	1	0.031	0.008	—	−0.509	−0.022	0.148	0.238
ν_{11}	$q_1^{(2)}$		2966 (s.)	2920—	2967	—	0.004	1	−0.714	—	0.008	−0.026	−0.675	−0.079
ν_{12}	$q_2^{(2)}$		2900 (s.)	—2980	2896	—	−0.060	0.712	1	—	−0.001	−0.043	−0.027	0.040
ν_{13}	τ	B_1	909 919 931 (v. s.)	**	915	—	−0.073	0.021	−0.006	—	1	−0.200	0.020	0.431
ν_{14}	$\alpha_2 = -\beta_1$		1250 1261 1273 (s.)	**	1268	—	0.191	−0.038	−0.052	—	0.193	1.447	1	−1.415
ν_{15}	$\alpha_1 = -\beta_1$		1434 (s.)	1380—1440	1432	—	−0.008	−0.041	0.029	—	−0.041	1	−1.437	0.253
ν_{16}	$\beta_2 = -\beta_1$		849—855 (s.)	855	841	—	−0.141	0.073	−0.064	—	−0.799	−0.269	0.555	1
ν_{17}	$q_1^{(2)}$		—	—	2967	—	—	1	—	—	−0.066	−0.072	—	−0.081
ν_{18}	τ		—	—	760	—	—	0.034	—	—	1	−0.147	—	−0.336
ν_{19}	α_1	A_2	—	—	1433	—	—	−0.029	—	—	0.042	1	—	−0.237
ν_{20}	β_2		—	—	857	—	—	−0.048	—	—	0.379	0.287	—	1
ν_{21}	τ		—	—	—	—	—	—	—	—	—	—	—	—
ν_{22}	$q^{(1)}$		2120 (s.)	2142 (s.)	2138	1	—	0.010	—	—	−0.022	0.023	—	−0.040
ν_{23}	$q_1^{(2)}$		2966 (s.)	2970 (m.)	2967	−0.010	—	1	—	—	−0.061	−0.072	—	−0.079
ν_{24}	τ		—	467 (m.)	469	−0.109	—	0.012	—	—	1	−0.065	—	−0.128
ν_{25}	α_1	B_2	1420 1434 1443 (m.)	**	1433	−0.009	—	−0.029	—	—	0.028	1	—	−0.243
ν_{26}	β_2		860 868 881 (v. s.)	**	868	−0.016	—	−0.048	—	—	0.198	0.303	—	1
ν_{27}	τ		—	—	—	—	—	—	—	—	—	—	—	—

*For the symbols of line intensities (in parentheses), see Table 2.
**P, Q, and R branches.

representation can be separated into the following irreducible representations:

$$\Gamma = 8A_1 + 4A_2 + 12E.$$

Vibrations of type A_2 are forbidden both in the infrared and in the Raman spectra. Vibrations of types A_1 and E are allowed in both spectra. We had at our disposal the experimental infrared absorption curves[8] and the frequencies determined from Raman spectra.[12] The assignment of the fundamental frequencies is presented in Table 5, and that of the overtones and combination frequencies observed in the infrared spectrum in Table 6. The raman frequency 600 (5) cm^{-1} is possibly the difference frequency $\nu_2 + \nu_{12} - \nu_{12}$. The ratio of the visually determined values for the intensities of the lines $\nu_2 + \nu_{12} - \nu_{12}$ and ν_2 equals 0.25. The Boltzmann factor $e^{-hc\nu_{12}/kT}$ for $\nu_{12} = 160$ cm^{-1} and T = 300°K equals 0.17.

2. The equilibrium configuration of the trimethylsilane molecule is schematically represented in Fig. 2. Thirty-seven natural coordinates were introduced:*

*The torsional vibrations of the $-CH_3$ groups were not considered.

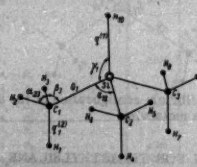

Fig. 2. Equilibrium configuration of the trimethylsilane molecule.

$q^{(1)}$, Q_i (i = 1-3), $q_i^{(2)}$ (i = 1-9), ε_{ij} (i, j = 1-3; $i \neq j$), α_{ij} (i, j = 1-9; $i \neq j$), γ_i (i = 1-3), β_i (i = 1-9).

We took as geometrical parameters[11] r(Si—C) = 1.873 A, r(Si—H) = 1.48 A, r(C—H) = 1.09 A; the angles

Table 5. Interpretation of the Vibrational Spectrum of the $(CH_3)_2SiH$ Molecule (Frequencies in cm^{-1})

Symbols	Coordinates*	Vibration type	Experimental frequency values: Ram.** according to ref. 12	IR** according to ref. 8	Calculated frequency values
ν_1	$q^{(1)}$		2118 (10)	2110 (s.)	2118
ν_2	Q (+)		623 (20)	—	629
ν_3	$q_1^{(2)}$ (−)		2967 (10)	2970 (s.)	2968
ν_4	$q_2^{(2)}$ (+)		2902 (10)	2900 (s.)	2898
ν_5	$\delta = -\tau$	A_1	219 (10)	—	225
ν_6	$\alpha_1 = -\beta_1$ (−)		1414	1426	1425
ν_7	$\alpha_2 = -\beta_1$ (+)		1258	1257—1269	1280
ν_8	$\beta_1 = -\beta_1$		—	855—870	874
ν_9	$q_1^{(2)}$ (−)		—	—	2966
ν_{20}	α_1 (−)	A_2	—	—	1422
ν_{21}	β_1		—	—	835
ν_{22}	τ		—	—	~160***
ν_{23}	Q (−)		718 (8)	707—718 (s.)	714
ν_{24}	$q_1^{(2)}$ (−)		2967 (10)	2970 (s.)	2967
ν_{25}	$q_2^{(2)}$ (−)		2967 (10)	2970 (s.)	2967
ν_{26}	$q_3^{(2)}$ (+)		2902 (10)	2900 (s.)	2899
ν_{27}	τ		254 (1)	—	244
ν_{28}	$\alpha_1 = -\beta_1$ (−)	E	1414	1426 (s.)	1426
ν_{29}	α_2^1 (−)		1414	1426 (s.)	1423
ν_{30}	$\alpha_2^2 = -\beta_1$ (+)		1258	1257—1269 (v. s.)	1247
ν_{31}	τ		908 (1)	902—910 (v. s.)	914
ν_{32}	β_2^2			855—870 (s.)	872
ν_{33}	$\beta_2^1 = -\beta_1$		839 (1)	839 (s.)	835
ν_{34}	τ		—	—	~160***

*The sign "+" denotes symmetrical vibrations, "−" asymmetrical.
**Ram.—Raman spectrum, IR—infrared absorption spectrum (intensities in parentheses).
***Estimated by extrapolation.

Table 6. Interpretation of the Overtones and Combination Frequencies in the Infrared Absorption Spectrum of the $(CH_3)_3SiH$ Molecule (Frequencies in cm^{-1})

Frequency*	Interpretation	Frequency*	Interpretation
4600 (v. w.)	$\nu_3+\nu_5+\nu_{15}$ (E)	1795 (w.)	$2\nu_{11}$ (A_1+E)
4400 (v. w.)	$\nu_3+\nu_{19}$ (E)	1716 (w.)	$2\nu_9$ (A_1)
3870 (v. w.)	$\nu_2+\nu_{19}$ (E), $\nu_3+\nu_{21}$ (E)	1587 (v. w.)	$\nu_3+\nu_{19}$ (E)
3800 (v. w.)	$\nu_4+\nu_{15}$ (E)	1514 (v. w.)	$\nu_7+\nu_{17}$ (E)
3180 (v. w.)	$\nu_3+\nu_{15}$ (E)	1458 (w.)	$\nu_3+\nu_{20}$ (E)
3100 (w.)	$\nu_3+\nu_{18}$ (E)	1332 (w.)	$\nu_3+\nu_{18}$ (E)
2870 (v. w.)	$\nu_{16}+\nu_{20}$ (A_1+E)	1144	
2500 (v. w.)	$2\nu_{20}$ (A_1+E)	1120 (w.)	$\nu_3+\nu_1$ (E)
1955 (w.)	$\nu_{18}+\nu_{20}$ (A_1+E)	1120	
1862 (w.)	$\nu_3+\nu_7$ (A_1)	1075 (w.)	$\nu_3+\nu_{16}$ (E)

*For the symbols of line intensities (in parentheses), see Table 2.

were assumed to be tetrahedral.

By taking into account four additional conditions for the angles, there were obtained 3 secular equations—of the 8th (the A_1 vibrations), the 3rd (A_2 vibrations), and the 11th (E vibrations) orders.

In the calculation of the frequencies, the secular equations were solved by the method of progressive diagonalization. The results are presented in Table 5.

4. DISCUSSION OF THE RESULTS

Comparison of the calculated and experimental vibrational spectra and analysis of the secular equations and of the results of the calculation have made it possible to draw the following conclusions:

1. The systems of dynamic coefficients obtained give a satisfactory description of the real distribution of forces within the $(CH_3)_nSiH_{4-n}$ molecules. The values of the calculated frequencies agree well with the experimental values.

2. Comparison of the force fields of the molecules under consideration allows us to note the presence of definite regularities in the changes in the values of a number of coefficients during the progressive transition from methylsilane to tetramethylsilane. Thus the value of the diagonal coefficient K_Q, corresponding to stretching of the Si—C bond, diminishes in the ratio 1:0.959:0.955: 0.953. A particularly sharp drop is noted in going from CH_3SiH_3 (one Si—C bond) to $(CH_3)_2SiH_2$ (two Si—C bonds). The coefficient $k_\chi(1)$ (Si—H) changes smoothly in the ratio 1:0.982:0.968. The values of k_α (H—C—H) and k_β (H—C—Si) also fall off systematically. The stiffness of the corresponding bonds and angles diminishes somewhat. On the other hand, the values of the diagonal coefficients k_δ(H—Si—H) and k_γ (H—Si—C) systematically increase in the same molecular sequence. The same may be said of some nondiagonal interaction constants: $A_\beta - B_\alpha$ (Si—C, H—C—H, H—C—Si) diminishes in the ratio 1:0.865:0.730: 0.608, while the quantity H_β (Si—C, Si—C) increases as 1:2:3 in the transition

$$(CH_3)_2SiH_2 \rightarrow (CH_3)_3SiH \rightarrow (CH_3)_4Si$$

3. The field of the CH_3 group changes in going from the saturated hydrocarbons to the methylsilanes.

4. The ν(Si—H) frequencies depend strongly only on the parameters $k_\chi(1)$ and h_δ; they depend slightly on H_γ, b_ε, a_γ, and b_γ, and are practically independent of the other parameters. The corresponding vibrations are fairly characteristic—the other bonds and angles change (relatively) by 3-4% at most.

5. In the calculation, only two values for C—H frequencies were obtained. These frequencies depend, for practical purposes, only on the parameters $k_\chi(2)$, h_α, and a. The corresponding vibrations are associated predominantly with stretching of the C—H bond. The changes in the H—C—H and H—C—Si angles amount to 6-8%, the changes in the Si—C bond to 5-6%.

6. The stretching frequencies ν(Si—C) correspond to stretching of the Si—C bond and to deformation of the angles (particularly H—Si—H and H—C—Si).

7. The results of the study of dimethylsilane show that (a) in the vibration ν_9, it is mainly the H—Si—H, C—Si—C, and H—Si—C angles which change. The H—C—H and H—C—Si angles change within the limits of 7-11%; (b) the asymmetrical deformation bands in the region of 1430 cm^{-1} are associated with changes in the H—C—H and H—C—Si angles; the symmetrical bands around 1260 cm^{-1} with changes in the same angles, the Si—C bond, and the H—Si—C angle; (c) the external deformation frequency of the $-CH_3$ group pertains to vibrations associated with changes in all the angles and the length of the Si—C bond; (d) the internal frequencies of the $=SiH_2$ group are associated with deformation of the angles and stretching of the Si—H bond.

8. From consideration of the secular equations for trimethylsilane it follows that: (a) the symmetrical and unsymmetrical normal vibrations associated with C—H stretching and deformation of the H—C—H angles ($\nu_5 - \nu_4$, $\nu_8 - \nu_7$, $\nu_{14} - \nu_{13}$, $\nu_{12} - \nu_{20}$) interact strongly, as do the vibrations pertaining to changes in the H—C—H and H—C—Si angles ($\nu_5 - \nu_3$, $\nu_7 - \nu_6$, $\nu_{12} - \nu_{23}$, $\nu_{19} - \nu_{22}$, $\nu_{20} - \nu_{22}$); (b) the interactions of the ν(C—H) vibrations with ν(H—C—H) and ν(H—C—Si) are significant ($\nu_5 - \nu_3$, $\nu_5 - \nu_2$, $\nu_4 - \nu_3$, $\nu_{14} - \nu_{13}$, $\nu_{14} - \nu_{23}$, $\nu_{13} - \nu_{22}$, $\nu_{13} - \nu_{23}$, $\nu_{12} - \nu_{13}$), and also those of the ν(C—Si—C) [or ν(H—Si—C)] vibrations with ν(H—C—Si) ($\nu_5 - \nu_3$, $\nu_{17} - \nu_{22}$, $\nu_{21} - \nu_{22}$); (c) the ν(Si—C) vibration interacts predominantly with ν(H—C—Si) ($\nu_1 - \nu_2$, $\nu_{15} - \nu_{22}$).

The author expresses his gratitude to M. M. Sushchinskii for his interest in the work, and also thanks D. Marais (Union of South Africa), M. Randič (Yugoslavia), and N. Sheppard (England) for the communication of experimental data on the spectra of the CH_3SiH_3 molecule in advance of publication.

REFERENCES

1. I. F. Kovalev. Opt. i Spektr. 2, 310 (1957); Fiz. Sbornik, L'vovsk. Gosudarst. Univ. 1, 304 (1957).
2. I. F. Kovalev. Opt. i Spektr. 6, 694 (1959).
3. I. F. Kovalev. Opt. i Spektr. 4, 560 (1958).
4. M. V. Vol'kenshtein, M. A. El'yashevich, and B. I. Stepanov. "Kolebaniya molekul." (Molecular Vibrations), Vol. 1. Gosudarst. Izd. Tekh.-Teoret. Lit., Moscow-Leningrad, 1949.
5. L. S. Mayants. Trudy Fiz. Inst. Akad. Nauk SSSR 5, 65 (1950); Doklady Akad. Nauk SSSR 89, 423 (1953).
6. L. S. Mayants. Opt. i Spektr. 5, 378 (1958).
7. D. Marais, M. Randič, and N. Sheppard. Private communication.
8. S. Kaye and S. Tannenbaum. J. Org. Chem. 18, 1750 (1953).
9. E. A. V. Ebsworth, M. Onyszchuk, and N. Sheppard. J. Chem. Soc. 4, 1453 (1958).
10. H. Westermark. Acta Chem. Scand. 9, 947 (1955).
11. A. C. Bond and L. O. Brockway. J. Am. Chem. Soc. 76, 3312 (1954).
12. V. A. Kolesova, E. V. Kukharskaya, and D. N. Andreev. Izvest. Akad. Nauk SSSR, Ser. Khim. 3, 294 (1953).

THE RAMAN SPECTRA OF THE STEREOISOMERS OF 1,2-DIALKYL CYCLOPENTANES

V. T. Aleksanyan, Kh. E. Sterin, A. A. Mel'nikov, and A. F. Plate

Received 14 May 1959

The Raman spectra of three 1,2-dialkyl cyclopentanes are investigated. It is shown that in the spectra of the cis- and trans-isomers it is possible to distinguish a group of characteristic indications, permitting a reliable identification of the stereoisomers. On the basis of the experimental results the trans-configuration is assigned to all of the low boiling isomers investigated, and the cis-structure to the high boiling ones.

In the synthesis of dialkyl cyclanes an important and very difficult problem consists in the establishment of the geometric configuration of their stereoisomers. Generally, in the determination of stereoisomers one is guided by the Auvers-Skit rules, according to which the trans-configuration is attributed to the stereoisomer with the lower constants (boilint point, specific gravity, refractive index). Since currently available data show that this rule is not valid in a series of cases, it is desirable to find other methods of fixing the geometric configuration of the steroisomers.

It is well known that the vibrational spectra of stereoisomers differ markedly from one another. However, the available data show a significant degree of random character and concern chiefly one, or in the best cast two, pairs of stereoisomers of one of the series of dialkyl cyclanes.

Not long ago two of us succeeded in showing in the example of a sufficiently long series of stereoisomers of 1,2- and 1,4-dialkyl cyclohexanes how both cis- and trans-forms of each series have in their Raman spectra a set of characteristic lines, which allow a confident determination of the stereoisomers of new members of the series indicated.[1]

The present work concerns an investigation, from the same point of view, of the Raman spectra of another series of dialkyl cyclanes—1,2-dialkyl cyclopentanes: 1-ethyl-2-n-propyl cyclopentane, 1-ethyl-2-n-butyl cyclopentane, and 1,2-di-n-butyl cyclopentane.[2]

The knowledge of the spectra of high boiling point cyclopentane hydrocarbons also has a practical interest. It is important from the viewpoint of further development of spectral methods of determining the hydrocarbon composition of the ligroin-kerosene fraction. In this range the spectra of cyclopentane hydrocarbons have been studied only to a small extent. Indeed, in this series, for example, for the composition $C_{10}H_{20}$-$C_{15}H_{30}$, the literature contains work on the spectra of only 13 hydrocarbons, and of this number only two are 1,2-dialkyl cyclopentanes. Thus, the present investigation fills this gap to a notable degree.

The method of obtaining and measuring the spectra has been described earlier.[3] Below are given the frequencies (in cm^{-1}), the line intensities, and characteristics (in brackets): b—broad, bkgd—background, d—double, sh—sharp; and also their physical constants (boiling point T_b in °C for a pressure of 30 mm Hg, refractive index n_D^{20}, density d_4^{20}, the calculated and experimentally determined molar refraction MR_D).

Cis-1-ethyl-2-n-propyl cyclopentane: T_b, 77.4°C; n_D^{20}, 1.4391; d_4^{20}, 0.8008; found MR_D, 46.08; calculated for $C_{10}H_{20}MR_D$, 46.18. Δν: 287 (1), 310 (19, b), 342 (2), 376 (5), 401 (7), 437 (4), 476 (3), 500 (2, b), 705 (1), 729 (3), 763 (6), 813 (1), 823 (10, b), 866 (2), 893 (27), 929 (5), 950 (7), 988 (6, b), 1014 (10, b, bkgd), 1048 (21), 1076 (6), 1094 (12), 1117 (6), 1146 (8), 1189 (7), 1231 (4), 1248 (6), 1272 (3, b), 1295 (11), 1319 (2, b), 1363 (6), 1448 (68), 2860 (230, b), 2872 (230, b), 2902 (150, b, bkgd, d), 2937 (280, bkgd), 2962 (240).

Trans-1-ethyl-2-n-propyl cyclopentane: T_b, 72.9°; n_D^{20}, 1.4337; d_4^{20}, 0.7898; found MR_D, 46.22; calculated for $C_{10}H_{20}MR_D$, 46.18. Δν: 210 (2, b), 303 (18), 320 (6, b), 368 (1), 402 (2), 425 (4), 456 (7), 491 (8), 563 (2), 615 (3, b), 740 (4), 767 (5), 807 (6, b), 845 (7, b), 889 (5, bkgd), 910 (30), 945 (6), 1007 (10), 1030 (17), 1042 (15, b), 1077 (6, bkgd), 1093 (12), 1135 (10, b), 1190 (7), 1228 (4), 1252 (10, b), 1295 (10, b), 1347 (10, b), 1446 (54, b), 2843 (200, b), 2855 (200, b), 2874 (250), 2907 (230, d), 2934 (230), 2960 (210).

Cis-1-ethyl-2-n-butyl cyclopentane: T_b, 95.3°; n_D^{20}, 1.4426; d_4^{20}, 0.8054; found MR_D, 50.75; calculated for $C_{11}H_{22}MR_D$, 50.80. Δν: 271 (2, bkgd), 288 (12, b), 321 (2, b, bkgd), 328 (1), 375 (1), 400 (8), 423 (3, b), 440 (2), 488 (2, b), 520 (1, b), 645 (1, b, bkgd), 720 (2, b), 765 (6), 793 (6), 820 (5, b, bkgd, d), 838 (5, b, bkgd), 871 (6), 891 (19, b, d), 911 (5), 935 (4), 953 (6), 972 (1), 989 (3), 1014 (6), 1043 (5, bkgd), 1056 (14), 1082 (11), 1097 (11), 1117 (10), 1145 (11), 1188 (11, b), 1215 (2), 1243 (4), 1260 (4), 1289 (8), 1298 (12, b), 1321 (3, b, bkgd), 1365 (6), 1437 (52), 1447 (43), 1459 (15, bkgd), 2856 (230, b), 2870 (260), 2891 (220, bkgd), 2906 (220, b, bkgd), 2934 (260), 2960 (220, b).

Trans-1-ethyl-2-n-butyl cyclopentane: T_b, 91.0°; n_D^{20}, 1.4376; d_4^{20}, 0.7950; found MR_D, 50.90; calculated for $C_{11}H_{22}MR_D$, 50.80. Δν: 255 (3), 286 (13, b), 312 (2), 357 (2), 370 (1), 400 (6, b), 414 (2, b, bkgd), 425 (4, b), 454 (2), 472 (5), 499 (5), 564 (1), 609 (2), 625 (1), 728 (1), 763 (8), 812 (5, b), 868 (2), 888 (5, bkgd), 898 (15), 912 (14), 946 (6), 967 (2), 999 (3, bkgd), 1013 (10), 1037 (11), 1058 (13), 1092 (18, b, d), 1133 (16, b), 1141 (16, b), 1175 (10), 1186 (12), 1218 (2), 1242 (2), 1280 (4, b), 1301 (11, b), 1348 (8), 1446 (66, b), 2852 (170), 2871 (230), 2904 (200, b), 2933 (210), 2959 (200).

Cis-1,2-di-n-butyl cyclopentane: T_b, 125.4°; n_D^{20}, 1.4467; d_4^{20}, 0.8111; found MR_D, 60.03; calculated for $C_{13}H_{26}MR_D$, 60.08. Δν: 225 (3, b, bkgd), 238 (4, b, bkgd), 247 (4, b, bkgd), 278 (5, b, bkgd), 310 (6, b, bkgd), 371 (1, b), 393 (0), 417 (2, b), 478 (1, b), 533 (1, b), 571 (0), 594 (0), 671 (1), 726 (2, b), 777 (5, b), 823 (3, b, bkgd), 836 (7, b), 871 (10, bkgd), 882 (17), 894 (21), 917 (8), 927 (4), 956 (3, d), 972 (7), 1009 (4, b), 1026 (8), 1060 (17), 1085 (14), 1103 (12), 1120 (10), 1144 (11), 1182 (6, b), 1207 (2, b), 1223 (2, b), 1246 (3, b, bkgd), 1267 (1, bkgd), 1301 (21), 1339 (4), 1438 (60), 1450 (60), 1476 (22, bkgd), 2852 (250, bkgd), 2867 (240, bkgd), 2888 (270, bkgd), 2912 (200, bkgd), 2935 (230), 2959 (190).

Trans-1,2-di-n-butyl cyclopentane: T_b, 122.6°; n_D^{20}, 1.4427; d_4^{20}, 0.8028; found MR_D, 60.18; calculated for $C_{13}H_{26}MR_D$, 60.08. Δν: 232 (3, b), 244 (2, b), 266 (3), 288 (4, b), 326 (2), 345 (1), 391 (2), 417 (2), 445 (1), 471 (2), 492 (2), 524 (1), 566 (0), 613 (2, b), 728 (2), 776 (8), 798 (1, bkgd), 817 (4), 869 (6, d), 885 (5, bkgd), 894 (25,

sh), 919 (6), 958 (5), 969 (4), 1000 (4), 1017 (3), 1033 (6), 1058 (13), 1084 (11), 1098 (10, b), 1136 (12, b, d), 1176 (7, d), 1207 (3), 1226 (3), 1249 (2), 1279 (5, bkgd), 1300 (22), 1342 (9), 1435 (52), 1449 (44), 1465 (20, bkgd), 2845 (220), 2856 (240), 2870 (210), 2895 (230), 2914 (210), 2938 (180), 2960 (200).

Analysis of the results of the experiment shows that in the transition from the simplest representatives of the investigated series to 1-ethyl-2-n-butyl and 1,2-di-n-butyl cyclopentane the spectral lines grow broad and diffuse; and their intensity, particularly in the region 700-800 cm^{-1}, decreases strongly. In essence in the spectral region indicated, which is most frequently used for analytical purposes, there are practically no suitable bands if we do not consider the weak lines in the region 300-350 cm^{-1}, having a limited analytical application. Simultaneously with the decrease of line intensity in the spectra of the investigated compounds with an increase in molecular weight there is observed a general increase of the background. These particulars were also observed by us in the Raman spectra of other homologs of cyclopentane with sufficiently high molecular weight, and particularly in sec-butyl cyclopentane and 2-cyclopentyl octane.[4]

From this it is possible to conclude that for complicated molecules the difference in the spectra of hydrocarbons of different structure (among them the differing cis- and trans-configurations of bonds relative to the naphthene ring) substantially decreases.

In the examination of the experimental results we used the same method as for the investigation of the series of 1,2- and 1,4-dialkyl cyclohexanes,[1] i.e., we obtained the spectra of the stereoisomers with the spectra of cis- and trans- 1,2-dimethyl cyclopentane, the configuration of which is securely established.*

*In the analysis of the experimental data obtained in the present work we also employed the spectra of cis- and trans-1-methyl-2-ethyl cyclopentane, obtained earlier by two of us.[3]

A comparison of the spectra of low and high-boiling preparations of each pair of stereoisomers shows that they all differ notably from one another. However, these differing appearances as a rule are not constant and frequently change on going from one pair of stereoisomers to another.

It is more or less possible to pick out a certain group of indications, present in the spectra of all six low-boiling stereoisomers known to us, and absent in the spectra of the high-boiling ones. Another group of indications, absent in the former, is observed in the spectra of high-boiling isomers. As seen from the tables, in the spectra of the low-boiling isomers there is observed a line in the region 1143-1147 cm^{-1}. In the spectra of the high-boiling isomers there are two lines in the regions 1107-1120 and 1144-1160 cm^{-1}.

Other indications of the spectra of these and other isomers are expressed less distinctly. Thus, the frequency of the intense line in the region 885-910 cm^{-1}, characterizing the pulsation vibration of the five-membered ring, appears several cm^{-1} higher in the spectra of the low-boiling isomers (cf. Table). In some cases there are observed in this region two intense lines (e.g., in the low-boiling isomers of 1-methyl-2-n-butyl cyclopentane and of 1-ethyl-2-n-butyl cyclopentane, and in the high-boiling isomers of 1-methyl-2-ethyl cyclopentane and of 1,2-di-n-butyl cyclopentane). Nevertheless, in all cases in the spectra of the high-boiling isomers there is an intense line in the region 882-893 cm^{-1}, while the frequency of the corresponding line in the spectra of the low-boiling isomers has a significantly greater magnitude. This indication of the examined spectra of the series of 1,2-dialkyl cyclopentanes also allows us to differentiate one isomer from the other.

The cited particulars give a basis for assigning to all of the low-boiling isomers investigated an identical geometric configuration, specifically the trans-configuration, by reason of the similarity of their spectra with the spectrum of trans-1,2-dimethyl cyclopentane; correspondingly, we assign the cis-structure to the high-boiling isomers.

Frequencies (cm^{-1}) and Intensities (in brackets) of the Raman Lines of 1,2-Dialkyl Cyclopentanes

Hydrocarbons	Region 1105–1160 cm^{-1}		Region 880–915 cm^{-1}	
	Low boiling isomers	High boiling isomers	Low boiling isomers	High boiling isomers
1,2-dimethyl cyclopentane (6)	1147 (11)	1107 (8) 1160 (4)	896 (38)	888 (42)
1-methyl-2-ethyl cyclopentane	1136 (10)	1114 (8) 1155 (6)	909 (26)	887 (14), 905 (24)
1-methyl-2-n-butyl cyclopentane (5)	1138 (9)	1120 (9) 1150 (4)	895 (24), 905 (10)	888 (29)
1-ethyl-2-n-propyl cyclopentane	1135 (10, b)	1117 (8) 1148 (8)	910 (30)	893 (27)
1-ethyl-2-n-butyl cyclopentane	1133 (16), 1141 (16)	1117 (10) 1145 (11)	898 (15), 912 (14)	891 (19, b)
1,2-di-n-butyl cyclopentane	1136 (12)	1120 (10) 1144 (11)	894 (25)	882 (17), 894 (21)

Note: The frequencies of lines with intensities greater than 5 are given.

REFERENCES

1. V. T. Aleksanyan, Kh. E. Sterin, A. L. Liberman, L. M. Kuznetsova, N. I. Tiun'kina, and B. A. Kazanskii. Sbornik "Pamyati Akad. G. S. Landsberga." Izd. Akad. Nauk SSSR, 1959.
2. A. F. Plate, A. A. Mel'nikov, R. A. Zelenko, and N. I. Lykova, Doklady Akad. Nauk SSSR 123, 1044 (1958).
3. V. T. Aleksanyan and Kh. E. Sterin. Opt. i Spektr. 3, 605 (1957);
   V. T. Aleksanyan, Kh. E. Sterin, A. L. Liberman, E. A. Mikhailova, M. A. Pryanishnikova, and B. A. Kazanskii. Izvest. Akad. Nauk SSSR, Ser. Fiz. 19, 225 (1955).
4. V. T. Aleksanyan, Kh. E. Sterin, A. L. Liberman, M. Iu. Lukina, G. S. Taits, G. A. Tarasova, and E. M. Terent'eva. Izvest. Akad. Nauk SSSR, Ser. Khim (in press).
5. B. A. Kazanskii, A. L. Liberman, G. V. Loza, I. M. Kuznetsova, V. T. Aleksanyan, and Kh. E. Sterin. Izvest. Akad. Nauk SSSR, Ser. Khim. No. 6, 1071 (1959).
6. G. S. Landsberg, P. A. Bazhulin, and M. M. Sushchinskii. "Osnovnye Parametry Spektrov Kombinatsionnova Rasseyaniya Uglevodorodov." (Fundamental Parameters of the Raman Spectra of Hydrocarbons), Akad. Nauk, SSSR, Moscow, 1958.

EMISSION AND ABSORPTION SPECTRA OF PERYLENE IN SOLID SOLUTIONS AT 77°K

E. V. Shpol'skii and R. I. Personov

Received 16 July 1959

The absorption and fluorescence spectra of solutions of perylene in ethyl alcohol and normal paraffins (from hexane to nonane) have been studied at room temperature and at 77°K. It has been shown that the spectra, which in alcoholic solutions consist of a series of diffuse bands, in frozen paraffin solutions display splitting into a series of narrow "lines." A vibrational analysis has been carried out and the frequencies of the normal vibrations of the perylene molecule in the ground and excited electronic states have been determined. The presence of mirror symmetry in the absorption and fluorescence spectra has been established. The results of the experiments are discussed, the peculiarities of the optical properties of the perylene molecule being taken into account.

INTRODUCTION

The aromatic hydrocarbon perylene (Fig. 1) is interesting from many points of view. From the point of view of the investigation of molecular structure, the optical and spectral properties of perylene discussed below, which in some respects set this compound apart from other aromatic polynuclear condensed hydrocarbons, offer considerable interest.

For example, a number of facts indicate the possibility of considering the perylene molecule as a combination of two relatively weakly bonded naphthalene nuclei. Chemically, this manifests itself in the ease with which the synthesis of perylene from naphthalene can be realized.[1] Furthermore, although a detailed calculation of the perylene molecule is lacking, it follows from general considerations of structural theory that, to a stable valence-structure model of this molecule, there must correspond the picture of two naphthalene nuclei united by ordinary (i.e., not double) bonds.[2] Finally, the X-ray determination of bond lengths performed by Robertson[3] shows that, while the bonds A, D, and E (Fig. 1) have the length 1.38 A, the length of bond G, which joins the two naphthalene nuclei, equals 1.50 A; i.e., it is anomalously large—according to Robertson's data, such long bonds are not encountered in a single other aromatic hydrocarbon.

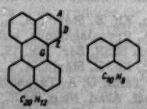

Fig. 1. Structural formulas of perylene and naphthalene.

In view of all these peculiarities in the structure of perylene, it is an unexpected fact that, in contrast to naphthalene which absorbs in the ultraviolet region, and also in contrast to other five- and six-ring condensed hydrocarbons which, on the long wavelength side, do not absorb beyond the extreme violet part of the spectrum, perylene shows intense absorption in the visible region, with a sharp maximum at about 4350 A (in solutions at room temperature). In the crystalline state, perylene has a dark brown color, while analogous hydrocarbons have a white or light yellow color in the crystalline state.

The spectroscopy of perylene also offers interest from the practical viewpoint, since the data obtained may be used for the determination of this substance by spectral analysis. Actually, perylene, together with other polycyclic aromatic hydrocarbons, is encountered among the pyrolysis products of organic substances: in soot, pitch, various tars,[3] and sometimes in natural products as well, for example, in petroleums[4] and bitumens[5]. Comparison of various petroleums and bitumens (extracted from rocks of different geological age) with respect to their perylene content is of considerable interest for the geochemistry of petroleum.

There are few data in the literature on the spectral properties of perylene. Absorption spectra of alcoholic solutions of perylene have been studied by Clar.[1] Bandow,[6] and Schoenthal and Scott[7] have measured some maxima of the fluorescence spectrum of perylene in alcohol and petroleum ether.

In our investigation of the absorption and fluorescence spectra of perylene we used the method of crystalline frozen paraffin solutions worked out in our laboratory,[8-13] which makes it possible to obtain spectra in the form of a succession of narrow "lines," the position of which may be measured with a high degree of accuracy. Bowen and Brokleburst[14] were the first to use this method for obtaining a quasi-linear fluorescence spectrum of perylene. However, the single prism monochromator used by them had very low dispersion and they obtained the maxima of only 16 principal bands. The spectrum obtained was not subjected to further analysis. Meanwhile, the vibrational analysis of such sharp spectra which makes it possible to find the frequencies of the normal vibrations of the molecule is particularly interesting in this case, since the use of Raman scattering in the middle of the visible region of the spectrum is very difficult on account of the strong absorption and fluorescence of perylene.

EXPERIMENTAL CONDITIONS

The fluorescence spectra of perylene in the crystalline state and in solutions were photographed by us with the help of a glass Fuoss spectrograph with a Rutherford prism (dispersion 42 A/mm around 4500 A). Ethyl alcohol and the normal paraffins from hexane to nonane were used as solvents (the latter were supplied to us by the Leningrad Scientific Research Institute for the Processing of Petroleum and the Production of Synthetic Liquid Fuel).

Fluorescence was excited by the group of mercury lines around 3650 A (a PRK-2 lamp with the corresponding filter). In a number of cases, excitation was also brought about by the group of lines of the mercury spec-

trum around 4046 and 4358 A. No dependence of the spectrum on the wavelength of the exciting light was found.

For obtaining spectra at T = 77°K, the cuvette with the fluorescing substance was placed in a transparent Dewar vessel with liquid nitrogen (a detailed description of the procedure used is given in reference 12). In order to avoid distortion of the first band of the fluorescence spectrum as a result of reabsorption, we used very low concentrations (of the order of 10^{-3}-10^{-7} mole/liter) in studying the spectra of frozen n-paraffin solutions, and also solutions of higher concentration (10^{-4}-10^{-5} mole/liter), but placed in a thin cuvette 0.25 mm in thickness.

The absorption spectra of perylene solutions at room temperature were measured with the help of an SF-4 spectrophotometer. Saturated solutions (concentrations of the order of 10^{-4}-10^{-5} mole/liter) were usually used, in layers 1 cm in thickness. The absorption spectra of frozen solutions were photographed with the help of the same spectrograph as for the fluorescence spectra. For studying the absorption spectra at T = 77°K, saturated solutions were used in layers 2.4, 0.9, and 0.25 mm in thickness. As in the case of fluorescence, the cuvette with the solution was immersed in a transparent Dewar vessel with liquid nitrogen. We used a 350 watt incandescent lamp with a single coil in a glass bulb as a source of a continuous spectrum.

The wavelengths of the bands and lines of the spectra being studied were determined by linear interpolation between nearby lines of the iron spectrum. The conversion of wavelengths into frequencies, taking account of the correction for the refractive index of air, was carried out with the help of Kayser's tables.[13] The precision of measurement of the wavelengths depended essentially on the character of the bands themselves and on the region of the spectrum. The maxima of the relatively broad absorption and fluorescence bands of alcoholic solutions were determined with a precision of the order of 10 A. In the case of the sharp spectra of frozen solutions in n-hexane, the error amounted to approximately 0.5-1 A for absorption and 1-2 A for fluorescence spectra. Correspondingly, the error in frequency differences was of the order of 10-15 cm^{-1}.

In this work we used perylene, synthesized and kindly placed at our disposal by Prof. I. Ya. Postovskii.

DESCRIPTION OF THE SPECTRA

1. Absorption spectra. At room temperature, the absorption spectra of alcoholic and n-paraffinic solutions of perylene are the same. Figure 2 shows the absorption spectrum of perylene in n-hexane. As can be seen from the Figure, two regions with 4-5 maxima in each are distinguished in this spectrum. The long wavelength region begins around 4350 A and extends to approximately 3700 A on the short wavelength side. The other, short wavelength region of stronger absorption begins at 3000 A and continues toward the short wavelength side, reaching a maximum at about 2525 A.

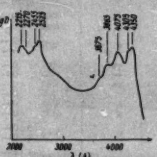

Fig. 2. Absorption spectrum of perylene in n-hexane at T = 293°K.

In view of the small quantity of perylene at our disposal, we did not determine exact values of the absorption coefficient. A rough estimate of the absorption maxima gives log ε ≈ 4.5, which agrees with Clar's results.[1]

Figure 3a shows a photograph of the long wavelength part of the absorption spectrum of a frozen alcoholic solution of perylene. Lowering of the temperature causes a marked narrowing of the bands. Groups of bands, separated by an interval of about 1330 cm^{-1}, are distinguished in the spectrum. Each group consists of 3 bands 100-150 cm^{-1} in width.

Fig. 3. Absorption spectra of perylene at T = 77°K in ethyl alcohol (a) and in n-hexane (b).

An essentially different picture is obtained when n-hexane is used as solvent (Fig. 3b). In this case the comparatively wide bands characteristic of a frozen alcoholic solution of perylene at 77°K are resolved into groups of narrow bands—lines of the order of 10 cm^{-1} in width. The wavelengths of the lines in the absorption spectrum of perylene in n-hexane are presented in Table 1.

Table 1. Absorption Spectrum of a Solution of Perylene in n-Hexane at a Temperature of 77°K

Line No.	Wave length (A)	Frequency of the lines (cm^{-1})	Intensity*	$\Delta\nu$(cm^{-1})	Possible interpretation
1	4454.0	22445	vs	0	0—0
2	4443.2	22500	m		
3	4384.8	22801	vs	356	0 + 358
4	4372.4	22864	s		
5	4348.4	22991	s	546	0 + 548
6	4317.1	23157	s	712	0 + 358 × 2
7	4303.4	23231	m		
8	4282.1	23346	s	901	0 + 358 + 548
9	4245.7	23547	m	1102	0 + 548 × 2
10	4212.4	23733	vs	1288	0 + 1290
11	4192.3	23847	vs	1402	0 + 1402
12	4182.8	23901	m	1456	0 + 358 + 548 × 2
13	4157.2	24048	vs	1603	0 + 1602
14	4144.0	24124	s	1678	0 + 1290 + 358
15	4130.1	24206	s	1761	0 + 1402 + 358
16	4117.5	24280	m	1835	0 + 1290 + 548
17	4096.5	24404	s	1959	0 + 1602 + 358
18	4087.0	24461	s	2016	0 + 1290 + 358 × 2
19	4076.8	24523	w		
20	4070.7	24559	vw	2114	0 + 1402 + 358 × 2
21	4055.1	24593	m	2148	0 + 1602 + 548
22	4057.5	24639	m	2194	0 + 1290 + 548 + 358
23	4037.9	24758	m	2313	0 + 1602 + 358 × 2
24	4025.1	24837	m	2392	0 + 1290 + 548 × 2
25	4007.0	24949	m	2504	0 + 1602 + 548 + 358 0 + 1402 + 548 × 2
26	3984.9	25025	m	2580	0 + 1290 × 2
27	3977.1	25137	s	2692	0 + 1402 + 1290
28	3959.8	25247	m	2802	0 + 1402 × 2
29	3945.4	25339	s	2894	0 + 1602 + 1290
30	3928.2	25450	s	3005	0 + 1602 + 1402
31	3920.7	25498	m	3053	0 + 1402 + 1290 + 358
32	3910.2	25567	vw	3122	0 + 1290 × 2 + 548
33	3904.2	25606	vw	3161	0 + 1402 × 2 + 358
34	3897.3	25652	m	3207	0 + 1602 × 2
35	3890.6	25696	m	3251	0 + 1602 + 1290 + 358
36	3874.0	25806	m	3361	0 + 1602 + 1402 + 358
37	3863.0	25879	vw	3434	0 + 1602 + 1290 + 548
38	3844.8	26003	w	3557	0 + 1602 × 2 + 358

*Symbols: vs—very intense line, s—intense, m—medium intensity, w—weak, vw—very weak.

In frozen solutions of other n-paraffins, the spectra duplicate the spectrum in n-hexane; i.e., they consist of narrow bands (almost lines) with the same frequency intervals. However, in going from solvent to solvent the spectra become somewhat fainter and shift toward the short wavelength side by approximately 40 cm^{-1} in heptane, 75 cm^{-1} in octane, and 110 cm^{-1} in nonane as compared with the spectrum in n-hexane.

2. Fluorescence spectra. In the crystalline state at room temperature, perylene has a bright orange red fluorescence. Its spectrum is diffuse and strongly shifted toward the long wavelength side as compared with the spectra of solutions (Fig. 4a). A maximum is observed at about 6150 A. Cooling the crystals to liquid nitrogen temperature (77°K) produces no marked changes in the spectrum.

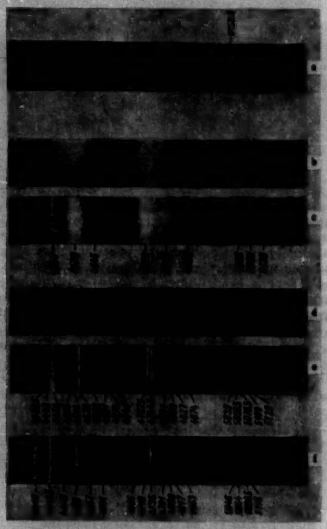

Fig. 4. Fluorescence spectra of perylene in the crystalline state at 293°K (a); in ethyl alcohol at 293°K (b) and 77°K (c); in n-hexane at 293°K (d) and 77°K (e); in n-heptane at 77°K (f).

In solutions the fluorescence of perylene becomes blue. At room temperature the spectrum consists of 4 washed-out bands (the last of these is of low intensity and is missing from the photographs presented in this article) 400-500 cm^{-1} in width. Here the fluorescence spectra of n-paraffin solutions (Fig. 4d) differ from the spectrum of an alcoholic solution (Fig. 4b) only in that two maxima are weakly evident in each band.

When an alcoholic solution is frozen, each of the broad fluorescence bands breaks up into 3 narrower bands 100-150 cm^{-1} in width (Fig. 4c). As in the case of absorption spectra, the distance between the band groups amounts to approximately 1300 cm^{-1}.

The fluorescence spectra of solutions in n-paraffins undergo very sharp changes when the temperature is lowered. The bands of the fluorescence spectrum of perylene in n-hexane, diffuse at room temperature (Fig. 4d), are resolved at a temperature of 77°K into groups of quite narrow lines of the order of 10 cm^{-1} in width (Fig. 4e). The wavelengths of the lines in the fluorescence spectrum of perylene in n-hexane are presented in Table 2.

The fluorescence spectra of frozen solutions in n-haptane, n-octane, and n-nonane are of the same quasi-linear character and duplicate the spectrum of a hexane solution with the same frequency intervals. However, in going from hexane to solvents with a greater number of C atoms, the lines become somewhat fainter, and the whole spectrum in its entirety undergoes a short wavelength shift relative to the spectrum in n-hexane, by the same amount as the absorption spectra. At the same time, there are observed a number of details which distinguish the spectra of solutions in the various paraffins. Thus, in the fluorescence spectrum of a solution of perylene in n-hexane, each of the first two maximum intensity lines at 4454 and 4526 A has two violet satellites, distant from it by 56 and 109 cm^{-1} respectively. These satellites are absent in the other n-paraffins. In heptane, octane, and nonane there appear three diffuse lines (wavelengths

Table 2. Fluorescence Spectrum of a Solution of Perylene in n-Hexane at 77°K

Line No.	Wave length (A)	Frequency of the lines (cm^{-1})	Intensity*	$\Delta\nu$(cm^{-1})	Possible interpretation
1	4432.5	22554	m		
2	4443	22501	m		
3	4454	22445	vs	0	0 — 0
4	4504	22196	s		
5	4514	22147	m		
6	4526	22088	vs	357	0 — 358
7	4541	22015	s		
8	4566	21895	s	550	0 — 550
9	4601	21728	s	717	0 — 358 × 2
10	4616	21658	s		
11	4641	21541	m	904	0 — 358 — 550
12	4656	21472	w		
13	4682	21352	w	1093	0 — 550 × 2
14	4727.5	21147	vs	1298	0 — 1298
15	4744.5	21071	vs	1374	0 — 1375
16	4761	20997	vs	1578	0 — 1578
17	4809	20789	s	1656	0 — 1298 — 358
18	4827	20711	s	1734	0 — 1375 — 358
19	4854	20596	vw	1849	0 — 1298 — 550
20	4874	20511	s	1934	0 — 1578 — 358 0 — 1375 — 550
21	4893	20432	m	2013	0 — 1298 — 358 × 2
22	4913	20348	m	2097	0 — 1375 — 358 × 2
23	4960	20158	m	2289	0 — 1578 — 358 × 2 0 — 1375 — 358 — 550
24	4980	20075	w	2370	0 — 1298 — 358 × 2
25	5006	19970	w	2475	0 — 1375 — 550 × 2
26	5039	19840	s	2605	0 — 1298 × 2
27	5056.5	19771	s	2674	0 — 1375 — 1298
28	5076.5	19693	m	2752	0 — 1375 × 2
29	5109	19568	m	2877	0 — 1298 — 1578
30	5129	19492	s	2953	0 — 1375 — 1578 0 — 1298 × 2 — 358
31	5149.5	19414	m	3031	0 — 1375 — 1298 — 358
32	5168	19344	w	3101	0 — 1375 × 2 — 358
33	5183	19288	m	3157	0 — 1578 × 2
34	5208	19214	m	3231	0 — 1578 — 1298 — 358 0 — 1375 — 1298 — 550
35	5222	19144	m	3301	0 — 1375 — 1578 — 358
36	5247	19053	w	3392	0 — 1375 — 1298 — 358 × 2
37	5279	18938	w	3507	0 — 1578 × 2 — 358 0 — 1375 — 1578 — 550
38	5301	18859	vw	3586	0 — 1375 — 1298 — 358 — 550
39	5321	18788	vw	3657	0 — 1375 × 2 — 358 — 550
40	5362	18575	vw	3670	0 — 1375 — 1578 — 358 — 550
41	5409	18483	m	3963	0 — 1375 — 1298 × 2
42	5433	18401	s	4044	0 — 1375 × 2 — 1298
43	5460	18310	w	4135	0 — 1375 × 3
44	5493	18200	m	4345	0 — 1375 — 1578 — 1298 0 — 1298 × 3 — 358
45	5515.5	18128	m	4319	0 — 1375 × 3 — 1578 0 — 1375 — 1298 × 3 — 358

*For symbols, see note to Table 1.

in heptane 4410, 4480, and 4686 A) (Fig. 4f), the analogs of which are not found in the spectrum of a hexane solution. The latter two of these form intervals of approximately 350 and 1335 cm^{-1} with the first. These intervals are close (on account of the diffuseness of the lines, the precision is not great) to the chief frequency differences in the principal spectrum of perylene (see Table 2).

VIBRATIONAL ANALYSIS

The preservation of the values of the intervals between lines in the spectra of all the paraffinic solutions confirms the fact that the observed spectra belong to the perylene molecule. The influence of the solvent drops, fundamentally, to an insignificant shift in the electronic levels with preservation of their vibrational structure.

Comparison of the sharp absorption and fluorescence spectra of perylene in n-hexane at T = 77°K (Tables 1 and 2) shows that the most intense short wavelength line of the fluorescence spectrum, at 4454 A, coincides with the longest wavelength intense line of the absorption spectrum. On this basis, we have assigned it to the 0-0 transition. The frequency differences formed between almost all the lines of the absorption spectrum (with a few exceptions) and the line at 4454 A (0-0), within the limits of error of the measurements, may be represented as combinations and harmonics of 5 frequencies: 358, 548, 1290, 1402, and 1602 cm^{-1}. The lines associated with the appearance of the frequencies 358 and 1402 cm^{-1} are the most intense. In exactly the same way, almost all the intervals between lines in the fluorescence spectrum, reckoned from the 0-0 line, can be interpreted with the help of 5 frequencies: 358, 550, 1298, 1375 and 1578 cm^{-1}. Of these, 358 and 1375 are the most intense.

Comparison of the fluorescence and absorption spectra of frozen solutions of perylene shows the presence of approximate mirror symmetry, the frequencies observed in the excited state differing only slightly, as shown above, from the frequencies of the ground state. The symmetry of the spectra shows up particularly visibly in the case of alcoholic solutions (Fig. 5).

Comparison of the vibrational frequencies of perylene and naphthalene is evidently of interest. In addition to the relationship considered above between the structures of these substances, both the molecules belong to the same point group $D_{2h} = V_h$, for which, according to the selection rules, the same vibrational frequencies—those symmetric with respect to the center of symmetry of the molecule (A_{1g}, B_{1g}, B_{2g}, B_{3g})—may appear in the electronic-vibrational and Raman spectra. Comparison of the observed perylene frequencies with the naphthalene frequencies obtained from Raman spectra[15] reveals the presence of two frequencies in the spectra being compared which coincide within the limits of error of the measurements (in cm^{-1}):

Naphthalene	Perylene
1379	1375
1576	1578

The frequencies 1379 and 1576 cm^{-1} are among those which are intense in the Raman spectrum of naphthalene and pertain to totally symmetric vibrations (Fig. 6).

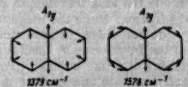

Fig. 6. Two totally symmetric vibrations of the naphthalene molecule, according to reference 16.

The causes for the appearance in the spectra of some details which are characteristic of a given solvent (the short wavelength satellites of the first intense lines of the fluorescence spectrum in n-hexane, the appearance of three diffuse bands in the other paraffins) are as yet unclear. It is very probable that one of the satellites of the 0-0 line (4443 A) coincides with the corresponding line in the absorption spectrum (see Table 1), while the line corresponding to the second satellite (4432.5 A) may not be observed in the absorption spectrum on account of its low intensity. In this case we are dealing with the presence of series which duplicate one another, the first two of which are very weak, so that only the first members of these series are observed; i.e., a picture analogous to that previously obtained for coronene,[10,14] pyrene, and 3,4-benzpyrene.[13]

DISCUSSION OF RESULTS

Certain characteristic features of the absorption spectrum of perylene are of considerable interest, especially the relationship between its absorption and luminescence spectra. In both respects perylene is essentially different from other polynuclear aromatic hydrocarbons. For the absorption spectra of these compounds in the crystalline state and in frozen solutions, the presence of a region of weak absorption ($\log \varepsilon \approx 2$-2.5), located between the fluorescence spectrum and the principal region of strong absorption ($\log \varepsilon \approx 5$-6), is characteristic. If we set aside the obvious cases where this weak absorption is brought about because a transition is forbidden by symmetry (as, for example, in benzene or coronene), the presence of this region and its peculiarities are of the greatest importance for interpretation of the mechanism of the origin and structure of fluores-

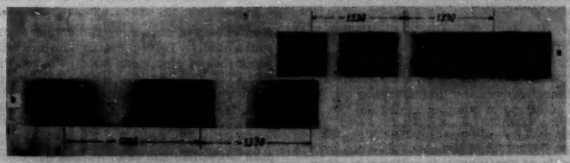

Fig. 5. Mirror symmetry of the fluorescence (a) and absorption (b) spectra of perylene in ethyl alcohol at 77°K.

cence spectra both in the crystalline state and in frozen crystalline solutions.

The spectra of pyrene and 3,4-benzpyrene investigated in one of the previous works[13] may serve as characteristic examples of the peculiarities of the region of weak absorption and its connection with the fluorescence spectrum. In the case of these substances in frozen paraffin solutions at 77°K, small sequences of "multiplets," including different numbers of lines depending on the solvent, precede the long wavelength edge of the region of strong absorption. Here the longest wavelength multiplet in absorption coincides, in resonance, with the leading multiplet of the fluorescence spectrum, which serves as the beginning of a like number (from one to five) of series which duplicate one another in the radiation spectrum. The peculiar nature of absorption in the long wavelength region also manifests itself in the fact that it is characterized by a complete absence of symmetry with the fluorescence spectrum; symmetry, however, does hold for the region of strong absorption.

It must be noted that a very similar picture is observed in the case of pure crystals at low temperatures, as has recently been shown in a series of works from Prikhot'ko's laboratory (see, for example, the review in reference 17). This face is particularly noteworthy because, in the case of frozen solutions, we are dealing not with the fundamental lattice but with absorption by an impurity. The fact that the impurity molecules themselves must play the role of "lattice defects" in this case may serve as an explanation.

The characteristic picture just described, which sheds light on the mechanism of the origin of quasi-linear spectra in frozen crystalline solutions, does not apply in the case of perylene. Here the principal region of strong absorption directly adjoins the fluorescence spectrum. In this case, symmetry of the two spectra is realized relative to the leading lines of these spectra, which coincide in resonance, but not relative to the center of symmetry located in the intermediate region which in this case is absent. All this apparently testifies to the fact that for perylene the model of an "oriented gas" must give entirely satisfactory results.

In conclusion the authors wish to express their gratitude to I. Ya. Postovskii for providing them with a sample of synthetic perylene.

REFERENCES

1. E. Clar. "Aromatische Kohlenwasserstoffe." 2nd ed., 1952.
2. J. M. Robertson. "Organic Crystals and Molecules." New York, 1953.
3. P. Wedgwood and R. L. Cooper. Analyst 80, 652 (1955).
4. R. Schnurmann, W. F. Maddams, and M. C. Barlow. Analyt. Chem. 25, 1010 (1953).
5. A. A. Il'ina. Proceedings of the Fourth Conference on Luminescence, Minsk, 1956.
6. F. Bandow. Z. phys. Chem. 196, 329 (1951).
7. R. Schoenthal and E. Scott. J. Chem. Soc. 1683 (1949).
8. E. V. Shpol'skii, A. A. Il'ina, and L. A. Klimova. Doklady Akad. Nauk SSSR 87, 935 (1952).
9. E. V. Shpol'skii and L. A. Klimova. Izvest. Akad. Nauk SSSR, Ser. Fiz. 18, 673 (1954).
10. E. V. Shpol'skii and L. A. Klimova. Izvest Akad. Nauk SSSR, Ser. Fiz. 20, 471 (1956).
11. E. V. Shpol'skii and L. A. Klimova. Doklady Akad. Nauk SSSR 3, 1227 (1956).
12. E. V. Shpol'skii, E. A. Girdzhiyauskaite, and L. A. Klimova. Proceedings of the Tenth All-Union Conference on Spectroscopy, 1, (1957). Izd. L'vovskogo Univ., 1957.
13. E. V. Shpol'skii and E. A. Girdzhiyauskaite. Opt. i Spektr. 4, 630 (1958).
14. E. J. Bowen and Brocklehurst. J. Chem. Soc., 4320 (1955).
15. H. Kayser. "Tabellen der Schwingungszahlen." Verlag S. Hirzel, 1925.
16. E. R. Lippincott and E. J. O'Reilly. J. Chem. Phys. 23, 238 (1955).
17. V. L. Broude, A. F. Prikhot'ko, and E. I. Rashba. Uspekhi Fiz. Nauk 67, 99 (1959).
18. A. L. McClellan and G. C. Pimentel. J. Chem. Phys. 23, 245 (1955).

ON THE INFLUENCE OF TEMPERATURE ON THE ELECTRONIC SPECTRA OF COMPLEX MOLECULES

L. G. Pikulik and M. A. Solomakho

Received 10 March 1959

The absorption and fluorescence spectra of a series of phthalimides and some dyes have been studied at +20°C and at liquid nitrogen temperature. It is shown that, when the temperature is lowered, a shift in the maxima of the absorption and fluorescence bands toward the frequency of the purely electronic transition takes place. An explanation of this shift is given.

It is necessary to carry on the study of luminescence spectra together with the study of absorption spectra. As a review of the work reported at the Sixth Conference on Luminescence[1] and at the Eleventh Conference on Spectroscopy[2] shows, combined study of the luminescence and absorption spectra of solutions of complex molecules* at low temperatures is virtually not taking place. Experimental data of such a character are encountered only sporadically. Together with this, the temperature dependences of electronic spectra have remained unclarified. The absence of experimental data gives no possibility of checking on series of conclusions which follow from the theory of the contour of spectral bands of complex molecules.

The theory of the contour of spectral bands of complex molecules has been worked out most systematically by Stepanov and Kazachenko.[3,4]

A complex molecule, from the point of view of vibrational energy, is comparable to a one-dimensional

*A complex molecule has a continuous electronic-vibrational spectrum. The definition of the concept "complex molecule" on the basis of spectroscopic criteria is given in monograph 3.

harmonic oscillator. At the same time, from the point of view of electronic energy, it retains quantum properties. In Fig. 1a are shown the potential curves of the ground and excited states which characterize this model.

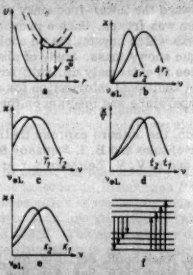

Fig. 1. Dependence of the contour of an absorption band on a change in various parameters which characterize the potential curves of the ground and excited states. a—potential curves of the ground and excited states (dashed curve represents the shifted position of the equilibrium in the higher electronic state); b—band shift predicted by theory for constant K and Δr and a fall in temperature T ($T_2 < T_1$); c—the same, for constant T and Δr and a diminution in K; d—the same for constant T and K and a diminution in Δr; e—observed band shift (t_1 = +20°C, t_2 = −196°C); f—transition scheme.

The analytical expression for the relative intensity of the contour of a luminescence or absorption band is a function of three* parameters: the difference between the equilibrium radii of the upper and lower electronic states Δr, the quasi-elastic constant of the potential curves K, and the temperature T. In Fig. 1b, c, and d is shown the character of the shift of a spectral absorption band depending on changes in these parameters (the shift of the fluorescence band will be mirror-symmetric).

*A fourth parameter—the frequency of the electronic transition, ν_{el}.—is not associated with the contour of the band, since it determines the position of the band on the frequency scale.

The action of external factors on the molecule (the solvent, for example) leads to changes in K and Δr, in consequence of which various spectral shifts are observed.[5,6] A significant shift of spectral bands is also observed on lowering the temperature of the medium.[7,8] At the same time, the regularity of the influence of the solvent on fluorescence spectra which is observed at +20°C is completely disrupted at −196°C.[7]

To clarify the nature of the spectral shift of solutions when the temperature is lowered, we have studied in this work the absorption and emission spectra of a series of phthalimides, as well as of some typical dyes, at liquid nitrogen temperature. The choice of solvents was dictated by the experimental conditions: on changing the temperature from that of the room to the temperature of boiling nitrogen, the medium must remain optically transparent. Of the liquid media which freeze without cracking,* we used ethyl, propyl, and isobutyl alcohols.

*A small addition of petroleum ether was helpful in this respect.

Furthermore, solid solutions were prepared, using gelatin, sugar, and starch as a base. Various films dyed with the substances being studied also proved convenient for experimental purposes. Plexiglass and film with a nitrocellulose base were used as media of this sort. The dyeing of the films was carried out in alcohol-water solutions of the substances being studied. Dyed samples of plexiglass were obtained, in addition, by the polymerization of a methyl methacrylate solution of the given substance. The spectra of plexiglass dyed by different methods differ somewhat, but the temperature regularities in the band shifts are alike.

The fluorescence spectra were investigated with a photoelectric apparatus built around a glass UM-2 monochromator, and the absorption spectra with an SF-4 spectrometer. For measuring spectra at low temperatures, special thermostatic cells were constructed.

In Fig. 2 are shown the spectra of 3-monomethylaminophthalimide in solid media at different temperatures. As can be seen from the figure, when the temperature is lowered, the maxima of the absorption and fluorescence bands shift toward each other, and this phenomenon does not depend on the peculiarities of the medium. An analogous phenomenon is also observed for the other phthalimides investigated (3-aminophthalimide, 3-amino-N-methylphthalimide, 4-aminophthalimide, 4-amino-N-methylphthalimide, 3-monomethylamino-N-methylphthalimide), the spectra of which were mainly obtained in the medium most convenient for the experiment—plexiglass. A series of control experiments leaves no doubt that, for all the compounds listed, the temperature shifts of the spectral bands are of the same character in the other media used as well.

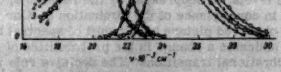

Fig. 2. Temperature dependence of the absorption and fluorescence spectra of 3-monomethylaminophthalimide in solid media. Curve 1—nitrocellulose base film at +20°C; curve 2—the same at −196°C; curve 3—plexiglass at +20°C; curve 4—the same at −196°C.

In Fig. 3 are shown, as an example, the fluorescence and absorption spectra of 4-aminophthalimide in one of the media which changes its state of aggregation when the temperature is lowered. In these cases the absorption and luminescence spectra also move toward each other. The significant shift in the fluorescence spectrum observed for such media is probably associated with the change in the state of aggregation of the solution.

It must be noted that when the temperature is changed from +20°C to −196°C, a reduction in band width takes place in both the fluorescence and the absorption spectra. For solid media it amounts to 5-10%; for media which change their state of aggregation, it amounts to 10-20%. The change in position of the maxima of the two bands amounts to 200 cm^{-1} on the average in the first case; in

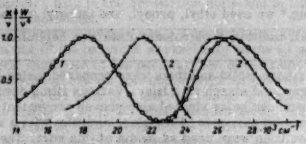

Fig. 3. Temperature dependence of the absorption and fluorescence spectra of 4-aminophthalimide in ethyl alcohol. Curve 1—t = +20°C; curve 2—t = −196°C.

the second case, the shift in the fluorescence band may reach 4000 cm^{-1}.

Thus, a shift of the maxima of the fluorescence and absorption bands toward each other takes place in the phthalimides considered here when the temperature of the medium is lowered. This phenomenon is also peculiar to other classes of substances. We have observed it in alcoholic solutions of several dyes: acridine yellow,* auramine, chrysoidine, coryphosphine, fluorescein, and aminochloromaleimide (for the nonfluorescing dyes, the shift of the long wavelength absorption band into the lower frequency region was observed). For 3,6-diaminoacridine it has been noted in reference 10.

The measurements were carried out at dye concentrations of an order not higher than 10^{-6} mole/liter. At such concentrations the dissolved dye is probably essentially in the monomeric form.

Let us compare the experimental facts with the conclusions which follow from the theory of the contour of spectral bands (Fig. 1b, c, d, e). The observed band shift when the temperature is lowered corresponds not to case b, as was anticipated, but to cases c and d. Thus, a change in temperature does not influence the spectra of the substance directly, but rather by means of a decrease in K or Δr. The anticipated shift of the absorption band into the higher-frequency region (Fig. 1b), produced by the redistribution of the molecules with respect to the vibrational levels, is suppressed by the reverse shift of the band in consequence of the diminution of K or Δr.

The observed picture of the shift of spectral bands actually indicates a change in the probabilities of electronic-vibrational transitions. The decisive role in this phenomenon must be ascribed to the solvent, which, as the temperature is lowered, exerts a stronger influence on the fluorescing molecule.[7,8] The reduction in the difference of the generalized equilibrium radii is the result of such an influence (see Fig. 1a). Evidently, during absorption, the relative number of transitions to lower vibrational levels of the upper electronic state increases—and the maximum of the absorption band shifts toward the lower frequency side. Correspondingly, during emission the number of transitions to lower vibrational levels of the ground electronic state increases—and the maximum of the emission band shifts toward the higher frequency side (Fig. 1e, f).

In all the cases considered here, the shift of the fluorescence band took place toward the higher frequency side. In reference 7 a shift of the fluorescence band of phthalimides toward the lower-frequency side was found when the solution was frozen. Such a phenomenon is observed in solvents which crystallize on cooling and appear as an opaque snowy mass. Study of absorption spectra in these cases is extremely difficult; however, it will undoubtedly give additional information for clarifying the influence of temperature and medium on the fluorescing molecule.

In conclusion, the authors express their deep gratitude to A. N. Sevchenko and B. I. Stepanov for their valuable comments and to V. V. Zelinskii for providing the phthalimides.

REFERENCES

1. Izvest. Akad. Nauk SSSR, Ser. Fiz. No. 11, 1958.
2. Izvest. Akad. Nauk SSSR, Ser. Fiz. Nos. 6, 9, 11, 1958.
3. B. I. Stepanov. "Liuminestsentsiya slozhnykh molekul." (Luminescence of Complex Molecules), Izd. Akad. Nauk Belorus. SSR, 1956.
4. L. P. Kazachenko and B. I. Stepanov. Opt. i Spektr. **2**, 339 (1957).
5. V. V. Zelinskii, V. P. Kolobkov, and L. G. Pikulik. Opt. i Spektr. **2**, 402, 405 (1957).
6. L. G. Pikulik. Trudy Inst. Fiz. i Mat., Akad. Nauk Belorus. SSR Pt. 3, (1958) (in press).
7. V. V. Zelinskii and V. P. Kolobkov. Opt. i Spektr. **5**, 423 (1958).
8. L. G. Pikulik and M. A. Solomakho. Izvest. Akad. Nauk SSSR, Ser. Fiz. **22**, 1391 (1958).
9. L. A. Kuznetsova and B. Ya. Sveshnikov. Izvest. Akad. Nauk SSSR, Ser. Fiz. **20**, 433 (1956).
10. V. L. Levshin and T. M. Tarasova. Izvest. Akad. Nauk SSSR, Ser. Fiz. **15**, 573 (1951).

Note added in proof: The marked short wavelength shift of the fluorescence spectra of phthalimides when liquid solutions are frozen (Fig. 3) is associated with the orientation polarization of the solvent. At room temperature, a change in the orientation polarization of the solvent takes place within the lifetime of the excited state, as a result of the change in the dipole moment of the molecule, and the electronic level is lowered (the fluorescence spectrum is shifted toward the long wavelength region). When the solution is frozen, the possibility of reorienting the solvent molecule within the lifetime of the excited state is eliminated, and therefore the additional influence of the solvent on the excited level ceases. This question was considered by us in a report at the Eighth Conference on Luminescence (Minsk, October, 1959).

TEMPERATURE DEPENDENCE OF THE BROAD ABSORPTION BANDS IN THE SPECTRA OF CRYSTALS OF VARIOUS STRUCTURES COLORED BY ISOMORPHOUS IMPURITIES

S. V. Grum-Grzhimailo and G. V. Klimusheva

Received 8 January 1959

The absorption spectra of crystals of various structures colored by isomorphous impurity ions with variable valencies were investigated between 103° and 823°K. Comparison of experimental data with calculations showed a satisfactory agreement between theory and experiment.

1. In order to check the applicability of the basic assumptions of the theories of Pekar[1] and Davydov[2] to ionic crystals whose color is caused by ions of variable valence, we undertook an investigation of various crystals between 103° and 823°K. The applicability of this theory to crystals whose coloration is caused by ions of variable valence was demonstrated previously[3,4] in the case of a single ruby sample. In the present investigation, crystals of different structures were studied. The investigation was performed on an improved apparatus with the aid of an SF-4 spectrophotometer.[5]

According to the theory of light absorption by impurities, developed by Pekar and Davydov, the wide absorption bands of impure crystals act in the following way when the temperature changes: At high temperatures, when there is strong coupling between electronic excitation and lattice vibration; the absorption curve has a shape similar to the emission curve of a free molecule when the Doppler effect is taken into account. If $2B/\Gamma \gg 1$, then the absorption band has the shape of a Gaussian error curve. (B is a parameter which is related to the half-width of the absorption band and Γ is the reciprocal of the average lifetime of an impurity center in the excited state.) An analysis of the shape of the absorption band at low temperatures, presented by Lubchenko[6,7] showed that as the temperature decreases, the spectral absorption curve departs from the Gaussian shape, becoming asymmetric with respect to a line passing through the maximum of the band perpendicular to the frequency axis.

According to the theory of Pekar and Davydov, the half-width of the absorption band and the magnitude and spectral location of the absorption maximum change in different ways at high and low temperatures (see below).

As the temperature is changed, the area enclosed by the spectral absorption curve and the frequency axis remains approximately constant, and the same is true of the product of the half-width of the band and the absorption coefficient at the maximum of the curve.

2. We obtained the absorption spectra of the crystals investigated previously at various temperatures.[8-12] These crystals possess various structures; their coloration is caused by Cr^{3+}, V^{2+}, $Mn^{2+} + Fe^{2+}$, and $Cr^{3+} + Fe^{2+}$.

The samples were in the form of polished, plane parallel platelets cut parallel to the optic axis. Ruby No. 84,* which contained 0.01% Cr_2O_3 (sample thickness was 2.04 mm) had been investigated previously.[8] For that particular ruby, the basic quantities which characterize absorption at various temperatures were calculated.[3,4] In this paper data on the absorption of ruby No. 44[8] (d = 0.41 mm) with a Cr_2O_3 concentration of 0.7% were obtained between 298° and 823°K. Calculations were made for two absorption bands of the ordinary ray and for two bands of the extraordinary ray (Figs. 1a and b).* Ruby

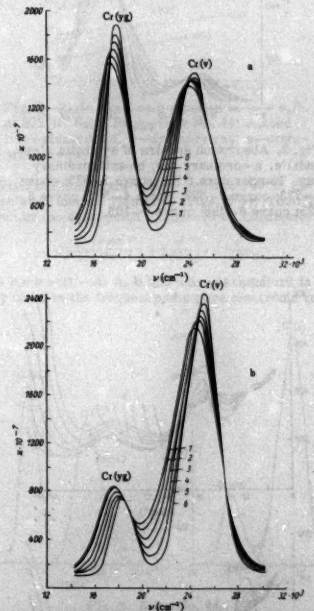

Fig. 1. Absorption spectra of ruby No. 44, which contains 0.7% Cr_2O_3. a—ordinary ray; b—extraordinary ray. Temperature (°K): curve 1—823; curve 2—723; curve 3—623; curve 4—523; curve 5—423; curve 6—298.

*The sample number refers to numbers in the mineral collection of the Crystallography Institute of the Academy of Sciences, U.S.S.R.

*The elements which give rise to a given absorption band are indicated at the maxima in the drawings. The region of the spectrum in which the absorption maximum is located is given in parentheses according to the following scheme of abbreviation: r—red; yg—yellow green; v—violet; ir—infrared; gb—green blue; b—blue; vb—violet blue.

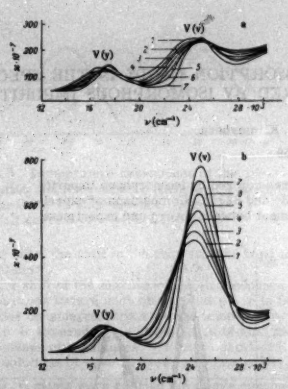

Fig. 2. Absorption spectra of synthetic alexandrite. a—ordinary ray; b—extraordinary ray. Temperature (°K): curve 1—823; curve 2—723; curve 3—623; curve 4—523; curve 5—423; curve 6—298; curve 7—103.

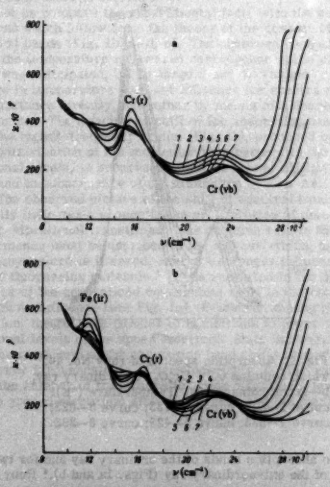

Fig. 3. Absorption spectra of emerald No. 165, which contains 0.17% Cr_2O_3. a—ordinary ray; b—extraordinary ray. Temperature (°K): curve 1—823; curve 2—723; curve 3—623; curve 4—523; curve 5—423; curve 6—298; curve 7—103.

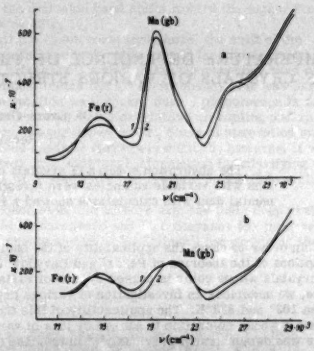

Fig. 4. Absorption spectrum of rose-brown tourmaline No. 120. a—ordinary ray; b—extraordinary ray. Temperature (°K): curve 1—298; curve 2—103.

No. 84, which had been investigated previously,[4] was studied at 103°K in the new apparatus.

Between 103° and 823°K, we also investigated V-corundum, a synthetic alexandrite in whose absorption spectrum (Figs. 2a and b) there are two bands for both the ordinary and extraordinary rays. These are caused by trivalent vanadium.

Another crystal which was studied was emerald No. 165[9] (Figs. 3a and b) whose crystal lattice differs from that of corundum (emerald is a cyclic silicate compound). The color of emerald, like that of ruby, is caused by trivalent chromium impurity. The sample investigated contained 0.17% Cr_2O_3.[9] The ions of trivalent Cr^{3+} substitute isomorphously for Al^{3+} with sixfold coordination. Previous investigations of beryls of various colors have shown that divalent iron, which produces the absorption band in the infrared, also has an effect on the color of emerald, which is a variety of beryl. We measured the absorption of this crystal between 103° and 823°K.

In addition to corundum and emerald, rose brown tourmaline No. 120[11] was also investigated (See Figs. 4a and b). (Tourmaline, which is also a cyclic silicate compound, has a different crystalline lattice from the other crystals discussed thus far.) The color of rose tourmaline is caused by Mn^{3+},[11] and the absorption band in the visible part of the spectrum has been attributed to this ion (Figs 4a and b). The band in the infrared part of the spectrum is caused by divalent iron.[12] The influence of the iron is also indicated in the ultraviolet where the absorption increases sharply. This sample was studied at room temperature and at 103°K. The crystal was not heated because, as is well known from data in references 13 and 14, this weakens the color of rose tourmaline and reduces the number of color-producing centers. This effect requires an additional investigation.

In contrast to rose tourmaline, emeralds,and crystals of corundum containing various impurities retain their color when heated to 823°K and subsequently cooled.

3. The spectral absorption curves of the samples under investigation change during heating according to the following scheme: as the temperature is increased, the absorption maximum decreases in those parts of the

spectrum where there is not superimposed on it any absorption associated with the location of a series of bands or absorption edges; the band widens and is displaced toward the long wavelength region of the spectrum. This is what happens to the absorption bands of ruby in the visible part of the spectrum for the strongly absorbed ordinary ray, which is designated in Fig. 1 by Cr(yg), and to the bands for the ordinary and extraordinary rays which are located at the boundary between the visible and ultraviolet parts of the spectrum, which are designated in Fig. 1b by Cr(v). The latter two bands change much less as a result of heating than does the band for the ordinary ray in the visible part of the spectrum. The visible band associated with the extraordinary ray Cr(yg) (See Fig. 1b) behaves differently. This band, on being displaced toward the long wavelength region of the spectrum, increases in magnitude. Obviously, this is due to the widening of neighboring absorption bands and an increase of absorption in the neighboring regions of the spectrum as a result of this widening.

In the case of alexandrite, the absorption maximum of the extraordinary ray in the ultraviolet decreases considerably more on heating than does the maximum in ruby. The latter is also located at about 400 mμ, but it is caused by chromium rather than vanadium. It was difficult to resolve other bands in the sample of alexandrite investigated.

When the temperature was lowered for both samples of corundum colored by Cr and V, the bands became narrower and higher. We did not observe any noticeable displacement of the absorption band maximum with respect to its room temperature location.

When the temperature was lowered, the absorption bands due to Cr in emerald behaved as they did in colored corundum. The bands in rose-colored tourmaline become higher when the temperature is lowered, while the bands located in the blue green are displaced somewhat toward shorter wavelengths.

When the temperature is increased, emerald becomes considerably more transparent. The band associated with Fe^{2+} flattens out, and finally disappears completely at 673°K. The wide absorption band in the red, caused by Cr^{3+}, acts like the absorption band in ruby: when the temperature is increased, it decreases and moves toward longer wavelengths. The increase in the absorption minimum, which occurs as temperature increases, causes the maximum to almost vanish at 673°K. The absorption band in the violet is displaced toward longer wavelengths as the sample is heated; at the same time, the absorption at the maximum increases because of the increased absorption of the crystal in the ultraviolet. The wide absorption bands of emerald were not calculated completely, since these bands are asymmetric and strongly affect each other.

4. In these investigations of light absorption in the above-mentioned crystals the following behavior pattern was discerned:

(a) The absorption curves have the shape of a Gaussian error curve at sufficiently high temperatures and become quite asymmetric at 103°K.

Calculations for four absorption bands in ruby sample No. 44 and for two bands in alexandrite at 823°K showed that the shape of the absorption bands was a good approximation to a Gaussian curve, since the experimental values of the absorption coefficient in the coordinates

$$\ln \varkappa = f[(\nu - \nu_0)^2],$$

(where ν_0 is the frequency of the absorption maximum) lie on a single straight line (Fig. 5). Only for frequencies which differ considerably from the maximum absorption frequency is there observed any asymmetry with respect to a line drawn through the band maximum perpendicular to the frequency axis. No calculations were performed for the two other bands in alexandrite or for the emerald bands obtained at 823°K, since at that temperature the absorption curves are flattened out considerably (Figs. 2a and b).

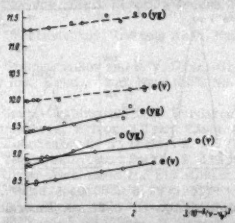

Fig. 5. Plot of $\ln \kappa$ as a function of $(\nu - \nu_0)^2$ at 832°K. Solid lines—ruby No. 44; dashed line—alexandrite. o—ordinary ray; e—extraordinary ray.

When the temperature is dropped to 103°K, the curves become even more asymmetric (Figs. 6-9). Their shape is given by the expression introduced by Lubchenko:[5]

$$S(\nu) = \frac{\text{const}}{2B}\left[1 + \beta\frac{\alpha^3}{8B^3}\right]e^{-\frac{\alpha^2}{4B^2}},$$

where $\alpha = \nu - \Omega - A$; A, B and β are parameters in the theory and Ω is the frequency of a pure electronic transition.

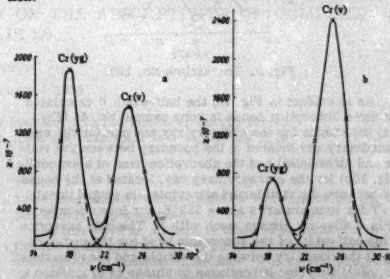

Fig. 6. Ruby No. 44.

Figures 6 through 9 compare absorption curves calculated from this equation (dashed lines) with experimental curves (solid lines). The theoretical parameters were evaluated by arbitrarily selecting three points on each curve (denoted by crosses). All the curves in Figs. 6 through 9 refer to a temperature of 103°K. The "a" part of each figure corresponds to the ordinary ray and the "b" part to the extraordinary ray.

The comparison indicates a satisfactory agreement between theory and experiment

(b) According to the theory of Pekar and Davydov, the half-width of the absorption bands is proportional to the square root of the absolute temperature at high temperatures and does not depend very much on temperature at low temperatures.

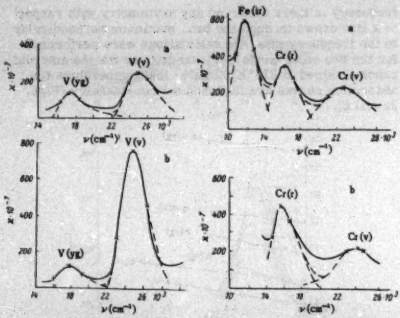

Fig. 7. Alexandrite.

Fig. 8. Emerald No. 165.

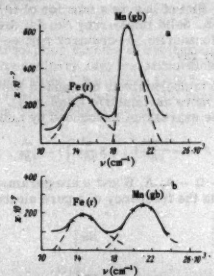

Fig. 9. Tourmaline No. 120.

As is evident in Fig. 10, the half-width δ calculated for three absorption bands in ruby sample No. 44 (Fig. 10a) (two bands for the ordinary ray and one for the extraordinary ray located at the boundary between the visible and ultraviolet) and the absorption band of alexandrite (Fig. 10b) for the extraordinary ray, located at the boundary between the visible and ultraviolet, is proportional to $\sqrt{T}$ for temperatures above 523°K; for lower temperatures δ does not change much with T. The only exception is the half-width of the absorption band for the ordinary ray at the boundary between the visible and the ultraviolet [Cr, o(v)] for ruby; it continues to change in proportion to $\sqrt{T}$ below 523°K. This can be explained by the difficulty encountered in resolving the two absorption bands which exist in ruby.

(c) The product of the half-width of the absorption band and the maximum absorption coefficient $\delta\kappa_{max}$ should remain approximately constant as the temperature changes, as follows from the Pekar and Davydov theory. Therefore, the quantity κ_{max} ought to be inversely proportional to $\sqrt{T}$ in the high temperature region and should slowly increase as the temperature decreases.

In the case of ruby sample No. 44 and the most sharply defined absorption band of alexandrite, the magnitude of the absorption maximum is inversely proportional to the square root of the absolute temperature, starting at approximately 523°K. At lower temperatures the absorption coefficient at the maximum depends on temperature to a considerably smaller degree (Fig. 11).

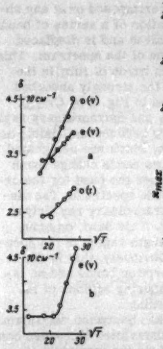

Fig. 10

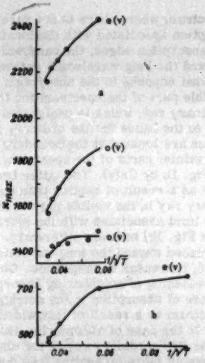

Fig. 11

Fig. 10. Half-width δ of the absorption band. a—ruby No. 44; b—alexandrite. o—ordinary ray; e—extraordinary ray.

Fig. 11. The absorption maximum κ_{max} as a function of $1/\sqrt{T}$. a—ruby No. 44; b—alexandrite. o—ordinary ray; e—extraordinary ray.

(d) The area under the absorption curve S as well as the product of the half-width and the absorption coefficient at the maximum ought to be nearly independent of temperature, according to the theory of impurity absorption. We demonstrated that the dependence of S on T and $\delta\kappa_{max}$ on T (see Figs. 12a and b) are in complete agreement with the theoretical conclusions of Pekar and Davydov. It is only in the case of the band in ruby-sample No. 44 located at the boundary between the visible and ultraviolet (ordinary ray) that the product $\delta\kappa_{max}$ and the area of the band increase with increasing temperature.

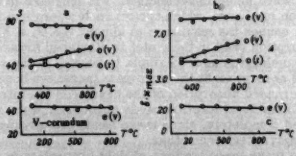

Fig. 12. The area S (a) and the product $\delta\kappa_{max}$ (b) as a function of temperature.

(e) The absorption band should be displaced toward longer wavelengths when the temperature is increased. Such a displacement is observed experimentally starting at 523°K (Fig. 13). In Figs. 1-3 it is seen that for ruby, alexandrite, and emerald the displacement of the absorption maximum in the red part of the spectrum is greater than that of the ultraviolet maximum. Virtually no displacement of the absorption maximum is observed at temperatures below 523°K.

(f) The data obtained for the absorption bands of tourmaline No. 120 show that the half-width of the curves, the area enclosed by the absorption curve and the frequency axis, and the product of the band half-width and

the absorption at the maximum are practically constant between room temperature and 103°K; as the temperature decreases, the absorption at the maximum increases slightly.

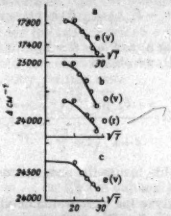

Fig. 13. The displacement of the absorption maximum Δ as a function of $\sqrt{T}$.

The study of the rules governing light absorption by impure crystals as a function of temperature showed satisfactory agreement between theory and experiment for all the maxima in those parts of the spectrum where there was no superposition of absorption from adjacent maxima. Thus, the theory of impure crystals is applicable to crystals of various structures colored by one or another of various ions of elements with variable valencies.

In conclusion we wish to thank A. F. Lubchenko for valuable discussions and for help in handling the experimental data and comparing them with the calculations.

REFERENCES

1. S. I. Pekar. Zhur. Eksptl. i Teoret. Fiz. **22**, 641 (1952).
2. A. S. Davydov. Zhur. Eksptl. i Teoret. Fiz. **24**, 197 (1953).
3. B. N. Grechushnikov. Doklady Akad. Nauk SSSR **49**, 7, 707 (1954).
4. B. N. Grechushnikov and S. V. Grum-Grzhimailo. Trudy Inst. Krist., Akad. Nauk SSSR No. 11, 189 (1955).
5. S. V. Grum-Grzhimailo, K. P. Bondarenko, and G. B. Klimusheva. Privory i Tekh. Eksper. **5**, 83 (1958).
6. A. F. Lubchenko. Opt. i Spektr. **3**, 195 (1957).
7. A. F. Lubchenko. Opt. i Spektr. **3**, 439 (1957).
8. S. V. Grum-Grzhimailo and E. I. Utkina. Trudy Inst. Krist., Akad. Nauk SSSR **8**, 99 (1953).
9. S. V. Grum-Grzhimailo. Trudy Inst. Krist., Akad. Nauk SSSR No. 2, 73 (1954).
10. S. V. Grum-Grzhimailo and L. A. Pevneva. Trudy Inst. Krist., Akad. Nauk SSSR No. 12, 85 (1956).
11. S. V. Grum-Grzhimailo. Doklady Akad. Nauk SSSR **60**, 8 (1948).
12. S. V. Grum-Grzhimailo. Trudy Inst. Krist., Akad. Nauk SSSR No. 12, 79 (1956).
13. N. E. Vedeneeva and S. V. Grum-Grzhimailo. Trudy Inst. Krist., Akad. Nauk SSSR No. 4, 215 (1948).
14. M. M. Slivko. "Investigations of tourmalines in certain deposits." Lvov University Press, Lvov, 1955.

THE EFFECT OF STRONG ILLUMINATION ON THE ABSORPTIVITY OF COMPLEX MOLECULES

A. P. Ivanov

Received 4 December 1959

Formulas are derived for the absorptivity of systems with two and three energy levels. Conditions under which negative absorption takes place are examined. It is shown that it is possible to observe clarification of a substance.

Until recently it was believed that the absorption coefficient does not depend on the intensity of the light. A large amount of experimental data and Maxwell's classical electromagnetic theory supported this belief. However, research carried out over the last three decades has cast some doubt on these ideas.

Vawilov,[1] in 1920, first expressed the idea of a possible dependence of the absorptivity of a substance on the radiant power of the incident radiation. Vawilov and Lewschin[2] observed a slight clarification of uranium glass when illuminated by the light of a spark. Considerably later, Lewis, Lipkin and Magel,[3,4] while studying the luminescence and absorption of "rigid" solutions, observed that under strong illumination the fundamental absorption band is weakened and a new band appears, which is characteristic of molecules in an excited state. A decrease in absorptivity with increasing intensity of illumination was also observed in radiospectroscopy, where it appeared as the broadening of narrow resonance absorption lines.[5-9] In connection with this effect, experimental and theoretical research on the microwave absorption band contour was undertaken.[5-9] Taking into account the influence of light intensity on the absorption index, Sveshnikov[10] showed that the well-known Burger's law is only a special case.

In this work an attempt is made to examine the influence of the electromagnetic radiation density on the absorptivity of complex molecules. The optical properties of complex molecules have been thoroughly studied by Stepanov and Neporent[11, 12] and by other investigators. This considerably simplified the solution of our problem. It seems to us that although the calculations given below are based on special properties of systems, some qualitative deductions can be applied to a broader class of materials.

Let us first consider the case in which absorption and radiation take place only for transitions between the first and second electronic levels, taking the vibrational sublevels into account. We will determine the number of molecules in these levels. Let n be the number of particles per unit volume. Under the influence of external radiation within the spectral interval containing the absorption region of the substance, a fraction of the molecules n_0 goes into the excited state with various vibrational energies; the remainder n_1 stays in the electronic ground state. When dynamic equilibrium is established,

the change in the number of molecules in the excited state dn_2 is equal to zero. For this particular case we can the therefore write the following set of equations:

$$n_1 \int_{\nu_p} \int_{E_n} a_\nu (E_m, \nu_p)\, \rho(E_n)\, d\nu_p\, dE_n$$

$$= n_2 \left\{ \int_{\nu_1} \int_{E_m^*} f_\nu (E_m^*, \nu_1)\, \rho^* (E_m^*)\, d\nu_1\, dE_m^* + \int_{E_m^*} d(E_m^*)\, \rho^* (E_m^*)\, dE_m^* \right\},$$

$$n_1 + n_2 = n. \qquad (1)$$

Here $a_\nu = B_{\nu 1} J$ is the spectral probability density for the transition to an excited state per particle, per unit time ($B_{\nu 1}$ is the Einstein coefficient for absorption, J is the volume spectral density of light radiation), $f_\nu = A_\nu + B_{\nu 1} J + d$ is the spectral probability density of a transition to the normal state with emission of quanta, A_ν is the probability of spontaneous transition and $B_{\nu 1} J$ is the probability of induced transition ($B_{\nu 1}$ is the Einstein coefficient for induced emission), d is the probability of a nonradiative transition to the ground state, and $\rho(E_n)$ and $\rho^*(E_m^*)$ are the particle distribution functions among the vibrational levels (E_n and E_m^*) of the ground and excited electronic levels.

On the right hand side of the first equation, integration is carried out over all the vibrational energies E_m^* and radiated frequencies ν_1; on the left hand side integration is carried out over all the vibrational energies E_n and the absorbed frequencies ν_p. Introducing the following notation:

$$B_1 = \int_{\nu_p} B_{\nu 1} d\nu_p;\quad \bar{B}_1 = \int_{\nu_p} B_{\nu 1} d\nu_1;\quad A = \int_{\nu_1} A_\nu d\nu_1$$

and solving the set of equations (1) we get

$$n_1 = \frac{\bar{A} + \bar{B}_1 J_{av} + \bar{d}}{\bar{A} + (B_1 + \bar{B}_1) J_{av} + \bar{d}}\, n. \qquad (2)$$

Here J_{av} is the average value of the volume spectral density of light radiation within the limits of the excited spectral region. The dashes over the letters indicate that the corresponding probabilities were averaged over the vibrational levels.

Let us clarify the relationship between the probabilities $\bar{B}_1$ and $\bar{B}_1$ of Eq. (2). By analogy with a calculation carried out by Stepanov,[13] it is not hard to show that

$$\frac{B_{\nu 1}}{B_{\nu 1}} = \frac{C^*}{C}\, e^{\frac{h(\nu_0 - \nu)}{kT}},$$

where ν is the frequency of the exciting light, ν_0 is the frequency of the electronic transition, and C and C^* are the normalizing factors. This relationship holds for a strong interaction of absorbing centers with the surrounding medium for $\nu \gtrsim \nu_0$. Since the frequencies of induced emission coincide with the frequencies of the absorbed light,

$$\frac{\bar{B}_1}{\bar{B}_1} = \frac{C^*}{C}\, e^{\frac{h(\nu_0 - \bar{\nu})}{kT}}. \qquad (3)$$

Let us now derive an expression for the absorption index. A parallel beam of light of radiant power $d\Phi$ in the spectral interval $d\nu$ traversing a path dl is weakened by the amount

$$d(d\Phi) = -Kd\Phi dl = -JKvd\omega dV, \qquad (4)$$

where v is the velocity of light in the given medium.

This decrease in flux is equal to the amount of energy absorbed in the volume dV = dSdl per unit time. The latter is equal to

$$d(d\Phi) = h\nu J d\omega dV (B_{\nu 1} n_1 - B_{\nu 1} n_2).$$

as was shown in reference 12 for example. It follows from comparison of (4) and (5) that

$$K = \frac{1}{v} h\nu (B_{\nu 1} n_1 - B_{\nu 1} n_2) = \frac{1}{v} B_{\nu 1} h\nu \left(n_1 - n_2 \frac{C^*}{C}\, e^{\frac{h(\nu_0 - \nu)}{kT}} \right). \qquad (6)$$

Substituting n_1 and $n_2 = n - n_1$ into (6), and taking account of Eq. (3), we obtain

$$K = K_0 \frac{\beta + \beta_1 \frac{C^*}{C} e^{\frac{h\nu_0}{kT}} \left(e^{-\frac{h\nu}{kT}} - e^{-\frac{h\bar{\nu}}{kT}} \right) J_{av}}{\beta + \beta_1 \left(1 + \frac{C^*}{C}\, e^{\frac{h(\nu_0 - \bar{\nu})}{kT}} \right) J_{av}}. \qquad (7)$$

Here $K_0 = (1/v) B_{\nu 1} h\nu n$ is the absorption index for low radiation density, and $\beta = \bar{A} + \bar{d}$.

Let us analyze the expression obtained.

1. For $\nu = \bar{\nu}$, Eq. (7) becomes

$$K = K_0 \frac{1}{1 + \beta_1 \tau \left(1 + \frac{C^*}{C}\, e^{\frac{h(\nu_0 - \bar{\nu})}{kT}} \right) J_{av}}, \qquad (8)$$

where $\tau = 1/(\bar{A} + \bar{d})$ is the average lifetime of the excited state. It follows from Eq. (8) that the greater the values of τ and J_{av}, the greater the decrease in K. For $J_{av} \to \infty$, $K \to 0$, despite the fact that a certain number of centers remains in the unexcited state (see Eq. 2). The absorptivity for a given frequency also strongly depends on the width of the spectral interval of the exciting light, because when it increases, $\bar{B}_1 = \int_{\nu_p} B_{\nu 1} d\nu_p$ increases too.

If there are no nonradiative transitions in the system, then $\bar{B}_1 \tau = B_1 / \bar{A}$. From Neporent's work[13] it follows that

$$\frac{B_{\nu 1}(\nu)}{\bar{A}_\nu(\nu)} = \frac{C}{C^*}\, e^{-\frac{h(\nu_0 - \nu)}{kT}} \frac{c^3}{8\pi h \nu^3},$$

which means that*

*This condition holds when the particles are excited by the light over the entire spectral absorption region.

$$\frac{B_1}{\bar{A}} = \frac{Cc^3 q}{C^* 8\pi h}\, e^{-\frac{h\nu_0}{kT}} \cdot e^{\frac{h\nu}{kT}}. \qquad (9)$$

Taking account of condition (9), when the nonradiative transitions to the ground state are absent Eq. (8) can be written as

$$\frac{K}{K_0} = \frac{1}{1 + \frac{Cc^3 q}{8\pi h C^* \nu^3} e^{\frac{h\nu}{kT}} \left(Ce^{-\frac{h\nu_0}{kT}} + C^* e^{-\frac{h\nu}{kT}} \right) J_{av}}. \qquad (10)$$

It is seen from (10) that K/K_0 is independent of τ. However, some authors[14, 15] mistakenly think that even when the quantum yield of luminescence (small value of d) is large, one does not observe clarification because of the short average lifetime of the excited state.

The fact that K/K_0 does not depend on τ can be explained as follows. As was shown by Einstein, the ratio of the coefficients $A \sim 1/\tau$ and B for any two levels depends only on the distance between them and on the degree of degeneracy, and is equal to $(g/g^*)(8\pi h\nu^3/c^3)$, where g and g^* are the statistical weights of the lower and higher levels respectively. Therefore, as the mean lifetime of the excited state increases, the absorptivity decreases and the produce $\bar{B}_1 \tau$ remains constant. In a system consisting of two electronic levels, a dependence

of K/K_0 on τ appears only when the probability of nonradiative transition is much greater than the probability of radiative transition.

The results obtained for $\nu = \bar{\nu}$ also apply perfectly to the case in which the excitation of molecules is produced by the monochromatic light for which the value of the absorption index is determined.

2. Let us consider the case in which $\nu \neq \bar{\nu}$. For the sake of concreteness, let $\bar{d} = 0$ and let the object be acted on by a radiation field corresponding to the radiation of an absolutely black body. In this case

$$J_{\nu\nu_0} = \frac{8\pi h\nu_{\nu\nu_0}^3}{c^3} \frac{1}{e^{\frac{h\nu_{\nu\nu_0}}{kT_1}} - 1}, \tag{11}$$

where T_1 is the temperature of the absolutely black body. Substituting the value $J_{\nu\nu_0}$ in (7) and using (9), we get (when $\nu \approx \nu_{\nu\nu_0}$)

$$\frac{K}{K_0} = \frac{e^{\frac{h\nu_0}{kT}}\left[e^{-\frac{h\bar{\nu}}{kT}}\left(e^{\frac{h\bar{\nu}}{kT_1}} - 1\right) + e^{-\frac{h\bar{\nu}}{kT}} - e^{-\frac{h\nu}{kT}}\right]}{e^{\frac{h(\nu_0-\bar{\nu})}{kT}}\left(e^{\frac{h\bar{\nu}}{kT_1}} - 1\right) + e^{\frac{h(\nu_0-\bar{\nu})}{kT}} + \frac{C}{C^*}}. \tag{12}$$

It follows from this expression that when $\nu > \bar{\nu}$ the absorption is always greater than zero. As the analysis of formula (12) shows, if $\nu < \bar{\nu}$ and the condition

$$\nu < \bar{\nu}\left(1 - \frac{T}{T_1}\right) \tag{13}$$

is satisfied, the absorption index becomes negative. Therefore, the intensity of the parallel light beam going through the medium does not decrease, but increases exponentially. This phenomenon occurs whenever the inequality $B_{ri}n_i < B_{ir}n_r$ holds because of some external influence on the substance (see Eq. 6). In this case, when the object is acted on by light covering a broad spectral range, light energy at some of the frequencies is used to excite the molecules, and is given off as light quanta of other frequencies. A peculiar source of light energy transformation is obtained.

The derivation of Eq. (7) is based on the assumption of strong interaction between absorbing centers and the surrounding medium. For noncondensed systems (vapors, gases) this condition does not hold in most cases.

As was shown in reference 11, one can state with a high degree of accuracy that

$$\rho^*(E_k^*) = \rho[E_k^* - h(\nu - \nu_0)],$$

for these systems, where ν is the frequency of the exciting light. Assuming that for the vapors of many complex molecules[16, 17] the oscillator strength is independent of temperature, one can consider $B_i(E_k)$ to be constant at different values of E_k. Therefore, if $g^*(E_k^*) = g(E_k)$ for $E_k^* = E_k$, it is easy to show that $\bar{B}_i = B_i = B$. If we calculate the absorption index for these conditions, we get

$$\frac{K(\nu)}{K_0(\nu)} = \frac{1}{1 + 2\frac{B}{\bar{\rho}} J_{\nu\nu_0}}. \tag{14}$$

It should be mentioned that if the vibrational structure of the levels is neglected, the equation for K/K_0 has the same form as (14) except that the mean probability values are replaced by the probabilities for the corresponding transitions between the two levels. In the latter case, if $d = 0$, then

$$\frac{K}{K_0} = \frac{1}{1 + \frac{c^3}{4\pi h\nu^3} J}. \tag{15}$$

and when degeneracy exists

$$\frac{K}{K_0} = \frac{1}{1 + \left(1 + \frac{g_2}{g_1}\right)\frac{c^3}{8\pi h\nu^3} J}, \tag{16}$$

where g_1 and g_2 are the statistical weights of the lower and upper energy levels respectively.

Let us consider the conditions under which one can actually observe the phenomenon of clarification in a substance. For example, let the object be acted on by radiation of intensity given by Eq. (11). In this case it is easy to determine the temperatures of the light source corresponding to the different values of K/K_0. In fact, if we substitute the value of J from (11) into (15), we obtain the expression

$$\frac{K}{K_0} = \frac{e^{\frac{h\nu}{kT_1}} - 1}{e^{\frac{h\nu}{kT_1}} + 1}, \tag{17}$$

It follows from (17) that in the visible part of the spectrum we need a temperature of the order of 10,000°K to decrease the absorption index by 10%, and 30,000°K to decrease it by 50%. If $g_2 > g_1$, absorption is decreased even more drastically.

At the present time, impulse light sources are widely used; in these light sources, the energy distribution in the visible and ultraviolet is close to black body radiation between 10,000°K and 100,000°K.[18–20] One would therefore expect to observe a change in the absorptivity of luminescent objects when working with these light sources.

So far, we have examined absorption processes arising from electron transitions between two electron levels. When electron transitions take place among three energy levels, absorption is of a somewhat different type.

In order to explain the main characteristics of such a system, we shall neglect the vibrational structure of electron levels. We will number the levels in such a way that the bigger the number of a level, the greater its energy. Let light of two frequencies ν_{13} and ν_{23}, corresponding to the transitions 1–3 and 2–3, fall on the object. When a stationary state is established, the particle distribution among the levels is easily determined by the method used, for example, in reference 21. Neglecting heat radiation, we have

$$\left.\begin{aligned} n_1 &= \frac{n}{\Delta}\left[p_{21}(p_{31} + p_{32}) + p_{31}B_{13}J_{13}\right. \\ &\left. + (p_{21} + p_{31})B_{23}J_{23} + B_{23}J_{23}B_{13}J_{13}\right], \\ n_2 &= \frac{n}{\Delta}\left[p_{32}B_{13}J_{13} + B_{13}J_{13}B_{23}J_{23}\right], \\ n_3 &= \frac{n}{\Delta}\left[p_{31}B_{13}J_{13} + B_{13}J_{13}B_{23}J_{23}\right], \end{aligned}\right\} \tag{18}$$

where n_1, n_2, n_3 are the number of particles per unit volume in levels 1, 2, 3; J_{13} and J_{23} are the light intensities of frequencies ν_{13} and ν_{23};

$$\Delta = p_{21}(p_{32} + p_{31}) + (p_{32} + 2p_{31})B_{13}J_{13} + (p_{21} + p_{31})B_{23}J_{23} + 3B_{13}J_{13}B_{23}J_{23}; \qquad p_{ji} = A_{ji} + d_{ji}.$$

It is interesting to examine two fundamentally different cases of absorption: absorption of the light of frequency ν_{31} and of frequency ν_{32}.

1. Remembering that the absorption index K_{ij} is determined from the equation

$$K_{ij} = \frac{1}{c} B_{ij} h\nu_{ij}(n_i - n_j),$$

we find for K_{13}

$$K_{13}=K_0\frac{p_{21}(p_{21}+p_{23})+(p_{21}+p_{31})B_{23}J_{23}}{p_{21}(p_{31}+p_{23})+(p_{23}+2p_{21})B_{13}J_{13}+(p_{21}+p_{31})B_{23}J_{23}+3B_{23}J_{23}B_{13}J_{13}}. \quad (19)$$

It follows from the analysis of this formula that if $J_{13} \to \infty$ then $K_{13} \to 0$ for any J_{23}. In addition, it should be pointed out that the absorption index never has values smaller than zero. For finite values of J_{13} and J_{23}, the presence of J_{23} radiation can either increase or decrease K_{13} depending on the relationship of the probabilities for corresponding transitions. If $J_{23} = 0$, then

$$K_{13}=K_0\frac{1}{1+\dfrac{p_{23}+2p_{21}}{p_{21}(p_{31}+p_{23})}B_{13}J_{13}}. \quad (20)$$

It follows from Eq. (20) that in this case, for a definite relationship of transition probabilities, the absorption index can be considerably smaller than in a two-level system.

2. For the absorption index K_{23} we have

$$K_{23}=\frac{1}{c}B_{23}h\nu_{23}n\times \quad (21)$$

$$\times\frac{(p_{23}-p_{21})B_{13}J_{13}}{p_{21}(p_{23}+p_{31})+(p_{23}+2p_{21})B_{13}J_{13}+(p_{21}+p_{31})B_{23}J_{23}+3B_{23}J_{23}B_{13}J_{13}}.$$

It is seen in (21) that if $p_{21} > p_{23}$ the absorption index becomes negative. Moreover, the presence of J_{23} simultaneously with J_{13} always decreases the absolute magnitude of K_{23}. For $J_{13} \to \infty$ we have

$$K_{23}=\frac{1}{c}B_{23}h\nu_{23}n\frac{p_{23}-p_{21}}{p_{23}+2p_{21}+3B_{23}J_{23}}, \quad (22)$$

so that if J_{23} is very large, K_{23} cannot be less than zero.

In conclusion, the author expresses his deep gratitude to A. S. Toporets for proposing this topic and for his interest in this work, and also to N. G. Bakhshiev and O. P. Girin for a number of comments and consultations.

REFERENCES

1. S. I. Vavilov. Izv. Fiz. Inst. pri. Moskov. Nauch. Inst. 1, 92 (1920); see also Sbornik Soch. (Collected Works) 1, 80 (1954).
2. S. I. Vavilov and W. L. Lewschin. Z. Phys. 35, 920 (1926); see also S. I. Vavilov. Sbornik Soch. 1, 195 (1954).
3. G. Lewis, T. Magel, and D. Lipkin. J. Am. Chem. Soc. 63, 3005 (1941).
4. G. Lewis, T. Magel, and D. Lipkin. J. Am. Chem. Soc. 66, 1579 (1944).
5. R. Karplus and J. Schwinger. Phys. Rev. 73, 1020 (1948).
6. R. Carten and W. Smith. Phys. Rev. 73, 1053 (1948).
7. H. Townes. Phys. Rev. 70, 665 (1946).
8. B. Bleaney and R. Penrose. Proc. Roy. Soc. A189, 358 (1947).
9. B. Bleaney and R. Penrose. Proc. Phys. Soc. 60, 83 (1948).
10. B. Ya. Sveshnikov. Doklady Akad. Nauk SSSR 51, 675 (1946).
11. B. S. Neporent and B. I. Stepanov. Uspekhi Fiz. Nauk 43, 380 (1951).
12. B. I. Stepanov. "Liuminestsentsia slozhnych molekul," Part I. (Luminescence of Complex Molecules), Izd. Akad. Nauk Belorus. SSR, 1955.
13. B. S. Neporent. Izvest. Akad. Nauk SSSR, Ser. Fiz. 22, No. 11, 1372 (1958).
14. Vawilov. "Mikrostruktura Sveta," p. 71. (Find Structure of Light), Izd. Akad. Nauk SSSR, 1950.
15. V. L. Levshin. "Fotoliuminestsentsia zhidkich i tverdych tel," p. 143. (Photoluminescence of Liquids and Solids), Gosudarst. Izd. Tekh.-Teoret. Lit., 1951.
16. F. Almasy and H. Laemmel. Helv. Chim. Acta. 33, 2092 (1950).
17. B. S. Neporent and N. G. Bakhshiev. Opt. i Spektr. 5, 634 (1958).
18. I. S. Marshak. Sbornik Mater. po Vakuum. Tech. 7, 3 (1955).
19. M. P. Vaniukov, A. A. Mak, and M. Ya. Ures. Opt. i Spektr. 4, 90 (1958).
20. N. N. Ogurtsova and I. V. Podmoshenskii. Opt. i Spektr. 4, 539 (1958).
21 V. V. Antonov-Romanovskii, B. I. Stepanov, M. V. Fok, and A. P. Khapaliuk. Doklady Akad. Nauk SSSR 105, 50 (1955).

ON THE INFLUENCE OF THE WIDTH OF THE MONOCHROMATOR SLITS ON THE ACCURACY OF PHOTOELECTRIC MEASUREMENTS OF THE INTENSITY OF RAMAN LINES

E. V. Chisler

Received 26 May 1959

The dependence of the mean-square error of the measurements of the line intensity on the width of the monochromator slits is examined from the viewpoint of the choice of optimum scanning conditions of the spectrum.

A large number of papers[1-9] have been devoted recently to the method of photoelectric recording of Raman spectra. One of the main questions of this method is the problem of increasing the signal-to-noise ratio at the output of the recording system. The aim of this note is to give a semiquantitative examination of the influence of the monochromator slit width on the value of the signal-to-noise ratio.

In the case of an ideal spectrometer (i.e., under the conditions where it is possible to neglect diffraction and aberrations of its optical part, and also in the absence of inertial distortions during the process of recording the spectrum) the value of the ordinate of the maximum $I(\nu_0)$ of the contour of the recorded spectral line of a dispersion form is defined by the expression

$$I(\nu_0) \sim \frac{\sigma^2}{2}\left(\alpha \arctan\alpha - \beta \arctan\beta + \frac{1}{2}\ln\frac{1+\beta^2}{1+\alpha^2}\right),$$

where $\alpha = (S_1 + S_2)/\sigma$, $\beta = (S_1 - S_2)/\sigma$, σ is the half-width of the line, and S_1 and S_2 are the widths of the entrance and exit slits of the monochromator, respectively.

In the recording of a continuous spectrum the value of the deflection of the needle of the electrophotometer I_Φ is proportional to the product S_1S_2. The dependence of $I(\nu_0)$ and I_Φ on S and σ for $S_1^2 = S_2 = S$ is presented in Fig. 1. (S and σ are expressed in the same arbitrary units.) As seen from the figure, for $\sigma \gg S$ the dependence of $I(\nu_0)$ on S is identical for all lines and is close to quadratic. For large values of the slits the relation of the measured magnitudes of the intensities of lines of different half-width changes continuously in its dependence on the monochromator slit width until, finally, there is established some constant value of the relation $(I(\nu_0) \sim S)$, appearing just as the ratio of the integrated intensities of the lines.

In Fig. 2 is presented the dependence of the quantity $I(\nu_0)$ on the width of the exit slit of the monochromator for a constant width of the entrance slit, $S_1 = 10$. The figure does not need any particular explanation. We will note only that the part of the graph common to all lines, where $I(\nu_0) \sim S_2$, is determined by the width of the entrance slit, and by the normalizing to 1 of the peak intensities of all lines in the plane of the picture.

While the curves in Figs. 1 and 2 were obtained for lines having a dispersion contour, it is evident from an examination of the graphs that the general character of the dependence applies also in the case of other possible forms of the Raman lines. In Particular, it is possible to assert that:

1. For $S_1 = S_2 = S$ and $S \ll \sigma$, independently of the form and width of the line, $I(\nu_0) \sim S^2$; and for $S \gg \sigma$, $I(\nu_0) \sim S$;

2. For S_1 = const. and $S_2 \leqslant S_1$, $I(\nu_0) \sim S_2$, and for $S_2 \gg S_1 + \sigma$, $I(\nu_0)$ = const.

It is also evident that for a given line the value of

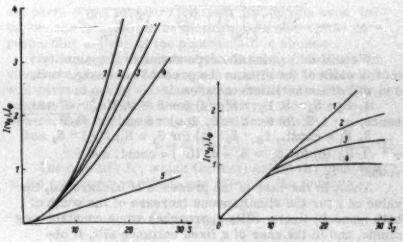

Fig. 1

Fig. 2

Fig. 1. Dependence of the quantities I_Φ (curve 1) and $I(\nu_0)$ (curves 2-5) on the width of the monochromator slits S ($S_1 = S_2 = S$) for different values of the line half-width, σ. Curve 1—$I_\Phi = S^2$; curves 2-5—σ is equal, respectively, to 20, 15, 10, and 2.

Fig. 2. Dependence of the quantities I_Φ (curve 1) and $I(\nu_0)$ (curves 2-4) on the width of the exit slit of the monochromator S_2 for a constant width of the entrance slit ($S_1 = 10$) and different values of the line half-width, σ. Curve 1—$I_\Phi = S_2$; curves 2-4—σ is equal, respectively, to 20, 10, and 2 (S and σ are expressed in the same arbitrary units).

$I(\nu_0)$ cannot increase faster than the quantity S^2 in the first, or the quantity S_2 in the second case.

Proceeding from these considerations we will find the dependence of the relative mean square error (γ) of the measurement of the line intensity at the maximum connected with the fluctuations of the current of the photomultiplier, on the monochromator slit widths, considering the dark current of the FEU to be small by comparison with the photocurrent.

We will examine the case where it is possible to neglect the intensity of the continuous background in the region of the line by comparison with the intensity of the line itself. As is well known, the mean square fluctuation of the current of the FEU is $\sqrt{\Delta i} \sim \sqrt{i}$, and, accordingly

$$\gamma = \frac{\sqrt{\Delta^2 I(\nu_0)}}{I(\nu_0)} \sim \frac{\sqrt{I(\nu_0)}}{I(\nu_0)}.$$

From this we find for the case $S_1 = S_2 = S$: (a) for $S \ll \sigma$, $I(\nu_0) \sim S^2$ and $\gamma \sim 1/S$; (b) for $S \gg \sigma$, $I(\nu_0) \sim S$ and $\gamma \sim \sqrt{1/S}$.

Analogously, in the case of a constant entrance slit, S_1 = const., we obtain: (a) for $S_2 \ll S_1$, $I(\nu_0) \sim S_2$ and $\gamma \sim \sqrt{1/S_2}$; (b) for $S_2 \gg S_1 + \sigma$, $I(\nu_0)$ = const. and γ = const.

Thus, in the absence of background, the quantity γ appears as a monotonic function of the width of the monochromator slits, and in the case of a simultaneous widening of both slits its value can be made as small as desirable.

In the presence in the region of the line of a continuous background of constant intensity I_Φ, comparable to the line intensity, the ordinate of the maximum of the recorded contour will be defined by

$$I(\nu_0) \pm \Delta I(\nu_0) = [I(\nu_0) + I_\Phi] \pm \Delta[I(\nu_0) + I_\Phi] - I_\Phi \pm \Delta I_\Phi$$

and the relative mean square error of the measurement will equal

$$\gamma = \frac{\sqrt{\Delta^2[I(\nu_0) + I_\Phi] + \Delta^2 I_\Phi}}{I(\nu_0)} \sim \frac{\sqrt{I(\nu_0) + 2I_\Phi}}{I(\nu_0)}.$$

We will determine the dependence of the quantity γ on the width of the slits in the presence of background, and will examine different cases.

1. $S_1 = S_2 = S$, $I_\Phi \sim S^2$: (a) for $S \ll \sigma$, $I(\nu_0) \sim S^2$ and, hence, $\gamma \sim 1/S$; (b) for $S \gg \sigma$, $I(\nu_0) \sim S$ and $\gamma \sim \sqrt{1/S + \text{const}}$.

2. S_1 = const., $I_\Phi \sim S_2$: (a) for $S_1 \geq S_2$, $I(\nu_0) \sim S_2$ and $\gamma \sim \sqrt{1/S_2}$; (b) for $S_2 \gg S_1 + \sigma$, $I(\nu_0)$ = const. and $\gamma \sim \sqrt{\text{const.} + S_2}$.

Thus, in the case of the presence of background, the value of γ for the simultaneous increase of the width of both monochromator slits approaches some constant magnitude, and in the case of a fixed entrance slit, it obviously has a minimum near $S_2 = S_1 + \sigma$.

The dependence of the quantity γ obtained can be useful for a choice of the optimum width of the slits in different concrete cases. In the general case, for the appearance of weak lines on a background of a continuous spectrum the conditions will evidently be optimum when $S_1 \approx S_2 \approx \sigma$. A further increase of the width of both slits (or of one of them), making the resolution poorer, gives a comparatively small gain in the photometric accuracy, since even in the first and by far the more common case, the dependence of γ on S will be close to $\sqrt{1/S}$. For the recording of single lines, when the resolution conditions do not limit the slit widths, the optimum will obviously be when S_1 has a maximum width and $S_2 = S_1 + \sigma$.

In conclusion, we will touch upon the question of contrast, i.e., the factor defining the possibility of photoelectric recording of weak lines on a background of an intense continuous spectrum. The idea of contrast in this sense is the equivalent current resolving power of the photometer, which is defined naturally as $\xi = r/\sqrt{\Delta^2 r}$, where r is the difference between the two currents and $\sqrt{\Delta^2 r}$ is the mean square error of the measurement of r. This definition is identical to the definition of ξ as $\xi = 1/\gamma$. Using the relationships obtained above, we find

$$\xi = \frac{1}{\sqrt{\frac{1}{S} + \text{const}}}.$$

Thus, the possibility of an increase in the contrast by opening the slits is limited not only practically but also fundamentally. In order to find the dependence of γ on the intensity of the exciting source of the spectrum, E, on the sensitivity of the FEU photocathode, m, and on the width of the transmission band of the photometer, $\Delta\omega$ (for constant slit widths), we write ξ in the form

$$\xi = \frac{\sqrt{\Delta^2[I(\nu_0) + I_\Phi] + \Delta^2 I_\Phi}}{I(\nu_0)}.$$

Putting $I(\nu_0) \sim maE$, $I_\Phi \sim mbE$, $\Delta^2[I(\nu_0) + I_\Phi] \sim \Delta\omega m(a + b)E$ and $\Delta^2 I_\Phi \sim \Delta\omega mbE$, where a and b are constants, we find

$$\xi \sim \sqrt{\frac{mE}{\Delta\omega}} \frac{a}{\sqrt{a + b}}.$$

It is evident that the possibility of an increase of the contrast due to m and E will be limited practically by the stability of these factors.

The author considers it his pleasant duty to thank P. P. Pavinskii, A. I. Stekhanov, and E. F. Gross for their interest in the present work and its discussion.

REFERENCES

1. M. M. Sushchinskii. Izvest. Akad. Nauk SSSR, Ser. Fiz. 14, 387 (1950).
2. M. M. Sushchinskii. Trudy Fiz. Inst. Akad. Nauk SSSR 5, 185 (1950).
3. Ya. S. Bobovich and V. M. Pivovarov. Zhur. Eksptl. i Teoret. Fiz. 29, 696 (1955).
4. Ya. S. Bobovich and D. B. Gurevich. Izvest. Akad. Nauk SSSR, Ser. Fiz. 19, 48 (1955).
5. I. S. Abramson and A. N. Mogilevskii. Izvest. Akad. Nauk SSSR, Ser. Fiz. 19, 49 (1955).
6. Ya. S. Bobovich and V. M. Pivovarov. Uspekhi Fiz. Nauk 60, 688 (1956).
7. O. Brandmüller and O. Moser. Z. angew. Phys. 8, 95 (1956).
8. O. Brandmüller and O. Moser. Z. angew. Phys. 8, 142 (1956).
9. S. G. Rautian. Uspekhi Fiz. Nauk 66, 475 (1958).

PHOTOELECTRIC METHOD OF RECORDING INTERFERENCE FRINGES IN WHITE LIGHT

T. S. Kolomiitsova and I. V. Novikova

Received 26 May 1959

Photoelectric methods of isolation and recording of the central white fringe in a system of white light interference fringes were examined. The results of the calculations of the magnitude of photocurrents that are obtained during such recordings are presented, and the experimental arrangements and investigations are described, based on the methods developed here. It is shown that, in principle, the automation of measurements on white light interferometers is possible.

At present many studies are known that are devoted to the discussion of photoelectric methods of recording of interference fringes in monochromatic light (for example, references 1 and 2). The aim of these investigations appeared to be the verification of the possibility of rapid counting of a large number of like interference fringes. A recent publication was devoted to the calculation of the distribution of energy in interference fringes for the case of a source emitting light in a spectral region of very narrow, though finite width.[3] In such a case the interference field contains a fairly large number of fringes.

It is well known that a white light interference pattern contains a small number of fringes which differ in brightness and in color. The most outstanding property of this pattern is the presence in the system of fringes of an achromatic fringe, which distinguishes itself from the others and which may be used as a reference mark for the setting and counting of fringes. For this reason, interferometers operating in white light, in contrast to interferometers working with monochromatic light, can be applied in all those cases where it is necessary to measure discontinuous changes in path differences (for example, for the comparison of the lengths of components with the length of an etalon).

A photoelectric method of isolation of the central achromatic fringe from a system of interference fringes and a method for the determination of its location are necessary for the automation of measurements on interferometers employing white light. This problem differs basically from the problem of the photoelectric recording of interference fringes in monochromatic light.

The central bright achromatic fringe is the brightest fringe in the system of white light interference fringes, since for path differences close to zero it is the only one for which the result of interference is the same with light of all (or nearly all) wavelengths.* In visual observation the eye distinguishes fringes from one another not so much by brightness as by color. Because of this, the observer easily isolates the achromatic fringe as the only white one in a system of colored fringes. It is well known that photoelectric receivers do not distinguish colors, and hence, when applying them to the setting onto white fringes it is only necessary to be aware of the energy relationship between the radiation flux from different parts of the interference field, for, in this case, interference fringes can be distinguished only by the corresponding signals of the photosensitive element.

*All further considerations in this article are based on the assumption that the bright fringe is achromatized and that there is no difference of the phase changes for the interfering rays. This does not affect the generality of the arguments, as the isolation of a fringe with the smallest signal does not differ in principle in any way from the isolation of a fringe with the largest signal when the relationship of light flux from the corresponding parts of the interference field is the same.

An energy calculation of the intensity of fringes for visual observation of the interference field in white light was carried out by Gershun,[4] who obtained the following expression for the resulting intensity B for the case of interference of two beams of equal intensity b

$$B = 2b\,(1 + S_\Delta). \tag{1}$$

The quantity S_Δ, which Gershun called the measure of the interference effect, was given by the formula

$$S_\Delta = \frac{\int_0^\infty v(\lambda)\, r_e(\lambda) \cos\frac{2\pi\Delta}{\lambda}\, d\lambda}{\int_0^\infty v(\lambda)\, r_e(\lambda)\, d\lambda}, \tag{2}$$

where $v(\lambda)$ is the visibility curve, $r_e(\lambda)$ is the spectral energy distribution of the emitting light source, Δ is the optical path difference of the interfering beams, and λ is the wavelength of the light.

Assuming that the function $r_e(\lambda)$ is given by Wien's law and the function $v(\lambda)$ by Gol'dhammer's empirical formula, Gershun calculated the values of S_Δ corresponding to various values of the path difference Δ. In Fig. 1, a graph is shown that was obtained in this way and which shows the dependence of S_Δ on Δ for an interference field containing the zero order fringe at the center. From the graph it is seen that alongside the zero order fringe, the eyes perceive 4-5 fringes of diminishing intensity. The difference in intensity between the zero order and the first fringes is very small, namely less than 10%, yet the eye easily distinguishes the fringes by their color.

In the present study, analogous energy calculations were carried out for the case of photoelectric recording of the white light interference field. During the interference of two light beams of equal magnitude and spectral composition, to each one of which corresponds a photoelectric current i, the resulting photoelectric current is given by the formula

$$I = 2i\,(1 + S_\Phi), \tag{3}$$

where the quantity S_Φ, which can also be called the measure of the interference effect, is given by the formula

$$S_\Phi = \frac{\int_{\lambda_1}^{\lambda_2} \gamma_\Phi(\lambda)\, r_e(\lambda) \cos\frac{2\pi\Delta}{\lambda}\, d\lambda}{\int_{\lambda_1}^{\lambda_2} \gamma_\Phi(\lambda)\, r_e(\lambda)\, d\lambda} \tag{4}$$

Here $\gamma_\Phi(\lambda)$ is the corresponding spectral sensitivity of the

photoelectrode; the remaining notation is the same as in formula (2).*

*When layers with selective spectral reflection or absorption are present in the interferometer, it is necessary to introduce into both expressions under the integral signs in formula (4) an additional multiplying factor which specifies the change in the spectral constitution of the interfering light beams after passing through the interferometer. This case is not considered in this paper.

The quantity S_Φ was evaluated by the method of graphical integration as the functions $\gamma_0(\lambda)$ and $r_*(\lambda)$ were given in the form of curves or tables.

Fig. 1. Curve representing the relationship of the quantity S_Φ on the path difference Δ (according to reference 4).

From formula (4) it can be seen that the quantity S_Φ is different for different interference fringes (because each fringe corresponds to a given path difference Δ). Thus, it defines the change due to interference in the photoelectric signal from different points of the interference field.

In order to be able to assess the possibility of the detection of the central fringe in a system of white light interference fringes, it is necessary to know how much larger is the photoelectric signal from the central fringe than the largest signal from any of the other fringes. Therefore, the difference between the photoelectric signal I_0 from the central fringe and the largest of the signals I_k, corresponding to the other fringes, divided by the magnitude of the signal I_0, can serve as a quantitative characteristic of the given photoelectric method. This quantity we shall here call the photoelectric difference and designate it by the letter m. Obviously

$$m = \frac{I_0 - I_k}{I_0} \cdot 100\ (\%). \qquad (5)$$

For the zero order fringe $S_{\Phi 0} = 1$, since $\Delta = 0$ for all λ. Thus, in an interference field with the zero order fringe at the center,

$$m = \frac{1}{2}(1 - S_{\Phi_k}). \qquad (6)$$

Calculations show that in an interference pattern with an achromatic fringe not of zero but, for instance, of the third or fifth order (as is the case in most interferometers) the photoelectric difference is noticeably reduced.

The question of possible ways of increasing the photoelectric difference is very important, because the quantity m determines the stability of operation of the photoelectric current amplifiers and the degree of dependence of the resultant signals on accidental disturbances and the instability of the voltage of the power supply. From formula (4) it follows that, for a given type of white light interference field, the photoelectric difference will be larger, the wider the spectral region of sensitivity of the photoelectric receiver.

A considerable widening of the region of sensitivity can be obtained by connecting in parallel the photomultipliers with different spectral characteristics. In Fig. 2

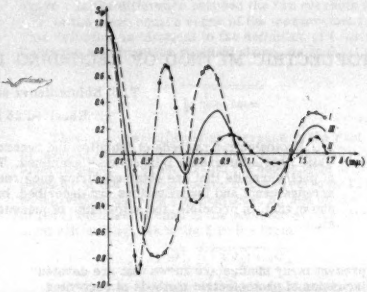

Fig. 2. Curve representing the relationship of the quantity S_Φ and the path difference Δ. Curve I—using photomultiplier FEU-22; curve II—same for FEU-19; curve III—when both photomultipliers are connected in series.

are shown curves of the dependence of S_Φ on the path difference, calculated for an interference field with a zero order fringe at the center. From the graph it is seen that when using one of the photomultipliers FEU-22 (maximum spectral sensitivity at $\lambda \cong 0.8\mu$) or FEU-19 (maximum spectral sensitivity at $\lambda \cong 0.4\mu$) the photoelectric difference m is about 15% (curves I and II, respectively). When these photomultipliers are connected in parallel, the photoelectric difference increases to 35% (curve III).*

*Germanium photodiodes, which are convenient in use and which, as is well known, possess a very wide region of spectral sensitivity, were applied in preliminary experiments as photoelectric receivers for the recording of white light fringes. These experiments showed that the photodiode allowed the central fringe to be isolated with precision in those interferometers in which the intensity of the interference pattern was sufficiently large. The development of a compact multistage amplifier well protected from external noise should also make possible the application of germanium photodiodes with interferometers of smaller intensities.

Several photoelectric methods of isolation of the achromatic fringe from a system of white light interference fringes, proposed by Academician Linnik, were tried out in this work: (1) based on the maximum energy value; (2) based on the magnitude of the maximum rate of increase of energy (with equal fringe widths the rate of increase of energy will be a maximum for the brightest fringe); and (3) based on the spectral composition (that is by the coincidence of the results of interference over a broad spectral region).

In this paper attention will be paid mainly to the first method, and the third method will not be examined at all.

For the experimental examination of the proposed methods of recording of white light fringes, we employed specially assembled laboratory equipment and commercially produced interferometers. The photoelectric arrangement, whose outline is shown in Fig. 3, was always applied for the recording. A real image of the interference pattern seen in the field of view of the apparatus was formed with the aid of a subsidiary optical system in a plane PP which is outside of the employed interferometer. A slit 1 was placed in this plane, whose width was about 6-8 times smaller than the width of the central white fringe and which was parallel to the interference

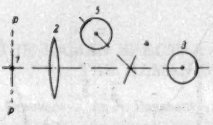

Fig. 3. Principal outline of the photoelectric arrangement for recording of interference fringes. 1—slit; 2—condensing lens; 3—photomultiplier FEU-22; 4—semitransparent mirror; 5—photomultiplier FEU-19.

fringes. The light, after passing through the slit, was directed by a condensing lens 2 onto the cathode of the photomultiplier 3 (FEU-22). In order to be able to use two different photomultipliers, without incurring significant light losses, a semitransparent mirror, 4, with a special coating and which directed the reflected light onto the photomultiplier 5 (FEU-19) was placed behind the condensing lens. The transmission curve of the mirror is shown in Fig. 4. It can be seen that onto each photomultiplier fell that spectral part of the illumination passing through the slit 1, which corresponded to the region of its spectral sensitivity. The absorption of the films in the coating was equal to zero.

The voltage of the power supply for the photomultiplier FEU-19 was chosen in such a way that, in the absence of fringes in the field of view of the interferometer, the photoelectric currents from both photomultipliers were equal. Both photomultipliers were connected in parallel through suitable resistances to the measuring instrument or to the terminal of a photocurrent amplifier. The measuring instrument registered the change in the output signal of the photomultipliers occurring when the interference fringes moved with respect to the slit 1.

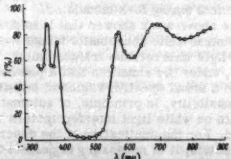

Fig. 4. Transmission curve of the semitransparent mirror.

A simulated command mechanism, consisting of an alternating current amplifier connected to a relay which closed the circuit of a power supply for a small electric lamp, was developed for the exploration of the fundamental possibility of automating the setting onto the central white fringe. The light falling onto the slit 1 was modulated by a disc-shaped shutter.* In order to reduce the noise level, a resonating circuit LC tuned to the frequency of the modulation of the light was connected to the terminal of the photomultipliers. A block diagram of the circuit for the recording of an alternating photoelectric current and of the simulated command mechanism is shown in Fig. 5.

The results of one series of experimental measurements are shown in Fig. 6.* Curves I–III represent the

*The use of modulation obtained by changing the voltage of the power supply of the light source is also possible.

*It must be mentioned that the results of many measurements with a direct photocurrent and with a modulated signal agree well with one another.

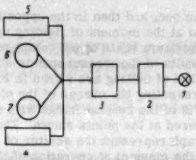

Fig. 5. Block diagram of the arrangement for the recording of an alternating photoelectric current and the simulated command mechanism. 6,7—photomultipliers FEU-19 and FEU-22; 5—resonating circuit; 4—millivoltmeter; 3—amplifier; 2—relay; 1—signal lamp.

change in the magnitude of the alternating photoelectric signal during the shift (with the aid of a compensator) of the interference fringes in the field of view of the interferometer, using successively the photomultipliers FEU-22, FEU-19, and both photomultipliers connected in parallel. The straight lines IV and V, parallel to the abscissa, indicate the magnitude of the signal corresponding to the background current in the absence of interference fringes. The asymmetry of the curves with respect to the central maximum shows the presence of imperfections in the adjustment of the apparatus; judging from the color of the fringes an achromatic fringe of the third or fourth order was observed in the interference field. It can be seen from this data that it would be impossible to isolate the central fringe from a system of fringes, using only one photomultiplier, because each of them gave two to three approximately equal maxima. But when the two photomultipliers were connected in parallel, the signal from the central fringe was approximately 25% greater than the largest signal from any other fringe (m = 25%).

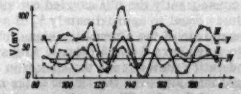

Fig. 6. The change in magnitude of the alternating photoelectric signal with a shift of the interference fringes (with the aid of a compensator) in the field of view of the interferometer (a—the scale units on the drum of the compensator). Curve I—when employing photomultiplier FEU-22 (m = 0); curve II—the same for FEU-19 (m = 10%); curve III—for both photomultipliers connected in parallel (m = 25%); curves IV, V—magnitude of the background signal in the absence of interference fringes.

Experiments were carried out which simulated automatic setting onto the central fringe. The amplifier of the simulated command mechanism (see schematic diagram in Fig. 5) was tuned in such a way that the relay operated and the small lamp lighted when a signal entered the amplifier, which was approximately 85% of the maximum signal, corresponding to the middle of the central fringe.* The interference fringes were shifted with a compensator past the slit of the photoelectric apparatus

*As is seen from Fig. 6, the signals from the other fringes are significantly lower than this level.

(Fig. 3) first in one, and then in the opposite direction, and every time at the moment of lighting up of the lamp a reading of the drum scale of the compensator was taken. The results of the measurements obtained using the above method of setting are shown in Fig. 7, where the curve representing the change of the photoelectric signal for shifts of the central fringe with respect to the slit was measured at the points shown. The shaded portions of the graph represent the scatter of readings corresponding to the moment of operation of the relay (points A_1 and A_2 show the mean values of these readings). The point B, placed at the center of the distance A_1A_2, nearly coincides with the point O, which is the coordinate of the center of the central fringe. By verifying that the scatter of points, corresponding to the moment of operation of the simulated command mechanism, does not exceed 0.05 of a fringe width, we can deduce that the accuracy of the photoelectric setting onto the center of the central fringe is also equal to 0.05 of a fringe width. When carrying out similar measurements on analogous arrangements with other interferometers, the accuracy of setting onto the central fringe was not less than 0.1 of a fringe width.

The equipment,described above for the isolation of the central white fringe by using the value of the maximum energy, possesses the disadvantage that it requires the stabilization of the power supply and the shielding of the equipment from external disturbances (electrical and luminous), as otherwise a good reproducibility of the results cannot be obtained. This can be overcome if one works instead with equipment which is based on the application of compensating methods.

The experimental examination of the possibility of the isolation of the central white fringe, using the method of maximum rate of increase of energy, was carried out with the aid of specially developed light modulators. The stationary slit, 1, in the photoelectric arrangement shown in Fig. 3, was replaced by a slit that was also placed parallel to the interference fringes, and which was fastened to the foot of a tuning fork. The electronic amplifying system actuated the tuning fork with an inverse coupling and consequently the slit carried out vibrations with an amplitude equal to approximately ½ of a fringe width. The magnitude of the alternating signal obtained from the photomultipliers 3 and 5 (Fig. 3) with such a system of modulation, determines the change in magnitude of the light intensity over the extent of the amplitude of vibration of the slit. The maximum value of the signal is then obtained at the locations in an interference field corresponding to the increase and decrease of intensity.

The curve I in Fig. 8 represents the magnitude of the direct photoelectric current, measured at the points shown, when the stationary slit is moved across the central fringe. Curve II represents the magnitude of the voltage of the alternating current, measured at the points shown for a corresponding shift across the fringe of the vibrating modulator. The analysis of the results of the experiment shows that, if the remaining conditions are equal, the accuracy of setting onto the central fringe is approximately twice as high when the simulated command mechanism is operating with the tuning fork modulator than the accuracy obtained with the disc modulator; this can be explained by the doubling of the number of maxima. At the same time however, (also because of the presence

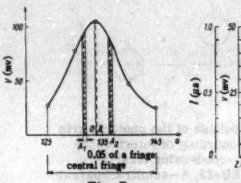

Fig. 7.

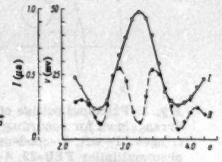

Fig. 8

Fig. 7. The areas of operation of the simulated command mechanism during the automatic setting onto the central fringe (a—scale units on the drum of the compensator). Fig. 8. The value of the direct photocurrent I and of the voltage of the alternating current V, measured during the shift across the central fringe of the stationary slit (curve I) and of the tuning fork modulator (curve II) respectively

of two equal maxima), the necessity appears of approaching the central fringe always from the same direction.

A more detailed investigation of the action of the tuning fork modulator, based on some supplementary experiments, showed that at times (especially when recording achromatic fringes of nonzero order, and also in the case of uneven distribution of intensity in the interfering beams) the method of isolation of the central fringe using the maximum rate of increase of energy proves to be the only one possible in practice. Also, in some cases it might be better (for instance, because of constructional considerations) to employ a stationary slit and an interference modulator of some other type in place of the mechanical tuning fork modulator.

Thus, the above work showed that it is possible to isolate the central white achromatic fringe from a system of white light interference fringes using photoelectric methods, under the condition that a photoelectric receiver with a broad spectral region of sensitivity is used. The possibility, in principle, of automation of measurements on white light interferometers was also demonstrated. For the application of the described method in practice, it is necessary to perfect the photoelectric and electronic amplifier parts of the apparatus, and also to adapt the construction of the photoelectric arrangement to the construction of an operating interferometer.

The authors express their deep gratitude to Academician V. P. Linnik for his interest in the problem and for his valuable advice.

REFERENCES

1. E. Peck and W. Obetz. J. Opt. Soc. Am. 43, 505 (1953).
2. R. Eisner. Rev. Sci. Instr. 29, 521 (1958).
3. G. D. Kahl and D. B. Sleator. J. Opt. Soc. Am. 48, 525 (1958).
4. A. A. Gershun. Doklady Akad. Nauk SSSR 53, 429 (1946).

THE RAMAN SPECTRA OF HYDROCARBONS OF DIFFERENT CLASSES
VI. THE RAMAN SPECTRA OF SOME ARYLCYCLOBUTANES

E. G. Treshchova, Iu. N. Panchenko, N. I. Vasil'ev, M. G. Kuz'min, Iu. S. Shabarov, and R. Ya. Levina

Received 3 July 1959

The Raman spectra of a series of arylcyclobutanes are obtained. In the spectra of all of the arylcyclobutanes studied frequencies are observed which are characteristic for the particular mono- and dialkylbenzenes and for alkylcyclobutanes. The Raman lines, characteristic of the four-membered ring, and of lines in the region ~1000-1600 cm^{-1}, characteristic of the benzene ring, have a higher intensity in the spectra of the arylcyclobutanes than the corresponding lines in the spectra of alkylcyclobutanes and alkylbenzenes, respectively. For the lines in the region ~600-800 cm^{-1}, characteristic of the benzene ring, such a rule is not observed.

In our preceding papers[1, 2] and in the work of other authors[3] it was shown that hydrocarbons with a three-membered ring show properties similar, to a certain degree, with the properties of olefins. In the Raman spectra of molecules containing a three-membered ring connected to a benzene ring, the intensity of some lines, characteristic of the benzene ring, appear greater than in the corresponding alkylbenzenes—an analogous situation to that observed if a double bond is conjugated with the benzene ring.

In the present work we posed the problem of deciding if the four-membered ring, bonded to the benzene ring, shows a similar influence, and of increasing the accuracy of the rules stated above.

We investigated the Raman spectra of phenyl cyclobutane and of a series of arylcyclobutanes with a different position of the second substituent on the benzene ring in relation to the four-membered ring: m-tolyl cyclobutane, p-tolyl cyclobutane, o-anisylcyclobutane, p-anisylcyclobutane, and also, for comparison, phenyl- and p-tolyl cyclopropane.

All of the arylcyclobutanes studied by us were synthesized by decomposition of the corresponding 3-aryl-1,4,5,6-tetrahydropyridazines in the presence of potassium hydroxide and platinum as described in the preceding papers:[2, 4, 5]

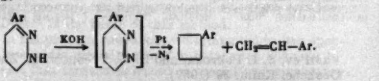

The physical constants of the arylcyclobutanes obtained in this manner (after their distillation in a column of 30 theoretical plates) are given in Table 1.

Table 1

Arylcyclobutane	Boiling point (°C) and vapor pressure (mm Hg)	n_D^{20}	d_4^{20}	MR_D Found	MR_D Calculated
Phenyl cyclobutane	189—190 (750)	1.5289	0.9375	43.32	43.06
m-tolyl cyclobutane	75.8—76.3 (9.5)	1.5346	0.9316	48.07	47.88
p-tolyl cyclobutane	93.5—93.7 (11)	1.5330	0.9275	48.16	
o-anisyl cyclobutane	90.5—91 (4)	1.5320	1.0040	50.05	49.44
p-anisyl cyclobutane	84.7—84.9 (4)	1.5360	1.0098	50.10	

The apparatus, the method of measurement, and the calculations of the Raman spectra were the same as described in the previous papers.[2]

In Table 2 are presented the Raman spectra of the arylcyclobutanes studied by us and, for comparison with them, the spectra of a few arylcyclopropanes. The intensities of the lines are given for optical slit widths ~23 and ~35 cm^{-1} (I_∞) and for some of them for an optical slit width ~16^{-1}, more convenient for analytical purposes.

The given values of I_∞ are connected with the integrated intensity of the lines by the relation

$$I_\infty = \frac{2}{\pi} \cdot I_{\text{int.}},$$

indicated in the monograph of Landsberg, Bazhulin, and Sushchinskii.[7] The intensities of the lines are expressed on an objective scale, in which I_∞ for the 802 cm^{-1} cyclohexane line is put equal to 500 units/mole.

As can be seen from Table 2, in the spectra of all of the arylcyclobutanes are observed intense frequencies, characteristic for mono- and disubstituted benzenes and for monosubstituted cyclobutane (lines in the region ~907-950 cm^{-1}). In Tables 3 and 4 the intensities of the lines characteristic of the benzene ring in the spectra of arylcyclopropanes, arylcyclobutanes, and alkylbenzenes are compared.

It is evident that it is profitable to compare the aryl cyclopropanes or aryl cyclobutanes with the alkyl benzenes having isopropyl or sec-butyl radicals, and having the identical positional substitution on the ring (ortho-, meta-, para-).

From Tables 3 and 4 it is seen that among the lines characteristic of the benzene ring, and given in these tables, the intensities of the lines with frequencies ~1000 cm^{-1} and greater in the spectra of the aryl cyclopropanes and aryl cyclobutanes, as has been stated, are higher than in the spectra of the corresponding alkyl benzenes.

The intensities of the lines indicated are several times higher for phenyl cyclopropane than for phenyl cyclobutane; however, in the spectra of p-tolyl cyclopropane and p-tolyl cyclobutane the intensities of these lines are close to one another. For the lines with frequencies less than ~1000 cm^{-1} (in the region ~600-800 cm^{-1}) the rules stated above do not hold. Thus the increase of the intensities of the characteristic lines of the benzene ring in aryl cyclopropanes, by comparison with alkyl benzenes which was noted earlier,[1, 2] is also observed in aryl cyclobutanes, with the exclusion of the lines of the benzene ring with frequencies less than ~1000 cm^{-1}, for which, as in the aryl cyclopropanes, such rules are not observed.

REFERENCES

1. R. Ya. Levina, Yu. S. Shabarov, K. S. Shanazarov, and E. G. Treshchova. Vestnik Moskov. Gosudarst. Univ., Khim. Nauk., No. 5, 145 (1957).
2. R. Ya. Levina, Yu. S. Shabarov, M. G. Kuz'min, N. I.

Table 2

Phenyl cyclopropane $C_6H_5-\triangle$		Phenyl cyclobutane $C_6H_5-\square$		p-tolyl cyclopropane $CH_3C_6H_4-\triangle$		p-tolyl cyclobutane $CH_3-C_6H_4-\square$		p-anisyl cyclobutane $CH_3OC_6H_4-\square$			o-anisyl cyclobutane $CH_3OC_6H_4-\square$			m-tolyl cyclobutane $CH_3C_6H_4\square$		
$\Delta\nu$, cm^{-1}	S 28 cm^{-1}	$\Delta\nu$, cm^{-1}	S 35 cm^{-1}	$\Delta\nu$, cm^{-1}	S 35 cm^{-1}	$\Delta\nu$, cm^{-1}	S 35 cm^{-1}	$\Delta\nu$, cm^{-1}	S * 18 cm^{-1}	S 35 cm^{-1}	$\Delta\nu$, cm^{-1}	S 18 cm^{-1}	S 35 cm^{-1}	$\Delta\nu$, cm^{-1}	S 18 cm^{-1}	S 35 cm^{-1}
316	40	257	30	239; b	185	215; bkgd	30	257; b	40	60	224	25	35	221; b	217	270
380; b	200	316; b	60	325	114	257; b	100	295	40	60	265	25	40	303	145	185
535	30	374; b	80	357	45	322; b	212	303	45	63	333	} 255	} 360	342	50	90
563	20	406	0	385	185	370; b	70	332; b	} 48	66 {	353			397; b	26	40
586	0	556	15	407	30	420	0	347			440	70	120	439	0	0
621	135	620	153	457	30	547	40	410; b	50	67	494	84	128	460	0	0
701	0	645	70	496	86	590; b	65	480; b	25	36	530	84	130	528	218	225
732	270	735	145	587	20	621	0	547; b	25	30	580	130	130	584	50	55
749	20	769	0	642	260	645	255	585	0	0	605	0	0	621	0	0
782	30	782	0	714; b	80	718; bkgd	30	603	75	90	640	140	146	651	116	120
819	140	809	0	767	40	738	45	635	200	215	667	26	46	695	50	55
836	30	842	45	788	176	782	875	671	0	0	724	400	480	724	290	315
875	210	872	120	807	} bkgd	809	30	695	25	40	746	220	380	776	50	58
902	565	907; d	287	822		875	260	735; b	95	130	792	330	400	816	135	200
1003	1295	950; d	185	833	0	908; b	480	788	25		808	33	40	864; b	42	80
1022; b	500	996	80	895	} 640	949	40	792	584	620	845	70	80	897	40	—
1045	0	1003	960	907		996	260	837	0	0	877	100	150	912	210	290
1080	45	1036	380	962	50	1085	45	845	0	0	912	330	450	947	187	295
1096	50	1104; b	120	996	0	1122	45	875	130	150	950	188	290	1000	1195	1250
1120	60	1154	294	1022	330	1151	50	912; d	270	340	996	329	408	1019	106	115
1156	340	1180	334	1048	212	1183	440	950	105	115	1038	70	85	1085	138	180
1183	250	1203; d	600	1107; b	70	1200; d	1200	996	156	170	1056	900	1050	1107	140	288
1220	860	1242	30	1160	25	1219	0	1015	26	35	1090	70	86	1170; b	245	400
1240	45	1300; b	360	1170	} 244	1245	45	1043	} 70	120 {	1117	30	45	1230	} 395	590
1268	45	1323	178	1184		1270	200	1070			1167	380	495	1250		
1296		1354	75	1210; b/bkgd	1070	1305	50	1090	34	56	1196			1270	250	390
1317	} 400	1380	20	1270; b	230	1334		1117	68	95	1204	} 340	645	1342; b	190	345
1368	600	1443	} 265	1314	270	1342	bkgd 438	1180	360	490	1240	800	1080	1382	193	320
1428	30	1465		1364	680	1368	430	1188			1304	800	980	1443		
1443	30	1582	65	1427	148	1443		1219	} 380	585 {	1350	40	56	1487	} 295	375
1463	330	1604	880	1470	420	1465	} 565	1248; b	300	400	1382	—	—	1593	300	—
1493	60			1518	135	1566; b	30	1304; b	275	340	1443					
1582	35			1615; b	1200	1610	1100	1340; b	} 170	200	1480	} 400	560	1610	580	870
1607	920							1354								
								1380	0	0	1493	250	305			
								1443	} 274	357	1600	1340	1435			
								1460								
								1582	100	100						
								1612	858	900						

Note: The following symbols are adopted: b – broad band; bkgd – a line on background; d – double line; s – optical slit width.
*For an optical slit width =16 cm^{-1}, the intensity of the standard line of cyclohexane at 802 cm^{-1} was conventionally put equal to 500 units/mole.

Table 3. Comparison of the Integrated Intensities of Some of the Lines, Characteristic of the Benzene Ring in Mono-Substituted Benzenes

Phenyl cyclopropane	Phenyl cyclobutane	Isopropyl benzene[7]	Sec-butyl benzene[7]
621 (135)	620 (153)	622 (130)	623 (100)
732 (270)	735 (145)	742 (290)	732 (170)
1000 (1300)	1003 (960)	1002 (930)	1002 (620)
1220 (860)	1203; d (600)	1212 (230)	1207 (170)
1607 (920)	1604 (690)	1606 (490)	1606 (300)

Note: In Tables 3 and 4 the intensities of all of the lines are expressed in units/mole.

Table 4. Comparison of the Integrated Intensities of Some of the Lines, Characteristic of the Benzene Ring in Disubstituted Benzenes

Ortho	Meta-		Para-			
o-anisyl cyclo-butane	m-tolyl cyclobutane	m-methyl isopropyl benzene	p-tolyl cyclo-propane	p-tolyl cyclo-butane	p-methyl isopropyl benzene	p-anisyl cyclo-butane
530 (130)	528 (225)	523 (248)	642 (260)	645 (295)	638 (192)	635 (215)
724 (880)	724 (315)	711 (547)	807 (880)	792 (900)	801 (800)	792 (620)
746			822	809	822	
1058 (1050)	1000 (1250)	1003 (1090)				
1240 (1080)	1230; b (590)	1248 (248)	1210; b (1070)	1200; d (1200)	1205 (500)	1219; b (585)
1600 (1435)	1610 (670)	1607 —	1615 (1200)	1610 (1100)	1612 (480)	1612 (900)

Vasil'ev, and E. G. Treshchova. Doklady Akad. Nauk SSSR 121, 303 (1958).

3. V. T. Aleksanyan, Kh. E. Sterin, M. Yu. Lukina, L. G. Sal'nikova, and I. L. Safonova. Proceedings of the Tenth All-Union Congress on Spectroscopy, Fiz. Sbornik 1, 3 (1957). Izd. L'vovskogo Univ., 1957.
4. R. Ya. Levina, M. G. Kuz'min, Iu. S. Shabarov. Vestnik Moskov. Gosudarst. Univ. No. 1, 170 (1957).
5. R. Ya. Levina, Yu. S. Shabarov, M. G. Kuz'min, N. I. Vasil'ev, S. I. Pokroka, and E. G. Treshchova. Zhur. Obshchei Khim. 29 (1959).
6. E. G. Treshchova, V. M. Tatevskii, V. R. Skvarchenko, and R. Ya. Levina. Opt. i Spektr. 5, 553 (1958).
7. G. S. Landsberg, P. A. Bazhulin, and M. M. Sushchinskii. "Osnovnye Parametry Spektrov Kombinatsionnovo Passeyaniya Uglevodorodov." (The Fundamental Parameters of the Raman Spectra of Hydrocarbons), Izd. Akad. Nauk SSSR, Moscow, 1956.

DETERMINATION OF ABSOLUTE OSCILLATOR STRENGTHS FROM SPECTRAL LINE WIDTHS

V. K. Prokof'ev, I. M. Nagibina, and G. P. Petrova

Received 3 July 1959

The paper describes a method for determining absolute oscillator strengths by measuring spectral line widths. The relative concentrations of Mg and Ca atoms and ions in the mantle of an arc discharge and at the electrodes were measured experimentally. The method presented was used to determine the absolute oscillator strength of the tin resonance line at 2863.33 A; the value obtained was 0.08.

INTRODUCTION

Oscillator strengths are important atomic constants. The interest of research workers in determining their absolute and relative values has grown recently, due in particular to the broad development of astrophysics and research on the physical processes in a discharge plasma.[1]

The following methods have been widely used for this purpose: (1) Rozhdestvenskii's "hook" method, (2) the emission method, and (3) the absorption method.

The most accurate of the three is the hook method. However it is not sensitive enough, especially for determining the f values for transitions involving high energy levels. This can be done by the emission method, but an accurate correction must be made for reabsorption and light source temperature.

The absorption method of determining absolute oscillator strengths requires allowance for the hyperfine structure of the line and the part of the growth curve on which the measurements are made.

Recently it has become possible to use a measurement of the contours of spectral lines excited in an arc discharge to determine relative oscillator strengths, as described in reference 2. An arc discharge is a particularly useful light source for studying refractory elements or those hard to volatilize. The working model of an inhomogeneous arc discharge given in the paper by Cowan and Dieke[3] is the basis of this method.

In the present research, we attempted to use spectral line width measurements to determine absolute f values. This method is based on the following considerations.

From the theory of the radiation of an inhomogeneous source[3] and the consequences of this theory, we obtain a relationship between the absorption parameters and the product $f\bar{N}_a$.

$$f\bar{N}_a = \frac{2mc}{\pi e^2 p(0)} p. \qquad (1)$$

Here $\bar{N}_a$ is the mean concentration of atoms or ions at the lower level; p is an absorption parameter which is a function of the ratio of the line width, u, when absorption occurs to the line width, δ, for an infinitesimally thin layer in the absence of absorption (or a function of the relative intensity in the maximum and minimum of a self-reversed line contour); m and e are the mass and charge of the electron; c is the velocity of light; and l is the length or diameter of the source;

$$p(0) = \frac{1}{\pi\delta}. \qquad (2)$$

It is assumed that the line in the arc discharge at atmospheric pressure has a resonance contour. The functional relationship $p = \varphi(I_{max}/I_{min})$ or $p = f(u/\delta)$ can be calculated theoretically and represented graphically.[4,5]

When the quantities $\bar{N}_a$ are equal (for example for two lines of a multiplet), determining the relative values of f amounts to measuring the parameter p and the line width δ for the lines forming the multiplet. From (1) we have for the oscillator strength ratio:

$$\frac{f_1}{f_2} = \frac{p_1 \delta_1}{p_2 \delta_2}. \qquad (3)$$

We may assume that it is also possible to determine the absolute values of oscillator strengths if we insure that the concentrations of atoms or ions of two or more elements in the gaseous phase are equal. In this case, f is known for one of the elements and the values of p and δ are measured for all the elements in the experiment; then the unknown value of f for the element under study is determined from (3). The basic conditions that must be observed to use the proposed method are as follows:

(a) It is desirable to choose serial transitions with closely similar lower state energies in the elements being compared. If this cannot be achieved, the population of the levels at the known discharge temperature must be taken into account.

(b) The elements being compared should have similar ionization potentials. If this condition is not satisfied, the degree of ionization of the elements must be taken into account.

(c) The concentrations of the two elements in the solid and gaseous phases must be made proportional.

Similar considerations were used by Allen in his paper[2] on determining absolute f values by the emission method.

To check the validity of the proposed method, we must first find out whether the concentration ratio is the same in the discharge cloud as in the solid. The first part of this paper is therefore devoted to an experimental study of the concentration ratio of atoms of the different elements in the discharge cloud for a given ratio of the numbers of atoms in the electrodes. In the second part of the paper we attempt to determine the absolute value of f for the tin resonance line by using the proposed method.

MEASUREMENT OF THE CONCENTRATION OF Mg AND Ca ATOMS AND IONS IN THE MANTLE OF AN ARC DISCHARGE

Specimens containing magnesium and calcium were used to determine the concentrations of particles in the mantle of a discharge. These elements are not very close in their ionization potentials and so the experimental conditions are more closely controlled than when

these quantities are equal. Table 1 gives the characteristics of the lines studied. The last column of the Table gives values of f taken from the literature.

Table 1. Characteristics of the Mg and Ca Lines Studied

Element	Wavelength (A)	Intensity	Excitation potential (ev)	Ionization potential (ev)	Transition	f
Mg I	2852.13	300 R	4.34	7.845	$^1S_0 - {}^1P_1$	1.2
Mg II	2795.53	150	4.43	15.032	$^2P^0_{3/2} - {}^2D_{5/2}$	0.8
Ca II	3933.67	600 R	3.15	11.868	$^2S_{1/2} - {}^2P^0_{3/2}$	0.8
Ca I	4226.73	500 R	2.93	6.112	$^1S_0 - {}^1P_1$	1.3

Chlorides of magnesium and calcium ($CaCl_2$ and $MgCl_2$) in water solution were chosen for the study. Saturated solutions of these salts were used to prepare a series of solutions of different concentrations, with a definite ratio (1.7) between the number of Mg atoms and the number of Ca atoms.

A Fabry-Perot etalon and an ISP-22 spectrograph were used to measure the widths of the line contours. The etalon had a 2 mm gap; its aluminized surfaces had a reflection coefficient of 0.82 to 0.80. Photographic photometry was used to measure the widths of the lines being studied.

In order to achieve the best possible reproducibility in the relative numbers of Ca and Mg particles in the vapor phase, the simplest methods possible were used for the evaporation. We tried two of the methods of introducing material into a discharge which are used at present in applied spectroscopy: (a) placing a drop of the solution under study on the end of a carbon electrode, which has been waterproofed with polystyrene, and then drying the solution, and (b) applying a thin film of the solution to the surface of copper plates and then drying it.

In the second case, the copper plate was made the lower electrode and was moved relative to the stationary upper electrode by means of a motor.

To determine the relative content of atoms and ions of the elements under study, a concentration of the two elements in the solution must be chosen for which there is broadening or self-reversal for two lines of the different elements simultaneously.

Then from (1)

$$\frac{N_{a\,Mg}}{N_{a\,Ca}} = \frac{I_{Ca} P_{Mg}{}^3 a_{Mg}}{I_{Mg} P_{Ca}{}^3 a_{Ca}}. \qquad (4)$$

For each line, we determined a concentration of element in solution which would correspond to an infinitely thin layer. This concentration may be different for magnesium and calcium. Then the line width u or $\log(I_{max}/I_{min})$ was measured at higher concentrations, and the parameter p was obtained from the theoretical curves.

Tables 2 and 3 give the results obtained by means of the above-mentioned two methods of introducing the material into the discharge. The second column of each Table gives the concentration of Mg and Ca used relative to copper, which was the internal standard. For all concentrations, the ratio of the numbers of Mg and Ca atoms in the solutions was 1.7 to 1. Column 7 or 8 gives the absolute concentrations of Mg and Ca in the discharge cloud, and the last column gives the concentration ratio in the discharge zone.

The u/δ ratios given in the Tables are corrected for instrumental broadening, which was calculated from a measured value obtained under conditions such that the line contour was of the dispersion type. In all cases the inhomogeneity parameter n was taken to be 1.5 for atoms and 1.3 for ions, as was shown in reference 4.

The Tables show that the relative number of atoms

Table 2. Measurements of the Concentrations of Mg and Ca Using Carbon Electrodes

Element and Wavelength (A)	C (%)	δ (A)	$\frac{C_{Mg}}{C_{Ca}}$	$\log\frac{I_{max}}{I_{min}}$	p	Mean value of p	$N_a \cdot 10^{20}$ (cm^{-3})	$\frac{N_{a\,Mg}}{N_{a\,Ca}}$
Mg I (2852)	2.5	0.043	1.70	0.04 0.06 0.04 0.03	2.75 2.91 2.75 2.27	2.67	14.1	1.34
	5.0			0.18 0.12 0.14 0.15	5.53 4.13 4.53 4.79	4.75	25	1.41
Ca I (4227)	2.5	0.045	1.70	0.07 0.10 0.18 0.15	3.43 3.84 5.53 4.70	4.40	10.5	1.38
	5.0			0.24 0.24 0.16 0.13	9.36 9.36 5.06 4.44	7.5	17.8	

Table 3. Measurement of the Concentrations of Mg and Ca Using Copper Plates

Element and Wavelength (A)	C (%)	$\frac{C_{Mg}}{C_{Ca}}$	δ	$\frac{u}{\delta}$	p	$N_a \cdot 10^{-20}$ (cm^{-3})	$\frac{N_{a\,Mg}}{N_{a\,Ca}}$
Mg I (2852)	2.5	1.7	0.043	1.42	0.69	3.7	1.32
Ca I (4227)				1.74	1.16	2.8	
Mg II (2795)	20.0	1.7	0.045	1.53	0.87	5.7	1.34
Ca II (3933)				1.57	0.93	4.6	

and ions in the discharge cloud is reproduced fairly well by the two methods used for introducing material into the discharge. When the solution was applied to the end surface of a carbon electrode, the mean value (1.4) was at most 18% away from the true value (1.7). Approximately the same value was obtained when the copper plates were used, but in this case the deviation from the true concentration averaged 20-25% for both atoms and ions.

It must be assumed that the material coated onto the copper surface as a very thin film is introduced into the discharge at a fairly uniform rate as the plates are moved.

From these data we can conclude that in both cases the relative concentrations applied to the electrodes are reproduced in the discharge plasma to within 20-25%. We chose the second method (introducing the material into the discharge on copper plates) because of its greater simplicity and reliability.

DETERMINATION OF ABSOLUTE f VALUES FOR TIN

The value of f for the tin resonance line at 2863.33 A ($5p^2P_0 - 6s^2P_1$) was determined. Manganese was used as the comparison element. The oscillator strength of the manganese line at 2798.27 A ($a^6S_{5/2} - y^6P^0_{5/2}$) is known to be 0.422.[7] The two elements are very close in ionization potential (Sn—7.33/ev, Mn—7.43/ev).

Both elements were simultaneously dissolved as chlorides of manganese and tin in equal atomic concentrations ($MnCl_2 \cdot 4H_2O$ and $SnCl_4 \cdot 5H_2O$).

It was assumed, on the basis of the above discussion, that the concentrations N_a for manganese and tin in the mantle of the discharge were equal. Table 4 gives the results of the measurements. The experiments showed that both the lines under study show broadening simultaneously at a concentration of 10% in the solution.

Table 4. Measurements of the Oscillator Strength for the Tin Line

Element and Wavelength (A)	δ (A)	a (A)	$\frac{a}{\delta}$	p	f	Corrected value of f
Mn I (2798.27)	0.018 0.021 0.019 0.020 0.022	0.027 0.028 0.029 0.030 0.031 0.031 0.029 0.030	1.45	0.74	0.42	—
Mean value	0.020	0.029	—	—	—	—
Sn I (2863.33)	0.013 0.015 0.011 0.013 0.014	0.020 0.019 0.019 0.019 0.018 0.017 0.017	1.39	0.845	0.24	0.08
Mean value	0.013	0.018	—	—	—	—

Each number in the Table is the mean of 2 or 3 individual measurements. The oscillator strength obtained from the measurements was 0.24; a correction must be applied to allow for the distribution of tin atoms over the lower states $^3P_{0,1,2}$. The line being studied corresponds to the lower state $^3P_0$, whereas at the temperature of the arc there are also atoms in the $^3P_1$ and $^3P_2$ states. If we assume an arc plasma temperature of 5000°, about one third of the atoms are in the $^3P_0$ state. After allowing for this we find $f_{2863} = 0.08$.

We cannot compare our results with those of other workers. However, a value of f = 0.08 for the 2863.38 A tin line is quite reasonable in view of Allen's data for the 3801 A tin line (f = 0.28).

No great accuracy is claimed for this method of determining f, but we believe that it permits a simple estimate of the absolute value of f with an accuracy of about 20%.

REFERENCES

1. V. K. Prokof'ev. Opt.-Mekh. Promyshl. 12, 13 (1958).
2. I. M. Nagibina. Izvest. Akad. Nauk SSSR, Ser. Fiz. 22, 681 (1958).
3. R. D. Cowan and G. H. Dieke. Revs. Modern Phys. 20, 418 (1948).
4. I. V. Dvornikova and I. M. Nagibina. Opt. i Spektr. 4, 421 (1958).
5. I. M. Nagibina. Opt. i Spektr. 4, 430 (1958).
6. C. W. Allen. Month. Not. 117, 622 (1957).
7. Yu. N. Ostrovskii. Opt. i Spektr. 3, 193 (1957).

EVALUATION OF THE ERROR OF INTERPOLATION BY THE NORMALS OF THE SPECTRUM SECTIONS ON THE ROWLAND CIRCLE

V. A. Loginov

Received 6 July 1959

The purpose of this article is to examine the problem of evaluating the error of interpolation by the normals of the spectrum sections on the Rowland circle. Results obtained for the DFS-2 diffraction spectrograph enable us to determine the magnitudes of spectrum sections on which linear and quadratic interpolations could be performed.

The problem of evaluating the error of interpolation along the etalon lines of spectrum sections on the Rowland circle, in particular, when using the DFS-2 spectrograph[1,2] becomes of special interest in molecular spectroscopy for the purpose of investigating the fine structure of strips.

Kayser[3] studied the problem of least deviation N of the function (3) from an approximating linear function for the range (−L, +L) located close to the normals of the grating in the Rowland mounting, and he came to the conclusion that

$$N = \frac{d}{24m}\left(\frac{L}{\rho}\right)^3. \qquad (1)$$

where d is the grating constant, L is the distance from the normal to the grating, m is the order of the spectrum, and ρ is the radius of curvature of the grating. Formula (1) is valid only under the condition of a specific and constant value of dispersion. This formula, however, is used sometimes for the determination of error when normal dispersion is assumed (see reference 4) but the conditions for which it is valid are not specified. If dispersion in the range (−L, +L) is assumed to be equal to its value at φ = 0, then the error will become 4 times larger than that calculated by formula (1). Since the conditions for determining dispersion by linear interpolation are different than those assumed to derive formula (1), this formula cannot be used to evaluate the error of linear interpolation by the normals even close to grating normals on the Rowland circle. Rowland's choice of the spectrum region, close to the grating normals, was dictated primarily by the fact that gratings were the best available instruments, at that time, for accurate measurements of wavelengths and because of that the constancy of dispersion became a very important factor. At present, however, with the availability of precise normals it became possible to take measurements of wavelengths on sections distant from the grating normals, while applying nonlinear interpolation formulas.

In this article the problem of interpolation by the normals of the spectrum sections on the Rowland circle is examined in the light of the theory of interpolation of a function, and the evaluation is made of an error committed when a given function is replaced by the Lagrange polynomial.[5] Furthermore, a partial solution of the problem is obtained for the DFS-2 spectrograph. The method of applying interpolation formulas when investigating diffraction spectrograms is given in references 4 and 6 and we shall refrain, therefore, from describing the apparatus and the technique of determining wavelengths by means of etalon lines.

The following equation holds true for the concave grating

$$m\lambda = d(\sin\varphi + \sin\psi). \qquad (2)$$

where φ is the angle of diffraction, ψ is the angle of incidence, d is grating constant, m is the order of spec-

trum, and λ is the wavelength; thereby, the slit, grating, and the spectra of diverse orders all lie on the Rowland circle of a diameter equal to the radius of curvature of the grating. Substituting φ in expression (2) by x/ρ, where x denotes the length of arc on the Rowland circle and ρ is the radius of curvature of grating, we obtain

$$\lambda - \lambda_0 = f(x) = \frac{d}{m} \sin \frac{x}{\rho}, \qquad (3)$$

where $\lambda_0 = (d/m) \sin \psi$ denotes the wavelength corresponding to the spectrum of mth order for $\varphi = 0$.

Differentiating Eq. (3) we obtain

$$\frac{d\lambda}{dx} = \frac{d}{m\rho} \cos \varphi, \qquad (4)$$

where $d\lambda/dx$ is the reciprocal linear dispersion having a maximum at $\varphi = 0$ and changing proportionally to $\cos \varphi$ (see also Tables 1 and 2). To interpolate by means of the Lagrange formula we substitute f(x) by polynomial $P_n(x)$,[2] which assumes, at n + 1 points, x_i given values λ_i of etalon lines.

Table 1. m = 1, N = 0.001 A, $\psi = 40°56'$, 1200 lines/mm

λ (A)	φ	$\frac{d\lambda}{dx}$ From (4) (A/mm)	l (mm) From (7)	l (mm) From (9)
10 000	33°01′	3.502	2.7	40.8
9000	25 08	3.781	3.0	39.8
8000	17 45	3.978	3.5	39.1
7000	10 39	4.105	4.7	39.7
6000	3 43	4.168	7.7	39.5
5893	2 46	4.172	8.9	39.5
5550	0 41	4.175	17.8	38.5
5460	0	4.176	19.7*	38.5
5350	− 0 41	4.175	17.8	38.5
5060	− 2 46	4.172	8.9	38.5
5000	− 3 10	4.170	8.3	38.5
4000	−10 05	4.112	4.7	38.7
3000	−17 11	3.990	3.6	39.0
2000	−24 32	3.799	3.1	39.7

*Calculated by formula (8).

Table 2. m = 1, N = 0.001 A, $\psi = 19°07'20''$, 600 lines/mm

λ (A)	φ	$\frac{d\lambda}{dx}$ From (4) (A/mm)	l (mm) From (7)	l (mm) From (9)
10 000	15°49′	8.026	2.7	31.0
9000	12 16	8.163	3.0	30.8
8000	8 46	8.255	3.5	30.7
7000	5 18	8.317	4.7	30.6
6000	1 51	8.349	7.7	30.6
5893	1 22	8.351	8.9	30.6
5460	0	8.353	15.6*	30.6
5000	− 1 22	8.351	8.9	30.6
5000	− 1 35	8.350	8.3	30.6
4000	− 5 01	8.321	4.7	30.6
3000	− 8 29	8.261	3.6	30.7
2000	−11 58	8.171	3.1	30.8

*Calculated by formula (8).

The error committed does not exceed the magnitude of

$$\frac{M(x-x_1)(x-x_2)\ldots(x-x_{n+1})}{(n+1)!}, \qquad (5)$$

where M is the maximum of the absolute value of the (n + 1) derivative, $f^{(n+1)}(x)$, of the function f(x) on the segment (x_1, x_{n+1}) (see reference 5).

For linear interpolation at (n = 1) the error of linear interpolation applying (5) will not be larger than

$$N \geq \frac{M}{2}(x-x_1)(x-x_2),$$

where in our case

$$M = \frac{d}{m\rho^2} \sin \varphi_2 = \frac{\lambda_2 - \lambda_1}{\rho^2}.$$

The limit of error of linear interpolation in the section $l = x_2 - x_1$, between the standard lines λ_2 and λ_1, will be

$$N = \frac{1}{8} Ml^2 = \frac{1}{8}(\lambda_2 - \lambda_1)\left(\frac{l}{\rho}\right)^2. \qquad (6)$$

The magnitude of spectral section l, for which the limit of error does not exceed the given magnitude N, is obtained from (6)

$$l < \frac{K}{\sqrt{\lambda_2 - \lambda_1}} \quad (K = \rho\sqrt{8N}). \qquad (7)$$

In the vicinity of the normal for $x_1 = 0$, $x_2 = l$, from (3) and (6) we obtain, with a known approximation,

$$N = \frac{1}{8}\frac{d}{m}\left(\frac{l}{\rho}\right)^3,$$

from which

$$l \leqslant \rho \sqrt[3]{\frac{8mN}{d}}. \qquad (8)$$

In the case of quadratic interpolation (n = 2) the error will not exceed

$$N > \frac{M}{6}(x-x_1)(x-x_2)(x-x_3) = \frac{Ml^3}{6} f(\mu, \mu_2).$$

Here

$$M = \frac{d}{m\rho^3} \cos \varphi_1$$

is the maximum value of the derivative $f^{(3)}(x)$ in the interval $l = x_3 - x_1$; $f(\mu, \mu_2) = \mu(\mu - \mu_2)(\mu - 1)$, where $\mu = (x - x_1)/l$, $\mu_2 = (x_2 - x_1)/l$, $\varphi = x_1/\rho$, and x_1, x_2, x_3 are microscope readings for standard lines with wavelengths λ_1, λ_2, λ_3, respectively.

The limit of error for quadratic interpolation in the region $l = x_3 - x_1$ becomes

$$N = \frac{d}{6m} f(\mu_{cr.}, \mu_2) \cos \varphi_1 \cdot \left(\frac{l}{\rho}\right)^3,$$

from which we derive

$$l \leqslant l_0 \sqrt[3]{\sec \varphi_1}, \quad \left(l_0 = \rho \sqrt[3]{\frac{6mN}{df(\mu_{cr.}, \mu_2)}}\right). \qquad (9)$$

Formulas (7), (8), (9) are applicable to the DFS-2 spectrograph, which is based on Paschen–Rünge design, and they can be helpful also in choosing the spectrum sections for interpolation by the normals.

The DFS-2 spectrograph has two gratings with 1200 and 600 lines/mm and a radius of curvature $\rho = 1995.3$ mm. It is designed to operate in the spectrum range of 2000–10000 A in the first orders of grating with $\lambda_0 = 5460$ A.

The constant K in formula (7) is equal to 178.5 for both gratings at N = 0.001 A. The values of l as a function of λ are determined from formulas (7) and (8) and tabulated in Tables 1 and 2, from which it can be seen that for N = 0.001 A, and depending on λ, the linear interpolation is permissible for the spectrum sections within 3–20 and 3–16 mm, corresponding to intervals 9–82 A and 22–130 A for the first orders of gratings and at 1200 and 600 lines/mm respectively.

By taking m = 1, N = 0.001 A, and $f(\mu_{cr}, \mu_2) = 0.1$ as used in reference 7, we can find from (9) that $l_0 = 38.5$ and 30.6 mm for the gratings with 1600 and 600 lines/mm, respectively. The numerical values of l as a function of λ are determined for these gratings by formula (9), and are shown in Tables 1 and 2. We can deduce, therefore, that quadratic interpolation may be performed on the spectrum sections approximately 39 and 31 mm long, containing 160 and 260 A in the first order of grating, and also that l is practically independent of λ.

We were taking into consideration only the error of interpolation resulting from the use of the equations of first and second degree, instead of the exact dispersion formula, and also assuming that the wavelengths of the standard spectral lines are known with a high degree of accuracy. The real accuracy of wavelength determinations by the method of interpolation on standard lines depends yet on many other factors (see reference 7).

The author is very grateful to Professor V. M. Tatevskii for valuable help and suggestions.

REFERENCES

1. V. K. Prokof'ev. Izvest. Akad. Nauk SSSR, Ser. Fiz. 18, 643 (1954).
2. R. I. Tveryankina. Izvest. Akad. Nauk SSSR, Ser. Fiz. 19, 28 (1955).
3. H. Kayser. Handbuch der Spektroskopie, 1. Leipzig, 1900.
4. R. Soier. "Eksperimental'naya Spektroskopiya." (Experimental Spectroscopy), Izd. Inostrannoi Lit., Moscow, 1953.
5. V. L. Goncharov. "Teoriya interpolirovaniya i priblizheniya funktsii." (The Theory of Interpolation and Approximation of a Function), Gosudarst. Izd. Tekh.-Teoret. Lit., Moscow, 1954.
6. S. E. Frish. "Tekhnika spektroskopii." (Techniques in Spectroscopy), Leningrad, 1936.
7. V. A. Loginov. Opt. i Spektr. 6, 692 (1959).

THE ENERGY SPECTRUM OF AN F-CENTER IN CONTINUUM THEORY

Yu. E. Perlin

Received 8 July 1959

A comparison of two categories of variational functions is made within the framework of the continuum theory of F-centers. It is shown that functions of the first kind (hydrogen model) give better results in the calculation of the energy of the ground state. For all excited electron states, functions of the second kind (polaron model) lead to lower energy values. Thus it is established that in the theory of excited states of F-centers (and other mixed centers of ionic crystals) it is necessary to take account of the collective motion of phonons produced by the excess electrons (polaron effect).

1. INTRODUCTION

In the current electron theory of ionic crystals, an important part is played by the constant α, characterizing the coupling between the "excess" electrons and the longitudinal optical vibration of the lattice. It is determined from the equation

$$\alpha = \left(\frac{\mu e^2 c^2}{2\hbar^3\omega}\right)^{\frac{1}{2}}, \qquad (1, 1)$$

where μ is the effective mass in the conductivity band of an ideal crystal;

$$c = \frac{1}{n^2} - \frac{1}{\varepsilon} \qquad (1, 2)$$

ε is the static dielectric constant, n the index of refraction in a transparent region, and ω is the limiting frequency of the longitudinal optical vibration.

The choice of the model of the current carrier depends particularly on the value of the coupling constant α (that is, a version of the theory of polarons).

The values of c and ω used in Eq. (1, 1) may be determined with sufficient reliability from the light dispersion curve of the pure crystal.[1] The greatest difficulty is offered by the determination of the effective mass μ. For ionic crystals with low carrier mobility, the only relatively reliable method of determining μ is apparently the method proposed by Pekar,[1] based on comparison of the theoretical expression for the frequency of the maximum of the F-band with the experimental values of this quantity. In this connection, it would be desirable to improve the accuracy of the theoretical expressions for the energy terms of the F-centers in the continuum theory. Although interesting in itself, an attempt to formulate a "microtheory" of F-centers cannot answer this question, since the formulas of a microtheory contain the mass of the free electron, but not its effective mass.

In the continuum theory (including the approximate method of effective masses), the Hamiltonian of the ionic crystal with F-centers has the form

$$\hat{H} = -\frac{\hbar^2}{2\mu}\Delta - \frac{e^2}{\varepsilon r} + \sum_{\chi} A_{\chi}(r)\, q_{\chi} + \frac{\hbar\omega}{2}\sum_{\chi}\left(q_{\chi}^2 - \frac{\partial^2}{\partial q_{\chi}^2}\right), \qquad (1, 3)$$

where q_χ are the normal coordinates of the longitudinal optical vibration, the dispersion of which we do not consider, and

$$A_{\chi}(r) = -\frac{e}{\chi}\sqrt{4\pi c\hbar\omega}\;\chi_{\chi}(r), \qquad (1, 4)$$

in which the functions χ_χ represent the result of differentiation of the orthogonal functions

$$\chi_{\chi}(r) = \sqrt{\frac{2}{L^3}}\begin{cases}\cos(\chi, r) & \text{for} \quad \chi_z \geqslant 0\\ \sin(\chi, r) & \text{for} \quad \chi_z < 0,\end{cases} \qquad (1, 5)$$

with respect to the argument χ_r, these functions being normalized in the fundamental region L^3.

We shall investigate crystals for which the condition of strong coupling is achieved at not too high a temperature; i.e.,

$$\alpha^2 \gg \frac{3\pi}{\beta}; \quad \beta = \frac{\hbar\omega}{kT}, \qquad (1, 6)$$

so that the states of the current carriers are realized in the ideal lattice in the form of the polarons of Pekar. The state of the electron in the polaron is described here by a wave equation of the damping type

$$\left.\begin{aligned}\psi_0(r) &= \left(\frac{\alpha_0^3}{7\pi}\right)^{1/2}(1+\alpha_0 r)\exp(-\alpha_0 r),\\ \alpha_0 &= \frac{\mu e^2 c}{2\hbar^2}.\end{aligned}\right| \qquad (1, 7)$$

and for a description of the collective motion of the phonons the translation vector ξ of the polaron is introduced, the components of which are related to the normal coordinates q_χ by the approximate relation

$$\frac{\partial \xi_i}{\partial q_{\chi}} = \frac{\hbar}{M\omega}\frac{\partial \psi_{\chi}}{\partial \xi_i}, \qquad (1, 8)$$

where M is the effective mass of the polaron, equal to

$$M = \frac{4\pi\alpha^3}{3\alpha_0^3}\int \psi_0^4(r)\, d\tau \qquad (1, 9)$$

and

$$q_{\chi} = -(\hbar\omega)^{-1}\int A_{\chi}(r)\,\psi_0^2(r-\xi)\, d\tau. \qquad (1, 10)$$

In conformity with reference 1, the configuration space of the phonon field (number of degrees of freedom ν) includes the translation vector ξ, $\nu - 6$ quantities

$$q'_s = q_s - q_{s\xi} \qquad (1, 11)$$

and three quantities

$$q'_{s_j} = \sqrt{q_{s_j}^2 + q_{s_{-j}}^2} \qquad (j = 1, 2, 3), \qquad (1, 12)$$

the choice of which is arbitrary.

For the calculation of the approximate eigenvalues of the Hamiltonian (1, 3) we use a straightforward variational method. It will be shown below that taking account of the symmetry of electron-phonon interaction in the choice of variation functions leads to a considerable lowering of the excited energy levels. This circumstance is explained by the transformation of the phonon part of the Hamiltonian (1, 3) to a modified polaron theory. The transformed Hamiltonian has the form

$$\hat{H} = -\frac{\hbar^2}{2\mu}\Delta - \frac{e^2}{\varepsilon r} + \sum_s{}' A_s(r)\,(q'_s + q_{s\xi}) + \frac{\hbar\omega}{2}\sum_s{}'\left[(q'_s + q_{s\xi})^2 - \frac{\partial^2}{\partial q_s'^2}\right] - \frac{\hbar^2}{2M}\Delta_\xi + \hat{H}' + \hat{H}'', \qquad (1, 13)$$

(for the details of the transformation, see reference 1) where the primed summation signs indicate the omission of the three vibrational degrees of freedom, and

$$\hat{H}' = \frac{\hbar^2}{2M}\sum_s{}'(\Delta_\xi q_{s\xi})\frac{\partial}{\partial q'_s}, \qquad (1, 14)$$

and

$$\hat{H}'' = \frac{\hbar^2}{2M}\sum_s{}'\sum_{s_1}{}'(\nabla_\xi q_{s\xi},\ \nabla_\xi q_{s_1\xi})\frac{\partial^2}{\partial q'_s \partial q'_{s_1}} \qquad (1, 15)$$

are the operators of one- and two-quantum scattering of polarons. In the temperature region defined by the inequality (1, 6) these operators may be regarded as small and, in the zeroth approximation, omitted. We shall also note that in the derivation of the Hamiltonian (1, 13) the individual terms which tend toward zero (as L^{-1} or L^{-2} when $L \to \infty$) are either omitted or altered.

Passing to the choice of type of variational function, it is necessary to distinguish two cases: (a) low discrete levels, for which the defining role in the electron state is the Coulomb interaction with the defects, and (b) excited states of large effective radius for which the Coulomb interaction plays a secondary role in comparison with the polaron effect. These cases are accordingly investigated in parts two and three of this paper.

2. LOW DISCRETE LEVELS (HYDROGEN MODEL)

In the present case of strong electron-phonon interaction (inequality (1, 6)) the electron of the F-center will adapt itself adiabatically to the vibration of the lattice. We therefore choose the variation function in the product form

$$\Psi(r, \xi, q') = \psi_\xi(r)\,\Phi_\xi(\xi, q'), \qquad (2, 1)$$

where the electron function ψ_ξ, which is independent of the coordinates of the phonon field, is the zeroth approximation to the electron wave function of the adiabatic method. It is assumed that the functions ψ_ξ and Φ_ξ are normalized, and that the center of localization of the electron functions coincides with the center of the Coulomb field. The variation functional is obtained in the form

$$\hat{H} = \int \Psi^* \hat{H} \Psi\, d\tau\, d\tau_\xi\, dq' = I[\psi_\xi] + \mathcal{H}_\xi, \qquad \left(dq' = \prod_s{}' dq'_s\right), \qquad (2, 2)$$

where

$$I[\psi_\xi] = \frac{\hbar^2}{2\mu}\int |\nabla\psi_\xi|^2\, d\tau - \frac{e^2}{\varepsilon}\int\frac{|\psi_\xi|^2\, d\tau}{r} - \frac{e^2}{2}\int\int\frac{|\psi_\xi(1)|^2\,|\psi_\xi(2)|^2\, d\tau_1 d\tau_2}{r_{12}}; \qquad (2, 3)$$

$$\mathcal{H}_\xi = \int \Phi_\xi^* \left\{\frac{\hbar\omega}{2}\sum_s{}'\left[(q'_s + q_{s\xi} - q_{s\xi})^2 - \frac{\partial^2}{\partial q_s'^2}\right] - \frac{\hbar^2}{2M}\Delta_\xi\right\}\Phi_\xi\, d\tau_\xi\, dq', \qquad (2, 4)$$

in which

$$q_{s\xi} = -(\hbar\omega)^{-1}\int A_s(r)\,|\psi_\xi(r)|^2 d\tau. \qquad (2, 5)$$

We shall carry out the minimization of the functionals (2, 2) in two stages—first on Φ_ξ with fixed ψ_ξ, then on ψ_ξ. We shall take Φ_ξ in the form

$$\Phi_\xi = \psi_0(\xi)\prod_s{}'\Phi_{a_s}(q'_s - r_{s\xi}), \qquad (2, 6)$$

where $\Phi_{a\chi}$ is the wave function of harmonic oscillators and

$$r_{s\xi} = q_{s\xi} - q_{s0}; \quad q_{s0} = q_{s\xi}|_{\xi=0}. \qquad (2, 7)$$

Then (2, 4) is transformed into

$$\mathcal{H}_\xi = \hbar\omega\sum_s{}'\left(a_s + \frac{1}{2}\right) + \hat{E}^\xi; \qquad (2, 8)$$

$$\hat{E}^\xi = \int\psi_0^*(\xi)\,\hat{\mathcal{E}}^\xi\,\psi_0(\xi)\, d\tau_\xi$$

$$= \int\psi_0^*\left[-\frac{\hbar^2}{2M}\Delta_\xi + \frac{\hbar\omega}{2}\sum_s{}'(q_{s\xi} - q_{s0})^2\right]\psi_0 d\tau_\xi. \qquad (2, 9)$$

With regard to the operator $\hat{\mathcal{E}}^\xi$, the quantity

$$W_0(\xi) = \frac{\hbar\omega}{2}\sum_s{}'(q_{s\xi} - q_{s0})^2 = \hbar\omega\sum_s{}'(q_{s0}^2 - q_{s0}q_{s\xi}). \qquad (2, 10)$$

plays the part of potential energy.

With the help of the function (1, 7), the latter quantity is computed in its final form. The calculation shows that W_0 produces a potential well which in the region of small $\xi < 1/a_0$ is in the form of a parabola

$$W_0(\xi) = \frac{1}{2}M\omega^2\xi^2 + O(\xi^4), \qquad (2, 11)$$

but in the region of $\xi > 1/a_0$ converges to the constant limit

$$\hbar\omega\sum_s{}' q_{s0}^2 = \frac{3e^2\hbar\omega}{7}$$

by the hyperbolic law ξ^{-1}. Consequently the minimum of $\hat{E}^\xi$ corresponds to a discrete energy level in the well W_0; that is, ψ_0 is a wave function of the localized kind. We shall look for it in the form

$$\psi_0(\xi) = \left(\frac{a_0^3\lambda^3}{\pi}\right)^{\frac{1}{2}}\exp(-a_0\lambda\xi), \qquad (2, 12)$$

where λ is the variational parameter whose value is given by minimizing the equation

$$\hat{E}^\xi(\lambda) = e^2\hbar\omega\left\{\frac{11\lambda^2}{a^4} + 0.429 - \lambda + \frac{2.04\cdot 10^{-2}\lambda^3}{(1+\lambda)^9}[49(1+\lambda)^7 + 77(1+\lambda)^6 + 84(1+\lambda)^5 + 73.5(1+\lambda)^4 + 52(1+\lambda)^3 + 28.9(1+\lambda)^2 + 11.2(1+\lambda) + 2.25]\right\}. \qquad (2, 13)$$

Numerical minimizing was carried out for the crys-

tals NaCl and KCl (the values of the parameters were borrowed from reference 1). For NaCl, $\bar{E}^*$ was 1.7 $\hbar\omega$ at $\lambda = 2.5\ \mu$, and for KCl $\bar{E}^*$ was 1.7 $\hbar\omega$ at $\lambda = 2.1\ \mu$. Thus, with an adequate degree of accuracy, it may be assumed that

$$\bar{E}^* = \frac{3}{2}\hbar\omega,$$

which in a manner of speaking follows immediately from (2, 11). This result is not connected with the choice of electron wave function $\psi_0(r)$. The latter is determined by minimizing the functional (2, 3) which agrees with the appropriate functional in the Pekar theory[1] of F-centers.

Finally, we obtain

$$H_{n_1 \ldots n_s \ldots} = I[\psi_{1s}] + \sum_s{}' \hbar\omega\left(n_s + \frac{1}{2}\right) + \frac{3}{2}\hbar\omega. \quad (2, 14)$$

This expression differs from the corresponding formula in reference 1 by the absence of three components in the expression for the phonon energy field, which is compensated by the supplementary term $(3/2)\hbar\omega$ (it is always possible to choose three n_s equal to zero). Thus the present variational method leads to the same formulas for the energy of discrete F-center levels as in the Pekar theory. However, unlike reference 1, the wave function of the stationary state (2, 14)

$$\Psi_{n_1 \ldots n_s \ldots} = \psi_{1s}(\mathbf{x})\,\psi_0(\xi)\prod_s{}'\Phi_{n_s}(q_s' - r_{s\xi}) \quad (2, 15)$$

is expressed in the modified polaron theory. In the author's paper[2] this wave function was used for the calculation of the probability of thermal ionization of F-centers.

The minimization of the functional (2, 3) for the ground state of an F-center was performed by Pekar and Deigen,[4] who obtained the following results

$$\psi_{1s} = \frac{\alpha_0^{3/2}\gamma^{3/2}}{\sqrt{7\pi}}(1 + \alpha_0\gamma r)\exp(-\alpha_0\gamma r);\quad \gamma = 1 + \frac{3}{4\varepsilon}; \quad (2, 16)$$

$$I[\psi_{1s}] = -\left(\frac{\alpha\gamma}{3}\right)^2\hbar\omega. \quad (2, 17)$$

Zil'berman[3] accomplished the minimizing of (2, 3) for the first and second excited levels using the hydrogen function with transformed parameters orthogonal to (2, 16). For the 2p state of the F-center in reference 5, it was found that

$$\left.\begin{aligned} \psi_{2p} &= \frac{8(\alpha_0\gamma\beta)^{5/2}}{\sqrt{2\pi}}\, r\cos\vartheta\exp(-2\alpha_0\gamma\beta r);\\ 2\gamma\beta &= \frac{1}{4\varepsilon} + 0.3914. \end{aligned}\right\} \quad (2, 18)$$

$$I[\psi_{2p}] = -(\alpha\beta\gamma)^2\hbar\omega. \quad (2, 19)$$

It should be noted here that the hydrogen model of excited states of the F-center can give fairly accurate results only when the contribution of the electron-phonon interaction to the energy of the electron is small compared to the contribution of the Coulomb field. It will be shown below (Section 3) that for the values of these parameters which usually characterize ionic crystals, these conditions are not satisfied for any of the excited electron states of the F-center.

3. EXCITED STATES (POLARON MODEL)

As is known, even in the absence of an additional potential, the electron-phonon interaction can lead to the localization of an electron in a polarized potential well, that is, to the formation of a polaron. As a consequence of the translational symmetry of the problem, the latter can freely migrate in the dielectric continuum, so that the electron wave function in the zeroth order has the form $\psi_0(\mathbf{r} - \xi)$ (in further calculations, formula (1, 7) is used). If the contribution of the additional potential to the electron energy is small compared to the polaron effect, then the potential mentioned will only insignificantly deform the wave function of the electron in the polaron.

In this case the variational wave function of the F-center may be sought for in the form:

$$\Psi(\mathbf{r}, \xi, q') = \psi_0(\mathbf{r} - \xi)\,\Phi(\xi, q'). \quad (3, 1)$$

Then the problem comes to minimizing the functional

$$I = \int \Psi^* \hat{H}\Psi\, d\tau_r d\tau_\xi dq' = I_0$$

$$+ \int \Phi^* \left[W(\xi) + \frac{\hbar\omega}{2}\sum_s{}'\left(q_s'^2 - \frac{\partial^2}{\partial q_s'^2}\right) - \frac{\hbar^2}{2M}\Delta_\xi\right]\Phi\, d\tau_\xi dq', \quad (3, 2)$$

where

$$W(\xi) = -\frac{e^2}{\varepsilon}\int\frac{\psi_0^2(\mathbf{r} - \xi)\, d\tau}{r}$$

$$= -\frac{\alpha^2\hbar\omega}{4\varepsilon}\left[\frac{1}{x} - \frac{e^{-2x}}{14}\left(\frac{14}{x} + 19 + 10x + 2x^2\right)\right] \quad (x = \alpha_0\xi). \quad (3, 3)$$

and

$$I_0 = \frac{\hbar^2}{2\pi}\int(\nabla\psi_0)^2 d\tau - \frac{e\varepsilon^2}{2}\iint\frac{\psi_0^2(1)\,\psi_0^2(2)\, d\tau_1 d\tau_2}{r_{12}} \cong -\left(\frac{\alpha}{3}\right)^2\hbar\omega. \quad (3, 4)$$

It now remains for us to find the minimum of the expression

$$\int\Phi^*\left[W(\xi) + \frac{\hbar\omega}{2}\sum_s{}'\left(q_s'^2 - \frac{\partial^2}{\partial q_s'^2}\right) - \frac{\hbar^2}{2M}\Delta_\xi\right]\Phi\, d\tau_\xi dq' = \min. \quad (3, 5)$$

Here the variables and q' are separated, so that it is necessary to suppose that

$$\Phi(\xi, q') = \varphi_n(\xi)\prod_s{}'\Phi_{n_s}(q_s'), \quad (3, 6)$$

where $\varphi_n(\xi)$ describes the motion of the polaron in the effective (shielded Coulomb) field (3, 3) and is determined by the condition

$$E_n = \int\varphi_n^*\left[-\frac{\hbar^2}{2M}\Delta_\xi + W(\xi)\right]\varphi_n d\tau_\xi = \min. \quad (3, 7)$$

The potential well $W(\xi)$ in which the polaron moves is a parabola

$$W(\xi) \cong -\frac{\alpha^2\hbar\omega}{4\varepsilon}\left(\frac{9}{14} - \frac{2x^2}{21}\right) \quad (3, 8)$$

for $x < 1$, and a Coulomb hyperbola for $x > 2$. Consequently, the spectrum of eigenvalues E_n includes not only the continuous region $E > 0$, but also the infinite manifold of discrete levels $E_n < 0$. In order to estimate the lowest of these levels, we may, according to (3, 8), replace the potential well $W(\xi)$ by the three-dimensional oscillator well

$$W(\xi) \cong -\frac{9\alpha^2\hbar\omega}{14\varepsilon} + \frac{M\omega_0^2\xi^2}{2} \quad (3, 9)$$

with the frequency

$$\omega_0 = 2\omega\sqrt{\frac{22}{21\varepsilon\alpha}}. \quad (3, 10)$$

Then

$$\left.\begin{aligned}\frac{E_1}{\hbar\omega} &= -\frac{9\pi^2}{14\varepsilon c}+\frac{3\omega_0}{2\omega};\\ \frac{E_2}{\hbar\omega} &= -\frac{9\pi^2}{14\varepsilon c}+\frac{5\omega_0}{2\omega};\end{aligned}\right\} \qquad (3,\ 11)$$

and so forth. If the minimizing of the functional (3, 7) is carried out with the help of the function

$$\varphi_{1s}=\left(\frac{\alpha_0^3\lambda_1^3}{\pi}\right)^{1/2}\exp\left(-\alpha_0\lambda_1\xi\right), \qquad (3,\ 12)$$

then for the crystal KCl we get $E_{1s} = -29.4\ \hbar\omega$, while formula (3, 11) gives $E_1 = -29.5\ \hbar\omega$. Thus formula (3, 11) for E_1 is accurate enough. The energy of the ground (electron) state of the F-center in the "polaron model" under consideration is equal to

$$\frac{E_{1s,\dots n_s\dots}}{\hbar\omega}=-\alpha^2\left(\frac{1}{9}+\frac{9}{14\varepsilon c}\right)+\frac{3\omega_0}{2\omega}+\sum_s\left(n_s+\frac{1}{2}\right). \qquad (3,\ 13)$$

Comparing (3, 13) with formulas (2, 14), (2, 17) of the hydrogen model, it is easy to conclude that for the usual values of the product εc, the latter gives significantly lower values of the energy. Only for abnormally high values $\varepsilon c \geq 10$ will the polaron model describe the ground state of the F-center more accurately than will the hydrogen model. Putting aside the above-mentioned abnormal case, let us use the approximate wave function (2, 15) for the fundamental state of the system. Then the additional requirement of orthogonality of (2, 15) with ψ_1 from (2, 16) is imposed in the wave function of the excited state.

If now we choose for the 2p state of the F-center

$$\varphi_{2p}=\frac{(\alpha_0\lambda_2)^{5/2}}{\sqrt{\pi}}\,\xi\cos\vartheta_\xi\exp\left(-\alpha_0\lambda_2\xi\right), \qquad (3,\ 14)$$

then, as is easily shown, the orthogonality condition is fulfilled for the calculation of the integral over ξ. The numerical minimization for the KCl crystal gives $E_{2p} = -27.7\ \hbar\omega$ (at $\lambda_2 = 3.5\ \mu$), while formula (3, 11) leads to $E_{2p} = -26.7\ \hbar\omega$. Thus formula (3, 11) is sufficiently accurate in this case. The energy in the 2p state of the F-center can be written

$$\frac{E_{2p,\dots n_s\dots}}{\hbar\omega}=-\alpha^2\left(\frac{1}{9}+\frac{9}{14\varepsilon c}\right)+\frac{5\omega_0}{2\omega}+\sum_s\left(n_s+\frac{1}{2}\right). \qquad (3,\ 15)$$

Comparison with formulas (2, 14)-(2, 19) shows that the energy of the first excited state of the F-center in the polaron model turns out to be substantially lower (by 13 $\hbar\omega$ for KCl) than in the hydrogen model. Whereas both of the compared derivations were derived by applying the direct variational methods to the same Hamiltonian, while both are orthogonal to the same approximate wave function of the ground state (2, 15), the polaron model should be preferred for the calculation of the excited electron levels of the F-center.

We note that the formulas of the polaron model may be derived without the use of variation methods by employing the adiabatic approximation. For this it is sufficient to consider the Coulomb interaction with a defect as a small perturbation in the electron equations in the adiabatic approximation. Then the correction of the first order in the electron energy proves to be equal to $W(\xi)$, which enters as a term in the adiabatic potential of the phonon subsystem. This method was used in the author's paper, reference 3, but the excited states of the discrete spectrum were not investigated in this work.

The excited states of an F-center in the continuum theory, that is, with the original Hamiltonians (1, 3), were also used by Buimistrov,[8] who employed a variational method useful for arbitrary values of the coupling constant α. However, apparently because the hydrogen approximation of the electron function was used in reference 6, the 2p state energies calculated by means of the formula given in this paper are almost identical with the results obtained by Zil'berman.[6]

4. DISCUSSION OF RESULTS

Making a comparison of two classes of variational functions in the continuum theory of F-centers permits the drawing of a number of conclusions. Functions of the first class (the hydrogen model) give better results in calculation of the energy of the ground state, but for all excited electron states, functions of the second class (polaron model) give lower energy values. Thus in the theory of excited states of F-centers (and of other impurity centers of ionic crystals), it is necessary to take into account the collective motion of phonons which generate excess electrons (polaron effect). A further refinement might be to compute the deformation of the electron wave function of the polaron by the electrical field of a defect. For the investigation of our first excited state such a refinement proves to be essential, since the effective radius of the electron orbits in this state are still not very large.

The change of the theoretical formulas for the energy of 2p states of an F-center requires the introduction of some corrections in the values of the parameters of ionic crystals and the parameters of the F-bands taken from reference 1. We shall quote the appropriate data in further publications.

In conclusion, we point out that one of the most difficult problems of the continuum theory of F-centers is the problem of the internal photoeffect. Experience shows[7] that already at temperatures of the order of −150°C, the quantum yield of photoconductivity in colored alkali halide crystals becomes practically 100%. This means that at comparatively low temperatures, an F-center excited by light is more likely to undergo ionization by radiationless transition than to return to the ground state. The optical lifetime of an excited F-center is about 10^{-7} sec. The probability of a thermal transition from the first excited state to the second should therefore be greater than 10^7 sec^{-1}. For the same optimal assumptions concerning the mechanism of the radiationless transition, the above-mentioned probability may be estimated by the formula

$$w\sim\omega\exp\left[-\frac{I(\psi_2)-I(\psi_1)}{kT}\right].$$

In the data of Zil'berman for KCl, $I(\psi_2) - I(\psi_1) \sim 15\ \hbar\omega$, so that for −150°C, w turns out to be of the order of 10 sec^{-1}! The hydrogen model of excited stated thus leads to a serious discrepancy with experiment. It is most probable that this difficulty may be resolved within the framework of the polaron theory because of the substantial reduction in the energy interval between excited states: The estimate by formula (3, 11) shows that the energy difference between the second and first excited states is of the order of $2\ \hbar\omega$. If it is assumed that the "tight spot" in the process of thermal ionization is the bridging of this gap, then the high probability of this process becomes understandable.

REFERENCES

1. S. I. Pekar. "A Study of Electronic Theory of Crystals." Gosudarst. Izd. Tekh.-Teoret. Lit., 1951.

2. M. A. Krivoglaz and S. I. Pekar. Izvest. Akad. Nauk SSSR, Ser. Fiz. 21, 16 (1957).
3. Yu. E. Perlin. Phys. Solid State 2, 246 (1960).
4. S. I. Pekar and M. F. Deigen. Zhur. Eksptl. i Teoret. Fiz. 18, 481 (1948).
5. G. E. Zil'berman. Zhur. Eksptl. i Teoret. Fiz. 19, 481 (1949).
6. V. M. Buistrov. Ukrain. Fiz. Zhur., Suppl. 3, 21 (1958).
7. N. Mott and R. Gurney. "Electronic Processes in Ionic Crystals." Izd. Inostrannoi Lit., Moscow, 1950.

THE TEMPERATURE DEPENDENCE OF THE INTENSITY OF STOKES AND ANTI-STOKES RAMAN LINES IN LIQUIDS

A. I. Sokolovskaya and P. A. Bazhulin

Received 18 July 1959

The temperature dependence of the intensities of the Stokes and anti-Stokes components and of the magnitude of their ratio in the Raman spectra of several liquids—$GeCH_2Br_2$, CCl_4, CS_2, and C_6H_6—are investigated. Temperature measurements of the intensity of the 992 cm^{-1} line of gaseous benzene are presented. The results obtained are compared with the theoretical conclusions.

In the papers concerning the study of the temperature dependence of Raman lines, a divergence of the experimental results of the Stokes component from the theoretical is observed.[1-6] Since, for the interpretation of the observed phenomenon, a knowledge of the temperature dependence of the anti-Stokes line is very desirable, we decided to continue the investigations with this aim in view.

It is of great interest, from the theoretical viewpoint, to make a comparison of the calculated ratio of the intensity of the Stokes to the anti-Stokes line with the ratio obtained experimentally.

The available experimental data on these questions are very few and incomplete.[7-10] We have investigated the temperature dependence of the Raman line intensities of a series of liquids—$GeCH_2Br_2$, CCl_4, CS_2, and C_6H_6. The choice of such materials provided a possibility of carrying out temperature measurements of the intensity in a wide range of Raman frequencies from 90 to 1000 cm^{-1}.

The measurements were made using an apparatus described earlier by us.[5] We will only add that due to the low intensity of the anti-Stokes 992 cm^{-1} line the spectrum of benzene was taken in a cell of 80 cm length with low pressure lamps, 1 meter in length. In view of the large difference in the intensities of the Stokes and anti-Stokes lines, particularly for high frequencies, the spectra were recorded after an attenuator, consisting of three steps with transmissions 100, 55, and 17%. The attenuator was carefully calibrated with the aid of a "Iu. E." spectrograph, on which the investigations were conducted. The height of the step attenuator did not exceed the height of the uniformly illuminated portion of the slit. For the 992 cm^{-1} line the transition from the anti-Stokes to the Stokes region was made with the help of the 606 cm^{-1} line. The integrated intensity was measured by the contour. For all of the molecules investigated the intensity of the strongest line in the spectrum at 25°C was taken as 100. The method of working out the results obtained was the same as in reference 6.

The experimental data on the temperature dependence of the Raman lines of $GeCH_2Br_2$, CCl_4, CS_2, C_6H_6 are presented in Table 1. In columns 1, 2, and 3 are shown, respectively, the substance under investigation, the vibrational frequency of the Raman line, and the temperature. In columns 4 and 6 are given the values of the intensity of the Stokes and anti-Stokes lines obtained experimentally; in columns 5 and 7, the intensities calculated from theory. In the last two columns of the table the ratio of the intensities of the Stokes and anti-Stokes components, obtained experimentally and calculated theoretically, are compared. The experimental results for the Stokes components are in complete agreement with the data for their substances published earlier by us.[5,6]

Table 1

Substance	ν (cm^{-1})	T°C	$I_{St.}$ Exp.	$I_{St.}$ Theor.	$I_{Anti\text{-}St.}$ Exp.	$I_{Anti\text{-}St.}$ Theor.	$\frac{I_{St.}}{I_{Anti\text{-}St.}}$	$\left(\frac{\nu-\nu_0}{\nu+\nu_0}\right)^4 \cdot \frac{h\nu}{kT}$
1	2	3	4	5	6	7	8	9
$GeCH_2Br_2$	96	+25	79	79	47	52	1.7	1.5
		+150	56	108	43	81	1.3	1.3
	128	+25	25	25	14	14	1.8	1.8
		+150	18	33	13	22	1.4	1.5
	164	+25	30	30	17	15	1.8	2.0
		+150	25	38	14	23	1.8	1.6
	264	−70	—	—	—	—	5.0	6.5
		−25	—	—	—	—	3.8	4.2
		+25	100	100	34	30	2.9	3.3
		+150	77	122	44	53	1.8	2.3
	315	+25	25	25	—	—	—	—
		+150	15.5	30	—	—	—	—
CCl_4	217	−20	100	81	31	25	3.2	3.2
		+25	87	87	33	32	2.6	2.7
		+70	75	96	37	40	2.0	2.4
	314	−20	105	91	19	17	5.5	5.4
		+25	97	97	23	24	4.2	4.0
		+70	83	104	26	31	3.2	3.4
	459	−20	104	96	9	8.3	11.6	11.5
		+25	100	100	11	11	9.1	9.1
		+70	85	104	12	18	6.8	5.8
CS_2	656	−50	188	98	2.4	1.8	83	55
		−20	155	99	3.4	3.0	46	33
		+25	100	100	7.1	5.2	14	19
C_6H_6	992	+20	100	100	1.1	1.15	91	87
		+70	74	103	1.8	2.3	42	45

As is seen from the presented data, the intensity of the Stokes satellites decreases with an increase in the temperature, in spite of the theory. The temperature shift of the intensity differs greatly for different liquids and, to a lesser degree, depends on the type of bonds participating in the vibration. In the present work the disagreement with theory for the lines of $GeCH_2Br_2$, corresponding to low frequencies, is particularly evident. A very narrow wing of the Rayleigh line in this case permits reliable measurements of the Raman line intensities down to 90 cm^{-1}. From Table 1 (columns 6, 7) it is also clear that the intensity of the anti-Stokes lines increases

with temperature, but always slower than required by theory.

For an examination of the validity of the statistical treatment of the temperature dependence of Raman line intensities in liquids it is essential to investigate the ratio of the Stokes and anti-Stokes components. If we start from elementary theory, then the ratio of the intensities should be described by the law

$$\frac{I_{St.}}{I_{Anti\text{-}St.}} = \left(\frac{\nu-\nu_i}{\nu+\nu_i}\right)^4 e^{\frac{h\nu}{kT}}.$$

This relationship has been verified experimentally by a series of authors for CCl_4 and crystalline quartz. In reference 9 it was found to be fulfilled within the limits of experimental error. However, Harrand,[10] on the contrary, observed a disagreement of experiment with theory. We have traced the dependence on temperature of the ratio of the intensities of the Stokes and anti-Stokes satellites for a series of lines of $GeCH_3Br_3$, CCl_4, CS_2, and C_6H_6 in the temperature interval from −80 to +150°C.

The results obtained are given in columns 7 and 8 of Table 1. Experiment showed that, in spite of the disagreement with theory of the temperature shift of the intensity of the Stokes and anti-Stokes lines, the magnitude of their ratio, at least in the temperature region from −20 to +50°C, is close to theoretical. For the lines 217, 314, and 459 cm^{-1} of carbon tetrachloride the divergence is essentially within the limits of the errors of measurement, and the result obtained agrees with the data of reference 9. The same is observed for the lines 96, 128, and 164 cm^{-1} of $GeCH_3Br_3$, and 992 cm^{-1} of benzene. At the same time, it must be noted that for the lines 264 cm^{-1} of $GeCH_3Br_3$ and 656 cm^{-1} of carbon disulfide at low temperatures, there is observed a divergence of experiment from theory, where the magnitude of the disagreement lies beyond the limits of the experimental error (the mean error of measurement did not exceed 10%).

From Table 1 it is also clear that it is not possible to detect any dependence of the temperature change of the intensity of the Stokes lines on the vibrational frequency. The intensity of low frequencies (from 96 cm^{-1} in the case of $GeCH_3Br_3$) as well as high (up to 992 cm^{-1} in benzene) decrease with an increase of the temperature independently of the vibrational frequency of the corresponding line. Such a behavior has been observed for Stokes lines of a series of other substances studied earlier by us.[5,6] On the other hand, the qualitative behavior of the frequency dependence for anti-Stokes lines corresponds to that expected from the theory. The anti-Stokes satellites with the highest vibrational frequencies experience the greatest changes with temperature. In our case these are the frequencies 459 cm^{-1} of CCl_4, 656 cm^{-1} of CS_2 and 992 cm^{-1} of C_6H_6. The intensity of the lines of low vibrational frequencies 96, 128, and 164 cm^{-1} of $GeCH_3Br_3$ are barely altered.

The data obtained by us on the intensities of the Stokes and the anti-Stokes lines, and on the magnitude of their ratio, leads to the conclusion that the temperature dependence of the intensity, obtained theoretically for an isolated molecule, is indeed observed in the liquid phase; however, it is evidently strongly obscured by intermolecular interactions in liquids. These distortions are at a maximum for the Stokes components since, as a result of theory, their intensity depends slightly on frequency and temperature.

For the anti-Stokes satellites, the intensity of which are far more sensitive to a change of the frequency and temperature, a qualitative agreement of theory with experiment is observed. Then we note that the influence of the intermolecular interactions on the ratio of the intensities of the Stokes to anti-Stokes components is minimal.

As is well known, the divergence of the temperature shift of the intensity on temperature is observed not only in Raman spectra but also in infrared spectra.[11] The question of the anomalous temperature shift of the intensity in Raman and infrared vibrational spectra has been considered before.[11-13] However, to the present time there does not exist a theoretical understanding of the observed phenomenon. From the viewpoint of an explanation of this question it is of interest to study the temperature dependence in vapors or gases, where the intermolecular interactions are not large. Similar measurements were carried out on gaseous N_2 and CO_2,[14] but of more interest is the comparison of the temperature shift of the same Raman line in the liquid and gas phases. Such measurements were made by us on benzene vapor for the 992 cm^{-1} line, and the results obtained were compared with the temperature shift of the same line in the liquid. The cell, constructed by us for such experiments, permitted a measurement of the temperature dependence of a Raman line for a constant vapor pressure. The latter is essential for a correct interpretation of the results, since the question of the influence of pressure on the line intensity to the present time has been insufficiently studied and is of independent interest. The intensity was determined from the contour and was computed for one molecule of the substance. In Table 2 are presented the results of the measurements.

Table 2

State	T°C	I Exp.	I Theor.
Liquid	+20	100	100
	+80	71±4	101
Vapor	+110	100	100
	+190	110±8	103

As seen from the data presented the intensity of the 992 cm^{-1} line increases approximately 10% for a change in the vapor temperature from 110 to 190°C. This result is close to theoretical. The intensity of the 992 cm^{-1} line in liquid benzene, on increasing the temperature from +20 to +80°C, decreases, and this change is completely opposite to the theoretical indication. The data obtained agree with the analogous measurements made on infrared absorption bands of vapors and liquids,[11,17] and confirm the proposed role of intermolecular interactions in the observed anomalous temperature dependence of the intensity of Raman lines in liquids.

REFERENCES

1. K. S. Krishnan. Nature **123**, 650 (1928).
2. R. Ananthakrishnan. Proc. Indian Acad. Sci. **7a**, 196 (1938).
3. L. M. Fishkova. Doklady Akad. Nauk SSSR **75**, 523 (1950).
4. Ya. S. Bobovich. Doklady Akad. Nauk SSSR **98**, 39 (1954).
5. A. I. Sokolovskaya and P. A. Bazhulin. Proceedings of the Tenth All-Union Congress on Spectroscopy 1, 225 (1957). Izd. L'vovskogo Univ., 1957.
6. A. I. Sokolovskaya and P. A. Bazhulin. Izvest. Akad. Nauk SSSR, Ser. Fiz. **22**, 9 (1958).
7. G. S. Landsberg and L. I. Mandel'shtam. Phys. **60**, 364 (1930).
8. L. S. Ornstein. Physica **2**, 503 (1935).
9. S. Venkateswarlu. Current Sci. (India) **16**, 15 (1947).
10. M. Harrand. Ann. phys. **2**, 5, 6, 309 (1957).

11. P. A. Bazhulin and V. M. Smirnov. Opt. i Spektr. 6, 6, 745 (1959).
12. Ya. S. Bobovich and V. M. Pivovarov. Doklady Akad. Nauk SSSR 97, 5, 801 (1954).
13. L. I. Stekhanov and E. V. Chisler. Zhur. Tekh. Fiz. 25, 2209 (1955).
14. F. C. Rössler. Acta Phys. 5, 477 (1952).
15. Ya. S. Bobovich and V. M. Pivovarov. Opt. i Spektr. 3, 227 (1957).
16. Ya. S. Bobovich and V. M. Pivovarov. Opt. i Spektr. 6, 2, 249 (1959).
17. V. M. Smirnov and P. A. Bazhulin. Opt. i Spektr. 7, 2, 193 (1959).

SHORT COMMUNICATIONS

HIGH-SPEED PHOTOELECTRIC SPECTROMETER FOR THE REGION 0.4-0.9 μ

N. G. D'yachenko

Received 12 March 1959

During the spectroscopic investigation of the kinetics of fast-flowing processes the need arises for the greatest possible speed of a sequence spectrogram obtainable with the instrument. The literature contains descriptions of high-speed spectrometers with scanning by means of an oscillating mirror yielding frequency sequences of 100-150 spectra sec.[1] A more complex instrument ("movable" slit) of a yield of a frequency sequence of 500 spectra sec is now under development.[2]

By means of a simple scanning device, containing an oscillating mirror, we obtained a frequency sequence of 400 spectra sec (800 for the case of "spectral" reflectance). The resolving power was of the order of 300.

Half of a double DMR-2 monochromator with glass optics was employed as the monochromator. In place of the first (according to entrance of the ray) movable prism there is a fixed scanning unit. It represents an electromagnet and rotor, vibrating on an elastic suspension device—a steel plate of cross section 10×1 mm. The horizontal speculum with the dimension $30 \times 25 \times 1$ mm is attached to the rotor. The length and flexibility of the steel plate are selected so that the frequency of the natural vibrations of the rotor with the speculum is equal to approximately 400 cps. For charging the electromagnet a generator of low frequency is used, adjusted in resonance with a variable mechanical system. The generator (with reversible connection through a phase-shifting RS circuit) and preliminary amplifier are assembled in lamps 6N9 and 6P9, respectively. The coil of the magnet is connected directly to the anode circuit of the amplifier of the output of class C (6P3).

When the scanning mirror during deflection from the position of equilibrium is receding from the exit aperture or approaching it, the apparatus is then employed for automatic focusing of the spectrum at the exit aperture during its scanning.

The receiver used is an FEU-22 photomultiplier. The signal with the photomultiplier through the cathode follower and 75-ohm cable was drawn to the vertical amplifier of the electronic oscillograph ENO-1. The oscillograph was worked into the system of a single sweep, syncronized with an impulse voltage, ending in a coiled magnet. A device was also used which permits one to increase the scale of the individual regions of the oscillogram of the spectrum.

The examples of the results obtained by means of the described instrument are spectrograms presented in Figs. 1 and 2. Figure 1b shows an oscillogram of the spectrum, stretched longitudinally on the axis of the wavelength. The instrument is designed in the form of three blocks.

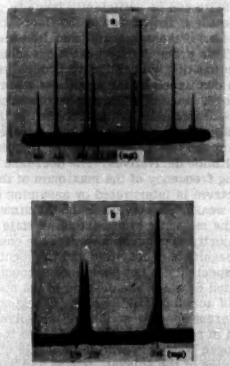

Fig. 1. Spectrum of radiation of lamp PRK-2. a—oscillogram, obtained for the period of oscillation of the scanning mirror ("mirror" spectra); time of recording of one spectrum $t \approx 1.2 \times 10^{-2}$ sec. b—the region of the same oscillogram, stretched longitudinally along the axis of the wavelength.

Fig. 2. Flash spectrum of the photoillumination compound ($Mg + KClO_4$). Series of sequence oscillograms is determined by the abscissa of black points on the curves. For each subsequent curve, the point is displaced along the axis of the abscissa to the side of short wavelengths. The above illustration is a graduated spectrum (glass PS7).

REFERENCES

1. O. D. Dmitrievskii, B. S. Neporent, and V. A. Nikitin. Uspekhi Fiz. Nauk 64, 447 (1958).

2. D. B. Gurevich, V. K. Prokof'ev, and Yu. A. Snegirev. Trudy Vsesoyuz. Nauch.-Issledovatel. Inst. Metrol., Sbornik, No. 1, 1958.

ON THE EFFECT OF THE SOLVENT ON THE FLUORESCENCE YIELD

A. S. Kochemirovskii and I. I. Reznikova

Received 9 May 1959

The magnitude of the fluorescence yield in liquid solutions depends on many factors, one of which, as indicated by Vavilov, can be the location of the fluorescent spectrum. Förster[3] later suggested that the energy of an excited state can be sufficiently large to predissociate a molecule if the energy of the fluorescence quanta is increased, i.e., if the spectrum is shifted toward higher frequencies. This process can cause a quenching of fluorescence by competing with radiative processes. This assumption is confirmed by the results of an investigation of the fluorescence of some nitro-compounds made by Lippert.[3] A dependence was established in the paper of Zelinskii, Kolobkov, and Pikulik[4] between the location of the spectrum and the magnitude of the fluorescence yield in phthalimide derivatives. The decrease in yield with increasing frequency of the maximum of the fluorescence spectrum is interpreted by assuming the disruption of the weakest double bond and the simultaneous transition of the molecule to a metastable state.

In the majority of papers, however, the connection between the magnitude of the yield and the location of the fluorescence spectrum is not taken into account. Thus in references 5 and 6, which are devoted to the study of the fluorescence of acridine solutions, the changing yield is related to different specific actions of the solvent. The changing yield in reference 5 is attributed to the formation of a hydrogen bond between the molecule of the solute and the molecules of the solvent. Bowen and Sahu[6] relate the effect of solvents on the yield of fluorescence to the amount of nonradiative energy losses, depending on the strength of intermolecular interactions. The change in the spectrum under the influence of the solvent is not taken into account in either paper and no information is given concerning the spectra themselves.

We investigated the spectra and the absolute quantum yields of the fluorescence of solutions of acridine in ethyl alcohol, glycerine, water, and trichloroacetic acid.*

*The trichloroacetic acid used contained water to the extent of about 0.8 mole H_2O/mole.

The yields were measured by means of a method which has been described previously.[7] Fluorescence spectra were obtained with a UM-2 monochromator and an FEU-18 photomultiplier. The short wavelength limit of sensitivity of the apparatus was approximately 25,000 cm^{-1}; for higher frequencies we used an ISP quartz spectrograph whose camera had been replaced by an FEU-18 photomultiplier. The excitation in both cases was produced by Mercury 365 mμ radiation obtained from an SVDSh-250 lamp and isolated by glass filters.

The fluorescence spectra of acridine solutions consist of wide bands with 2 maxima, the distance between the maxima being constant and equal to 1100 cm^{-1} in all of the solvents which we investigated. As can be seen in Fig. 1, both the long wavelength and short wavelength fluorescence maxima fall on a straight line in the solvent scale proposed by Zelinskii, Kolobkov, Pikulik, and Reznikova.[8,9]

The correspondence between the fluorescence yields of solutions of acridine in ethyl alcohol and in trichloroacetic acid is in agreement with the qualitative results obtained by Mataga and Tsuno[5] on the intensity of acridine fluorescence in benzine containing ethyl alcohol and trichloroacetic acid. The yield value which we obtained for acridine in water (33%) proved to be somewhat smaller than the value cited in the paper of Bowen and Sahu[6] (45%). A value of 4% is obtained for the yield of a solution in ethyl alcohol, according to a curve shown by these authors. In our measurements, the yield of an alcohol solution was about 2%. It is necessary to point our, however, that the measurement of such small yields is fraught with considerable inaccuracies. The yield of a solution in trichloroacetic acid considerably exceeds the yield of an aqueous solution.

The change in the fluorescence of acridine solutions with a change in solvent is concurrent with the change in the location of the fluorescence band. The displacement of the band to lower frequencies leads to an increase in

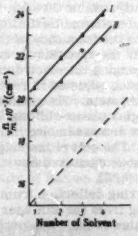

Fig. 1

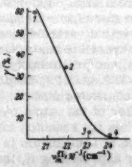

Fig. 2

Fig. 1. Dependence of the location of fluorescence maxima of acridine (ν_{max}^{fl}) on the solvent (the position of solvents on the x-axis is given according to the scale of solvents[8,9]). Curve I—location of the short wavelength maximum; curve II—location of the long wavelength maximum. A dotted straight line is shown for the standardizing substance 4 amino-N-methylphthalimide. Numbering of solvents: 1, trichloroacetic acid; 2, water; 3, glycerine; 4, ethyl alcohol.

Fig. 2. Dependence of the absolute fluorescence yield (γ) of acridine solutions on the location of the fluorescence spectrum. The numbering of solvents is the same as in the description of Fig. 1.

the quantum yield of fluorescence (Fig. 2). The results obtained indicate that acridine solutions, like phthalimide derivatives,[4] show a connection between the location of the spectrum and the magnitude of the quantum yield of fluorescence.

Inasmuch as the same dependence of the location of the fluorescence spectrum is observed for acridine as for compounds investigated in references 8 and 9, one can expect that in most organic solvents the fluorescence spectrum of acridine will be located in a shorter wavelength region than in ethyl alcohol. It can be seen in Fig. 2 that the fluorescence will be completely quenched in such a spectrum. This fact also prevents the fluorescence of solutions of acridine in most of the organic solvents cited by Bowen and Sahu.

One can therefore conclude that the fundamental reason for the change in the fluorescence yield of acridine under the influence of the solvent is given by the change in the positions of the molecular energy levels, which determine intramolecular processes of fluorescence quenching.

REFERENCES

1. S. I. Vavilov. Acta Phys. Polon. 5, 417 (1936).
2. T. Förester. Fluoreszenz organisher Verbindungen. Göttingen, 1951.
3. E. Lippert. Z. physik. Chem., N. F. 2, 328 (1954).
4. V. V. Zelinskii, V. P. Kolobkov, and L. G. Pikulik. Opt. i Spektr. 1, 161 (1956).
5. N. Mataga and S. Tsuno. Naturwiss. 44, 304 (1957).
6. E. Bowen and T. Sahu. J. Chem. Soc., 3716 (1958).
7. V. V. Zelinskii, V. P. Kolobkov, and L. G. Pikulik. Opt. i Spektr. 1, 570 (1956).
8. V. V. Zelinskii, V. P. Kolobkov, and L. G. Pikulik. Opt. i Spektr. 2, 402 (1957).
9. V. V. Zelinskii, V. P. Kolobkov, and I. I. Reznikova. Trudy soveshchaniya po termodinamike i stroeniyu rastvorov. (Proceedings of the conference on thermodynamics and structure of solutions), Izd. Akad. Nauk SSSR, Moscow, 1958.

ON THE COMPENSATION OF ROWLAND'S "GHOSTS" IN SPECTROGRAPHS WITH DOUBLE DIFFRACTION ON THE GRATING

V. N. Karpinskii

Received 10 July 1959

The behavior of "ghosts" in spectrographs with manifold diffraction of rays on the grating was investigated by Stepanov and Kopystyanskii[1] and also by Fasti and Sinton.[2]

In 1956 the author studied the ghosts and the methods of their compensation in spectrographs at the State University of Lvov[3] and in the Principal Astronomical Observatory of The Academy of Sciences of SSSR.

The behavior of ghosts was examined on the emission lines of mercury at 5461 A. Two schemes were investigated. In the scheme with the flat mirror M (Fig. 1), the displacement of the line is achieved by turning the mirror about the axis parallel to the lines of grating. This causes the brightness of ghosts to change periodically, allowing us to observe consecutive maxima and minima of the intensity. Relative intensity of ghosts, closest to the line, is approximately 30 times higher at maximum than at minimum. Moving the mirror M away from the grating diminishes the magnitude of period of ghosts in the focal plane proportionally to the distance.

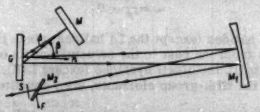

Fig. 1. M—flat mirror, G—grating (n—the direction of normal) M_1—spherical mirror, M_2—flat mirror, S—slit, F—focal plane.

For every diffraction the periodical errors due to the positioning of grating lines with the period, Δx, cause the appearance of periodical distortions of the diffracted frontal wave with the period, $\Delta x \cos \beta$, where β is the angle of diffraction. The values of phase difference obtained at every diffraction add up with different phases, depending on the angle of rotation of the mirror M; if the phases are opposite, following two diffractions, a wave is obtained whose front is not distorted by the periodical errors of the grating. Since red and violet ghosts are diffracted in different directions, the positions of their maxima are different also.

Turning the mirror M by an angle which corresponds to the value of the period of change in the intensity of first ghosts conforms exactly to the displacement of a ray on the grating, equal in magnitude to the period of error made during the cutting of lines. When the angle Δ between the incident and reflected rays approaches 0.5 deg, the maxima and minima of ghosts become less distinct, because the distortion of the front obtained at the first diffraction is projected on the grating with the period

$$\frac{\Delta x \cos \beta}{\cos (\beta - \Delta)},$$

different from the period of the errors of the grating, and such that the resulting phase difference varies from one edge of the grating to the other. The out of focus image of every ghost consists of a number of bright and dark lines changing their positions with the turning of the mirror M.

Some weakening of ghosts can be achieved by applying a scheme described by Walsh,[3] using a pair of flat mirrors at right angles. Such a spectrograph is shown schematically in Fig. 2. We have used such an arrangement to investigate ghosts in the spectrograph with the fourth order grating GOI (150 × 150 mm, 600 lines/mm), for double diffraction. The slit was 0.4 mm wide, and the focal lengths of mirrors M_1 and M_2 were 8 meters. The deflection of the frontal wave of light striking the grating, after second diffraction, is accomplished here by rotating the glass wedge K, deflecting the rays by 1'. For different angles of rotation of the wedge the magnitude of deflection changes in the direction perpendicular to the lines of the grating. It is ob-

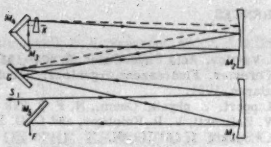

Fig. 2. M_1 and M_2—spherical mirrors, G—grating, M_3, M_4, and M_5—flat mirrors, K—wedge, S—slit, F—focal plane.

vious, therefore, that for the half-period deflection, the ghosts will compensate each other. If the grating is located at one focal point of the mirror M_2 and the square M_3M_4 at the other, one side of which is parallel to the lines of the grating (required accuracy 3'-5'), then for the light of all wavelengths striking the square M_3M_4, together with the ghosts, the primary and secondary Rowland's ghosts change their intensity periodically with the rotation of the wedge K. Furthermore, red and violet ghosts disappear at the same time and the period of primary ghosts corresponds to the displacement of the ray by the period of grating error, and the period of secondary ghosts to half this value. The intensity of ghosts of first and second order can be decreased 20 times compared to their maximum value, without even changing the position of the wedge, for any wavelength in the region of 4000-6600 A, mainly because the dispersion in such a wedge is negligible and has practically no effect on the magnitude of the ray displacement. When the line is more than 40 mm away from the edge of the square M_3M_4, the intensity of ghosts will diminish at maximum and increase at minimum, analogous to the case with flat mirrors observed when the angle Δ was increased. For the use of the photoelectric method of spectrum registration it is necessary to perform scanning by translation of the square M_3M_4: in the vicinity of edge M_3, various sections of the spectrum will find their way into the stationary slit and this will not disturb the compensation of ghosts.

If the image of the line or one of the ghosts at its maximum intensity is blocked just in front of the square M_3M_4, the corresponding ghost in the spectrum of double diffraction becomes bright. This indicates that the minimum intensity is obtained through ghost interference between ghosts of first and second diffractions. The results presented are somewhat different from those given in references 2 and 4. In conclusion, we would like to point out that these are only preliminary results of our investigation.

The author expresses gratitude to V. A. Krat, V. E. Stepanov, I. V. Yudina, A. V. Merkulov, and the team at the Optical and Mechanical Institute (GAO) for valuable suggestions and help in his work.

REFERENCES

1. V. E. Stepanov and A. A. Kopytyanskii. Byull. Kom. po Issled. Solntsa, Akad. Nauk SSSR, No. 10, 24 (1954). (Bulletin of the Commission for the study of the sun).
2. O. Fatie and O. Sinton. J. Opt. Soc. Am. 44, 103 (1954).
3. A. Walsh. Nature, 167, No. 4225 (1951).
4. D. Rank, O. Guenther, O. Burnet, and A. O. Wiggins. J. Opt. Soc. Am. 47, 631 (1957).

CALCULATION OF THE VIBRATIONAL FREQUENCY OF DIATOMIC MOLECULES FROM THE REDUCED MASS

K. S. Krasnov and A. I. Maksimov

Received 6 July 1959

A number of empirical formulas have been proposed for calculating the vibrational frequencies of diatomic molecules. These formulas connect the vibrational frequency ω_e with the interatomic distances d and other parameters of the molecules.[1,2] Unfortunately, their inadequacy lies in the fact that the interatomic distances are not always known. Formulas connecting the vibrational frequency of a diatomic molecule, ω_e, with parameters which are known for all cases without exception, e.g., the reduced mass of the molecule μ,[3,4] the nuclear charge, etc., are therefore of interest.

Of these formulas, the best were proposed by Carelli and Frantteur[3] for light ($\mu < 50 \times 10^{-24}$ gm) and heavy ($\mu > 50 \times 10^{-24}$ gm) molecules of halides and oxides. However, the division of molecules into light and heavy often ignores the nature of the chemical bond. A check of their formula against up-to-date information shows that the average relative error is more significant than the authors supposed, and amounts to 5% in the first and 8-15% in the seventh group of the periodic table.

We have attempted to express the dependence of ω_e on μ by means of a formula which will be an improvement on the formulas of Carelli.

The exact dependence of ω_e on the reduced mass must take into account the type of chemical bond according to the natural chemical classification based on the periodic table. Our analysis of the data for more than one hundred molecules has shown that the dependence of ω_e on μ for groups of similar diatomic molecules XY, where X belongs to one group of the periodic table and Y to another, can be expressed with sufficient accuracy by the equation

$$\omega_e = \frac{A}{\mu} + B \qquad (1)$$

The alkali halides (except the Li halides, since the Li^+ ion differs from the rest in the structure of its outer electron shell), the alkali hydrides (except LiH), the halides of the fifth-group elements, etc., constitute such groups.

The highest accuracy is attained when X (or Y) refers to the elements of one subgroup, or else when X (or Y) represents an atom of a given element in combination with elements Y which pertain to one subgroup (or group) of the periodic table. The choice of one of these methods of grouping in the determination of ω_e depends on the available information on molecules of the same type: the more extensive the information, the more complete is the breakdown according to bond type and the more accurate the result.

Table 1 gives the coefficients of Eq. (1) and the

values of the average relative errors ε for various groups of molecules. Calculation of ω_e for the halides according to Eq. (1), under the grouping rules set forth above, lowers the average relative error according to Carelli and Frantteur from 4.5-15.8% to 1.75-5.5% (ω_e taken from references 1, 6, and 7).

Table 1. Principle of Grouping for Calculation According to Eq. (1)

Types of compound	Group of the periodic table	Compounds	Coefficients of Eq. (1) A	Coefficients of Eq. (1) B	Average error (%) ε
Halides	VII	Interhalogen compounds	8775	+85	2.8
	V	Mn	8118	+28	2.7
	IV	–	7793	+74	4.9
	IV	Fluorides	10320	–58	2.8
	IV	Chlorides and bromides	6878	+106	3.0
	III	B	16260	–1038	5.4
	III	Al	7657	–17	2.8
	III	Ga, In, Tl	7089	+63	2.3
	II	Fluorides of the main subgroup	7784	–12	2.7
	II	Chlorides of the main subgroup	5685	+70	1.4
	II	Bromides of the main subgroup	5559	+77	1.9
	II	Iodides of the main subgroup	4765	+80	1.8
	II	Halides of the secondary subgroup	8071	+37	4.2
	I	Na subgroup	4402	+47	2.3
	I	Secondary subgroup	7621	+88	4.5
Hydrides	V	–	24125	–22345	0.4
	IV	–	12136	–10383	5.2
	III	–	11318	–9622	1.7
	II	Main subgroup	8621	–7443	1
	II	Secondary subgroup	2380	–909	4.8
	I	Na subgroup	6270	–5380	2
Others		CO, CS, CSe	23275	–1266	5.8
		SiO, SiS, SiSe, SiTe	13567	–108	3.8
		GeO, GeS, GeSe, GeTe	11857	+71	3.1
		SnO, SnS, SnSe, SnTe	10027	+106	2.6
		PbO, PbS, PbSe, PbTe	9147	104	2.8

Table 2 gives values of ω_e, calculated by us according to (1), for some molecules for which there are no experimental data.

Let us consider the application of Eq. (1) in more detail, using the alkali halides as examples.

Table 2. Vibrational Frequencies ω_e (cm^{-1}); Experimental (boldface), Calculated According to (1), Extrapolated by Rice and Klemperer (square brackets), and According to Gordy's Formula (parentheses)

	H	F	Cl	Br	I	At
Na	–	465±20	**366±6** 363 (398)	**302±6** 293 (330)	**258±4** 273 (296)	260±10
K	–	386±20	**281±4** 284 (309)	**213±4** 215 (248)	189 [173]	181±6
Rb	–	325±15	**228±4** 223 (260)	– 149 [166]	– 128 [128]	120±5
Cs	–	307±15	**209±4** 205 (237)	– 130 [139]	– 111 [104]	101±4
Fr	868±20	296±10	191±6	122±4	103±4	88±4
Ca	–	502±20 *	–	–	–	–
Ba	–	–	–	–	153±5	–
Ra	1148±60	430±15	255±5	171±5	137±5	–
Ga	1468±25	–	–	–	–	–
In	1405±25	–	–	–	–	–
Ge	1823±100	625±20	–	–	–	–
Sn	1758±100	–	–	–	–	–
As	1910±10	–	–	–	–	–
Sb	1785±10	–	–	–	–	–

Note: The value $\omega_{CaF} = 857.3$ is given in summary of reference 1. We consider this unreliable, since it is higher than ω_{MgF}. Such an anomaly is not observed in other groups.

For the seven molecules denoted in Table 2 by boldface type (NaCl, NaBr, NaI, KCl, KBr, RbCl, and CsCl), the frequencies ω_e determined by Rice and Klemperer from infrared spectra[a] may be described by Eq. (1) with A = 4401.7 and B = 47.3. The results of calculation according to (1) are compared with the experimental data in Table 2. The discrepancies in five cases out of seven lie practically within the limits of experimental error. The average relative error equals 2.3%. (The greatest deviation, as might be expected, is found in NaI (6%), inasmuch as it is the only iodide among the seven molecules.) For comparison, we have calculated ω_e according to the equation of Gordy[2] for the force constant k_e:

$$k_e = 1.67\left(\frac{x_A x_B}{d^2}\right)^{3/4} + 0.30^* \qquad (2)$$

*x_A and x_B according to reference 9, d according to references 10-12.

These values of ω_e are systematically higher than the experimental ω_e's according to Rice and Klemperer (by 30 cm^{-1} on the average) and those calculated by us according to formula (1).

It is evident that ω_e calculated according to (1) is significantly closer to the experimental data of Rice and Klemperer, and therefore we have used Eq. (1) in the form

$$\omega_e = 4401.7 \cdot \frac{1}{\mu} + 47.3$$

to calculate ω_e for the remaining alkali halides (Table 2). The table also contains values calculated for some of them by Rice and Klemperer by a special extrapolation, along with values calculated according to Gordy's formula. The very slight difference between the ω_e's calculated by us and those extrapolated by Rice and Klemperer makes it possible for us to consider both of them as being close to the actual values.

The values of ω_e for the fluorides and the astatine compounds must be considered the least reliable, since the coefficients of Eq. (1) were determined on the basis of known values of ω_e for molecules among which there was not a single fluoride or astatide.

REFERENCES

1. G. Herzberg. "Spektry i stroenie dvukhatomnykh molekul." (Spectra and Structure of Diatomic Molecules), Izd. Inostrannol Lit., Moscow, 1949.
2. J. P. Varshni. J. Chem. Phys. 28, 1078 (1958).
3. R. L. Purbrick. Phys. Rev. 71, 137 (1947).
4. C. H. D. Clark and C. W. Scaife. Trans. Faraday Soc. 33, 1394 (1937).
5. A. Carelli and P. Frantteur. Nuovo Cimento 14, 301 (1937).
6. S. A. Rice and W. Klemperer. J. Chem. Phys. 27, 573 (1957).
7. K. Butkov. Z. Physik 58, 232 (1929).
8. W. Gordy. J. Chem. Phys. 14, 305 (1946).
9. W. Gordy and W. J. Orville-Thomas. J. Chem. Phys. 24, 439 (1956).
10. A. Honig, M. Mandel, M. L. Stitch, and C. H. Townes. Phys. Rev. 96, 629 (1954).
11. K. S. Krasnov. Zhur. Neorg. Khim. 3, 1993 (1958).
12. K. S. Krasnov. Zhur. Neorg. Khim. 4, 530 (1959).

ABSORPTION SPECTRA OF DIAMONDS

G. O. Gomon

Received 22 July 1959

In spite of the fact that a number of papers[1-3] have been devoted to the study of the absorption of light by diamonds, no investigations of this type have been carried out so far on specimens from domestic deposits. It therefore seemed worth while to study the absorption spectra of diamonds from different deposits in the Soviet Union at various temperatures, and to compare the results with data from the literature.[1-3]

Octahedra and plates were selected from a collection of diamonds—in all, about 40 differently colored and luminescent specimens. The absorption spectra were measured with the aid of an SF4 spectraphotometer, and were also photographed with a quartz ISP-28 spectrograph. Our data and the results of other authors are given in the Table.

Wavelength λ of the maxima of the bands in the Absorption Spectra of Diamonds (A)

Data of ref. 1	Data of ref. 2	Data of ref. 3				Our data	
		Series	Line	λ*	Group	λ	Δ (ev)
		1	a	8250	?		
			b	7950			
			c	7500			
		2	a	4778	B	4785	
			b	4619		4619	
			c	4510		4530	
		3	a	4149	B	4152	
			b	4086		—	
			c	4031		4040	~0.080
			d	3942		3950	
			e	3841		3850	
				3757		—	
		4	a	3442	B	3450	~0.080
			b	3367		3380	
						3354	
						3300	
3298			c	3300		—	
		5	a	3294	A	3200	~0.025—0.030
3201				—		3180	
3176				—		3154	
3154	3157	6	a	3153	A		
						3110	
3085	3075					3088	
3064	3060	7	a	3062	A	3064	~0.030
3034						3036	
						3020	
		8	a	2960	A	—	

*Weak lines are underlined.

As is evident from the Table, the locations of the weak absorption bands near the values 4785, 4619, and 4520 A, observed in the absorption spectra of diamonds colored a golden yellow, agree satisfactorily with the wavelengths of the No. 2 band series presented in the work of Clark, Ditchburn, and Dyer.[3]

All of the remaining absorption lines and bands of the diamonds are arranged in four groups or series, the distance between two neighboring bands within each series being approximately constant (see the Table).

In the broad absorption band adjacent on the short wavelength side to the narrow line at 4152 A, vibrational structure is resolved, consisting of narrower bands near 4040, 3950, and 3850 A (see the Figure, curve 1). There is a set of narrow emission bands situated toward the red in the luminescence spectrum, which form a mirror image of these absorption bands with respect to the line at 4152 A. This fact indicates that in diamonds the centers of blue luminescence and the centers of absorption are identical. The intensity of luminescence of diamonds is proportional to the intensity of absorption in the band near 4152 A; in nonluminous diamonds there is no absorption in this region (curve 2). We might point out that in the absorption spectra of diamonds of various shades of yellow this same absorption band is present.

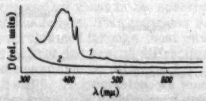

Curves of the spectral absorption of diamonds: luminescent (curve 1) and nonluminescent (curve 2) during photoexcitation.

In the absorption spectra of eight of the diamonds which we investigated at 80°K, there was detected a group of 3-4 narrow bands located near 3300, 3354?, 3380, and 3450 A. At room temperature, these bands shifted slightly (~5A) toward the red and became somewhat broader.

In the absorption spectra of all the diamonds investigated by us which were transparent in the ultraviolet region up to 3100-2900 A, there is a group of lines with wavelengths 3154, 3180, and 3200 A at 80°K. At room temperature this group of lines is shifted approximately 4 A toward the red. Unlike Sunanda Bai,[2] we failed to establish the presence of any correlation between the intensity of luminescence of diamonds and this group of absorption lines.

In the absorption spectra of diamonds which are transparent no further than 2900 A, the absorption rises sharply (stepwise) near 3120-3100 A. Between 3100 and 3000 A (at room temperature) one can distinguish one or two weak absorption bands which, on cooling of the specimen to 80°K, are shifted slightly toward the blue and become much sharper. In the absorption spectra of certain diamonds one can also detect from three to five narrow bands of the indicated series located near 3020, 3036, 3088, and 3110 A. The energy gap (Δ) between two neighboring bands of this series is constant and equals approximately 0.030 ev.

Analysis of the experimental data shows that if in the first group of lines the broader bands adjoin the line at 4152 A on the short wavelength side, then in the remaining three groups the shortest wavelength bands with wavelengths 3020, 3154, and 3300 A are the narrowest principal lines of the series and the broad bands accompanying them are located in the longer wavelength region within each series.

The authors of reference 3 divided all of the lines and bands detected by them in the absorption spectra of diamonds into two groups. The widths and intensities of the absorption lines of group A depend on temperature, while the lines of group B are relatively sharp even at room temperature. The other difference between groups A and B is that the lines of group A are single, but the lines of group B are accompanied by a system of subsidiary bands. The Table shows the data obtained in reference 3, as well as the classification of absorption lines into groups A and B.

An analysis of our data (see the Table) shows that the lines of series No. 6 and No. 7 (according to reference 3) are not single, and should be placed in group B. However, on the other hand, absorption bands located near the line at 4152 A are included in group B, and this means that the "centers" of the blue luminescence of diamonds must be connected with lattice defects which are responsible for the absorption of these crystals in the region near 3000 A. Moreover, as already noted above, we did not detect any direct relationship between the absorption in the 3000-3300 A region and the blue luminescence of diamonds.

Besides studying the absorption spectra of diamonds, we also determined their absorption edge in the ultraviolet. According to this criterion, the authors of reference 1 divided diamonds into two types: continuous absorption of diamonds of type I begins near 3000 A, while diamonds of type II are transparent up to 2250 A. Thus it is characteristic that diamonds of type I luminesce, but diamonds of type II do not show luminescence when excited by ultraviolet light, $\lambda = 365$ mμ.

Among the diamonds we investigated, there were specimens which were transparent up to 2250 A; some of these showed luminescence when excited by ultraviolet light. In the absorption spectra of such specimens one could detect the line at 4152 A with a broad band adjoining it (see the Figure). However, the series of bands with principal lines near 3020, 3154, and 3300 A are absent in the absorption spectra of diamonds transparent beyond 2900 A. Thus, in the case of crystals which are transparent to 2900-3000 A it is possible to detect three or four (if the diamond luminesces) groups of bands in the absorption spectra. According to the degree of transparency of the specimen, the three short wavelength series of bands disappear in its absorption spectrum.

According to the data of reference 1, the limit of transparency of diamonds lies either near 2250 A or near 3000 A. In this connection, we might note that among our specimens the limits of transparency were located at various points between 2250 and 3000 A.

We have pointed out previously[4] that the classification of diamonds into two types proposed in reference 1 could not encompass all the diverse physical properties of these crystals observed in individual specimens, and proposed a scheme which satisfactorily accounted for the data quoted in the present communication.

REFERENCES

1. R. Robertson, I. Fox, and A. Martin. Phil. Trans. Roy. Soc. **A232**, 463 (1934).
2. Symposium of papers on the structure and properties of diamond, Proc. Indian Acad. Sci. **A19** (1944).
3. C. D. Clark, R. W. Ditchburn, and H. B. Dyer. Proc. Roy. Soc. **234**, 363 (1956).
4. G. O. Gomon. Doklady Akad. Nauk SSSR **105**, 713 (1955).

ON THE SENSITIZATION OF PHOTOGRAPHIC PLATES IN THE ULTRAVIOLET REGION OF THE SPECTRUM

I. A. Berezin and A. I. Stepanova

Received 30 July 1959

A commonly used method of increasing the sensitivity of photographic materials in the far ultraviolet region is based on covering the photosensitive emulsion with a thin layer of luminescent material. The materials ordinarily used as sensitizers are various types of oils[1-4] or sodium salicylate. However, the choices of sensitizer and photographic material are haphazard, as a rule. Consequently, the sensitizations are not always fully effective.

We have studied the sensitization of photographic plates in the ultraviolet region as a function of luminescent material and the type of emulsion. Types of emulsion investigated were spectral types I, II, and III, micro and iso-ortho, and sensitizers investigated were transformer oil, vaseline oil, and sodium salicylate.

Characteristic curves for photographic plates of spectral type III with the various sensitizers are given in Fig. 1. The characteristic curves for the sensitized micro and iso-ortho plates have a similar form. Exposure conditions selected were such that for plates of spectral types I and II the entire spectra were more or less underexposed. Spectra taken on unsensitized micro and iso-ortho plates were also more or less underexposed. A comparison of the characteristic curves for the various types of plates, sensitized with the various materials, shows that the photographic plates of spectral type III sensitized with sodium salicylate have the highest sensitivity in the far ultraviolet region.

The dependence of the sensitization on wavelength is shown in Fig. 2. As a measure of the sensitization we use the ratio S_s/S_a, where S_s is the absolute blackening of a spectral line on the sensitized plate and S_a is the absolute blackening of the same line on an unsensitized plate for the same exposure time. The sensitization threshold occurs at a longer wavelength (2400 A) for sodium salicylate than for transformer oil or vaseline oil (2250 and 2200 A, respectively).

The dependence of the sensitization on the concen-

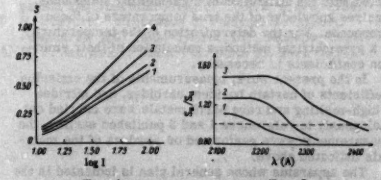

Fig. 1

Fig. 2

Characteristic curves for plates of spectral type III with various sensitizers (λ2136 A). Curve 1—unsensitized, curve 2—vaseline oil, curve 3—transformer oil, curve 4—sodium salicylate.

Fig. 2. Dependence of sensitization on wavelength for plates of spectral type III. Curve 1—vaseline oil, curve 2—transformer oil, curve 3—sodium salicylate

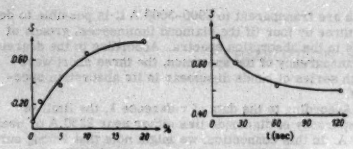

Fig. 3 Fig. 4

Fig. 3. Dependence of sensitization on concentration of the sodium salicylate solution (abscissa). S = blackening of a spectral line (λ2136 A).

Fig. 4. Dependence of the sensitization on soaking time (abscissa). S = blackening of a spectral line (λ2136 A).

tration of sodium salicylate was investigated. It was determined that the sensitization improved with increasing concentration (Fig. 3).

Increasing the time that the plates are soaked in the sodium salicylate solution worsens the sensitization (Fig. 4). Washing the plates with water before development has no positive effect.

Reproducibility of the results was checked in terms of the absolute blackening of spectral lines by means of multiple exposures of spectra on sensitized and unsensitized plates. For unsensitized plates of type III it is 8.8%, while for the same type of plates sensitized by a 3-second soaking in sodium salicylate it is 10.6%, and for plates soaked 2 minutes it is 13.8%.

The investigation of the dependence of sensitization on the storage time of the plates showed that sensitized plates retained their properties completely after storage for a week.

CONCLUSION

A 20% solution of sodium salicylate in a 50% aqueous solution of ethyl alcohol is recommended for sensitization of photographic plates in the 2000-2300 A region. Photographic plates of spectral type III are recommended. The photographic plates are soaked in the solution of sodium salicylate for three seconds and are then dried for several minutes in a stream of air. The layer of sodium salicylate must not be washed off before development of the plates. The sensitized plates retain their properties for a week.

REFERENCES

1. S. L. Mandel'shtam. "Vvedenie v spektral'nyi analiz." (Introduction to Spectral Analysis), Gosudarst. Izd. Tekh.-Teoret. Lit., Moscow, 1946.
2. N. S. Sventitskii. Invest. Akad. Nauk SSSR, Ser. Fiz. 11, 319 (1947).
3. V. K. Prokof'ev. "Fotograficheskie metody kolichestvennovo spektral'novo analiza metallov i splavov." (Photographic Methods of Quantitative Spectral Analysis of Metals and Alloys), Gosudarst. Izd. Tekh.-Teoret. Lit., Moscow, 1951.
4. F. Z. Pedos and N. S. Sventitskii. Opt. i Spektr. 5, 706 (1958).
5. O. N. Setkina. Zavodskaya Lab. 9, 232 (1940).
6. B. G. Voronov. Proceedings of the Tenth Congress on Spectroscopy, 2, 395 (1958).
7. E. M. Akimov and I. P. Malkov. Opt. i Spektr. 6, 96 (1959).

EMISSION COEFFICIENTS OF SOME POWDERED HIGH-MELTING COMPOUNDS

T. I. Serebryakova, Yu. B. Paderno, and G. V. Samsonov

Received 8 August 1959

Development of high temperature techniques, connected with the utilization of high-melting compounds, requires knowledge of the true temperature of these compounds. For the determination of the temperature by a pyrometrical method, a calculation of their emission coefficients is necessary.

In the present work, measurements of the emission coefficients of certain borides, carbides, and nitrides of high-melting and rare earth metals were carried out. Analogously to references 1 and 2 published earlier, the measurements were performed on powders of the materials indicated above.

The apparatus whose general plan is indicated in the Figure was employed for the measurements. It fitted sufficiently closely the model of an absolute black body. A tantalum cylinder 5 (diameter 20 mm, height 50 mm) manufactured from sheet tantalum with a thickness from 0.1 to 0.2 mm served for a heater. The cylinder contained an aperture 7 with a diameter of 5 mm in its wall. A second tantalum cylinder 6 with a diameter of 8 mm and a height of 20 mm was placed concentrically inside the cylinder. The inner cylinder contained an aperture (diameter 1 mm) whose axis coincided with the axis of

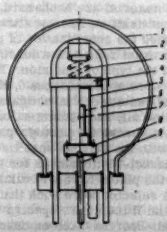

the aperture of the first cylinder. The inside of the cylinder was tightly closed at the ends by means of spot welded tantalum discs.

The tantalum cylinders were fastened by their lower ends on a molybdenum stage 8 placed on the curved end of the lower current lead, and the upper contact (pressed by means of spring 3) was made through a molybdenum crossbar 4 loosely placed on the upper current lead 2.

The working space of the apparatus was confined by a bell jar 1.

A layer of paste, prepared from fine powder (2-3 μ) of a high-melting compound suspended in a nitrate binder, was applied on the surface of the inner cylinder in a uniform homogeneous layer with a thickness of about 100 μ, and then dried at 40-60°C. The temperature of the surface of the inside cylinder (luminance temperature) and the temperature in the aperture (the true temperature) were determined by means of an optical pyrometer (OPPIR-09). Correction for light absorption by the bell jar of the oven proved to be very insignificant and was not considered in the calculations. Measurement of the intensity of the emission was carried out at the wavelength (650 mμ) of the emitted light.

Calculation of the emission coefficients was made according to the formula

$$\ln \varepsilon_\lambda = \frac{c}{\lambda}\left(\frac{1}{T_{true}} - \frac{1}{T_{lum.}}\right),$$

where c = 1.438 cm/deg.

The use of a small diameter inside cylinder, in contrast to the methods used for these same purposes previously,[2,3] provides a quite uniform temperature distribution on the surface on which the powder of the high-melting compound is applied and minimizes errors in the measurement. Besides, the small dimensions of the inside cylinder make it possible to perform measurements while utilizing a very small amount of material.

The method developed by us was used for a determination of the emission coefficient of pure tantalum in the temperature interval from 800 to 2000°C; whereupon, good agreement was obtained with well known data from the literature (Table 1).

Table 1. Emission Coefficients of Pure Tantalum

Literature source	Temperature (°C)						
	850	1200	1350	1450	1550	1650	1750
According to our data	0.49	0.44	0.42	0.44	0.42	0.42	0.42
According to reference 4	0.46	0.44	0.43	0.42	0.42	0.42	0.41

It is possible that certain of the results which are too large were caused by the surface roughness of the layer which was studied; however, the role of this factor, evidently, is small so that in all cases the temperature dependence of the emission coefficient is typical for polished metallic surfaces.[5]

The data obtained from the work are given in Table 2.

Considering the results which were obtained, one must note that the compounds of metals which have unfilled electronic d-shells are characterized by similar values of the emission coefficients, and the emission coefficients somewhat exceed those for the rare earth metals in which a deep lying and strongly screened 4f-shell is unfilled (with the exception of yttrium which is related to the d-transition metals). This can be connected with the ease of electronic transitions in the first case. Besides this, the borides of the rare earth metals have a peculiar crystal structure which is characterized by the presence of a rigid framework of boron atoms. The valence electrons of the metal atoms participate in the formation of the framework, and this also hinders possible electron transitions.

Table 2. Emission Coefficients for Powders of High-Melting Carbides, Borides, and Nitrides

Compound	Temperature (°C)								
	850	900	1000	1150	1250	1350	1450	1550	1650
LaB_6	0.68	0.68	0.69	0.69	0.69	0.70	0.70	0.70	0.71
NdB_6	0.56	0.56	0.56	0.57	0.58	0.58	0.58	0.58	0.59
SmB_6	0.71	0.70	0.70	0.69	0.69	0.68	0.68	0.67	0.67
GdB_6	0.61	0.61	0.62	0.62	0.63	0.63	0.63	0.63	0.64
YB_6	0.63	0.64	0.65	0.66	0.66	0.66	0.67	0.67	0.68
ZrB_2	0.86	0.87	0.88	0.90	0.91	0.92	0.91	0.93	0.95
HfB_2	0.85	0.86	0.87	0.88	0.89	0.90	0.92	0.92	0.94
B_4C	0.84	0.85	0.85	0.86	0.86	0.87	0.87	0.88	0.88
TiC	0.84	0.85	0.85	0.86	0.86	0.87	0.87	0.88	0.88
CrC_3	0.91	0.91	0.91	0.91	0.91	0.91	0.91	0.91	0.91
BN	0.58	0.59	0.59	0.59	0.60	0.60	0.60	0.60	0.60

The higher emission coefficient of boron carbide in comparison with boron nitride which have similar characters of chemical binding (covalent for the carbide and covalent with elements of ionic binding for the nitride) can be explained by the easy excitation of the electrons of the carbide which are responsible for the bond between carbon atoms in the linear chain —C—C—C— located along a body diagonal of the unit cell of B_4C.[6] Let us note that the same thing explains the relatively low electrical resistance of the carbide, which is less by several orders of magnitude than the resistance of the nitride, and also the rapid decrease of the resistance of B_4C with increasing temperature.

REFERENCES

1. G. A. Kudintseva and B. M. Tsarev. Radiotekh. i Elektron. 3, 427 (1958).
2. F. Morgan. J. Appl. Phys. 22, 108 (1951).
3. D. Jillson. J. Metals 188, 1006 (1950).
4. M. Ardenne, "Tabellen der Elektronenphysik, Ionenphysik und Übermikroskopie." Vol. 2, p. 892, 1956.
5. R. Bosvort. "Processes of Thermal Transport." Gosudarst. Izd. Tekh.-Teoret. Lit., Moscow, 1957.
6. G. V. Samsonov. Zhur. Fiz. Khim 32, 2424 (1958).

EFFECT OF SOLVENTS ON THE ELECTRONIC SPECTRA OF ORGANIC MOLECULES

I. A. Zhmyrev, V. V. Zelinskii, V. P. Kolobkov, A. S. Kochemirovskii, and I. I. Reznikova

Received 12 August 1959

In 1878 Kundt[1] proposed a rule relating the frequency shifts of absorption spectra to the refractive index of the solvent, but in the majority of cases, this rule does not agree with experimental results. On the other hand, in his first investigation of the effect of solvent on fluorescence spectra of complex organic compounds, Kaufmann[2] showed that the change in the color of fluorescence occurred parallel with a change in the dielectric constant of the solvents. Explanations for this phenomenon were sought in the simultaneous effect of the dielectric constant and of the refractive index on the spectra. A number of attempts have been made to compare quantitatively the spectral changes with the above-mentioned properties of the solvents.[3-6] However, none of the above attempts can be considered successful. The most complete treatment of quantitative correlation of the solvent effect on electronic spectra of organic compounds with the refractive index and dielectric constant of the solvents, is given in the papers of Bakhshiev.[7,8]

The experimental results given in those papers, agree very well with the formulas proposed by their author. However, substitution of values of A* and $\Delta\nu_{sl}$ for a wider selection of solvents leads to considerable deviation of experimental results from the theoretical straight line. Figure 1 reproduces $\Delta\nu_{sl}$ as a function of A from reference 8 and shows the points relating A and $\Delta\nu_{sl}$ for a number of solvents not given in reference 8.

*See the caption to Fig. 1.

As can be seen from the figure, the deviation of some points from the straight line amounts to 75% of the measured value of A or $\Delta\nu_{sl}$. Figure 1 shows all the data for only one derivative of phthalimide, but it is easy to verify that the same situation holds true for other phthalimide derivatives.

It can be attempted to explain the presence of shifts greater than those determined by the magnitude of A, as being due to additional specific interactions between the solvent molecules and the solute molecules, e.g., formation of hydrogen bonds or salt formation. However, because of a number of reasons, such explanations can not be considered as satisfactory.*

*Lack of space prevents us from examining this problem in detail. This will be done elsewhere.

It is even more difficult to explain the deviations upward from the straight line, i.e., small $\Delta\nu_{sl}$ at large values of A, when the "acting cause" is large and the effect small.

The reverse dependence of the susceptibility of spectra to the effect of solvents, on the radius of the molecule, also does not agree with experimental results. In the case of derivatives of phthalimide and maleinimide, it is possible to give many examples of the absence of the effect of molecular volume on the susceptibility of spectra to the effect of solvents. In the case of 4-amino-N-methylphthalimide and 4-amino-N-cyclohexylphthalimide, where the volume of the latter is about one and a half times the molecular volume of the former (Fig. 2), the straight lines characterizing the dependence of the fluorescence spectra of these compounds on the solvent, coincide. There is very little difference between the

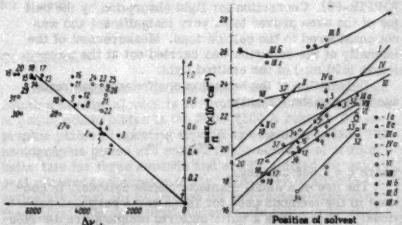

Fig. 1

Fig. 2

Fig. 1. $\Delta\nu_{sl}$ is a function of A for 4-aminophthalimide. Full points—results of reference 8; circles—results obtained in the present investigation.
Numbering of the solvents: 1-vapor, 2-n-heptane, 3-carbon tetrachloride, 4-benzene, 5-toluene, 6-xylene, 7-dioxane, 8-diethyl ether, 9-anisole, 10-butyl acetate, 11-chloroform, 12-ethyl acetate, 13-pyridine, 14-isoamyl alcohol, 15-isobutyl alcohol, 16-acetone, 17-ethyl alcohol, 18-methyl alcohol, 19-glycerol, 20-water, 21-chlorobenzene, 22-ethylene bromide, 23-ethyl bromide, 24-ethylene chloride, 25-isopropyl bromide, 26-propyl bromide, 27-methylal, 28-caproic acid, 29-octyl alcohol, 30-butyric acid, 31-acetic acid, 32-n-octane, 33-n-hexane, 34-propyl acetate, 35-isoamyl acetate, 36-pinacoline, 37-ethyl orthoformate.

$$A = \frac{2\varepsilon - 1}{2\varepsilon + 2} + p\,\frac{2n^2 - 1}{2n^2 + 2}.$$

Fig. 2. The position of maxima of fluorescence spectra (ν_{fl}^{max}) and absorption spectra (ν_{abs}^{max}) as a function of solvent.
Fluorescence: Curve I—4-amino-N-methylphthalimide, curve II—4-acetylamino-N-methylphthalimide, curve III—3-amino-N-methylphthalimide, curve IV—3-acetylamino-N-methylphthalimide; curve Ia—4-amino-N-cyclohexylphthalimide, curve IIa—4-benzoylamino-N-cyclohexylphthalimide, curve IIIa—3-amino-N-phenylphthalimide, curve IVa—3-benzoylamino-N-cyclohexylphthalimide; curve V—4-diphenylamino-N-methylphthalimide, curve VI—aminochloromaleinimide, curve VII—cyclohexylaminomaleinimide.
Absorption: Curve IIIb—3-aminophthalimide, curve IIIc—3-amino-N-methylphthalimide, curve IIId—3-amino-N-phenylphthalimide.
The method of plotting the position of solvents along the abcissa axis is the one used in references 10, 12, and 13. The numbering of solvents is the same as in Fig. 1.

straight lines for 3-amino-N-methylphthalimide and 3-amino-N-phenylphthalimide, although the molecule of the latter is one and half-times larger than the molecule of the former. The molecule of 4-amino-N-methylphthalimide is two times smaller than that of 4-diphenylamino-N-methylphthalimide, but the frequency shift of the fluorescence spectrum, in any two solvents, is the same for both compounds; e.g., the frequency shift in going from octane to propylacetate, is 3800 cm^{-1}.* Hence, at present, the correctness of the point of view, according to which the solvent effect on spectra is determined by the macroproperties of the solvents, can not be experimentally justified. According to another point of view,[9-13] it is essentially incorrect to ascribe the effect of solvents on spectra to the macroproperties of the solvents, because they are primarily determined by the nearest-order intermolecular interactions, which are, in their turn, determined by the microproperties and not the macroproperties of the solvents. The known parallelism between the changes in ν_{a1} and ε, is determined by the fact that the magnitude of the dielectric constant is determined mainly by the same microproperties of the solvents.

*In the case of phthalimide derivatives, the change in fluorescence spectra from solvent to solvent is much greater than in the case of absorption spectra. Thus, the change in ν_{a1} is mainly determined by change in ν_{fl}^{max}. However, as can be seen from Fig. 2, the absorption spectra, or their frequency shifts in going from one solvent to another, are also the same for compounds differing in their molecular dimensions.

REFERENCES

1. A. Kundt. Ann. Phys. 4, 34 (1878).
2. O. Kaufmann and O. Beisswanger. Z. phys. Chem. 50, 350 (1904).
3. V. Ooshika. J. Phys. Soc. Japan 9, 594 (1954).
4. N. Mataga, Y. Kaifu, and M. Kouzumi. Bull Chem. Soc. Japan 29, 115, 165 (1956).
5. E. Lippert. Z. Naturforsch 10a, 541 (1955).
6. E. Lippert. Z. phys. Chem. N.F., 8, 125 (1956).
7. N. G. Bakhshiev. Izvest. Akad. Nauk SSSR, Ser. Fiz. 22, 1387 (1958).
8. N. G. Bakhshiev. Opt. i Spektr. 7, 52 (1959).
9. V. V. Zelinskii and V. P. Kolobkov. Report presented at the VI Symposium on Luminescence, Leningrad, 1958.
10. V. V. Zelinskii, V. P. Kolobkov, and I. I. Reznikova. Reports of Conference on Thermodynamics and Structure of Solutions, Moscow, 1958.
11. E. Kosower. J. Am. Chem. Soc. 80, 3253 (1958).
12. V. V. Zelinskii, V. P. Kolobkov, and L. G. Pikulik. Opt. i Spektr. 2, 402 (1957).
13. I. A. Zhmyreva, V. V. Zelinskii, and V. P. Kolobkov. Doklady Akad. Nauk SSSR 129, 1089 (1959).

THE EFFECT OF TEMPERATURE ON THE ELECTROLUMINESCENCE OF A SUBLIMED ZnS-Mn PHOSPHOR

N. A. Vlasenko

Received 17 August 1959

Studying the effect of temperature on electroluminescence (EL) can give valuable information on the mechanism of this phenomenon. Up till now research workers have usually confined themselves to studying the temperature variation of EL brightness and comparing this with the thermal luminescence of the phosphor. The data on this topic available at present are very contradictory. For example, for zinc sulfide activated with manganese Mattler[1] obtained a monotonic decrease in brightness with temperature between −120 and +120°C. Halstead and Koller[2] observed a brightness maximum below room temperature, and Kazankin and Petoshina[3] found that the brightness changes little with temperature below −50°C, then increases sharply as the temperature rises, passes through two maxima and begins to fall at approximately 50°C. Some authors[4,5] state that there is a relationship between the temperature variation of EL brightness and thermal luminescence; others[3,6,7] find no connection between these characteristics. Most workers are agreed, however, that both phenomena are related to electrons accumulated in traps. The importance of donor centers on the temperature variation of EL has not been explained yet.

Using different coactivators and fluxes, and changing the annealing atmosphere in preparing the phosphor make it possible to form different types of impurity center, which may greatly complicate and change the temperature variation of EL brightness. Possibly this accounts for the inconsistent results obtained by different authors mentioned above.

It is therefore interesting to study the effect of temperature on the properties of EL phosphors with a very simple chemical constitution. A method which we developed[8,9] makes it possible to prepare sublimed phosphors which are luminescent under an applied electric field: we diffused an activator metal into the basic lattice material without any impurities. Sublimed phosphors are convenient for studying the temperature variation of EL, since they eliminate the problem of finding a dielectric with temperature-invariant properties, and the measurements may be made over an unlimited temperature range. In addition, the conductivity of the phosphor can be studied because the specimens obtained by sublimation are uniform.

ZnS-Mn sublimed phosphor was studied in this project, in the temperature range 100-500°K. A special optical cryostat was used for measurements below room temperature. The specimen was pressed against a copper finger of the inner cylinder of the cryostat into which liquid nitrogen was poured. The space between the inner and outer cylinders was evacuated to 10^{-4} mm Hg to avoid icing of the specimen and the window. The heating rate could be varied over a wide range by means of a heater in the cryostat, and the specimen temperature raised to +70°C. For the measurements at higher temperatures, the specimen was clamped to a heavy copper block in a special oven. The data obtained with the specimen in the cryostat and in the oven were easily related by combining the results in the range 20-70°C. A copper-constantan thermocouple measured the temperature. The radiation

detector was an FEU-17 photomultiplier with an amplifier and galvanometer as indicator. The EL was excited by a sinusoidal voltage, and photoluminescence was excited by the 365 mμ mercury line. Above room temperature, the luminescence was measured under equilibrium conditions a few minutes after establishing the required temperature; at low temperatures, the measurement was made with the specimen slowly warming up (1.5 deg/min).

As we mentioned, up till now most research has been confined to the temperature variation of the integral EL brightness, while from a physical point of view the characteristic of interest is the temperature variation of the number of quanta emitted per unit time. These two variations may be different in form, since the luminescence spectrum changes with temperature and the sensitivity of a radiation detector varies with wavelength. We therefore studied the EL spectrum at different temperatures. On the basis of these measurements, the radiation curves were integrated graphically, giving the temperature variation of the relative number of quanta emitted in unit time for a given type of excitation. A similar relationship was obtained in the same way for photoluminescence. Figure 1 gives the experimental results. It shows that with increasing temperature, the electroluminescence and photoluminescence spectra undergo a spectral redistribution of the radiant energy, consisting of a change in the intensity of the band and an increase in its width [sic]. (In addition, a small shift in the maximum of the photoluminescence spectrum to the short wavelength region was observed). The half-width of radiation band changed in proportion to $\sqrt{T}$ for $T > 250°K$.

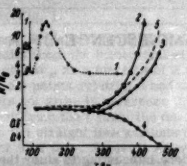

Fig. 1. Curves of thermoluminescence (curve 1), temperature variation of integral electroluminescent brightness (curve 5), and relative number of quanta emitted per unit time for electrical excitation (curves 2, 3), and photoexcitation (curve 4) for a sublimed ZnS-Mn phosphor. Field voltage and frequency: curve 2—2×10^3 volts/cm, 200 cps; curve 3—2×10^3 volts/cm, 2000 cps.

N, the number of quanta emitted, remains constant for temperatures below 200°K. With a further increase in temperature, N falls; this apparently is associated with the appearance of temperature quenching. Beginning at a certain temperature, the variation of the number of quanta emitted per unit time becomes different for photoluminescence and electroluminescence: for the former, the number of quanta continues to fall; for the latter, it begins to rise rapidly with temperature. The rise in EL intensity is monotonic and is accompanied by an increase in the current through the specimen. The same results were obtained when the phosphor was heated and cooled several times. No slowing down of the increase in the EL was observed right up to 500°K. Measurements could not be made at higher temperature due to electrical breakdown and burning of the sample.

Figure 1 also shows the temperature variation of the integral EL brightness (curve 5), taken under the same conditions as curve 3. It is seen that these curves differ, especially in the low temperature region.

Thermal luminescence (Fig. 1 curve 1, heating rate 5 deg/min) was also studied on the same specimens that were used to study the temperature variation of photoluminescence and electroluminescence. The curve of the thermal luminescence of a sublimed ZnS-Mn phosphor has only one maximum in the region of 130°K. This maximum is observed in all ZnS phosphors and is apparently caused by the presence of excess zince atoms. Thermal luminescence was not observed if the specimen was excited with an electric field, instead of ultraviolet radiation, before heating. This is probably because the presence of a strong electric field reduces the depth of traps and therefore lower temperatures are needed to accumulate electrons in them. Comparison of the thermal luminescence curve with the temperature variation of EL shows that there is no correspondence between them. Therefore, the traps responsible for the peak of the thermal luminescence curve in the region of 130°K have no importance in the EL process in the temperature region that we studied, and no deeper trapping levels were detected in the sublimed ZnS-Mn phosphor.

To examine the effect of donor centers on EL, we studied the temperature variation of the conductivity of the phosphor and its relationship to the temperature variation of EL. Figure 2 gives the results for one specimen. The phosphor conductivity was measured with a vacuum tube megohmmeter in a dc field of about 5×10^3 volts/cm. The logarithm of the phosphor conductivity plotted against the reciprocal of the absolute temperature has two straight-line portions, which indicates the presence of two types of donor levels. The depths of these levels, determined from the slopes of the straight line portions, are 0.11 and 0.38 ev. It is striking that the EL intensity begins to rise sharply in the temperature region where the deeper donor level system begins to make an appreciable contribution to the phosphor conductivity. For convenience in making the comparison, Fig. 2 shows the temperature variation of the number of activator centers excited per unit time by the application of an electric field. This relationship was obtained by dividing the number of quanta emitted at a given temperature by the coefficient of temperature quenching, the latter being determined from the temperature variation of photoluminescence.

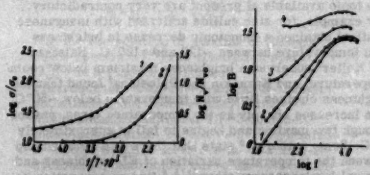

Fig. 2

Fig. 3

Fig. 2. Temperature variation of the conductivity (curve 1) and the relative number of activator centers excited by the electric field in unit time (curve 2) in a sublimed ZnS-Mn phosphor. Field strength 2×10^3 volts/cm. Frequency 2000 cps.

Fig. 3. Frequency variation of the electroluminescent brightness of a sublimed ZnS-Mn phosphor at different temperatures. Temperature (°K): curve 1—105; curve 2—293; curve 3—360; curve 4—410.

We can explain the observed temperature variation of EL if we start from a collision mechanism of EL excitation and thermal ionization of donors, aided by the presence of a field. At low temperatures, the concentration of conduction electrons is determined by shallow donor levels. In the presence of a strong external field (10^5 volts/cm), these levels are almost completely ionized at any temperature, that is, the number of electrons which can be accelerated by the field and which can excite the activator centers in collisions, is independent of temperature in this region; consequently the EL intensity is also. However, when the temperature is raised so that considerable ionization of the deep donor levels also begins, the EL intensity begins to increase with temperature due to the increase in the number of collisions leading to excitation of activator centers.

Johnson, Piper, and Williams[5] have suggested that the increase in EL intensity with increase in the concentration of free electrons may be associated with an increase in the local field in a layer impoverished in electrons at the phosphor/metal electrode interface. However, as our studies showed, the shape of the light pulses and the relative size of the peaks corresponding to voltage half-cycles of different polarity do not change in the temperature region where the strong growth in EL is observed, whereas the peak corresponding to the negative polarity (the metal electrode negative) would increase considerably more rapidly with temperature if the increase in the field at the surface layer were responsible for the EL intensity increase.

As the frequency of the field applied to the phosphor is raised, a considerable increase in EL begins at the higher temperatures (Fig. 1, curves 2, 3). This apparently indicates that the number of donor centers ionized in a given voltage half-cycle decreases as the field frequency increases. For the same reason, apparently, a change in the character of the frequency variation of EL brightness occurs with rising temperature (Fig. 3), observed in the same temperature range where there is an increase in the probability of thermal ionization of deep donors, aided by the field.

In conclusion I thank K. D. Sinel'nikov for his interest and I. N. Shklyarevskii and V. K. Miloslavskii for valuable discussions.

REFERENCES

1. J. Mattler. Compt. Rend. 239, 1116 (1954).
2. R. Halsted and L. Koller. Phys. Rev. 93, 349 (1954).
3. O. N. Kazankin and L. N. Petoshina. Opt. i Spektr. 4, 76 (1958).
4. H. Gobrecht, D. Hahn, and A. E. Gumlich. Z. Physik 136, 623 (1954).
5. P. D. Johnson, W. W. Piper, and F. E. Williams. J. Electrochem Soc. 103, 221 (1956).
6. C. H. Haake. Phys. Rev. 98, 1544 (1955).
7. F. G. Alfrey and J. B. Taylor. Brit. J. Appl. Phys. 6, Suppl. 4 (1955).
8. N. A. Vlasenko. Doklad na VII Soveshch. po liuminests. (Report on the Seventh Conference on Luminescence), Moscow, 1958.
9. N. A. Vlasenko and Yu. A. Popkov. Opt. i Spektr. 8, 81 (1960).

A SIMPLE DERIVATION OF THE KRAMERS-KRÖNIG RELATIONS

V. S. Galishev

Received 30 September 1959

Toll[1] performed a theoretical investigation of the so-called dispersion relations for a generalized amplitude of scattering and proved their equivalence to a strict causality condition. The results of this work are partially interchangeable with the results which Bogoliubov et al.[2] obtained by a different method.

This note shows that using these investigations it is possible, in a very simple way, to obtain Krönig's[3] relation between the index of refraction and the linear absorption coefficient, and also Kramers'[4] relation between the real and imaginary components of the dielectric constant.

It is assumed that the amplitude of forward scattering is analytic in the upper half of the complex frequency plane $\omega = \omega_r + i\omega_i$ and has its pole at an infinity of zero order. In this instance, we can use particular cases of formulas (5, 2) and (5, 6) from reference 1. These formulas contain two arbitrary parameters: a positive integer j and a real frequency λ. Since the order of the pole of the amplitude of scattering at infinity is determined by the difference $j - 1$, we have the parameter $j = 1$, according to our earlier assumption. For convenience we select the parameter λ to equal zero. Therefore, substituting $\lambda = 0$ and $j = 1$ in the abovementioned formulas, we obtain

$$A(\omega_r) - A(0) = \frac{\omega_r}{\pi i} P \int_{-\infty}^{\infty} \frac{[A(x) - A(0)]}{x(x - \omega_r)}\, dx, \qquad (1)$$

where P is the principal value of the integral. But if $A(\omega)$ corresponds to the amplitude of the coherent scattering of a photon by an isolated atom, then $A(0) = 0$ because of the zero charge of the atom. Therefore, taking the real component of (1) we have

$$\mathrm{Re}\, A(\omega_r) = \frac{\omega_r}{\pi} P \int_{-\infty}^{\infty} \frac{\mathrm{Im}\, A(x)}{x(x - \omega_r)}\, dx. \qquad (2)$$

The propagation of light in the medium is described by the "plane" wave

$$\exp\left[-i\omega_r\left(t - \frac{n'}{c}x\right)\right]$$

with the complex index of refraction

$$n'(\omega_r) = n(\omega_r) + i\frac{\alpha(\omega_r)c}{2\omega_r}, \qquad (3)$$

where $n(\omega_r)$ is the ordinary index of refraction $\alpha(\omega_r)$ is the linear absorption coefficient, and c is the velocity of light in vacuum. Then the connection between $n'(\omega_r)$ and the amplitude of forward scattering, using the known optical relations of Lax,[5] formula (5, 14), and Bethe and Morrison,[6] formula (11, 10), is expressed by the equation

$$[n'(\omega_r)]^2 = 1 + \frac{4\pi e^2}{\omega_r^2} N A(\omega_r), \qquad (4)$$

where N is the number of atoms per unit volume. When the index of refraction differs only insignificantly from unity, formula (4) becomes

$$n'(\omega_r) = 1 + \frac{2\pi e^2}{\omega_r^2} N A(\omega_r). \tag{5}$$

Using formulas (3) and (5) and also the condition $A(\omega_r) = -A(-\omega_r)$, it is easy to convert expression (2) into the desired relationship between the index of refraction and the linear absorption coefficient (see Krönig,[3] formula (9))

$$n(\omega_r) - 1 = \frac{c}{\pi} P \int_0^\infty \frac{a(x)dx}{x^2 - \omega_r^2}. \tag{6}$$

This can also be written as follows:

$$n'(\omega_r) - 1 = \frac{c}{\pi} \lim_{\varepsilon \to 0^+} \int_0^\infty \frac{a(x)\,dx}{x^2 - (\omega_r + i\varepsilon)^2}, \tag{7}$$

which can be easily demonstrated by using the symbolic identity

$$\frac{1}{y \mp i\varepsilon} = \frac{P}{y} \pm i\pi\delta(y). \quad (\varepsilon \to 0^+). \tag{8}$$

Our method of deriving formula (5) is slightly different for establishing the second of the abovementioned relations. We now assume that the amplitude of forward scattering is analytic when $\mathrm{Im}\,\omega > 0$ and that its pole at infinity is of an order not higher than first. Then expression (1) can be replaced by

$$A(\omega_r) - A(0) - A^{(1)}(0)\,\omega_r = \frac{\omega_r^2}{\pi i} P \int_{-\infty}^{\infty} \frac{[A(x) - A(0) - A^{(1)}(0)\,x]}{x^2 (x - \omega_r)}\,dx. \tag{9}$$

Because of the zero charge of the atom the terms with A(0) and $A^{(1)}(0)$ drop out of Eq. (9). The relation between the dielectric constant $\varepsilon = (n')^2$ and the amplitude of scattering is expressed by formula (4). Therefore, taking the real and imaginary components of (9) and taking account of Eq. (4), we find the desired relationship between the real ε' and the imaginary ε'' components of the dielectric constant ε. (Kramers,[4] formulas (19) and (21); Landau and Lifshits,[7] formulas (61, 8)–(64, 9)):

$$\varepsilon'(\omega_r) - 1 = \frac{1}{\pi} P \int_{-\infty}^{\infty} \frac{\varepsilon''(x)}{x - \omega_r}\,dx. \tag{10}$$

$$\varepsilon''(\omega_r) = -\frac{1}{\pi} P \int_{-\infty}^{\infty} \frac{\varepsilon'(x) - 1}{x - \omega_r}\,dx. \tag{11}$$

From the present derivation of the Kramers-Krönig relations (6), (10), and (11) it is seen that the following two suppositions are essential for the derivation of each of these relations: (1) that the forward scattering amplitude is analytic in the upper half of the complex plane, and (2) that it behaves at infinity as stated above. For Krönig's relation, the supposition about the smallness of the complex index of refraction compared to unity is also essential.

In conclusion, the author expresses his deep gratitude to A. V. Sokolov and A. N. Orlov for their interest in this work.

REFERENCES

1. J. S. Toll. Phys. Rev. 104, 1760 (1956).
2. N. N. Bogoliubov, B. V. Medvedev, and M. K. Polivanov. "Voprosy teorii dispersionnykh sootnoshenii." Gosudarst. Izd. Fiz.-Mat. Lit., 1958.
3. R. Krönig. J. Opt. Soc. Am. 12, 547 (1926).
4. H. A. Kramers. Estratto dagli Atti del Congresso Internazionale dei Fisici a Como. Bologna, 1927.
5. M. Lax. Revs. Modern Phys. 23, 287 (1951).
6. H. Bethe and F. Morrison. "Elementarnaya teoriya yadra." Izd. Inostrannoi Lit., Moscow, 1958.
7. L. D. Landau and E. M. Lifshitz. "Elektrodinamika sploshnykh sred." Gosudarst. Izd. Fiz.-Mat. Lit., 1959.

MICROWAVE INVESTIGATION OF THE MOLECULES F_3BNH_3 AND $F_3BN(CH_3)_3$

A. M. Prokhorov and G. P. Shipulo

Received 9 October 1959

The molecules F_3BNH_3 and $F_3BN(CH_3)_3$ are symmetrical tops. An estimation of the values of the rotational constants of these molecules has been made on the basis of data on their structure in the solid state;[1] for F_3BNH_3, the value B = 4740 Mc was obtained, and for $F_3BN(CH_3)_3$, B = 1830 Mc.

We have carried out an investigation of the rotational spectra of these molecules in the vapor with the help of a microwave spectroscope with Stark modulation, the absorbing cell of which was equipped for work at temperatures up to 200°C.

The search for the absorption lines of F_3BNH_3 was carried out in the range 9000–35000 Mc. Only the absorption lines of ammonia, NH_3, were found, their intensity increasing as the temperature of the cell was raised. The absence of absorption lines of the F_3BNH_3 molecule may be ascribed to the fact that in the vapor this molecule is strongly dissociated into BF_3 and NH_3. This conclusion is confirmed, in particular, by the lack of success in determining the temperature dependence of the saturation vapor pressure of this substance.[2] On the other hand, such a dependence has been established for $F_3BN(CH_3)_3$, and it was shown[2] that dissociation does not take place up to a temperature of 230°C.

In the investigation of the molecule $F_3BN(CH_3)_3$ in the range 7000–35000 Mc, 10 rotational transitions were found, characteristic of a symmetrical top with the constant B = 1750 Mc. The 1-2 and 2-3 transitions were registered with the help of a recorder. They appear as broad unresolved lines, the average frequencies of which equal 6990 and 10480 Mc, while the widths amount to 60 and 100 Mc respectively. The dipole moment was estimated on the basis of the intensity ($\sim 5 \times 10^{-4}$) and first-order Stark effect of the 2-3 transition; it approximately equaled 5 debye units in both cases. The 8-9 (located in the frequency range around 31500 Mc) and 9-10 (around 35000 Mc) transitions can be well observed on the oscilloscope screen and consist, each, of several lines of width 20-30 Mc.

The spectrum found undoubtedly belongs to the mole-

cule $F_2BN(CH_3)_2$, since it is characteristic of a symmetrical top and the measured value of the rotational constant differs from the calculated one by 4% in all. Furthermore, the measured value of the dipole moment coincides with that determined by other methods.[4]

The complex character of the observed rotational transitions must be principally due to the nonrigidity of the molecule and the presence in it of the two groups F_2B and $N(CH_3)_2$ which are capable of executing torsional vibrations. Furthermore, each transition must contain lines of molecules with the isotopes B^{11} (81%) and B^{10} (19%).

REFERENCES

1. Z. V. Zvonkova. Kristallografiya 1, 73 (1956).
2. A. W. Laubengayer and G. F. Condike. J. Am. Chem. Soc. 70, 2274 (1948).
3. A. B. Burger and A. A. Green. J. Am. Chem. Soc. 65, 1838 (1943).
4. G. Buz and D. Martin. "Khimiya trekhftoristogo bora i ego proizvodnykh." (Chemistry of boron trifluoride and its derivatives), Izd. Inostrannoi Lit., Moscow, 1955.

INFLUENCE OF GAS ADSORPTION ON ELECTROLUMINESCENCE

I. K. Vereshchagin

Received 12 October 1959

It is well known that data exist which make it possible to consider the electroluminescence of crystal phosphors in a dielectric as a surface effect.[1,2] In particular, it has been demonstrated that the catalytic activity (a pure surface effect) and electroluminescence of zinc oxide show parallel changes upon changing the preheating temperature of the sample.[3] On the other hand, since catalytic activity is usually connected with adsorption, the amount of gas adsorbed must influence the intensity of electroluminescence. The results of a measurement of ZnO electroluminescence in air and in vacuum are represented in the Figure (similar effects were also observed on some luminescent ZnS material). A number of conclusions can be drawn from an analysis of the data reported.

The electroluminescence of ZnO increases in intensity upon evacuation, giving an initial flash that fades in a few minutes; the brightness acquires a stationary value, which exceeds the corresponding value in air by a factor of 2-3.

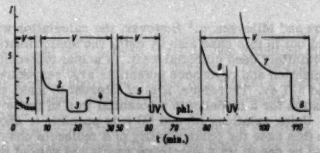

Average brightness I of ZnO electroluminescence in air[1,2,5] and in a vacuum of 10^{-2} mm Hg[2,4-7] as a function of time t test conditions. Curve 1—after 21 hr. exposure in air without applied field V; curve 2—after evacuation without field; curve 3—after admission of air; curve 4—after evacuation, with field; curve 5—after retention in vacuum for 20 min; curve 6—after irradiation in vacuum with ultraviolet light (UV) with an applied field for 5 min and exposure in vacuum without field for 13 min (phl—decay of photoluminescence); curve 7—after ultraviolet irradiation in vacuum with an applied field for 5 min; curve 8—after an admission of air. The sample: ZnO powder heated in vacuum at 200°C for 15 min, average crystallite size 1 μ. Experimental conditions: voltage V on the capacitor 200 volts, frequency 1000 cycles, thickness of the layer of powder insulated from the electrodes 0.1 mm, layer temperature +20°C.

After admission of air the luminescence drops rapidly to its original level. The magnitude of the initial peaks depends strongly on the exposure time of the ZnO sample without field. If evacuation is made in presence of a field, the flashes are absent and the brightness of the electroluminescence is almost immediately established at a level which is lower than the level corresponding to an evacuation without field. If the voltage is then removed for a certain time the level of luminescence is increased, and illumination with ultraviolet light leads to a further increase in the steady state brightness of electroluminescence.

Simultaneous measurements of the electrical conductivity of the samples under the same conditions showed that the conductivity increases by 9-10% upon evacuation, and that irradiation with ultraviolet light leads to an additional increase of the conductivity by a factor of approximately 2. The causes of the change in the electrical conductivity of ZnO have been explained in a number of papers: slight desorption of oxygen or other electronegative compounds takes place upon evacuation, resulting in the liberation of electrons.[4,5] Irradiation with ultraviolet light leads to photodesorption.[5,6]

According to reference 4, evacuation at room temperature cannot remove any significant amounts of adsorbed oxygen from the surface of ZnO. Prolonged heating at 400-500°C in vacuum is necessary to remove the main quantity of chemisorbed O_2. Consequently, the desorption of O_2 is slight with a simple evacuation; this produced only a slight change in electrical conductivity. On the other hand, electroluminescence exhibits a tremendous change upon evacuation. The same is the case with the photo emf, whose drop is not compensated by the subsequent admission of dry O_2,[7] obviously because in both cases the physical adsorption of other gases or vapors plays a dominant role. Adsorption of negative ions, always present in air, is also possible.[8]

A desorption of chemisorbed oxygen takes place under the influence of ultraviolet light; this appears as a considerable increase in electrical conductivity. Changes of electroluminescence and of conductivity occur simultaneously (the increases are 1.9 and 1.7 fold, respectively, as compared to vacuum values before irradiation) because the number of luminescence centers quenched by oxygen

is decreased ("blocking" of the centers[9]) simultaneously with the number of electrons bound by oxygen. The decrease in the brightness of electroluminescence upon adsorption of gas molecules can also be caused by the appearance of surface conduction and by other causes which would change the conditions of excitation and of electron injection into a strong field region at the surface of the crystals.

Chemical as well as physical adsorption leads to a bending of energy bands near the surface. An applied alternating field periodically decreases the height of these barriers and facilitates the bringing of electrons to the surface. This decreases the probability of desorption and of liberation of oxygen levels, which is apparently the cause of a reduction in brightness upon evacuation with an applied voltage.

The width of potential barriers at their maximum possible height is about 10^{-3} μ near the crystal surface, with almost complete ionization of the excess zinc (the concentration of the latter is of the order of 10^{17}-10^{18} cm^{-3}).[8, 10] From the values of the decrease in brightness of electrical conductivity and photoluminescence in air (5-10%), one can calculate the approximate width of the layer participating in electroluminescence. It turns out to be 10^{-1}-10^{-2} μ.

Thus the experiments described directly indicate the strong dependence of electroluminescent properties on crystal surface conditions. A further, more detailed investigation of the connection between adsorption effects and electroluminescence will no doubt make it possible to obtain new information on the mechanism of this effect.

REFERENCES

11. P. Zalm, G. Diemer, and H. A. Klasens. Philips Repts. 9, 81, 1954.
2. S. Larach and R. E. Shrader. Phys. and Chem. Solids 3, 159, 1957.
3. I. K. Vereshchagin. Izvest. Vyssh Uche. Zav. Fiz. 2, 114 (1960).
4. I. A. Myasnikov. Problem. Kinetiki i Kataliza 8, 34 1955; Doklady Akad. Nauk SSSR 99, 125 (1954).
5. I. A. Myasnikov. Zhur. Fiz. Khim. 31, 1721, 2004 (1957).
6. A. N. Terenin. Problem. Kinetiki i Kataliza 8, 23, 1955.
7. E. K. Putseiko and A. N. Terenin. Doklady Akad. Nauk SSSR 101, 645 (1955).
8. W. Brattain and J. Bardeen. Bell System Tech. J. 32, 1 (1953); "Problemy fiziki poluprovodnikov." (Problems of Semiconductor Physics), Izd. Inostrannoi Lit., Moscow, 1957.
9. K. V. Tagantsev and A. N. Terenin. Doklady Akad. Nauk SSSR 112, 241 (1957).
10. V. I. Kudryavtseva and G. I. Sinyapkina. Trudy Sibirsk. Fiz.-Tekh. Inst. pri Tomsk. Univ. 34, 214 (1947).

CALCULATION OF THE POLARIZABILITY OF MOLECULES WITHIN THE LIMITS OF THE METALLIC MODEL

Yu. N. Zhivliuk

Received 21 October 1959

The calculation of molecular polarizability within the limits of the metallic model is generally carried out using the approximation of an infinitely deep potential well.[1, 2] The purpose of the present communication is to show that, using the operator form of the second-order correction of perturbation theory

$$\sum_{k \neq n} \frac{X_{kn} X_{nk}}{E_n - E_k \pm \omega}, \qquad (1)$$

it is not difficult to make the calculation in the case of a rectangular potential well of finite depth. It is easy to convince oneself that expression (1) is equivalent to

$$\int \psi_n^* \hat{X} (E_n - \hat{H} \pm \omega)^{-1} (\hat{X} - X_{nn}) \psi_n d\tau, \qquad (2)$$

where $\hat{H}$ is the Hamiltonian of the unperturbed molecule, ψ_k is the wave function in zero approximation, $\hat{X}$ is the perturbation operator, ω is the frequency of the perturbation, and E_n is the eigenvalue of the operator $\hat{H}$.

The method, based on expression (1), was proposed by Dalgarno[3] in the form of (2) and later was used by other authors for the solution of concrete problems. The calculation consists of the solution of the differential equation

$$(\hat{H} - E_n \pm \omega) f = (\hat{X} - X_{nn}) \psi_n, \qquad (3)$$

where $f = (\hat{H} - E_n \pm w)^{-1} (\hat{X} - X_{nn}) \psi_n$, followed by integration.

In essence, this method was used in another form by Adamov and Milevskaya.[1] However, the calculation was carried out in this case also by using the approximation of an infinitely deep potential well. In actual molecules, the ionization and resonance potentials are, respectively, ~10 and 5-7 ev. Therefore, it is of interest to make the calculation for a model with a potential well of finite depth. Using relations (2) and (3) it is possible to show that in this case the polarizability of a molecule contributed by one of its π-electrons equals the sum of the following three integrals:

$$a = a_1 + a_2 + a_3,$$

where

$$a_1 = A_1 \int_{-\infty}^{0} \left(C_1^+ e^{\gamma_1^+ x} + C_1^- e^{\gamma_1^- x} - \frac{2A_1 k_1}{\omega^2} e^{k_2 x} \right) x \cdot e^{k_2 x} dx,$$

$$a_2 = A_2 \int_{0}^{L} \left(C_2^+ \sin \gamma_2^+ x + C_2^- \sin \gamma_2^- x + C_3^+ \cos \gamma_2^+ x + C_3^- \cos \gamma_2^- x + \frac{2A_1 K_2}{\omega^2} \sin k_2 x - \frac{2A_1 k_1}{\omega^2} \cos k_2 x \right) \cdot x \cdot \left(\frac{k_1}{k_2} \sin k_2 x + \cos k_2 x \right) dx,$$

$$a_3 = A_3 \int_{L}^{\infty} \left(C_4^+ e^{-\gamma_1^+ x} + C_4^- e^{-\gamma_1^- x} + \frac{2A_2 K_3}{\omega^2} e^{-k_2 x} \right) \cdot x \cdot e^{-k_2 x} dx.$$

The constants $C_1^{\pm}$, $C_2^{\pm}$, $C_3^{\pm}$, $C_4^{\pm}$ are determined from the conditions of continuity of the function f at the boundaries of the well:

$$C_1^{\pm} = C_3^{\pm} = \frac{2A_1U}{\omega^3} \cdot \frac{\frac{\gamma_1^{\pm}}{\gamma_2^{\pm}}\cos\gamma_2^{\pm}L + \sin\gamma_2^{\pm}L + \frac{2U\gamma_2^{\pm}}{\gamma_1^{\pm}(k_1^2-k_2^2)}\cos k_2 L}{2\gamma_2^{\pm}\cos\gamma_2^{\pm}L + \gamma_1^{\pm}\sin\gamma_2^{\pm}L - \frac{(\gamma_2^{\pm})^2}{\gamma_1^{\pm}}\sin\gamma_2^{\pm}L},$$

$$C_2^{\pm} = \frac{2A_1U}{\omega^3} \cdot \frac{\frac{\gamma_2^{\pm}}{\gamma_1^{\pm}}\sin\gamma_2^{\pm}L - \cos\gamma_2^{\pm}L + \frac{2U}{k_1^2-k_2^2}\cos k_2 L}{2\gamma_2^{\pm}\cos\gamma_2^{\pm}L + \gamma_1^{\pm}\sin\gamma_2^{\pm}L - \frac{(\gamma_2^{\pm})^2}{\gamma_1^{\pm}}\sin\gamma_2^{\pm}L},$$

$$C_4^{\pm} = \frac{2A_1Ue^{\gamma_1^{\pm}L}}{\omega^3} \cdot \frac{\frac{\gamma_2^{\pm}}{\gamma_1^{\pm}} + \left(\frac{\gamma_2^{\pm}}{\gamma_1^{\pm}}\cos\gamma_2^{\pm}L + \sin\gamma_2^{\pm}L\right) \cdot \frac{2U}{k_1^2-k_2^2}\cos k_2 L}{2\gamma_2^{\pm}\cos\gamma_2^{\pm}L + \gamma_1^{\pm}\sin\gamma_2^{\pm}L - \frac{(\gamma_2^{\pm})^2}{\gamma_1^{\pm}}\sin\gamma_2^{\pm}L},$$

where

$$k_1 = \sqrt{2(U-E_n)}, \quad k_2 = \sqrt{2E_n}, \quad \gamma_1^{\pm} = \sqrt{2(U-E_n \mp \omega)},$$

$$\gamma_2^{\pm} = \sqrt{2(E_n \pm \omega)},$$

$$A_1 = \sqrt{\frac{2k_1^2k_2^2}{2k_1k_2^2 + 2k_1^2k_2 + k_2^2k_2(k_1^2+k_2^2)L}},$$

$$A_2 = A_1 e^{k_1 L}\left(\frac{k_1}{k_2}\sin k_2 L + \cos k_2 L\right).$$

The width L and depth U of the potential well are chosen in accordance with the ionization potential and frequency of the electronic resonance transition. Consideration of the finiteness of the well gives rise to a significant correction to the polarizability, which can consist of several tens of per cent. Thus, for example, the longitudinal polarizability of butadiene, computed in this manner, is equal to $\alpha = 280$ atomic units, while in the case of the infinitely deep potential well, $\alpha = 220$ atomic units.

The example analyzed shows the advantage of the operator form (2) of the second-order correction of perturbation theory, which allows one to obtain an accurate solution of a number of problems. The use of expression (2) is also frequently convenient when an accurate solution of the Schrödinger equation is impossible. In this case one may have recourse to a numerical solution, since for the solution of some problems it is sufficient to know the eigenvalue of the energy and the wave function of only one state of the molecule, and Eq. (3) closely resembles the corresponding equation of Schrödinger.

The author takes this opportunity to thank I. I. Sobel'man for stating the problem and for advice during discussion of the present communication.

REFERENCES

1. M. N. Adamov and I. S. Milevskaya. Opt. i Spektr. 2, 339 (1957).
2. M. N. Adamov, M. G. Veselov, and T. K. Rebane. Izvest. Akad. Nauk SSSR, Ser. Fiz. 22, 1015 (1958).
3. A. Dalgarno and I. Lewis, Proc. Roy. Soc. A233, 70 (1955).

A CONTINUOUS EMISSION SOURCE GIVING SHORT-LIVED SINGLE FLASHES

A. M. Shukhtin, V. S. Egorov, and G. K. Tumakaev

Received 12 November 1959

In present-day laboratory work there frequently arises a need for a source of continuous radiation giving high intensity flashes of short duration. The present article gives a short description of a typical source of this type, simple in construction and convenient in performance.

This source is an easily demountable capillary pulsed discharge tube (Fig. 1). The body of the tube, 13, is a hollow thick-walled cylinder of plastic, incide of which porcelain capillary, 14, with an inside diameter of 3-4 mm is snuggly fitted. Electrodes 1 and 10 are attached to the end of the cylinder with the aid of four half-rings, 8. One electrode is constructed so as to improve breakdown conditions in the tube and to prevent the discharge from running along its surface. The external ends of the electrodes, with help of flange, 3, and adjustable socket, 12, are covered by windows, 2. One of these is the "working" window (quartz or glass) and serves for the emission of radiation. The second window and the socket with small lamp, 12, are used for adjusting the optical system.

While operating, the windows become coated, and it is occasionally necessary to wipe or to change them. A lens, 5, is clamped to a flange, 3, with the help of retaining washer, 4, making it possible to obtain a parallel beam of light. All vacuum seals at points of contact are effected with rubber gaskets, 6. One of them, snuggly fitted onto the protruding end of the porcelain capillary, serves to preclude the possibility of a breakdown between the body

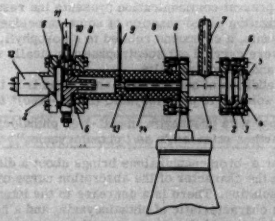

Fig. 1. The structural arrangement of the source.

of the tube and the capillary, which could cause failure of the source. Ignition electrode, 9, is introduced into the middle section of the discharge gap. To reduce the parasitic inductance (leakage) in the discharge circuit, the source is connected directly to the condenser leads. The tube is filled with air pumped through the nipple, 7, by an air pump. The air pressure in the tube can be regulated by a simple valve (rubber tube with clamp, 11). The pressure is so chosen that on the one hand spontaneous breakdown will not occur at the given difference of potential, (total gap length ~6 cm) and on the other hand the discharge can readily be initiated by application of igniting

impulse. In our case these conditions were realized with an air pressure of 130-150 mm Hg.

The power supply and ignition circuit is shown in Fig. 2. The employment of hydrogen Thyratron TGI 1-400/16 insures initiation of the discharge within approximately 1 μsec after sending a positive control signal to the thyratron grid. In our case, the capacity of the supply condenser, which was charged to 25-30 kv, was 0.56 mf. After a large number of flashes, the diameter of the capillary increases, but only very slightly, so that the source has a long lifetime.

Figure 3, I shows the oscillograms of the discharge current and light pulse obtained by using a Rogovsky loop and an FEU-18 photomultiplier, respectively, as detectors. Registration of signals was accomplished by means of an OK-17M double beam triggered oscilloscope. As is seen from the oscillogram, the strong light pulse exists only during the first half-cycle of the discharge. The duration of this half-cycle thus also determines the time of exposure. Under our conditions, this time was 3-5 μsec.

Figure 3, II shows oscillograms of light flashes and the time scale (time scale—1 μsec). The spectrum of the light is continuous over the entire visible and ultraviolet regions (6500-2200 A); line emission is almost completely absent.

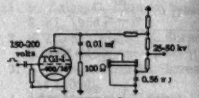

Fig. 2

Fig. 3

Fig. 2. Power supply and ignition circuit for discharge tube.

Fig. 3. I—Oscillograms of discharge current (a) and light pulse (b). II—Oscillogram of light pulse, with time scales.

With the aid of this continuous spectrum source, it is possible to obtain interference pictures in the ultraviolet and visible with one flash, using a slow optical system consisting of a Rozhdestvenskii interferometer and a spectrograph.

SPECTROPHOTOMETRIC STUDY OF THE INTERACTION BETWEEN PHTHALOCYANIN AND IRON TRICHLORIDE

T. S. Glikman and Z. L. Barvinskaya

Received 16 November 1959

Butsko and Dain[1] have shown that the reaction of chlorophyll (and pheophytin) with iron trichloride results in the formation of molecular complexes. Chlorophyll reacts similarly with $SnCl_2$.[2]

The present communication presents the results of an investigation of the reaction of some chlorides with phthalocyanin, a compound related to chlorophyll. The studies were carried out spectrophotometrically with dry solvents and anhydrous salts.

The addition of an excess of anhydrous iron trichloride to a solution of phthalocyanin (metal-free)* in α-chloro- or α-bromonaphthalene brings about a distinct change in the character of the absorption curve of the pigment solution. There is a decrease in the intensity of the bands characteristic of phthalocyanin, and a new band in the red region of the spectrum with a maximum at 750 mμ simultaneously appears. The greater the excess of $FeCl_3$ in the solution, the more intense is this change (Fig. 1).

*By analogy with pheophytin, metal-free phthalocyanin will be further referred to as "phthalocyanin."

The character of the changes observed in the absorption curve of phthalocyanin indicate that the addition of $FeCl_3$ results in the formation of a new product. By analogy with what is observed in the case of chlorophyll,[1,2] it may be assumed that this product is a molecular compound produced as a result of the association of phthalocyanin with iron trichloride. Actually, the addition to such a system of 7-10% of water leads to the complete regeneration of the original pigment. The instability constant of this complex apparently is small, since even with very low concentrations of the components (10^{-4} mole/liter of phthalocyanin and 5×10^{-3} mole/liter of $FeCl_3$) almost complete disappearance of the band for the free pigment is observed.

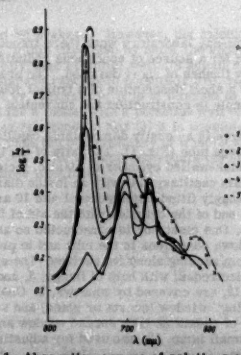

Fig. 1. Absorption curves of solutions of phthalocyanin in α-bromonaphthalene in the presence of added $FeCl_3$. 1—phthalocyanin solution without additive, concentration $C = 3.1 \times 10^{-4}$ mole/liter; 2—with added $FeCl_3$, $C = 1.5 \times 10^{-3}$ mole/liter; 3—with added $FeCl_3$, $C = 3.0 \times 10^{-3}$ mole/liter; 4—with added $FeCl_3$, $C = 4.4 \times 10^{-3}$; 5—with added HCl.

Addition of anhydrous $FeCl_3$ or $SnCl_4$ to a solution of phthalocyanin in α-chloronapthalene also leads to the formation of a complex with a maximum at 750 mμ. The same result is observed when dry HCl is introduced. However, in this case the absorption maximum of the solution is located at 740 mμ.

It is notable that oxygen plays a unique role in the formation of the complex of phthalocyanin with iron trichloride. It has been established that a molecular compound is formed only in air. If the solutions of iron chloride and of phthalocyanin are first well degassed and only then mixed together (without breaking the vacuum), the formation of a complex is not observed. Furthermore, if the system (phthalocyanin + $FeCl_3$ in α-chloronaphthalene) is subjected to careful degasification to a residual pressure of ~10^{-4} mm or dry, pure argon is bubbled for a long time through the solution, then the band characteristic of the complex disappears completely, and the bands for free phthalocyanin appear in the absorption curve of the solution. It is interesting, however, to note that subsequent introduction of oxygen leads only to a very slight regeneration of the molecular complex. Apparently, only those oxygen molecules that are adsorbed by solid phthalocyanin participate in the formation of the molecular complex. In fact, if solid phthalocyanin that has first been well degassed is dissolved (under vacuum conditions) and then, after the vessel is opened, is mixed in the air with a solution of $FeCl_3$, no change is observed in the character of the absorption curve (in the region 500-800 mμ) (Fig. 2, curve 1). If, however, after removal of the gases from the solid phthalocyanin, dry, pure oxygen is admitted to the vessel and only then the pigment is dissolved, the subsequent addition of $FeCl_3$ solution brings about the appearance of the absorption band characteristic of the complex. (Fig. 2, curve 2).

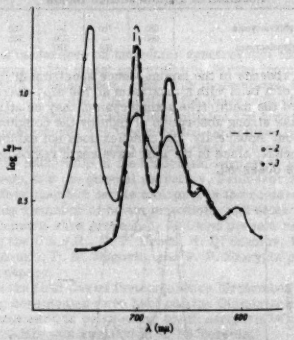

Fig. 2. Change in character of absorption curves of solutions (in α-chloronaphthalene) of phthalocyanin + $FeCl_3$ depending on the conditions of solution of the phthalocyanin. 1—phthalocyanin + $FeCl_3$, before solution solid phthalocyanin was well degassed (residual pressure 10^{-4} mm); 2—phthalocyanin + $FeCl_3$, solid phthalocyanin was well degassed, dry oxygen was admitted to vessel before solution; 3—solution of phthalocyanin in α-chloronaphthalene without additive (curve 2 obtained with a different layer thickness).

The tendency of some complexes of bivalent iron to reversible addition of molecular oxygen has been observed in the work of various authors.[3, 4] A similar phenomenon on the part of salts of trivalent iron, so far as we know, is here observed for the first time. It requires further investigation.

REFERENCES

1. S. S. Butsko and B. Ya. Dain. Zhur. Obshchei Khim. 28, 2603 (1958).
2. I. I. Dilung and B. Ya. Dain. Zhur. Fiz. Khim., in press (1959).
3. K. Kunz and A. Kress. Ber. deut. chem. Ges. 60, 367 (1927).
4. J. Drake and R. J. P. Williams. Nature 182, 1084 (1959).

INFLUENCE OF SOME ELECTRONOPHYLIC COMPOUNDS ON THE ABSORPTION AND LUMINESCENCE SPECTRA OF MAGNESIUM PHTHALOCYANIN SOLUTIONS

I. A. Akimov and G. A. Korsunovskii

Received 16 November 1959

In the work of Ashkinazi, Glikman, and Dain[1] it was determined that when ferric chloride and chlorophyll interact in solution, pheophytin is formed by the action of hydrochloric acid produced by solvolysis of the salt. When solutions of anhydrous ferric chloride and chlorophyll in dry acetone are mixed, Butsko and Dain[2] observed the formation of intermediate products which subsequently were converted into iron pheophytinate.

We have investigated the influence of hydrochloric acid and of the chlorides of various metals on the absorption and luminescence spectra of solutions of an analogue of chlorophyll-magnesium phthalocyanin, whose spectrum has been thoroughly investigated in our laboratories.

If an acetone solution of ferric chloride ($FeCl_3 \cdot 6H_2O$) is added in air to an acetone solution of magnesium phthalocyanin, the blue color of the solution changes to olive green, and the absorption spectrum changes as shown in Fig. 1.

The absorption bands of magnesium phthalocyanin with maxima at 665 and 601 mμ disappear, and new bands appear with maxima at 707 and 682 mμ. If the solution is allowed to stand, the intensity of these bands decreases, and after several hours weak bands appear with maxima around 688 and 655 mμ, characteristic of the metal-free phthalocyanin. Simultaneously, the formation of a precipitate occurs, a dioxane solution of which gives the spectrum characteristic of the metal-free phthalocyanin in this solvent.

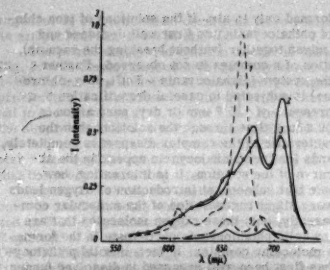

Fig. 1. The change in absorption spectrum of an acetone solution of magnesium phthalocyanin containing 1×10^{-5} mole/liter upon addition of 1×10^{-3} mole/liter of ferric chloride in acetone. Curve 1, original solution; curve 2, the spectrum of the mixture 5 min after addition of $FeCl_3 \cdot 6H_2O$; curve 3, the same 1 hr after mixing; curve 4, the same 24 hr after mixing; curve 5, spectrum of solution of precipitate in dioxane.

Similar phenomena were observed upon mixing an acetone solution of magnesium phthalocyanin with an acetone solution of hydrochloric acid at a concentration of 10^{-2} mole/liter.

These experiments suggest the hypothesis that the similar reaction mentioned above involving the pheophytinization of chlorophyll under the influence of hydrochloric acid takes place, either directly or as a result of solvolysis, by the replacement of the central magnesium atom with hydrogen. This reaction is accompanied by the formation of an unstable intermediate complex, having as noted above absorption bands at 707 and 682 mμ.

According to the results of Glikman and Barvinskoi,[3] the absence of water in the reaction of metal-free phtnalocyanin with feric chloride stabilizes the complex formed.

The formation of an unstable complex is also observed when $SbCl_3$, $SnCl_4$, and SnI_4 are added to acetone solutions of magnesium phthalocyanin. However, in the case of these substances, we did not succeed in observing the absorption band of the metal-free phthalocyanin as the final product.

The addition of bases—pyridine, aniline, or concentrated aqueous potassium hydroxide—to the solution containing the complex converts the latter back to magnesium phthalocyanin with its characteristic spectrum.

Parallel with the study of the absorption spectra, we have investigated the luminescence spectra of the above-mentioned mixtures of solutions. The spectra were recorded on a recording spectrophotometer,[4*] with excitation produced by the 365/366 mμ group of lines from a mercury lamp of the type SVDSh-250. Figure 2 shows luminescence spectra of solutions of magnesium phthalocyanin, of the complex, and of metal-free phthalocyanin. From the Table below, it can be seen that the bands obtained by excitation of the complex and located at 683 and 745 mμ coincide in location with bands of magnesium phthalocyanin, and the bands with maxima at 720 and 780 mμ are located very close to the bands of the metal-free phthalocyanin.

Location of Luminescence Bands

Magnesium phthalocyanin	685	710	—	750	—
Complex	683	—	720	745	780
Metal-free phthalocyanin	—	708	730	—	775

The absence in the luminescence spectrum of the complex of a band with a maximum at 708 mμ, characteristic of the metal-free phthalocyanin, may be attributable to the strong absorption of light by the complex in this region. Apparently, the complex does not exhibit luminescence, since in the long wavelength region no new bands are observed.

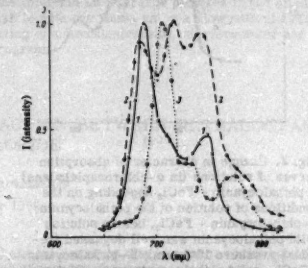

Fig. 2. Luminescence spectra of solutions of phthalocyanins. Curve 1, magnesium phthalocyanin in acetone; curve 2, the same after addition of $SbCl_3$; curve 3, metal-free phthalocyanin in dioxane.

The influence noted above of pyridine and aniline is apparent also in the luminescence spectra. Upon the addition of these substances to the complex, the bands of the metal-free phthalocyanin disappear, and the bands of magnesium phthalocyanin are considerably intensified.

*The authors express their gratitude to A. V. Shablya for his offer of the apparatus for these measurements.

REFERENCES

1. M. S. Ashkinazi, T. S. Glikman, and B. Ya. Dain. Doklad Akad. Nauk SSSR 73, 743 (1950).
2. S. S. Butsko and B. Ya. Dain. Zhur. Obshchei Khim. 28, 2603 (1958).
3. T. S. Glikman and Z. L. Barvinskaya. Opt. i Spektr. 8, 425 (1960).
4. A. V. Shablya and A. V. Karyakin. Opt. i Spektr. 5, 44 (1958).

NEWS ITEMS

THE INTERNATIONAL CONFERENCE ON MOLECULAR SPECTROSCOPY AT BOLOGNA (ITALY)

V. Chulanovskii

The conference on molecular spectroscopy took place in Bologna at the oldest university in Europe from the 7th to the 12th of September, 1959. The international Society for Pure and Applied Chemistry, the University of Bologna, and several other organizations initiated and cooperated on the conference. The Organization Committee was made up of representatives from the different countries and was under the leadership of the chairman, Professor H. W. Thompson, and the general secretary, Professor A. Mangini. More than 500 people took part in the conference, including a number of Soviet scientists, and some 200 or more reports were presented. Of those present representing the U.S.S.R., E. F. Gross, N. D. Sokolov, V. M. Chulanovskii, D. N. Shigorin, and P. P. Shorygin presented papers.

On the first day of the conference (September 6) the opening ceremonies were held and the Ciamician medals were presented to outstanding spectroscopists. One of these medals was awarded to A. N. Terenin.

The main work of the conference took place in six sections, two of which were divided into subsections, and three or four sections were held simultaneously. The sectional meetings usually started with a general report, and in addition, a number of general reports were presented outside the section meetings. With such a conference program, each of the delegates could take part in discussion of a limited range of topics. This limitation and the unavoidable subjectivity relative to problems considered are also reflected in this account.

Only three of the general reports will be discussed here in any detail. First, the paper on molecular spectra in the vacuum ultraviolet presented by G. Herzberg (Ottawa, Canada).* The report was devoted to the author's studies in the field of electron spectra, chiefly in the absorption of the diatomic molecules CO, O_2, NO, H_2, CH_2, and also several of the simpler polyatomic molecules. Second, the paper given by R. C. Lord (Cambridge, Mass.) on his work in the far infrared region (200-20 cm^{-1}) Third, a detailed report by J. A. A. Ketelaar (Amsterdam, Holland) on the infrared spectra of crystals (especially those that absorb strongly), which aroused a great deal of interest.

*This report was previously read by G. Herzberg in Leningrad and Moscow during his stay in the Soviet Union.

The work of the first section, devoted to the general theory of molecular spectra, embraced a broad range of topics: calculation of the vibrational spectra of complex molecules, the theory of intermolecular interactions, computation of transition probabilities, and the fine structure of electron shells of the simpler molecules, etc.

The work of the second section pertained to electron absorption and emission spectra, mainly in relation to their significance for the solution of structural problems. I. Tanaka's (Bedford, Mass.) paper was devoted to a description and explanation of the nature of continuous emission spectra in the far ultraviolet region of electrical discharges in inert gases.

Papers were given by D. N. Shigorin et al. during this same section on the spectrum of anthraquinone and its derivatives in frozen solutions, and by P. P. Shorygin et al. on the dependence of the spectra of methoxy- and dimethylamine groups on the angle of twist with respect to the plane of the benzene ring. An appreciable part of the section was concerned with the consideration of exciton spectra, particularly in connection with the work of E. F. Gross in this field. A number of reports were devoted to questions of fluorescence and phosphorescence.

The problem of reflection spectra in the ultraviolet and infrared regions of the spectrum was discussed between the second and third sections. Two general reports (J. Lecomte—Paris, France, and G. Kortüm—Tübingen, German Federal Republic) were devoted to it. In a private discussion on this topic J. Fahrenfort (Amsterdam, Holland) proposed a new method of observing infrared reflection spectra of weakly absorbing materials by bonding a layer of the material between windows of a substance with a very large coefficient of refraction (KRS5). In this method the contrast in the spectrum is greatly enhanced, and makes quantitative measurements possible.

The third section on infrared spectroscopy can be more fully presented in this account inasmuch as the author participated direction in the work of this particular section. A great number of the reports of this section were devoted to the study of the structure of the infrared spectra of different molecules and their connection with the structure of the molecules themselves. For some time past, considerable interest has been paid to the infrared spectroscopy of the liquid state, and this was reflected in the program of this section. Attempts to seek the true mechanism of intermolecular interactions occupied a special position in the papers of foreign scientists, but it always transpired that the theoretical schemes for such interactions were either lacking or one-sided, and failed to explain many variations. Apropos of this topic, in their general report, R. Mecke (Freiberg, German Federal Republic) and H. W. Thompson (Oxford, England) proposed a general formula for the dependence of the relative displacement on factors characterizing the absorbing medium

$$\frac{\Delta\nu}{\nu} = C_1 + C_2\frac{\varepsilon-1}{2\varepsilon+1} + C_3\frac{n^2-1}{2n^2+1} + C_4\sigma^*.$$

The symbol σ^* here denotes the characteristic of local bonding. The constants C_1, C_2, C_3, and C_4 are selected to best satisfy the experiment during the transition from one solvent to another. Experiment shows that such a general formula is also limited in its applicability. Another type of classification of solutions according to the nature of the intermolecular bond (volume or local), which is independent of the mechanism of the bond, was proposed by the author of this account.

V. Chulanovskii et al. presented a report on a spectroscopic study of the hydrogen bond, in which they showed the importance of the role of not only the proton but also the donor and acceptor proton in the infrared

absorption spectrum. J. Lascombe and M. L. Josien (Bordeau, France) reported that discreet changes in the vibrational frequency of the C=O group associated with formation of hydrogen bonds had been detected in a number of solutions of several ketones. E. Fishman and N. Krascella (Syracuse, N.Y.), studied the temperature dependence of the shifting of C=O and C=N bands in different solutions. M. Horák, J. Jonáš, and J. Plíva (Prague, Czechoslovakia) established a linear dependence between the magnitude of the displacement of the C=O group band in carboxylic acid and its frequency value.

L. J. Bellamy (ERDE, Waltham Abbey, England) pointed out the importance for analytical purposes of calculation of the change in band intensities during a transition in a solution.

The entire paper by M. Clark and N. Sheppard (Cambridge, England) was devoted to spectra of adsorbed films. Three other papers were concerned with polymer spectra.

A detailed description of changes in the spectrum of HCl in different solutions during the transition from the gaseous state to the frozen solid state (at different pressures and temperatures) was given in a report by B. Vodar (CNRS, France).

New operating techniques were also reflected in many of the papers; three of these papers will be cited. C. E. Weir, E. R. Lippincott, A. Van Valkenburg and E. N. Bunting (Washington, D.C., and Maryland) described a cell with diamond windows for operation in the infrared region (1-15 μ) under pressures up to 50,000 atm. M. Delhaye (Lille, France) reported on a study of Raman spectra using cinematographic exposure; this technique can be utilized to follow the progress of a chemical reaction. A. Hadni, E. Decamps, and C. Janot (Nancy, France) presented a paper on spectroscopy in the far infrared region.

Only few of the reports can be mentioned in this account for the reasons indicated above. The reports by Italian scientists, in particular, are not presented here primarily because of the author's inadequate knowledge of the Italian language. Also, the fourth section which was devoted to papers on Raman spectra and the section encompassing work in the microwave region are not covered.

As can be seen from the above, the conference embraced a wide range of topics and generally speaking was conducted on a high level. The papers of this conference can be considered as being on the same level as those presented at meetings arranged by the Commission on Spectroscopy of the Academy of Sciences of the U.S.S.R. Attention should be paid to foreign scientists' high development of technical practices and knowledge in the field of theoretical spectroscopy and also to the high class spectral equipment with which even university laboratories abroad are equipped.

VIII INTERNATIONAL SYMPOSIUM ON SPECTROSCOPY

The eighth International Symposium on Spectroscopy took place from the 14th through the 18th of September, 1959, in Lucerne (Switzerland) under the auspices of the Swiss Society for Spectral Analysis. Professor E. Lüscher (Zürich) was chairman of the Organization Committee and Scientific Council and Doctor J. Guy was general secretary. Some 400 people from more than 30 countries took part in the Symposium. The Soviet Union was represented by three delegates: S. A. Ukholin, M. A. Mazing, and S. E. Frisch, corresponding member of the Academy of Sciences of the U.S.S.R.

The Symposium was divided into three sections: (1) Emission Spectroscopy, (2) Mass Spectroscopy, and (3) X-Ray Spectroscopy. Four survey papers were read: (1) H. C. Van de Hulst (Holland) "A study of interstellar gas by methods of optical and radiospectroscopy," (2) Lochte-Holtgreven (German Federal Republic) "Spectroscopic study of the physics of hot plasma," (3) Mavrodineanu (U.S.A.) "Some data on quantitative spectral analysis using flames," (4) Schumacher (Switzerland) "Problems of mass spectroscopy." A fifth survey report on the development of quantometry that was scheduled did not take place.

The largest number of reports was presented at the Emission Spectroscopy section and most of these pertained to problems in spectral analysis. Papers in the sections were allowed 20 minutes; in the majority of cases discussion of the papers was very brief. Several reports in the Emission Spectroscopy section dealt with general processes taking place in light sources. Cases in point were the reports by E. Laqua and W. D. Hagenah on the dependence of the spectral radiation of sparks on changes of discharge current with time and the report by Veresh on the recombination of ions and electrons in spark discharges in vapors of zinc, cadmium, etc. A report on entry of electrode material into a flame arc of alternating current was very nicely illustrated by slowed-down color motion pictures (1200-1300 frames per sec). A report by M. Pierucci was devoted to the pinched-down electric arc as a source of very high temperatures. An appreciable number of the reports dealt with problems of flame spectrometry. The reports in the Mass Spectroscopy and X-Ray Spectroscopy sections were well presented, and the papers in these two sections indicated that mass spectroscopy and X-ray analysis bear considerable attention as analytical methods. X-ray fluorescence spectra are being used for analytical purposes.

Attempts to use spectrographs in the extreme ultraviolet (vacuum) region for analytical purposes attracted attention in the field of optical emission spectroscopy. For example, a paper by Balloffet, Romand, and Vodar reported on spectral analysis of germanium, arsenic, selenium, antimony, and several other elements by the lines located in the 1500-700 A region. The same authors reported on spectral determination of gases in titanium by the lines of multiply ionized ions of nitrogen (NIV and NV) and oxygen (OIII, OIV, OV and OVI) located in the extreme ultraviolet region.

On the last day of the Symposium several papers were devoted to spectral apparatus. Among these papers mention should be made of the report by P. Kröplin (German Democratic Republic) on a 2 meter spectrograph with a plane diffraction grating, the report by Scheller (German Democratic Republic) on a new instrument for industrial visual analysis, and a paper by B. Saudreau (France) on a vacuum spectrograph for analytical purposes.

A report on "The nonsteady state theory of broadening and displacement of spectral lines" was given by M. A. Mazing from the Soviet delegation. This paper was well presented and generated a lively interest. It should be noted that the Soviet Union could have been far more fully represented; we have a number of interesting papers on spectral analysis, which would have demonstrated the

general high level of spectral-analytical research in the Soviet Union. In order to do this it would have been necessary to make decisions beforehand on the participation of Soviet scientists in the Symposium, so that time would have been available to prepare reports and inform the committee of the proposed contributions.

On the second day of the Symposium excursions to factories inspected spectral-analytical laboratories; at the Sulzer Brothers' plant in Winterthur, the operation of a quantometer made by the ARL Co. (Lausanne) was demonstrated.

An exhibition of spectral apparatus held during the Symposium was of considerable interest. Of the large-scale equipment the big Jarell-Ash diffraction grating spectrograph should be mentioned; it has a maximum dispersion of 0.17 A/mm, and a practical resolving power of 300,000. The instrument is very well assembled in over-all arrangement, has a generator, and is provided with an illuminating device containing a direct vision prism for separating spectra of different orders. The Steinheil Company (German Federal Republic) exhibited a three-prism spectrograph for industrial analyses with a very compact arrangement of the spectrograph in the over-all assembly with the generator (the spectrograph is mounted vertically). In addition to this the same company exhibited a fine photoelectric attachment for a spectrograph for automatic recording of spectra. The automatic recording attachment for the spectrophotometer and assembly combines a double spectrum projector with a spectrophotometer. A number of interesting displays were presented by the Zeiss factory in Jena (German Democratic Republic): a 2 meter spectrograph with a plane diffraction grating, a three-prism spectroscope for industrial purposes, and a photoelectric microphotometer.

Finally, mention should be made of the wide application of photoelectrics, automatic recording, and program control, etc., illustrating general trends in the development of spectral-analytical instrumentation.

NOTICE

In the first part of July 1960 the XIII All Union Conference on Spectroscopy will be held in Leningrad.

The program of the Conference includes reports on physical problems of atomic and molecular spectroscopy:

1. Theoretical and experimental determination of atomic constants.
2. Spectroscopy of plasmas.
3. Spectroscopy of molecular electron states.
4. Spectroscopy of molecular vibrational states.
5. Spectroscopy of crystals.
6. Spectroscopy of gases and condensed systems.
7. Spectral methods of research on intermolecular interactions.
8. Radiospectroscopy, including electron paramagnetic and nuclear magnetic resonance.

Applications to contribute reports and theses of the reports should be sent, prior to April 5, to the Commission on Spectroscopy of the OFMN Academy of Sciences of the U.S.S.R. (Moscow, K-12, proezd Capunova, d. 13-15. tel. kommut KO-14-40, dob. 31).

THE OPTICAL SOCIETY OF AMERICA

Why should you join OSA?

There is no other association of opticists in existence to promote and disseminate knowledge in this field. The Optical Society of America was organized in 1916 "to increase and diffuse the knowledge of optics in all its branches pure and applied, to promote the mutual interests of investigators of optical problems, of designers, manufacturers and users of optical instruments and apparatus of all kinds, and to encourage co-operation among them".

What about the advantages of membership?

You receive three monthly publications:

THE JOURNAL OF THE OPTICAL SOCIETY OF AMERICA: *This is the official publication of OSA*

OPTICS AND SPECTROSCOPY: *an English translation of the leading scientific journal of the USSR Academy of Sciences in this field*

PHYSICS TODAY: *as OSA is a member society of the American Institute of Physics, OSA members receive this publication**

From JOSA and OPTICS AND SPECTROSCOPY you will not only learn what your American colleagues are doing, but also discover what the Russians are working on in your field. Together these two journals publish the work of American and Russian scientists in all branches of optics and spectroscopy, including X-ray, ultraviolet, visible, infrared and microwave, filters, lens design, thin layer optics, geometric optics, electron optics, diffraction gratings, electroluminescence, wave mechanics, thermal radiation backgrounds, detectors, infrared polarizers, and their many applications in science and industry.

You will also receive announcements and programmes of all meetings (OSA holds at least two a year) and, even if you cannot attend many of these, you will know what is going on in your area. And you can submit a paper and have it given by proxy.

Who can join?

OSA invites to membership all who are interested in any branch of optics, either in research, in teaching, in optical applications, in the manufacture and distribution of optical equipment of all kinds, or in physiological and medical optics.

What are the membership dues? $13.00 per annum.

How can you join?

Write Dr. Mary E. Warge, Executive Secretary, Optical Society of America, 1155 16th Street, N. W., Washington 6, D. C., for an application form.

*OSA members may also subscribe to other AIP publications at a reduced rate.

OPTICAL SOCIETY *of* AMERICA

1155 SIXTEENTH STREET, N. W. WASHINGTON 6, D. C.

TRANSLITERATION OF CYRILLIC CHARACTERS

used by the Optical Society of America

А	а	a	Р	р	r
Б	б	b	С	с	s
В	в	v	Т	т	t
Г	г	g	У	у	u
Д	д	d	Ф	ф	f
Е	е	e	Х	х	kh
Ж	ж	zh	Ц	ц	ts
З	з	z	Ч	ч	ch
И	и	i	Ш	ш	sh
Й	й	i	Щ	щ	shch
К	к	k	Ъ	ъ	"
Л	л	l	Ы	ы	y
М	м	m	Ь	ь	'
Н	н	n	Э	э	e
О	о	o	Ю	ю	yu
П	п	p	Я	я	ya

ANNUAL REVIEWS
RUSSIAN TRANSLATION PROGRAM

Annual Reviews, Inc., is a non-profit corporation engaged in the publication of ten Reviews that cover a number of the sciences from Psychology to Nuclear Science. The reviews, 20 or 25 in number, published in each annual volume, are written by scientists from all over the world. When the scientific literature from the USSR began to enter this country in the postwar years, Annual Reviews attempted to make the contents available to its readers by publishing in several of the Reviews, a special chapter entitled, "The current status of _____ in the USSR." Such articles were written by scientists of native linguistic competence, resident in the western world, who, at the same time, were well recognized by their colleagues for their scientific competence.

Although this effort was pursued for three years, it was finally largely abandoned because of the difficulties that were experienced in attempting to evaluate the present status of, for examples, optics, in one 30-page chapter. Fortunately, by this time, translation programs had begun to develop. These have made it possible for Annual Reviews to subscribe to 31 of the translated periodicals and to make these available to its authors, some 200 in any given year, who are interested in the contents. Thus, papers on optics in Russian are distributed among at least 20 authors, each a specialist in his field, instead of leaving to a single author the very difficult task of reviewing the whole of the Russian literature in optics. The recipients are completely free to review or to discard the material received. In the case of one of its Reviews, Annual Reviews is still using the earlier approach, largely because a substantial portion of the original literature is not encompassed by present translation programs.

INSTRUMENT SOCIETY OF AMERICA
FOREIGN TRANSLATION PROGRAM

The Instrument Society of America was awarded a grant by the National Science Foundation to continue the translation and publication of the 1959 issues of English editions of four leading Russian technical journals:

The Russian original of Measurement Techniques (Izmeritelnaia Tekhnika) was published as a monthly in 1959 by the Committee of Standards, Measures and Measuring Instruments of the Council of Ministers, USSR. There are approximately 100 pages per issue with articles of particular interest to all who are engaged in the study and application of fundamental measurement.

Instruments and Experimental Techniques (Pribory i Tekhnika Eksperimenta) is published bi-monthly by the Academy of Sciences, USSR. Over 175 pages per issue deal with articles on function, construction, application and operation of instruments in various fields of experimentation.

The Russian monthly Automation and Remote Control (Avtomatika i Telemekhanika) is published by the Institute of Automation and Remote Control of the Academy of Science, USSR with approximately 150 pages per issue. It is considered to be the leading Soviet journal in the automatic control field and contains articles on all phases of automatic control theories and techniques.

Industrial Laboratory (Zavodskaya Laboratoriya) is published by the Ministry of Light Metals, USSR. This monthly contains articles on instrumentation for analytical chemistry and physical and mechanical methods of material research and testing. There are approximately 125 pages per issue.

For information write Instrument Society of America, 313 Sixth Avenue, Pittsburgh 22, Pennsylvania.

Emission Coefficients of Some Powdered High-Melting Compounds . . . . . T. I. Serebryakova, Yu. B. Paderno, and G. V. Samsonov 212
Effect of Solvents on the Electronic Spectra of Organic Molecules . . . . . L. A. Zhmyrev, V. V. Zelinskii, V. P. Kolobkov, A. S. Kochemirovskii, and I. I. Reznikova 214
The Effect of Temperature on the Electroluminescence of a Sublimed ZnS-Mn Phosphor . . . . . N. A. Vlasenko 215
A Simple Derivation of the Kramers–Krönig Relations . . . . . V. S. Galishev 217
Microwave Investigation of the Molecules F_3BNH_3 and $F_3BN(CH_3)_3$ . . . . . A. M. Prokhorov and G. P. Shipulo 218
Influence of Gas Adsorption on Electroluminescence . . . . . I. K. Vereshchagin 219
Calculation of the Polarizability of Molecules within the Limits of the Metallic Model . . . . . Yu. N. Zhivliuk 220
A Continuous Emission Source Giving Short-Lived Single Flashes . . . . . A. M. Shukhtin, V. S. Egorov, and G. K. Tumakaev 221
Spectrophotometric Study of the Interaction Between Phthalocyanin and Iron Trichloride . . . . . T. S. Glikman and Z. L. Barvinskaya 222
Influence of Some Electronophylic Compounds on the Absorption and Luminescence Spectra of Magnesium Phthalocyanin Solutions 223

NEWS ITEMS

The International Conference on Molecular Spectroscopy at Bologna (Italy) 225
VIII International Symposium on Spectroscopy 226

EDITOR'S NOTE

Comments on the scientific content of the translated Russian articles published in OPTICS AND SPECTROSCOPY are invited. They should be addressed as a Letter to the Editor of the Journal of the Optical Society of America and forwarded to the Editor of that journal, Dr. W. R. Brode, National Bureau of Standards, Washington 25, D.C.

VOL. VIII, NO. 3 OPTICS AND SPECTROSCOPY MARCH 1960

CONTENTS

The Hyperfine Structure of Multielectron Atoms . . . G. M. Bukat, A. Z. Dolginov, and R. A. Zhitnikov 151
An Approximate Method for Calculating Franck-Condon Factors . . . L. M. Biberman and I. T. Yakubov 155
Calculation of the Probability of Autoionization in Helium and Lithium Atoms . . . R. Kh. Propin 158
Transition Probabilities in the γ– and β– Band Systems of NO . . . S. P. Erkovich and Yu. V. Pisarevsky 160
Coefficient of Continuous Absorption of Radiation by Quasi Molecules of Hydrogen . . . S. P. Erkovich 162
The Importance of H_2O in the Combustion of Carbon Monoxide in Oxygen . . . R. B. Tagirov 164
Vibrational Spectra and Potential Functions of the Methylsilanes CH_3SiH_3, $(CH_3)_2SiH_2$, and $(CH_3)_3SiH$ . . . I. F. Kovalev 166
The Raman Spectra of the Stereoisomers of 1,2-Dialkyl Cyclopentanes . . . V. T. Aleksanyan, Kh. E. Sterin, A. A. Mel'nikov, and A. F. Plate 170
Emission and Absorption Spectra of Perylene in Solid Solutions at 77°K . . . E. V. Shpol'skii and R. I. Personov 172
Temperature Dependence of the Broad Absorption Bands in the Spectra of Crystals of Various Structures Colored by Isomorphous Impurities . . . S. V. Grum-Grzhimailo and G. V. Klimusheva 179
On the Influence of Temperature on the Electronic Spectra of Complex Molecules . . . L. G. Pikulik and M. A. Solomakho 180
The Effect of Strong Illumination on the Absorptivity of Complex Molecules . . . A. P. Ivanov 183
On the Influence of the Width of the Monochromator Slits on the Accuracy of Photoelectric Measurements of the Intensity of Raman Lines . . . E. V. Chisler 187
Photoelectric Method of Recording Interference Fringes in White Light . . . T. S. Kolomiitsova and I. V. Novikova 189
The Raman Spectra of Hydrocarbons of Different Classes. VI. The Raman Spectra of Some Arylcyclobutanes . . . E. G. Treshchova, Iu. N. Panchenko, N. I. Vasil'ev, M. G. Kuz'min, Iu. S. Shabarov, and R. Ya. Levina 193
Determination of Absolute Oscillator Strengths from Spectral Line Widths . . . V. K. Prokof'ev, I. M. Nagibina, and G. P. Petrova 195
Evaluation of the Error of Interpolation by the Normals of the Spectrum Sections on the Rowland Circle . . . V. A. Loginov 197
The Energy Spectrum of an F-Center in Continuum Theory . . . Yu. E. Perlin 199
The Temperature Dependence of the Intensity of Stokes and Anti-Stokes Raman Lines in Liquids . . . A. I. Sokolovskaya and P. A. Bazhulin 203

SHORT COMMUNICATIONS

High-Speed Photoelectric Spectrometer for the Region 0.4–0.9 μ . . . N. G. D'yachenko 205
On the Effect of the Solvent on the Fluorescence Yield . . . A. S. Kochemirovskii and I. I. Reznikova 206
On the Compensation of Rowland's "Ghosts" in Spectrographs with Double Diffraction on the Grating . . . V. N. Karpinskii 207
Calculation of the Vibrational Frequency of Diatomic Molecules from the Reduced Mass . . . K. S. Krasnov and A. I. Maksimov 208
Absorption Spectra of Diamonds . . . G. O. Gomon 210
On the Sensitization of Photographic Plates in the Ultraviolet Region of the Spectrum . . . I. A. Berezin and A. I. Stepanova 211

(Contents continued on inside back cover)